Reliable Life Prediction Models for Various Material Damage Processes

by

Shaik Mohammed Najeeb

A Thesis Presented to the

FACULTY OF THE COLLEGE OF GRADUATE STUDIES

KING FAHD UNIVERSITY OF PETROLEUM & MINERALS

DHAHRAN, SAUDI ARABIA

In Partial Fulfillment of the
Requirements for the Degree of

MASTER OF SCIENCE

In

MECHANICAL ENGINEERING

November, 1990

RELIABLE LIFE PREDICTION MODELS FOR VARIOUS MATERIAL DAMAGE PROCESSES

BY

SHAIK MOHAMMED NAJEEB

A Thesis Presented to the

FACULTY OF THE COLLEGE OF GRADUATE STUDIES

KING FAHD UNIVERSITY OF PETROLEUM & MINERALS

DHAHRAN, SAUDI ARABIA

In Partial Fulfillment of the
Requirements for the Degree of

MASTER OF SCIENCE

In

MECHANICAL ENGINEERING

NOVEMBER, 1990

KING FAHD UNIVERSITY OF PETROLEUM & MINERALS

DHAHRAN, SAUDI ARABIA

This thesis, written by

SHAIK MOHAMMED NAJEEB

under the direction of his thesis committee, and approved by all the members, has been presented to and accepted by the Dean, College of Graduate Studies, in partial fulfillment of the requirements for the degree of

MASTER OF SCIENCE IN MECHANICAL ENGINEERING

Thesis Committee

Anwar Khalil Sheikh
Chairman (Dr. Anwar Khalil Sheikh)

S. M. Zubair
Member (Dr. Syed Mohammed Zubair)

Munir Ahmad
Member (Dr. Munir Ahmad)

Dr. H.I. Abualhamayel
Department Chairman

Dr. Ala H. Rabeh
Dean College of Graduate Studies

Date : 12-1-91

Dedicated to

My beloved parents, wife, brothers & sister

whose sacrifices made this task possible

ACKNOWLEDGEMENT

Praise and gratitude be to Allah the Almighty, with whose gracious help it was possible to accomplish this work. Acknowledgement is due to King Fahd University of Petroleum and Minerals for extending all facilities and providing financial support.

I would like to offer my indebtedness and sincere appreciation to my advisor and committee chairman, Dr. Anwar Khalil Sheikh, who has been a constant source of help and encouragement during my M.S. programme. I also greatly appreciate the invaluable co-operation and support extended by Dr. Syed Mohammed Zubair, and Dr. Munir Ahmad who served as my committee members.

I owe the spirit of my M.S. programme to my family for inculcating in me the zeal and enthusiasm which has always been a source of inspiration for me. I am also grateful for their patience, understanding and encouragement.

Lastly, but not the least, I am thankful to all faculty, staff, colleagues and friends who made my stay at K.F.U.P.M. a memorable experience.

TABLE OF CONTENTS

LIST OF TABLES

LIST OF FIGURES

THESIS ABSTRACT

NAME OF STUDENT : SHAIK MOHAMMED NAJEEB

TITLE OF STUDY : RELIABLE LIFE PREDICTION MODELS FOR VARIOUS MATERIAL DAMAGE PROCESSES

MAJOR FIELD : MECHANICAL ENGINEERING

DATE OF DEGREE : NOVEMBER, 1990

Service failures in most of the engineering systems (structures, machines, or components) are caused by a variety of material degradation processes which leads to the gradual decline in the quality and performance of the system, and ultimately causes the failure of the system. The life of a component is terminated when the damage D(t) reaches or exceeds a limiting value which is the critical level D_l i.e., failure occurs when $D(t) \geq D_l$, where D(t) represents a certain manifestation of damage at time t. The time dependent stochastic characterization of damage functions observed in different types of material damage processes is presented and the corresponding reliability models are developed as well as the link between the parameters of the damage processes and the reliability models is established. These damage functions and reliable life prediction models are developed for several irreversible material degradation processes, such as wear, corrosion, fouling and creep. These reliability models when incorporated in the process of decision making helps to select the best among the available technical alternatives of replacing or maintaining the existing system, as well as to compare the reliability of competing systems supplied by different manufacturers.

MASTER OF SCIENCE

KING FAHD UNIVERSITY OF PETROLEUM & MINERALS

Dhahran, Saudi Arabia.

بسم الله الرحمن الرحيم

خلاصة الرسالة

الإســـــــــم : شيخ محمد نجيب

عنوان الدراسة : نماذج موثوقة للتنبأ بعمر مادة نتيجة تعرضها لعمليات تلف مختلفة .

القســـــــــم : الهندسة الميكانيكية .

التاريـــــــــخ : نوفمبر ١٩٩٠م .

يتأتى فشل الخدمة في معظم النظم الهندسية (انشاءات ، آلات أو عناصر) نتيجة عدة عمليات تحللية (تفسخية) للمواد ، مما يؤدي الى انخفاض تدريجي في جودة وأداء النظام ويؤدي بالنهاية الى اخفاق عمل النظام . ينتهي عُمْر العنصر عندما تصل أو تتعدى درجة التلف $D(t)$ قيمة قصوى مقدارها D_f ، (بمعنى آخر ، يحدث الفشل عندما تكون $D(t) > D_f$ ، حيث أن $D(t)$ تمثل مقدار معين من التلف عند وقت معين t) . تمت دراسة دوال تلف عشوائية متغيرة زمنياً لعمليات تلف مختلفة للمادة ، كما تم تطوير النماذج الموثوقة المقابلة ، كما تم ايجاد العلاقة بين العوامل التي تتحكم في عمليات التلف والنماذج الموثوقة . تم تطوير الدوال التلفية ونماذج تنبأ العمر الموثوقة لعدة عمليات تحللية غير انعكاسية مثل التآكل ، الصدأ ، الترسب والزحف . يمكن إستخدام هذه النماذج الموثوقة في عمليات الإنتقاء بين الإختيارات المتاحة لإستبدال أو صيانة النظام الموجود ، كما يمكن أستخدامها لمقارنة مدى الإعتماد على النظم التي يقدمها مختلف المصنعين .

ماجستير في العلوم
جامعة الملك فهد للبترول والمعادن
الظهران - المملكة العربية السعودية

CHAPTER 1

INTRODUCTION TO MATERIAL DAMAGE PROCESSES AND RELIABILITY MODELLING

1.1 INTRODUCTION

The consumption of existing materials in the present world is very high , but also there is always new demands for better and cheaper materials. The search for energy alternatives is creating the need for high temperature, high strength materials which have high reliability in such an environment. Therefore the reliability assessment of the materials is one of the most important features of material evaluation.

With tens of millions of manufactured products and equipment, there is a substantial danger of mechanical failures leading to severe consequences such as death or disability, and economic and material loss. A part or assembly is considered to have failed under three conditions :

(a) when it becomes completely inoperable,

(b) when it is still operable but is no longer able to perform its intended function satisfactorily due to a shift from its permissible limits, and/or

(c) when serious deterioration has made it unreliable or unsafe for

continued use, thus necessitating its immediate removal from service for repair or replacement.

There are a variety of factors which leads to the failure of the product. They include many aspects of design, material selection, fabrication and processing, inspection and quality control, maintenance and unanticipated exposure to overload or normal mechanical or chemical damage in service.

1.2 CLASSIFICATION AND CAUSES OF FAILURE

The factors responsible for failure may be grouped as

(i) external factors,

(ii) internal factors, and

(iii) initial quality factors.

(i) External Factors

These factors are originated from the external sources of the system and are extrinsic in character. They represents the environmental conditions such as speed, temperature, pressure, corrosive media etc., under which the machine or equipment is operating. The occurrence rate of the failure depends on the severeness of the environmental conditions. The random failure is normally caused by the external factors.

(ii) Internal Factors

These factors are due to the internal causes that takes place within the system. These factors are significant in the initial failure due to the inherent defects of the system such as faulty design, manufacture or assembly and in the final phase known as the wear-out failure, which occurs when the system wears out.

(iii) Initial Quality Factors

These factors occurs at the beginning of the operation (i.e., initial damage at time t=0). This includes the defects such as dimensional inaccuracies in manufactured products, inherent variability of material properties combined with faulty production processes, assembly, and improper quality control leading to considerable variation at the beginning of the operation.

1.3 MODELS OF DAMAGE PROCESSES

The life of the component or a system is reduced by two types of failure namely gradual failure and sudden or instantaneous failure. Most of the component failures are caused by various damage processes occuring in the system which leads to the gradual decline in the initial efficiency of the component, which in turn leads to a component failure when the accumulated damage reaches a critical level. Damage or failure of components result from irreversible material degradation processes such as wear, corrosion, creep, fouling, fatigue, diffusion, biological attack, seasonal fluctuations in

temperatures redistribution of internal stresses etc. The life of the component is terminated when the damage D(t) reaches or exceeds a limiting value which is the critical damage level D_l i.e., failure occurs when $D(t) \geq D_l$.

When we view the occurrence of irreversible damage processes, we find a remarkable degree of similarity in their response and it is also possible to distinguish a certain type of relationship as plausible models for the damage function D(t), where D(t) represents a certain manifestation of damage at time t. The specific type of manifestation representing the damage depends upon the underlying processes such as in the case of ***wear***, D(t) represents material loss, volume or depth of wear, in ***pitting corrosion*** it represents the depth of the pit, in ***stress cracking corrosion*** it represents crack length, in ***oxidation*** it represents the thickness of the film, in ***creep*** it is the magnitude of the strain. Typical examples of damage functions (i.e., the models of damage) are given in Fig. 1.1. The damage models are briefly mentioned here [1]:

(a) The combined affect of the rate of all factors affecting the given damage process is such that a linear relationship as shown in Fig. 1.1a. is observed.

(b) The damage may not occur for some period t_o, but after which it may cause rapid failure of the component. This is due to the accumulation of the initial factors and high cycle fatigue is an example of it. [Fig. 1.1b].

(c) The rate of damage during the initial period of operation (also

known as running-in period) often decreases with time until it reaches a steady state value. For example in the case of wear, this happens because of the changes in the irregularities on the surfaces of rubbing parts. [Fig. 1.1c]. In this type of damage process various factors contribute in such a way that the damage intensity gradually decline.

(d) In the case of some types of corrosion or fatigue processes, factors causing the damage gradually intensify and the rate of damage increases at a faster rate after the initiation of the process [Fig. 1.1d].

(e) Sometimes due to the sudden and sharp fluctuations in operating conditions .the process causing the damage remains unstable in nature [Fig. 1.1e].

(f) Damage of most of the components usually proceeds in several stages as shown in Fig. 1.1f. Wear and creep are the examples of this type.

(g) Deformation of a component as a result of redistribution of internal stresses first occurs at a high rate and then gradually slow down [Fig. 1.1g].

1.4 DETERMINISTIC REPRESENTATION OF DAMAGE MODELS

From the last section, it can be seen that the damage process is a certain function of time i.e.,

$$D(t) = \varphi(t) = \varphi\,(t{:}\varepsilon_i, \varepsilon_e, \varepsilon_o) \tag{1.1}$$

The different damage processes follow various rate laws of damage which are generally treated in literature as deterministic functions inspite of the significant variability within their outcomes. Table 1.1 lists a variety of damage kinetic models with appropriate references as proposed by various researchers in different areas of material degradation. The different damage laws presented in the literature to characterize damage function D(t) as a deterministic function of time are the following [2,3,4,5,6]:

$$D(t) = D_i + rt \tag{1.2}$$

$$D(t) = D_i + r \ln t \tag{1.3}$$

$$D(t) = D_i + rt^n \tag{1.4}$$

$$D(t) = D_i t^B \tag{1.5}$$

$$D(t) = D_{max}(1 - e^{-\lambda t}) \tag{1.6}$$

where D_i, r, B, λ, and n are treated as deterministic (fixed) parameters.

1.5 STOCHASTIC NATURE OF DAMAGE PROCESSES

The external and internal factors, in general, show significant fluctuations or perturbations around their nominal values. These perturbations are reflected in the average value and the scatter of the damage process. The variations in the initial quality factors determine the average and dispersion of the initial level of material damage. Thus the damage process in reality represents a ***stochastic phenomenon*** and need to be modelled by using the theory of probability.

For example consider, the life of a machine or its elements depending upon the rate of damage process and the limiting conditions of the machine or the system. The rate of damage process (for example wear) dD(t)/dt is a function of several independent variables :

$$\frac{dD(t)}{dt} = \dot{\varphi}\left[\varepsilon_e, \varepsilon_i, \varepsilon_o, t\right] \tag{1.7}$$

where

$\dot{\varphi}\left[\varepsilon_e, \varepsilon_i, \varepsilon_o, t\right] = d\varphi\left[\varepsilon_e, \varepsilon_i, \varepsilon_o, t\right]/dt$

ε_i = set of internal factors causing damage to the system

ε_e = set of external factors causing damage to the system

ε_o = set of initial quality factors at time $t=0$.

t = operating time

From eq (1.7) a general form of damage function can be written as

$$D(t) = \int_0^t \dot{\varphi}\left[\varepsilon_o, \varepsilon_i, \varepsilon_e, \tau\right] d\tau \tag{1.8}$$

When the machine is in the working condition there will be many variations and fluctuations in the external factors (ε_e) such as loads (P), velocities (V), method of lubrication, temperatures and the degree of contamination of the friction surfaces etc. Variability in the manufacturing or assembling will result into variability in the initial quality of the product (ε_o) where as the inherent variabilities of material characteristics and properties will result into variability in the in the internal factors (ε_i) of the system. Even though some of these

variables such as pressure, velocity and initial quality can be controlled at a fixed level without fluctuations (i.e., deterministic quantities), it is extremely difficult to have control at a desired level on all the other factors. Since most of the input variable ε_i, ε_e, ε_o are in general random in nature, the damage function in real life represents a stochastic phenomenon. The various types of damage functions in Fig. 1.1 represents merely a single realization of each specific random process. When several machine parts are tested and damage is monitored as a function of time, a set of realizations are observed, leading to a random phenomenon as shown in Fig. 1.2, which is mathematically expressed as

$$D(t) = D[\varepsilon_o, \varepsilon_i, \varepsilon_e, t] \qquad t \in T \qquad (1.9)$$

Each curve in this set of realizations of damage process has a given probability of occurrence.

1.6 PROBABILISTIC REPRESENTATION OF DAMAGE MODELS

As discussed in the previous section that the damage process is a stochastic or random phenomenon with respect to time, all the models can be mathematically represented by a set of random realizations in time (T) and space D(t) The real life or field data examples of various damage processes are shown in Figs. 1.3 to 1.6, which reinforce the concept of viewing the damage as a stochastic phenomena. In a most general way the damage can be represented by the following random functions of time which are the stochastic counterparts of eq (1.2) to (1.6)

$$\text{(i)}\ D(t) = D_i + \varphi(t) \qquad t \in T \qquad (1.10)$$

where

$$\varphi(t) = rt \qquad t \in T \qquad (1.11)$$

$$\varphi(t) = r \ln t \qquad t \in T \qquad (1.12)$$

$$\varphi(t) = rt^n \qquad t \in T \qquad (1.13)$$

$$\text{(ii) } D(t) = D_i t^B \qquad t \in T \qquad (1.14)$$

$$\text{(iii) } D(t) = D_{max}\,(1 - e^{-\lambda t}) \qquad t \in T \qquad (1.15)$$

where D_i, B, D_{max}, r are random quantities λ, n are fixed quantities.

Since D_i, B, D_{max}, r are random variables, $D(t)$ will also become random in nature. The random variables D_i, B, D_{max}, and r can be hypothesized to have certain distribution which can be validated from experimental data. Corresponding to a critical limit of damage D_l, distribution of time to failure T can be determined from the damage growth laws, and the reliable life of the material processes can be assessed from the corresponding reliability function. The relationship between distribution of damage at some time t, and the distribution of time to failure corresponding to a critical damage D_l is illustrated in Fig. 1.2. Before we explore this approach in more detail and develop specific models of time to failure distribution for above mentioned stochastic damage models, it is necessary to review the fundamentals of reliability theory and empirical approach of analysing the time to failure data to represent it by some well known reliability models.

1.7 FUNDAMENTALS OF RELIABILITY ANALYSIS

Let **T** be the random variable denoting the time to failure of the part subjected to a consistent criterion of failure. If m identical parts are put in operation at some time t=0, and operated upto failure then in general all of them will experience a different time to failure. These m observations of time to failure ($t_1, t_2, t_3, \ldots\ldots t_m$) represents a set of realizations or an outcome of the random variable **T.** Basically there are two approaches in characterizing a random variable :

(a) By developing certain indicators of central tendency and scatter of the random variable.

(b) By completely characterizing the random variable by an appropriate probability distribution.

***Main indicators of random variable life* T :**

The main indicators of random variable **T** are :

1. Mean life $\overline{T}$, [E(t), $\mu(T)$, μ]
2. Median life T_m, [C]
3. Standard deviation of life $\sigma(T)$ or variance of life $\sigma^2(T)$. [$\sigma(T)$ has the same units as **T**]
4. Coefficient of life variation or coefficient of variation $K = \sigma(T)/\overline{T}$

An illustrative example is given below to highlight the calculation procedure for developing these indicators.

Example: Time to failure data for a machine part is recorded as 67, 120, 130, 220, 290 hours. Find the mean time to failure, median life, standard deviation and coefficient of variation of the part.

Mean Time to Failure or average life $\bar{T}$

$$\bar{T} = \frac{t_1 + t_2 + t_3 + \ldots\ldots + t_k + \ldots\ldots\ldots + t_m}{m} = \frac{\sum_{k=1}^{m} t_k}{m}$$

$$\bar{T} = \frac{67 + 120 + 130 + 220 + 290}{5} = 165 \text{ hrs}$$

Median life T_m is the middle value of the ordered data i.e., T_m = 130 hrs.

Standard Deviation of Time to Failure $\sigma(T)$ is

$$\sigma(T) = \sqrt{\frac{(t_1 - T)^2 + (t_2 - T)^2 + \ldots\ldots\ldots\ldots + (t_m - T)^2}{m\text{-}1}}$$

$$\sigma(T) = \sqrt{\frac{(67-165)^2 + (120-165)^2 + (130-165)^2 + (220-165)^2 + (290-165)^2}{5\text{-}1}}$$

$$= 88.74 \text{ hrs}$$

Coefficient of variation, K is the non-dimensional measure of the dispersion or scatter in data, and for this case

$$K = \sigma(T)/\bar{T} = \frac{88.74}{165} = 0.54$$

Complete characterization of the random variable life **T :**

Complete characterization of the random variable **T** can be done by any of the following probability functions :

(a) Probability density function PDF = f(t) = f(t; θ_1,θ_2)

(b) Cumulative distribution function CDF = F(t) = F(t; θ_1,θ_2)

(c) Reliability function RF = R(t) = R(t; θ_1,θ_2)

(d) Hazard function HF = h(t) = h(t; θ_1,θ_2)

θ_1,θ_2 are parameters of these functions, in which one of them is usually related to mean life (or median life) and the other is either linked with σ or K.

The probability density function, f(t) is defined as the function such that f(t) Δt is the probability that the random variable **T** lies between t and [t + Δt] or the failure takes place at a time between t and [t + Δt].

$$f(t)\Delta t = P[t \leq T \leq t + \Delta t] \tag{1.16}$$

The cumulative distribution function, F(t) is defined as the probability that the component will fail before time T, i.e.,

$$F(t) = P[T < t] \qquad t \geq 0 \tag{1.17}$$

$$= \int_0^t f(t)\, dt \tag{1.18}$$

The reliability function R(t) is defined as the probability that the component will perform its intended function beyond some time t, i.e.,

$$R(t) = P[T > t] = 1 - P[T < t] = 1 - F(t) \tag{1.19}$$

Reliability is also known as the probability of survival.

The hazard function is defined as the function such that h(t) Δt represent the probability that the part will fail at some time [t + Δt], given that it has not

yet failed at $T = t$.

$$h(t)\Delta t = P[T < t + \Delta t \mid T > t] = \frac{P[t < t + \Delta t]}{P[T > t]} = \frac{f(t)\Delta t}{R(t)} \qquad (1.20)$$

The link between hazard function h(t), reliability function R(t), and probability density function f(t) is given by

$$h(t) = \frac{f(t)}{R(t)} = -\frac{dR(t)}{R(t)dt} \qquad (1.21)$$

Thus knowing any one of the above functions other functions can be found by using eq (1.21) which can also be expressed as

$$R(t) = \exp\left[-\int_0^t h(t)dt\right] \qquad (1.22)$$

Since T is measured in time units and R(t) being probability is a dimensionless number, therefore the other related functions will have the following units

$$f(t) = -\frac{dR(t)}{dt} \text{ (1/time) units}$$

$$h(t) = -\frac{dR(t)}{R(t)dt} \text{ (1/time) units.}$$

Influence of coefficient of variation on the nature of the probability density function :

Since coefficient of variation of life K plays a dominant role in reliability analysis, it is worth while to mention its influence on the possible shape of the distribution.

(a) If data has no uncertainty around its mean value, then $\sigma(T)=0$ which means $K=0/\bar{T}=0$, which indicates that the data is purely deterministic. (Fig. 1.7a)

(b) If data has small scatter, for example $\sigma(T)=0.05\bar{T}$ which means $K=0.05$, then the distribution of data will be as shown in Fig. 1.7b (Narrow peaked distribution).

(c) If the data has a moderate scatter for example $\sigma(T)=0.30\bar{T}$ which means $K=0.30$, then the corresponding distribution will be such as shown in Fig. 1.7c (Broad peaked distribution)

(d) If the data has relatively large scatter, for example $\sigma(T)=\bar{T}$ which means $K=1$, then the distribution will become as shown in Fig. 1.7d (Exponential distribution with peak at time $t=0$).

Analysis of time to failure data for fitting the reliability models :

Some well known reliability models often used in life analysis are

1. Normal

$$R(t) = \Phi\left[\frac{t-\mu}{\sigma}\right] \qquad -\infty < t < \infty,\ \mu > 0,\ \sigma > 0 \tag{1.23}$$

2. Log normal

$$R(t) = \Phi\left[\frac{\ln t - \mu_1}{\sigma_1}\right] \qquad -\infty < t < \infty,\ \mu_1 > 0,\ \sigma_1 > 0 \tag{1.24}$$

3. Weibull

$$R(t) = \exp\left[-(t/\eta)^{\gamma}\right] \qquad \eta > 0,\ \gamma > 0 \tag{1.25}$$

To illustrate the methodology of analysing time to failure data and empirically fitting the appropriate distribution an illustrative example is presented for the case of the weibull model.

Example : Weibull Analysis of time to failure data in hours

[120, 295, 130, 220, 67]

Step 1 : Rank the data $t_1 < t_2 < t_3 ... < t_i < ....t_m$

Step 2 : Calculate the plotting position of estimated CDF $\hat{F}(t_i)$ by using $\hat{F}(t_i) = \frac{i}{(m+1)}$ [See the Table below].

Step 3 : Plot $\hat{F}(t_i)$ versus t_i on an appropriate probability paper [Refer Fig. 1.8, Weibull probability paper in this case].

Step 4 : Estimate the parameters of the model θ_1, θ_2. (η and γ in this case).

Rank i	Time to failure t_i	$\hat{F}(t_i) = \frac{i}{(m+1)}$
1	67	0.166
2	120	0.330
3	130	0.500
4	220	0.666
5	295	0.833

Concept of Reliable Life and its Utilization :

Life corresponding to a given risk of failure (= 1 - probability of survival) is called ***reliable life.*** Suppose we have to operate a device with a reliability of 99% or (0.99), then the corresponding reliable life $t_{0.01}$ will be a solution of $R(t_{0.01}) = 0.99$, where $t_{0.01}$ indicates that the risk of failure associated with this life is 1 - 0.99 = 0.01. Physically it means, if 100 such parts are put into operation at some time t=0, then at a time location $t_{0.01}$, only one part would have been failed and 99 parts would still be functioning.

The knowledge of reliable life (or reliability model) can be used in a number of decision making processes. Some of them are

- -- Scheduling of part replacements.
- -- Selection of optimal maintenance or replacement strategies.
- -- Calculating the type and quantity of spare parts needed in a given planning horizon.
- -- Economic forecasting based on projected part replacements and maintenance.
- -- Comparative evaluation of two similar products made by different manufacturers.
- -- For improvement in the performance of existing design by changing the operating conditions.

In many cases time to failure data is directly available, then a set of

reliability models can be fitted empirically, (analytically or graphically) and the best one is selected and its parameters can be determined from the analysis. The selected reliability model can be used for the above mentioned purposes.

Often we have a situation where enough time to failure data is not directly available. In such cases the damage process which lead to the failure can be generated (or simulated under accelerated conditions) in the laboratory or by continuously monitoring the damage in actual operating environment. These damage processes behave ***stochastic*** in nature and their ***average*** and ***dispersion*** characteristics can be utilized to determine the reliable life (reliability) models. The rest of this chapter will be devoted to develop various reliability models directly from the material damage model discussed in section 1.6. This development will provide a ***generalized systems approach*** (***a global mathematical framework***) in modelling a variety of analog damage processes and their corresponding time to failure distributions (reliability models).

Using the above systems approach (or the mathematical framework) the following damage processes and their statistical characteristics, as well as their resulting time to failure distributions are analysed in depth in the forthcoming chapters i.e.,

(a) Wear [Chapter 2]

(b) Corrosion and Oxidation [Chapter 3]

(c) Fouling [Chapter 4]

(d) Creep and Rupture life [Chapter 5].

1.8 GENERALIZED DAMAGE MODEL $D(t) = D_i + rt^n$

Consider a most generalized model of non-linear, non-stationary damage process.

$$D(t) = D_i + r\,\varphi(t) \qquad t \in T$$

where

D_i = initial level of damage at $t = 0$

$r = \dfrac{dD(t)}{d\varphi(t)}$ = rate of damage with respect to function $\varphi(t)$

If $\varphi(t) = t^n$ then the damage process is represented as

$$D(t) = D_i + rt^n \qquad t \in T \qquad (1.26)$$

where n is a fixed quantity

The life of the component or part is terminated when the damage D(t) exceeds or reaches a critical level D_l, thus the random variable T defining the component life is given by

$$T = \left[\frac{D_l - D_i}{r}\right]^{1/n} \qquad (1.27)$$

and its realizations are denoted by t. D_i and r are assumed to be statistically independent and normally distributed with $D_i \sim N\left[\mu(D_i), \sigma^2(D_i)\right]$ and $r \sim N\left[\mu(r), \sigma^2(r)\right]$ respectively.Both initial damage D_i and the rate of damage r which means the condition $P[D_i < 0] = 0$ and $P[r < 0] = 0$ must be satisfied. For normally distributed variates this condition is satisfied if the coefficient of

variation of distribution is less than 0.3. (i.e., $\sigma(\mathbf{r})/\mu(\mathbf{r})$ and $\sigma(\mathbf{D_i})/\mu(\mathbf{D_i}) \leq 0.3$)

As a consequence of these assumptions the random function **D**(t) in eq (1.26) will also be normally distributed with mean $\mu[\mathbf{D}(t)]$ and standard deviation $\sigma[\mathbf{D}(t)]$ where

$$\mu[\mathbf{D}(t)] = E[\mathbf{D_i} + \mathbf{r}t^n] = E[\mathbf{D_i}] + t^n E[\mathbf{r}]$$
$$= \mu(\mathbf{D_i}) + \mu(\mathbf{r})t^n \qquad (1.28)$$

$$\sigma^2[\mathbf{D}(t)] = V[\mathbf{D_i} + \mathbf{r}t^n] = V[\mathbf{D_i}] + t^{2n} V[\mathbf{r}]$$
$$= \sigma^2(\mathbf{D_i}) + \sigma^2(\mathbf{r})t^{2n} \qquad (1.29)$$

The failure of the component subjected to the non-linear damage process given in eq (1.26) is defined when **D**(t) reaches D_l, then the probability of the event $(\mathbf{T} > t)$ is equivalent to the probability of the event $[\mathbf{D}(t) < D_l]$, and is given by

$$R(t) = P(\mathbf{T} > t) = P[\mathbf{D}(t) < D_l]$$
$$= \Phi\left\{\frac{D_l - \mu[\mathbf{D}(t)]}{\sigma[\mathbf{D}(t)]}\right\} \qquad (1.30)$$

where R(t) is the reliability of the component and $\Phi(z)$ is the Gaussian function given by

$$\Phi(z) = \frac{1}{\sqrt{2\pi}} \int_{-\infty}^{z} e^{-t^2/2}\, dt$$

Substituting eqs (1.28) and (1.29) into (1.30) we get [5]

$$R(t) = 1 - \Phi\left\{\frac{t^n - c}{\sqrt{\alpha\, t^{2n} + \beta}}\right\} \qquad -\infty < t < \infty, c > 0, \alpha > 0, \beta > 0 \qquad (1.31)$$

where

$$c = [D_1 - E(D_i)] / E(r) \tag{1.32}$$

$$\alpha = V(r) / [E(r)]^2 \tag{1.33}$$

$$\beta = V(D_i) / [E(r)]^2 \tag{1.34}$$

The probability density function is given by

$$f(t) = \frac{1}{\sqrt{2\pi}} \frac{nt^{n-1}(\beta + c\alpha t^n)}{(\beta + \alpha t^{2n})^{3/2}} \exp\left\{ \frac{-1}{2}\left[\frac{t^n - c}{\sqrt{\alpha t^{2n} + \beta}} \right]^2 \right\} \tag{1.35}$$

and hazard function is

$$h(t) = \frac{nt^{n-1}}{\sqrt{2\pi}} \frac{(\beta + c\alpha t^n)}{(\beta + \alpha t^{2n})^{3/2}} \frac{\exp\left\{ \frac{-1}{2}\left[\frac{t^n - c}{\sqrt{\alpha t^{2n} + \beta}} \right]^2 \right\}}{1 - \Phi\left\{ \frac{t^n - c}{\sqrt{\alpha t^{2n} + \beta}} \right\}} \tag{1.36}$$

Some special cases can be deduced from the above generalized model which are commonly observed in a number of material damage processes.

1.8.1 Three Parameter Bernstein Model

when $\alpha \neq 0$; $\beta \neq 0$; $n = 1$.

The generalized damage model will have sample functions [$D(t) = D_i + rt$] as shown in Fig. 1.9. The various probability functions for this model are obtained by letting $n = 1$, in eqs (1.31), (1.35) and (1.36) respectively.

$$R(t;\alpha,\beta,c) = 1-\Phi\left\{\frac{t-c}{\sqrt{\alpha t^2+\beta}}\right\} \qquad t>0,\ c>0,\ \alpha>0,\ \beta>0 \qquad (1.37)$$

$$f(t;\alpha,\beta,c) = \frac{1}{\sqrt{2\pi}}\frac{(\beta+c\alpha t)}{(\beta+\alpha t^2)^{3/2}}\exp\left\{\frac{-1}{2}\left[\frac{t-c}{\sqrt{\alpha t^2+\beta}}\right]^2\right\} \qquad (1.38)$$

$$h(t;\alpha,\beta,c) = \frac{1}{\sqrt{2\pi}}\frac{(\beta+c\alpha t)}{(\beta+\alpha t^2)^{3/2}}\frac{\exp\left\{\frac{-1}{2}\left[\frac{t-c}{\sqrt{\alpha t^2+\beta}}\right]^2\right\}}{1-\Phi\left\{\frac{t-c}{\sqrt{\alpha t^2+\beta}}\right\}} \qquad (1.39)$$

This model was earlier proposed by Gertsbakh and Kordonsky [7] and was discussed in detail by Ahmad and Sheikh [8]

1.8.2 Normal Model

when $\alpha = 0$; $\beta \neq 0$; $n=1$.

The random function characterizing this type of model is shown in Fig. 1.10. and is expressed mathematically as $D(t) = D_i + rt$. When $V(r)=0$, then $\alpha=0$ which means that the rate of the damage remains constant. This condition reduces the eqs (1.37), (1.38) and (1.39) to the following :

$$R(t;\beta,c) = 1-\Phi\left\{\frac{t-c}{\sqrt{\beta}}\right\} \qquad t>0,\ c>0,\ \alpha>0,\ \beta>0 \qquad (1.40)$$

$$f(t;\beta,c) = \frac{1}{\sqrt{2\pi\beta}} \exp\left\{\frac{-1}{2}\left[\frac{t-c}{\sqrt{\beta}}\right]^2\right\} \tag{1.41}$$

$$h(t;\beta,c) = \frac{1}{\sqrt{2\pi\beta}} \frac{\exp\left\{\frac{-1}{2}\left[\frac{t-c}{\sqrt{\beta}}\right]^2\right\}}{1-\Phi\left\{\frac{t-c}{\sqrt{\beta}}\right\}} \tag{1.42}$$

These probability functions represent normal distribution which is a well known reliability model.

1.8.2.1 Parameter Estimation for Normal Model

From a set of m realizations of damage process :

If each realization is fitted with a straight line then the j^{th} realization will be $D_j(t) = D_{i,j} + rt$, in other words this represent the damage of the j^{th} component and if m such realizations are known then the parameters c and β can be estimated from the following equations [2] :

$$\hat{c} = \frac{\left[D_1 - \sum_{j=1}^{m} \frac{D_{i,j}}{m}\right]}{r} \tag{1.43}$$

$$\hat{\beta} = \frac{\sum_{j=1}^{m}\left[D_{i,j} - \sum_{j=1}^{m} \frac{D_{i,j}}{m}\right]^2/(m-1)}{r^2} \tag{1.44}$$

Maximum likelihood estimates of time to failure data :

If directly time to failure data , $(t_1,t_2,.....,t_M)$ are given, then the maximum likelihood estimates of the parameters of the normal model which are well known are given by

$$\hat{c} = \frac{1}{M}\sum_{j=1}^{M} t_j \tag{1.45}$$

$$\hat{\beta} = \frac{\left[\sum_{j=1}^{M}(t_j - c)^2\right]/M}{\left\{\left(\frac{1}{M}\right)\left[\sum_{j=1}^{M} t_j\right]\right\}^2} \tag{1.46}$$

1.8.3 Inverted Normal Model

when $\alpha \neq 0$; $\beta = 0$; $n=1$.

In this case the initial damage is deterministic i.e., $V(D_i) = 0$ which makes $\beta = 0$ and the rate of damage is a random variable. The random function which characterizes this type of damage is shown in Fig. 1.11. which can be mathematically expressed as $D(t) = D_i + rt$. Since **r** is normally distributed, therefore **T** will be inverted normally distributed or $\frac{1}{T}$ will be normally distributed. This distribution of time to failure is also known as $\alpha-$ distribution. The various probability functions of this model are [2,8]

$$R(t;\alpha,c) = 1 - \Phi\left\{\frac{t-c}{\sqrt{\alpha}t}\right\} \qquad t>0,\ c>0,\ \alpha>0 \tag{1.47}$$

$$f(t;\alpha,c) = \frac{1}{\sqrt{2\pi}}\frac{c}{\sqrt{\alpha}\,t^2}\exp\left\{\frac{-1}{2}\left[\frac{t-c}{\sqrt{\alpha}\,t}\right]^2\right\} \tag{1.48}$$

$$h(t;\alpha,c) = \frac{1}{\sqrt{2\pi}}\frac{c}{\sqrt{\alpha}t^2}\frac{\exp\left\{\frac{-1}{2}\left[\frac{t-c}{\sqrt{\alpha}\,t}\right]^2\right\}}{1-\Phi\left\{\frac{t-c}{\sqrt{\alpha}\,t}\right\}} \tag{1.49}$$

1.8.3.1 Parameter Estimation for Inverted Normal Model

From a set of m realizations of damage process :

In this case the equation, $D_j(t) = D_i + r_j t$, characterizes the damage of the j^{th} component and if m such realizations are available then [2,8]

$$\hat{\alpha} = \frac{\sum_{j=1}^{m}\left[r_j - \sum_{i=j}^{m}\frac{r_j}{m}\right]^2 / (m-1)}{\left[\sum_{j=1}^{m}\frac{r_j}{m}\right]^2} \tag{1.50}$$

$$\hat{c} = \frac{[D_1 - D_j]}{\left[\sum_{j=1}^{m}\frac{r_j}{m}\right]} \tag{1.51}$$

Maximum likelihood estimates of time to failure data :

The maximum likelihood estimates of the parameters of the inverted normal model have been developed by Ahmad and Sheikh [8] for both the complete family of distribution ($\sqrt{\alpha} \leq 0.35$) and for incomplete (truncated) family of distribution ($\sqrt{\alpha} \geq 0.35$). The resulting equations for estimating the parameters from a set of M observations on component life (i.e., $t_1, t_2, \ldots\ldots, t_M$) are presented here [8] :

$$\hat{c} = \frac{1}{\left[\left(\frac{1}{M}\right)\sum_{j=1}^{M}\frac{1}{t_j}\right]} \tag{1.52}$$

$$\hat{\alpha} = \left[\left(\frac{1}{M}\right)\sum_{j=1}^{M}\left(\frac{1}{t_j} - \frac{1}{\hat{c}}\right)^2\right]c^2 \tag{1.53}$$

Eqs (1.52) and (1.53) correspond to the case of complete family of distribution, for incomplete (truncated) family of distribution the parameters will be estimated from the following equations [8]

$$\hat{c}\, h^{-1} = 1 + R_\alpha \sqrt{\alpha} \tag{1.54}$$

$$K(\hat{\alpha}) = S\, h^2 \tag{1.55}$$

where $\frac{1}{h} = \frac{1}{M}\sum_{j=1}^{M}\left[\frac{1}{t_j}\right]$

$$R_\alpha = \left(\frac{1}{\sqrt{\hat{\alpha}}}\right) / \Phi\left(\frac{1}{\sqrt{\hat{\alpha}}}\right)$$

$\Phi\left(\frac{1}{\sqrt{\hat{\alpha}}}\right)$ = probability density function of normal model with argument

$(1/\sqrt{\alpha})$ and

$$S = \frac{1}{M}\sum_{j=1}^{M}\left[\frac{1}{t_j^2}\right]$$

1.9 DAMAGE MODEL $D(t) = D_i t^B$

Some of the material damage processes follows a non-linear deterioration of material. This type of damage function is shown in Fig. 1.12.

$$D(t) = D_i t^B \qquad t \in T \qquad (1.56)$$

where

D_i = initial value of damage at $t = 1$

$$B = \frac{dD(t)/D(t)}{dt/t}$$

Equation (1.52) can be rewritten as

$$\ln D(t) = \ln D_i + B \ln t \qquad t \in T \qquad (1.57)$$

Both $\ln D_i$ and B are assumed to be statistically independent and normally distributed with mean $\mu_{lnD_i} = E[\ln D_i]$, $\mu_B = E[B]$ and variance $\sigma^2_{lnD_i} = V[\ln D_i]$, $\sigma^2_B = V[B]$, respectively. Also the condition $P(\ln D_i < 0) = 0$ and $P(B < 0) = 0$, must be satisfied since both the initial damage and rate of damage are always positive quantities. Therefore $\ln D(t)$ will also will be normally distributed with

$$E[\ln D(t)] = E[\ln D(t)] + E[B] \ln t \tag{1.58}$$

$$V[\ln D(t)] = V[\ln D(t)] + V[B \ln t] \tag{1.59}$$

If the damage level criterion is D_1, then the following relationship holds :

$$P[D(t) < D_1] = P[\ln \{D(t)\} < \ln D_1]$$

$$= P(\ln T > \ln t) = P(T > t) = R(t) \tag{1.60}$$

Here T is the random variable characterizing the life which is expressed as

$$\ln T = \frac{\ln D_1 - \ln D_i}{B} \qquad D_i \in D(t) \tag{1.61}$$

Therefore the reliability function can be written as

$$R(t; \alpha_1, \beta_1, c_1) = 1 - \Phi\left\{\frac{\ln t - c_1}{\sqrt{\alpha_1 (\ln t)^2 + \beta_1}}\right\} \quad t > 1, c_1 > 0, \alpha_1 > 0, \beta_1 > 0 \tag{1.62}$$

where

$$c_1 = [\ln D_1 - E(\ln D_i)] / E(B) \tag{1.63}$$

$$\alpha_1 = V(B) / [E(B)]^2 \tag{1.64}$$

$$\beta_1 = V(\ln D_i) / [E(B)]^2 \tag{1.65}$$

The probability density function is given by

$$f(t; \alpha_1, \beta_1, c_1) = \frac{1}{\sqrt{2\pi}\, t} \frac{(\beta_1 + c_1 \alpha_1 (\ln t))}{\left[\beta_1 + \alpha_1 (\ln t)^2\right]^{3/2}} \exp\left\{\frac{-1}{2}\left[\frac{\ln t - c_1}{\sqrt{\alpha_1 (\ln t)^2 + \beta_1}}\right]^2\right\}$$

(1.66)

and the hazard function is

$$h(t;\alpha_1, \beta_1, c_1) = \frac{1}{\sqrt{2\pi}t} \frac{(\beta_1 + c_1\alpha_1(\ln t))}{\left[\beta_1 + \alpha_1(\ln t)^2\right]^{3/2}} \frac{\exp\left\{\frac{-1}{2}\left[\frac{\ln t - c_1}{\sqrt{\alpha_1 (\ln t)^2 + \beta_1}}\right]\right\}}{1 - \Phi\left\{\frac{\ln t - c_1}{\sqrt{\alpha_1 (\ln t)^2 + \beta_1}}\right\}} \tag{1.67}$$

This model is known as three parameter Log Bernstein model [1].

1.9.1 Log-Normal distribution

when $\alpha_1 = 0$; $\beta_1 \neq 0$.

In this case when $V(\ln B) = 0$ which makes $\alpha_1 = 0$. $V(\ln B) = 0$ implies that B is a deterministic quantity i.e., the rate of change of $\ln D(t)$ is constant with respect to $\ln t$, and the corresponding damage function is represented by

$$D(t) = D_i t^B$$

$$\ln D(t) = \ln D_i + B \ln t \tag{1.68}$$

The various probability functions for this case are :

$$R(t; \beta_1, c_1) = 1 - \Phi\left\{\frac{\ln t - c_1}{\sqrt{\beta_1}}\right\} \qquad t > 1, c_1 > 0, \beta_1 > 0 \tag{1.69}$$

$$f(t;\beta_l, c_l) = \frac{1}{\sqrt{2\pi\beta_l t}} \exp\left\{\frac{-1}{2}\left[\frac{\ln t - c_l}{\sqrt{\beta_l}}\right]^2\right\} \tag{1.70}$$

$$h(t;\beta_l, c_l) = \frac{1}{\sqrt{2\pi\beta_l t}} \frac{\exp\left\{\frac{-1}{2}\left[\frac{t - c_l}{\sqrt{\beta_l}}\right]^2\right\}}{1 - \Phi\left\{\frac{\ln t - c_l}{\sqrt{\beta_l}}\right\}} \tag{1.71}$$

These probability functions represent the well known lognormal distribution model.

1.9.1.1 Parameter Estimation of Log Normal model

From a set of m realizations of damage process :

A least square curve of type $D_j(t) = D_{i,j}t^B$, is fitted to each of the realizations of the damage process and the parameters are estimated from the following equations [1] :

$$\hat{c}_l = \left[\ln D_l - \sum_{j=1}^{m}(\ln D_{i,j})/m\right] / B \tag{1.72}$$

$$\hat{\beta}_l = \frac{\sum_{j=1}^{m}\left[\ln D_{i,j} - \sum_{j=1}^{m}\ln\frac{D_{i,j}}{m}\right]^2 / (m-1)}{B^2} \tag{1.73}$$

where m is the total number of damage curves in the set of sample functions.

Maximum likelihood estimates of time to failure data :

Maximum likelihood estimates of the parameters can be obtained directly from the component failure data, [1] i.e.,

$$\hat{c}_1 = \frac{1}{M}\left[\sum_{j=1}^{M} \ln t_j\right] \tag{1.74}$$

$$\hat{\beta}_1 = \sqrt{\left[\sum_{j=1}^{M} (\ln t_j - c_1)\right] / (M-1)} \tag{1.75}$$

1.9.2 Inverted Log-Normal distribution

when $\alpha_1 \neq 0$; $\beta_1 = 0$.

In this model $V(\ln D_i)=0$ which makes $\beta_1=0$ i.e., the initial damage is a deterministic value. The corresponding damage function is $D(t) = D_i t^B$ or

$$\ln D(t) = \ln D_i + B \ln t \tag{1.76}$$

The distribution of time to failure corresponding to this type of damage model is known as inverted log-normal distribution and its various probability functions are

$$R(t; \alpha_1, c_1) = 1 - \Phi\left\{\frac{\ln t - c_1}{\sqrt{\alpha_1}(\ln t)}\right\} \qquad t>1, c_1>0, \alpha_1>0 \tag{1.77}$$

$$f(t; \alpha_1, c_1) = \frac{1}{\sqrt{2\pi}} \frac{c}{\sqrt{\alpha_1}(\ln t)^2 t} \exp\left\{\frac{-1}{2}\left[\frac{\ln t - c_1}{\sqrt{\alpha_1}\, t}\right]^2\right\} \tag{1.78}$$

$$h(t;\alpha_l, c_l) = \frac{1}{\sqrt{2\pi}} \frac{c_l}{\sqrt{\alpha_l}(\ln t)^2 t} \frac{\exp\left\{\frac{-1}{2}\left[\frac{\ln t - c_l}{\sqrt{\alpha_l} t}\right]^2\right\}}{1 - \Phi\left\{\frac{\ln t - c_l}{\sqrt{\alpha_l}(\ln t)}\right\}} \qquad (1.79)$$

1.9.2.1 Parameter Estimation of Inverted Log-Normal model

From a set of m realizations of damage process :

In this case the equation $D_j(t) = D_{i,j}t^B$, characterizes the damage of the j^{th} component and if m such realizations are available then

$$\hat{c}_l = \frac{[\ln D_l - \ln D_i]}{\sum_{j=1}^{m}(B_j / m)} \qquad (1.80)$$

$$\hat{\alpha}_l = \frac{\sum_{j=1}^{m}\left[B_j - \sum_{j=1}^{m}\frac{B_j}{m}\right]^2 / (m-1)}{\left[\sum_{j=1}^{m}\frac{B_j}{m}\right]^2} \qquad (1.81)$$

Maximum likelihood estimates of time to failure data :

The maximum likelihood estimates for a set of M observations are [1]

$$\hat{c}_l = \frac{1}{M}\left[\sum_{j=1}^{M}\ln t_j\right]^{-1} \qquad (1.82)$$

$$\hat{\alpha}_l = \left\{\frac{1}{M}\sum_{j=1}^{M}\left[1 - \frac{\hat{c}_l}{\ln t_j}\right]^2\right\} \qquad (1.83)$$

1.10 DAMAGE MODEL $D(t) = D_i + r \ln t$

In the most generalized model eq (1.10) if $\varphi(t) = \ln t$, then the damage process is represented as

$$D(t) = D_i + r\ln t \qquad t \in T \qquad (1.84)$$

where

D_i = initial level of damage at $t = 1$

$r = \dfrac{dD(t)}{d(\ln t)}$ = rate of damage with respect to $\ln t$.

The damage model will have sample functions as shown in Fig. 1.13. Eq (1.26) can be obtained from eq (1.57) by replacing $\ln D(t)$ and $\ln D_i$ by $D(t)$ and D_i respectively and the r in this case will represent the rate of change of damage $D(t)$ with respect to $\ln t$. The corresponding probability functions for this model are :

$$R(t; \alpha_1, \beta_1, c_1) = 1 - \Phi\left\{\frac{(\ln t) - c_1}{\sqrt{\alpha_1 (\ln t)^2 + \beta_1}}\right\} \quad t > 1, c_1 > 0, \alpha_1 > 0, \beta_1 > 0 \quad (1.85)$$

$$f(t; \alpha_1, \beta_1, c_1) = \frac{1}{\sqrt{2\pi}} \frac{(\beta_1 + c_1\alpha_1(\ln t))}{(\beta_1 + \alpha_1(\ln t)^2)^{3/2}} \exp\left\{\frac{-1}{2}\left[\frac{(\ln t) - c_1}{\sqrt{\alpha_1(\ln t)^2 + \beta_1}}\right]^2\right\}$$

(1.86)

$$h(t;\alpha_1, \beta_1, c_1) = \frac{1}{\sqrt{2\pi}} \frac{(\beta_1 + c_1\alpha_1(\ln t))}{(\beta_1 + \alpha_1(\ln t)^2)^{3/2}} \frac{\exp\left\{\frac{-1}{2}\left[\frac{(\ln t) - c_1}{\sqrt{\alpha_1 (\ln t)^2 + \beta_1}}\right]^2\right\}}{1 - \Phi\left\{\frac{(\ln t) - c_1}{\sqrt{\alpha_1 (\ln t)^2 + \beta_1}}\right\}} \tag{1.87}$$

This model is also known as Log Bernstein model.

Since eqs (1.85), (1.86), and (1.87) are identical in structure with eqs (1.62), (1.66) and (1.67), therefore two special cases will be lognormal [eqs (1.69) to (1.71)] when $V(\dot{r})=0$ i.e., $\beta_1=0$ and inverted lognormal [eqs (1.77) to (1.79)] when $V(D_i)=0$ i.e., $\alpha_1=0$.

1.10.1 Parameter Estimation

From a set of m realizations of damage process :

(1) Lognormal distribution

Each realization is represented by $D_j(t) = D_{i,j}(t) + r \ln t$ and the parameters are estimated from the following equations :

$$\hat{c}_1 = \frac{\left[D_1 - \sum_{j=1}^{m} \frac{D_{i,j}}{m}\right]}{r} \tag{1.88}$$

$$\hat{\beta}_1 = \frac{\sum_{j=1}^{m}\left[D_{i,j} - \sum_{j=1}^{m}\frac{D_{i,j}}{m}\right]^2/(m-1)}{r^2} \qquad (1.89)$$

(2) Inverted lognormal distribution

Each realization is represented by $D_j(t) = D_i(t) + r_j \ln t$ and the parameters are estimated from the following equations :

$$\hat{\alpha}_1 = \frac{\sum_{j=1}^{m}\left[r_j - \sum_{i=j}^{m}\frac{r_j}{m}\right]^2/(m-1)}{\left[\sum_{j=1}^{m}\frac{r_j}{m}\right]^2} \qquad (1.90)$$

$$\hat{c} = \frac{[D_i - D_j]}{\left[\sum_{j=1}^{m}\frac{r_j}{m}\right]} \qquad (1.91)$$

Maximum likelihood estimates of time to failure data :

The maximum likelihood estimates eqs (1.74) and (1.75) for lognormal and eqs (1.82) and (1.83) for inverted lognormal remain valid.

1.11 DAMAGE MODEL $\tilde{D}(t) = \tilde{D}(1) + \gamma \ln t$

Some of the material damage processes such as in the case of pitting corrosion, the damage D(t) observed at any time t, is extreme value distributed. The kinetics of such processes can often be expressed by the growth of some characteristic damage $\tilde{D}(t)$ as linear function of lnt. If the distribution of D(t) is

assumed as type-I extreme value then the following holds true

$$F[D(t)] = P[D(t) < D(t)] = \exp[-\exp\{-Y(t)\}] \qquad (1.92)$$

where

$Y(t)$ = reduced variate = $\alpha(t)\,[D(t) - \tilde{D}(t)]$

$D(t)$ = the deepest (or maximum) damage at time t, representing the realization of $D(t)$ at time t

$\tilde{D}(t)$ = is the characteristic value or most probable value of the damage at time t

$1/\alpha(t)$ = a measure of variance given as $\frac{\sqrt{6}}{\pi} \times \sigma(t)$, where $\sigma(t)$ is the standard deviation of the distribution at time t.

Let us consider the damage model varies with logarithmic time in a linear form as follows (Fig. 1.14)

$$\tilde{D}(t) = \tilde{D}(1) + r \ln t \qquad \ln t \in \ln T \qquad (1.93)$$

where

$\tilde{D}(1)$ is the characteristic initial extreme value distributed damage at $t = 1$

r is the slope of D(t) vs ln(t) which is a fixed quantity

For this model instead of actual realizations of the process, various quantiles of damage $D(t)$ (i.e., $D_q(t)$, where $P[\,D(t) \le D_q(t)\,] = q$ are plotted as a function of ln t, and each quantile has the same slope r. For any quantile of damage, the following probability statement holds true, [9]

$$P[\,D(t) \le D_q(t)\,] = q = P[\,T > t_q\,] \qquad (1.94)$$

$$F[D_q(t)] = R(t_{1-q}) = q \tag{1.95}$$

Mode value or characteristic damage $\tilde{D}(t)$ is also a quantile such that $q = 0.37$ or $P[\,D(t) \le \tilde{D}(t)\,] = 0.37$, and the corresponding reliability will also be $R(t_{1-q}) = 0.37$ or $F(t_{0.63}) = 1 - 0.37 = 0.63$. This relationship is shown in Fig. 1.15.

$$D(t) = \tilde{D}(1) + r \ln t$$

for $\tilde{D}(t) = D_l$

$$D_l = \tilde{D}(1) + r \ln t_{0.63}$$

$$= \tilde{D}(1) + r \ln\eta \tag{1.96}$$

where η is the characteristic life.

The reliability function is given by

$$R(t) = P[D(t) < D_l]$$

$$= \exp[-\exp\{-Y(t)\}]$$

$$= \exp[-\exp[-\alpha(t)[D_l - \tilde{D}(t)]]]$$

$$= \exp[-\exp[-\alpha(t)[\tilde{D}(1) + r\ln\eta - \tilde{D}(1) - r\ln t]]]$$

$$= \exp[-\exp[-\alpha(t)[-r(\ln t - \ln\eta)]]]$$

$$= \exp\left[-\exp\left[\alpha(t) r \left[\ln\left\{\frac{t}{\eta}\right\}\right]\right]\right]$$

$$= \exp\left[-\left\{\frac{t}{\eta}\right\}^{\alpha(t)r}\right]$$

If $\alpha(t)$ is constant, then $\alpha(t)r = \gamma$ is the shape parameter of the weibull distribution. Therefore the reliability function is

$$R(t) = \exp\left[-\left(\frac{t}{\eta}\right)^{\gamma}\right] \qquad t>1,\ \eta>1,\ \gamma>1 \tag{1.97}$$

The probability density function is given by

$$f(t) = \frac{\gamma}{\eta}\left(\frac{t}{\eta}\right)^{\gamma-1} \exp\left[-\left(\frac{t}{\eta}\right)^{\gamma}\right] \tag{1.98}$$

and hazard function is

$$h(t) = \frac{\gamma}{\eta}\left(\frac{t}{\eta}\right)^{\gamma-1} \tag{1.99}$$

where γ is the shape parameter and represents the scatter in the life, and η is scale parameter and represents the life corresponding $R(\eta) = 0.37$.

1.12 DAMAGE MODEL $D(t) = D_{max}(1 - e^{-\lambda t})$

Some of the material damage processes follow an asymptotic form of damage with respect to time which is shown in Fig. 1.15.

The damage process equation is given by

$$D(t) = D_{max}(1 - e^{-\lambda t}) \tag{1.100}$$

where

D_{max} is the random variable and

λ is the fixed quantity.

D_{max} is assumed to be statistically independent and normally distributed random variable with mean $\mu[D_{max}]$ and variance $V[D_{max}]$ $D_{max} \sim N[\mu(D_{max}), \sigma^2(D_{max})]$.

Again the component subjected to this type of damage is termed inoperable when the damage D(t) exceeds or reaches a critical damage level D_l, thus the corresponding random variable **T** defining the life of the component is given by

$$\frac{D_l}{D_{max}} = 1 - e^{-\lambda t}$$

$$e^{-\lambda t} = 1 - \frac{D_l}{D_{max}} = \frac{D_{max} - D_l}{D_{max}}$$

$$T = -\frac{1}{\lambda} \ln\left[\frac{D_{max} - D_l}{D_{max}}\right]$$

$$T = \frac{1}{\lambda} \ln\left[\frac{D_{max}}{D_{max} - D_l}\right] \qquad (1.101)$$

$$T_i = -\frac{1}{\lambda} \ln\left[1 - \frac{D_l}{D_{max,i}}\right]$$

where $D_{max,i} = (-2 \ln r_1)^{1/2} \cos(2\pi r_2)$

r_1 and r_2 are random numbers.

The distribution of **T** can be developed analytically or by Monte carlo simulation. Since the mathematical derivation of this distribution is quite complex, therefore in the present investigation the distribution of **T** was determined by using Monte carlo simulation technique, and it was demonstrated that the underlying reliability function also represents a Weibull model.

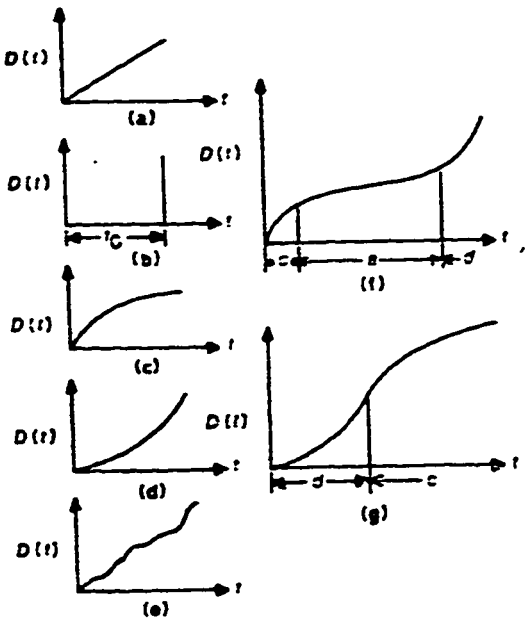

Fig. 1.1 Various plausible deterministic models of damage; $D(t)$ represents the degree of total damage at time t.

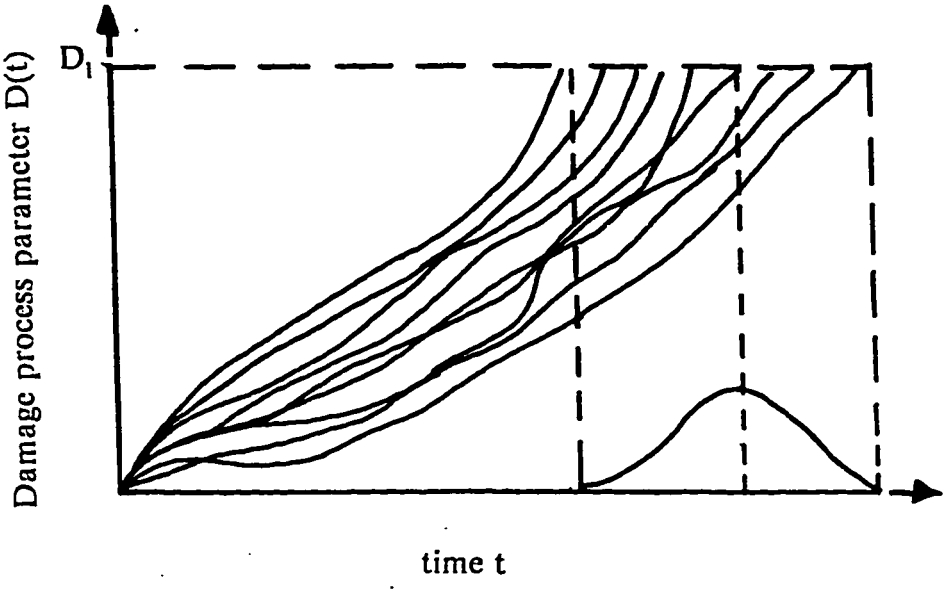

Fig. 1.2 A typical set of sample functions of a stochastic damage processes.

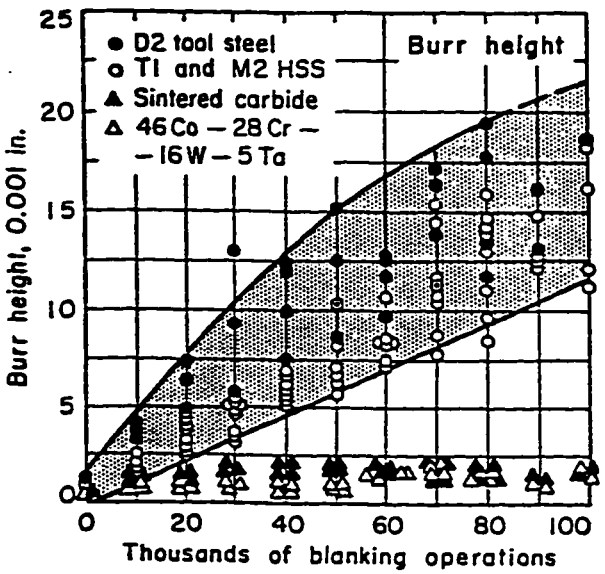

Fig. 1.3 Sample functions of the random process $D(t) = D_i + rt$ where D(t) represent the burr height as a function of die life [22].

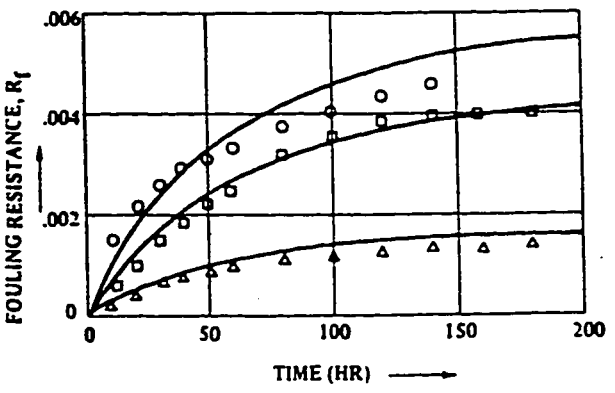

Fig. 1.4 Sample functions of random process represented by $D(t) = D_i + rlnt$ where D(t) is the fouling resistance as a function of time [53].

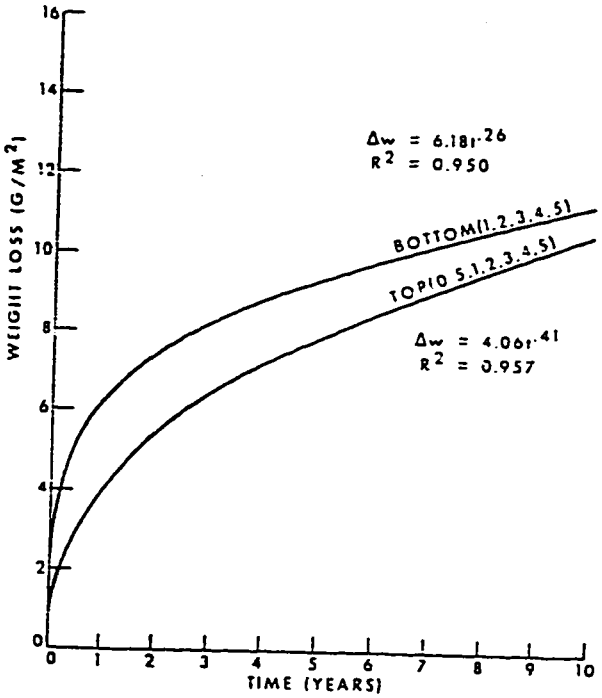

Fig. 1.5 Sample functions of random process of the type $D(t) = D_i t^B$ where D(t) is the weight loss as a function of time [49].

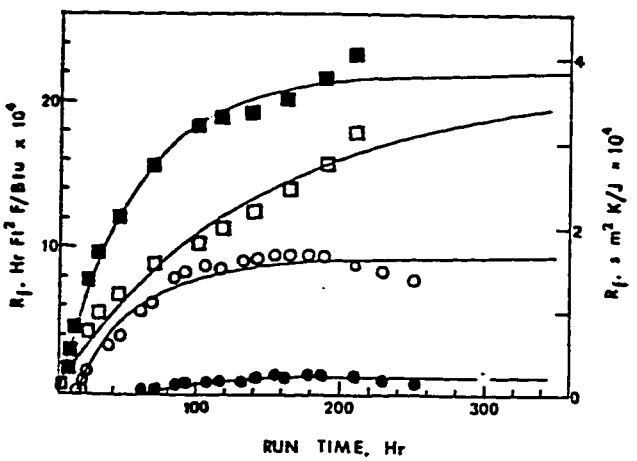

Fig. 1.6 Sample functions of represented by random process $D(t) = D_{max}(1 - e^{-\lambda t})$ where D(t) is the fouling resistance and λ is the time constant necessary to reach 63.2% of the maximum damage D_{max} [56].

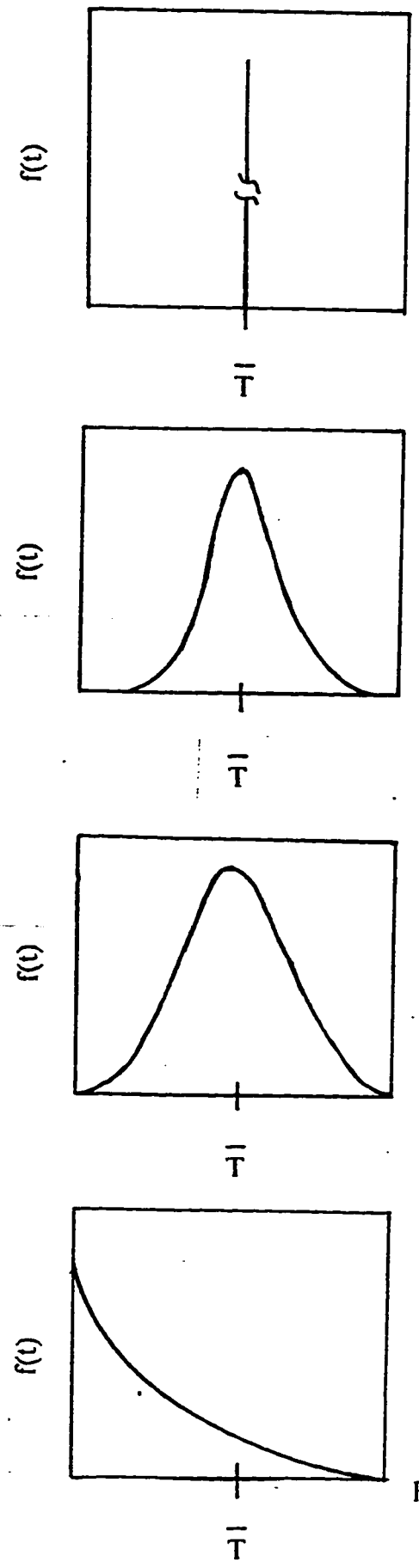

Fig. 1.7 Influence of coefficient of variation on probability density function.

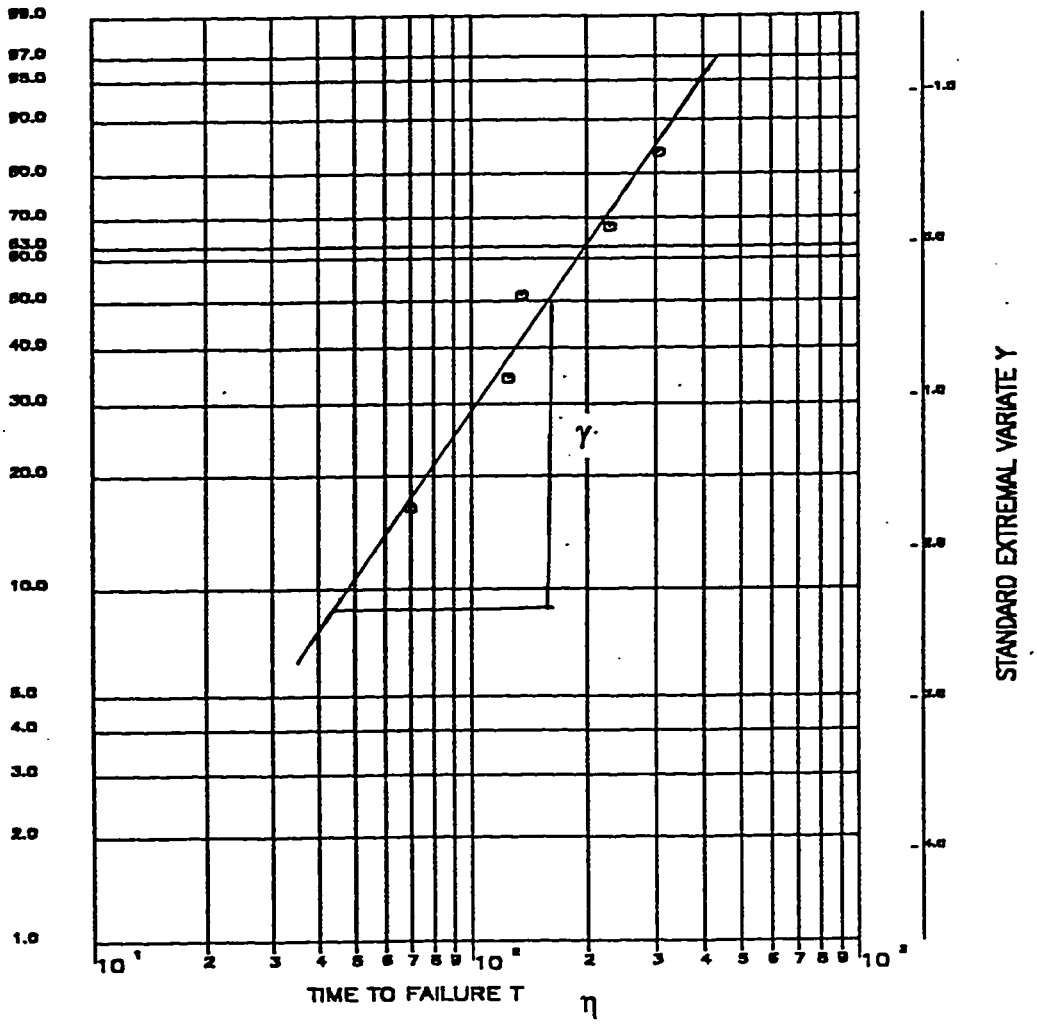

Fig. 1.8 Example of Weibull analysis.

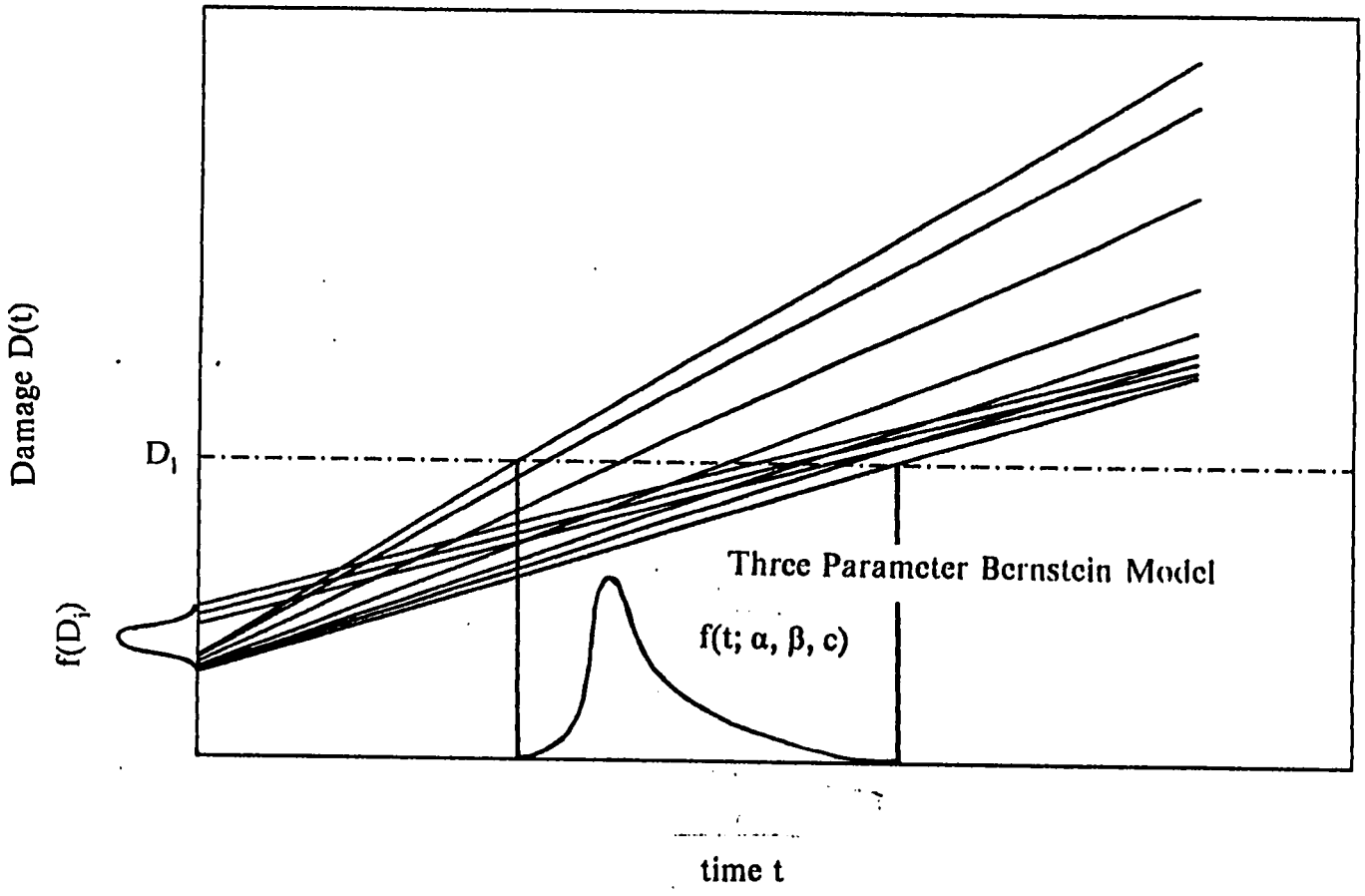

Fig. 1.9 Sample functions of linear, non-stationary random damage process $\mathbf{D(t) = D_i + rt}$.

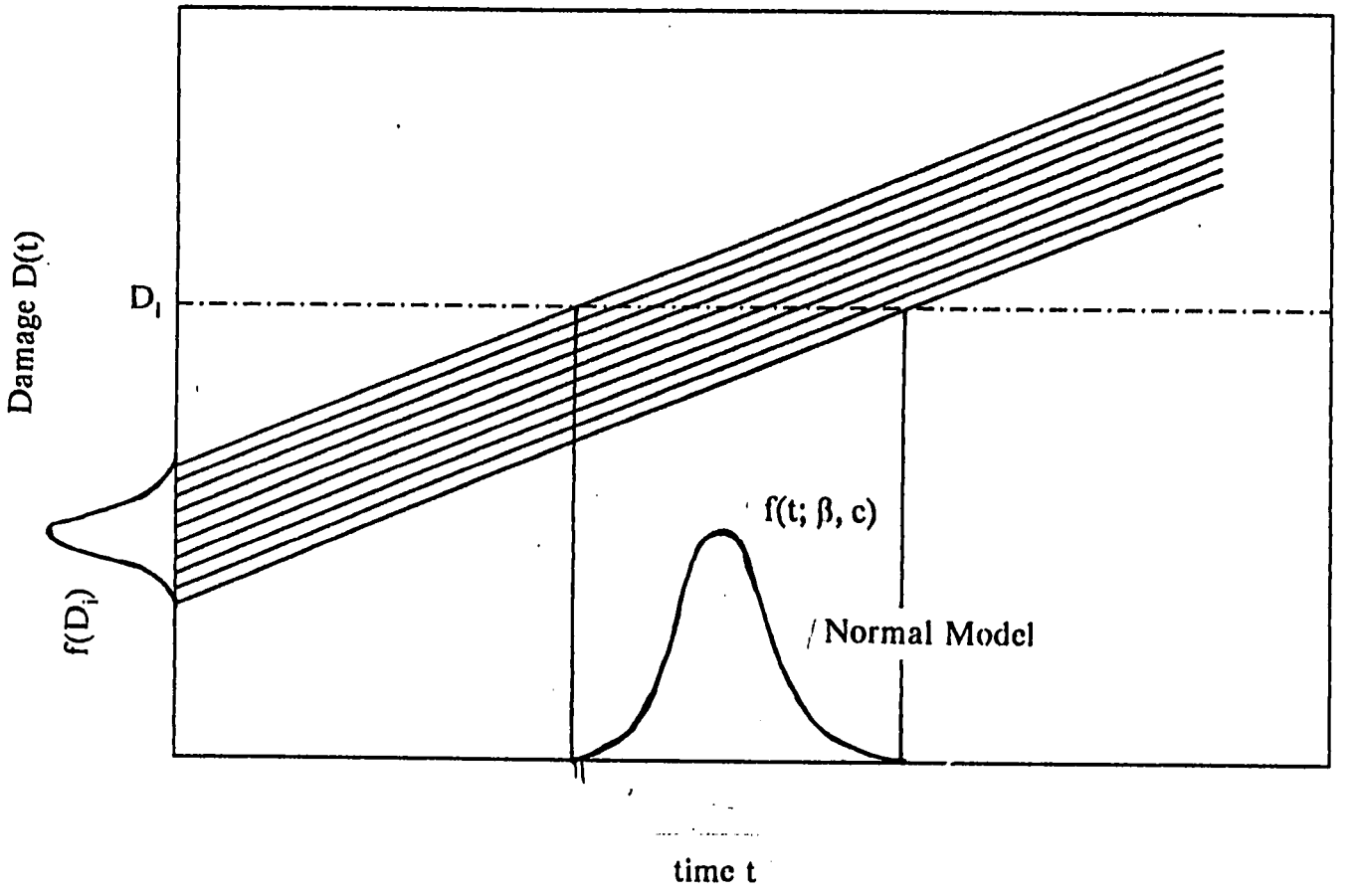

Fig. 1.10 Sample functions of random damage process $D(t) = D_i + rt$.

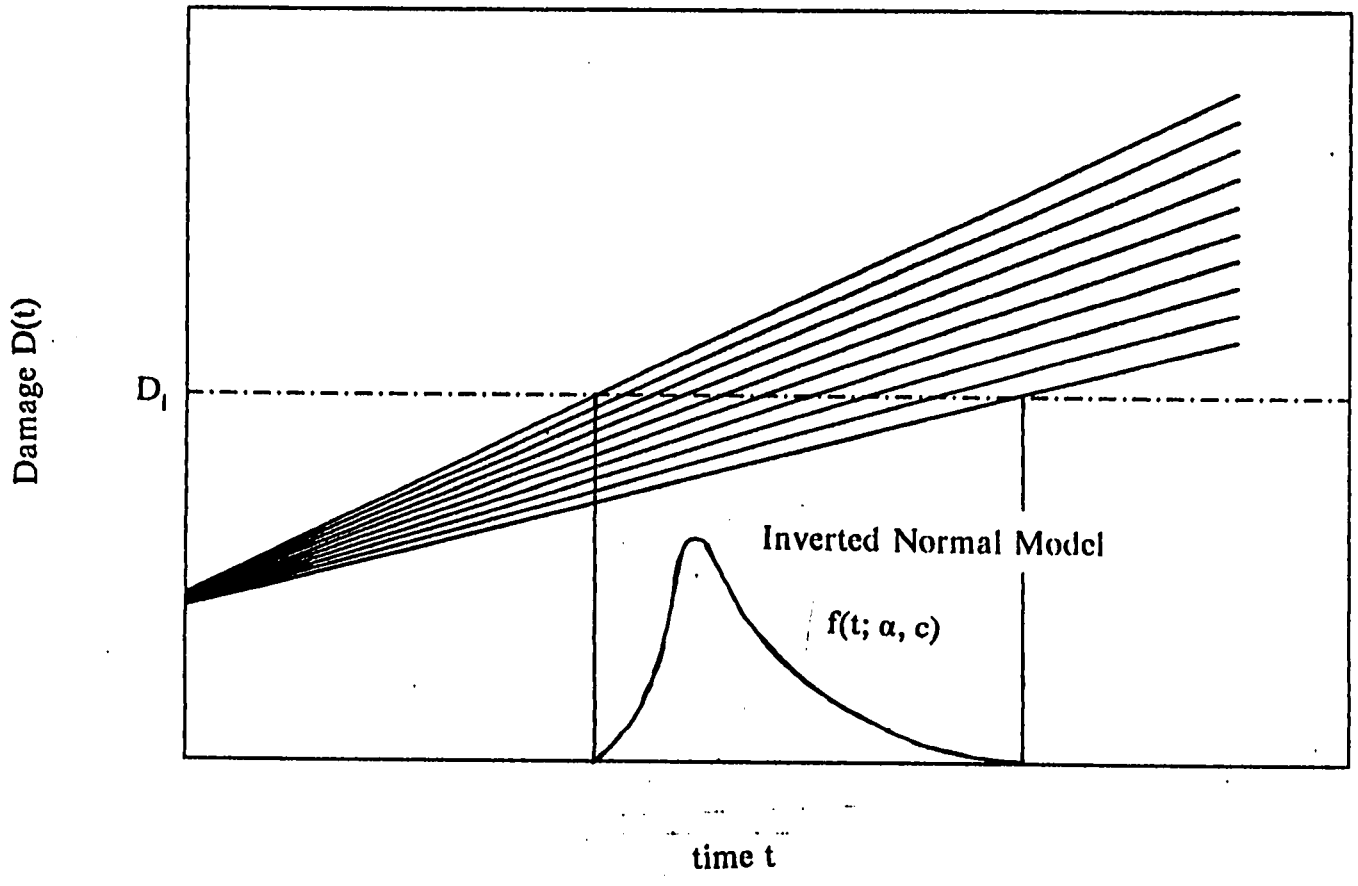

Fig. 1.11 Sample functions of random damage process $\mathbf{D(t) = D_1 + rt}$.

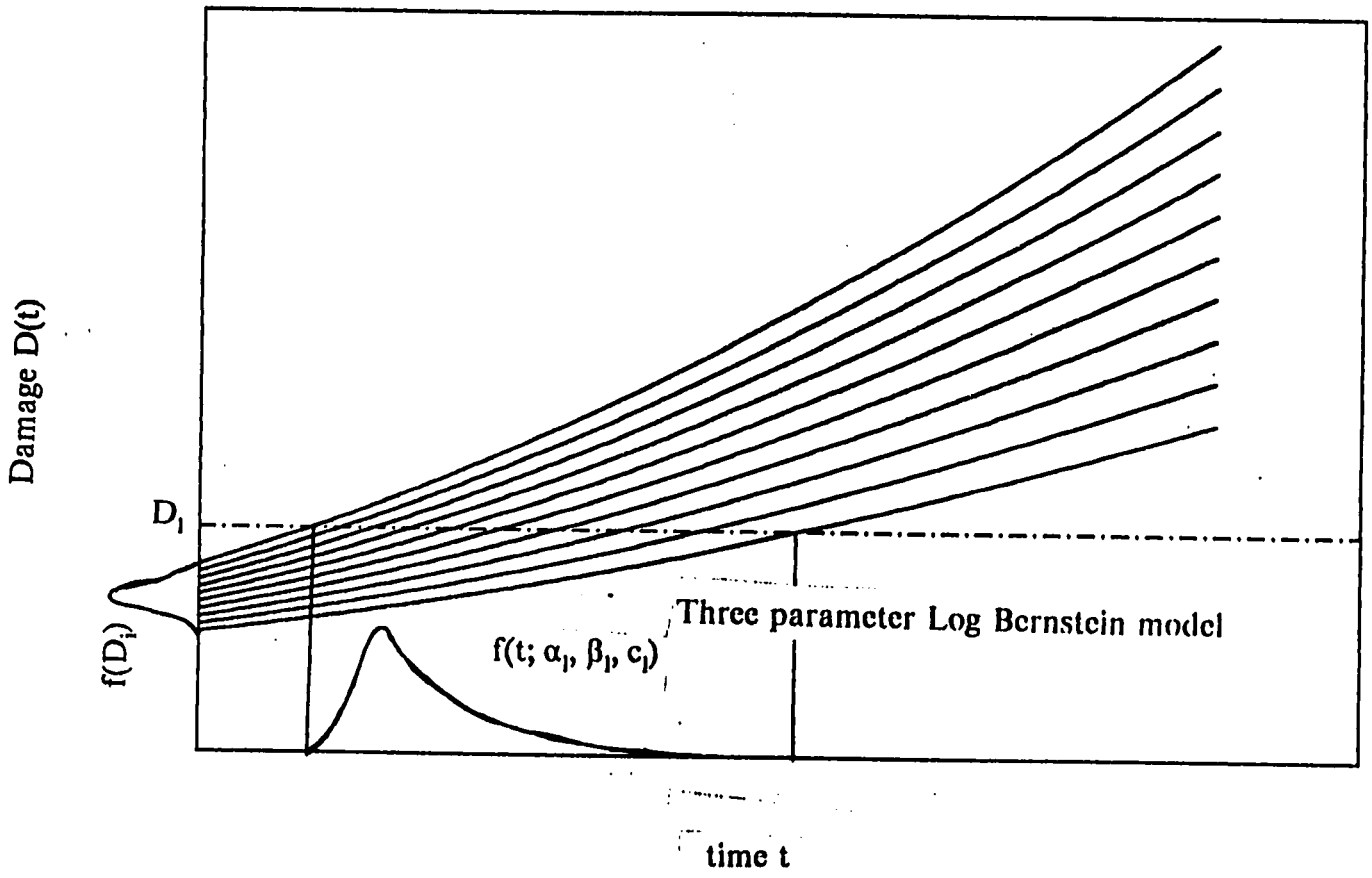

Fig. 1.12 Sample functions of non-linear, non-stationary random damage process $D(t) = D_l\, t^B$.

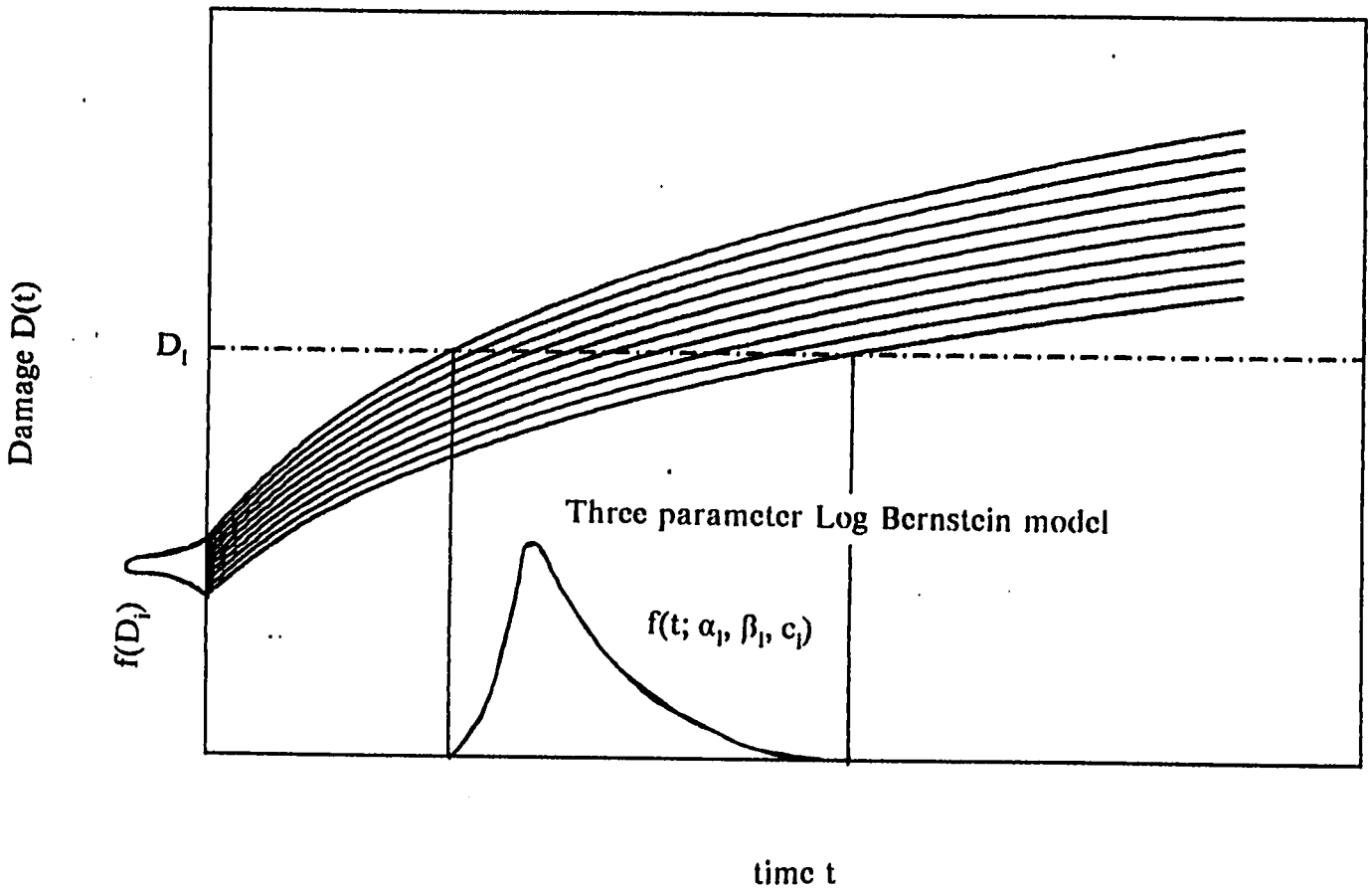

Fig. 1.13 Sample functions of random damage process $D(t) = D_i + rint.$

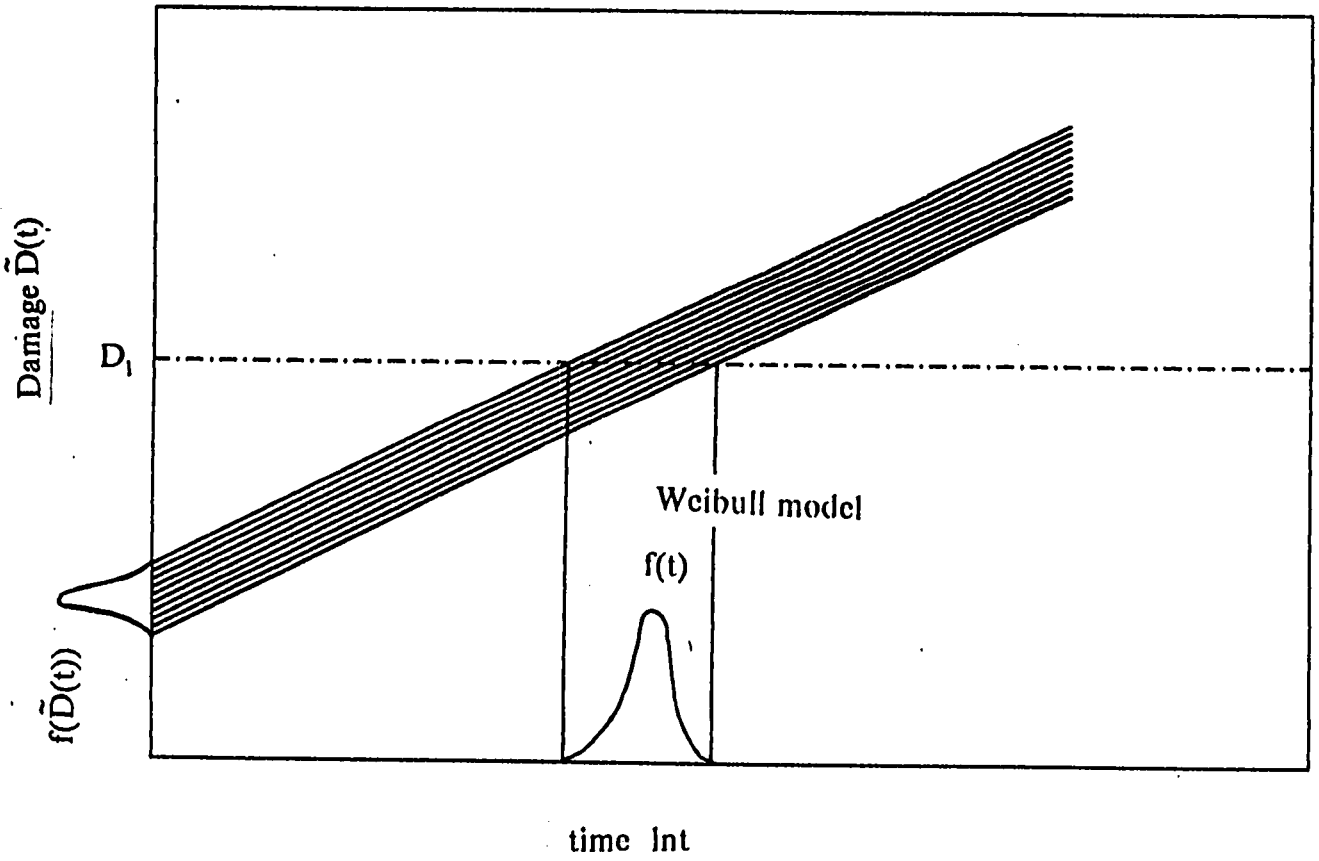

Fig. 1.14 Sample functions of random damage process $\tilde{D}(t) = \tilde{D}(t) + r\,lnt$.

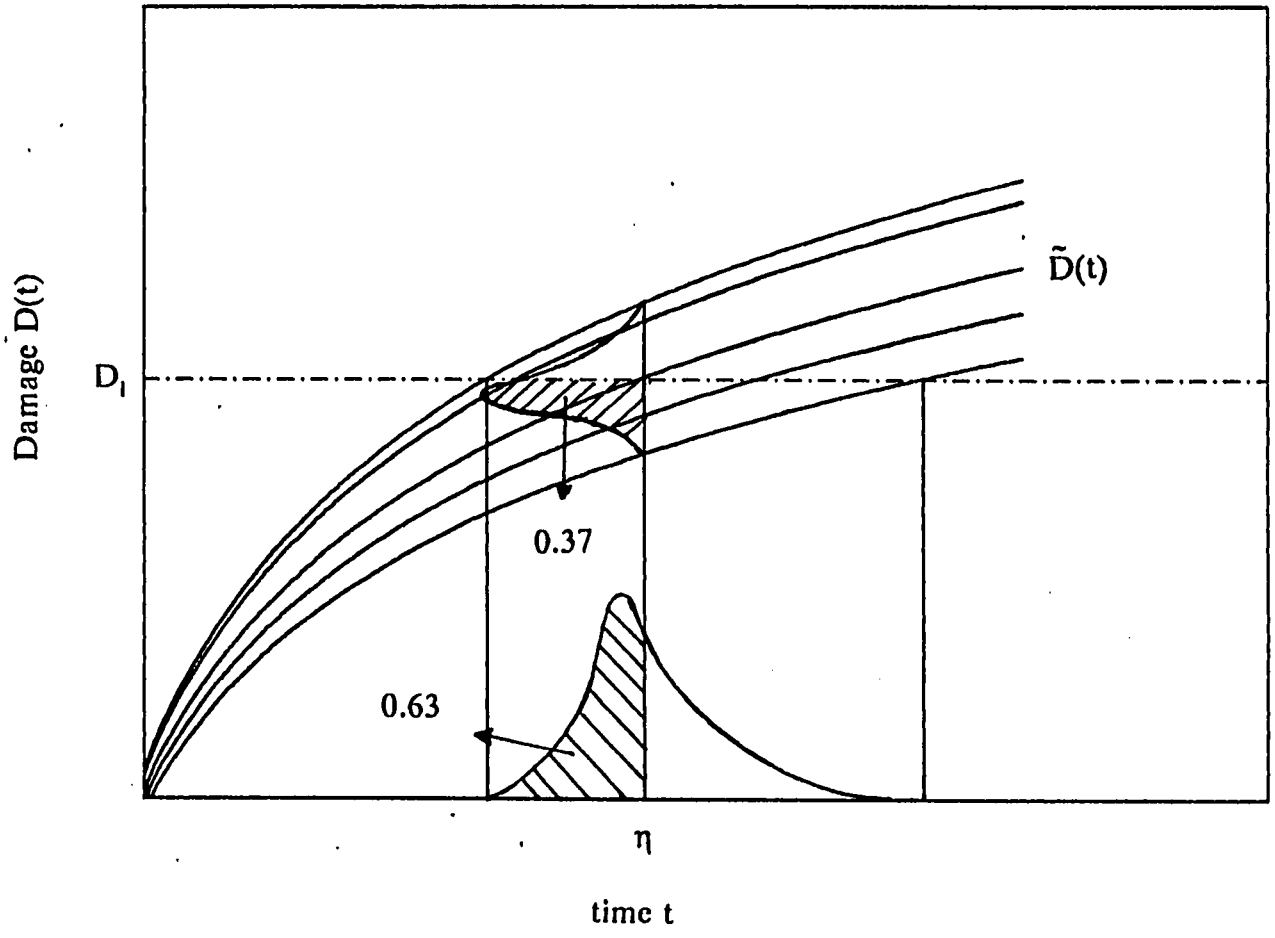

Fig. 1.15 Sample functions of quantiles of pit growth.

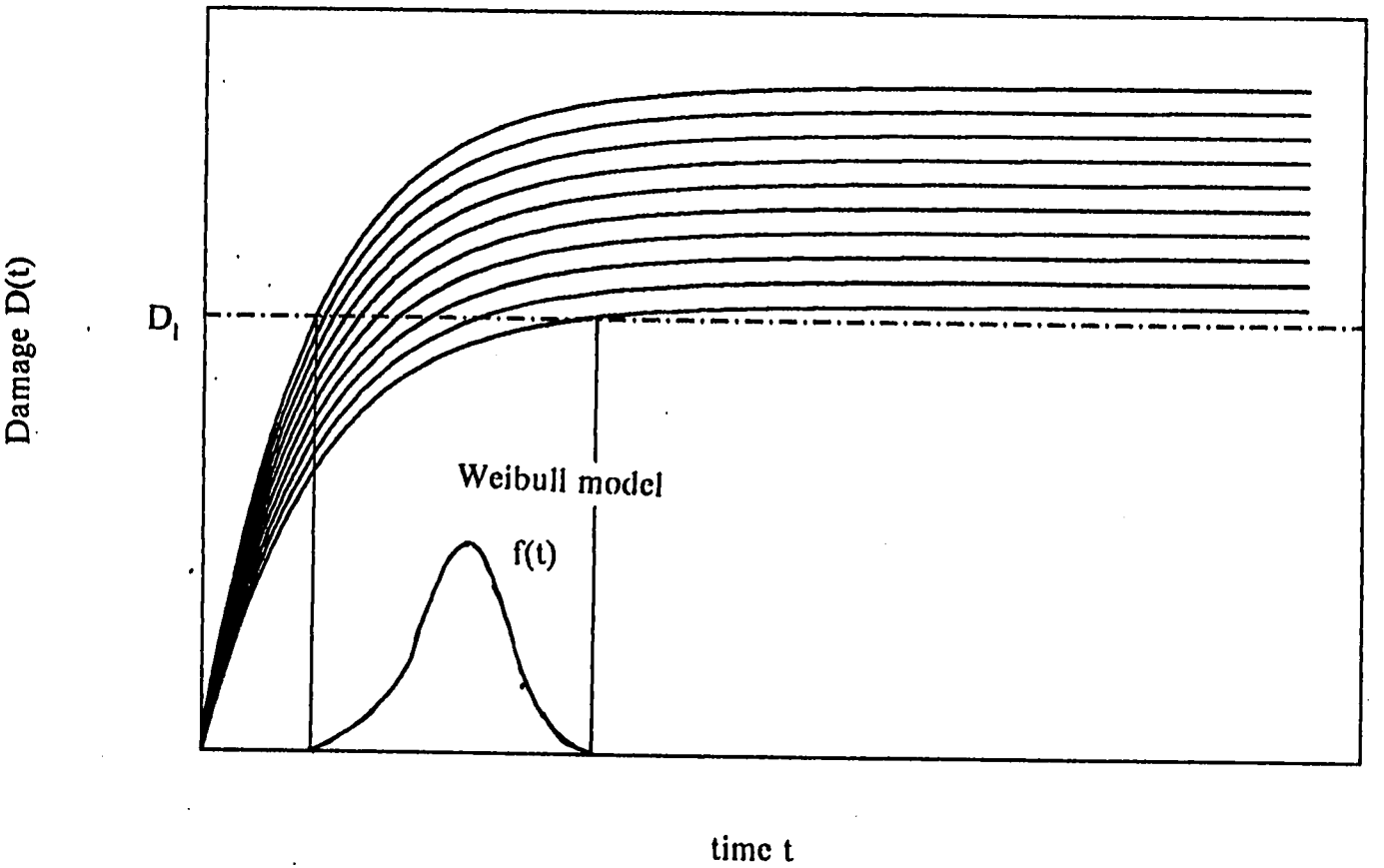

Fig. 1.16 Sample functions of random damage process $D(t) = D_{max}(1 - e^{-\lambda t})$.

Table 1.1. Representation of Various Damage Models for Different Processes

PROCESS \ MODEL		$D(t)=D_i+rt$	$D(t)=D_i+r\ln t$	$D(t)=D_i t^B$	$D(t)=D_i+rt^n$	$D(t)=D_{max}(1-e^{-\lambda t})$	$D(t)=rt^*$	$D(t)=\sqrt{rt}^*$	$D(t)=D_i\ln(rt+C)^*$
Wear		x [7]	--	x [1]	x [5]	--	--	--	--
Corrosion	Pitting	--	x [3]	x [4]	--	--	--	--	--
	Oxidation	x [48]	x [49]	x [49]	--	--	x [47]	x [47]	x [47]
	Stress Corrosion Cracking	--	x [27]	--	--	--	--	--	--
Fouling		x [66]	x [53]	--	--	x [6]	--	--	--
Creep		x [68]	--	--	--	--	--	--	--

$D(t)$ is the damage manifestation with time.

where D_i,r are random variables and n,C, λ are fixed quantities.

* these models are especially for Oxidation, can be modified into general models.

CHAPTER 2

WEAR

2.1 INTRODUCTION

Wear is defined as the progressive loss of substance from the operating surface of a body occuring as a result of relative motion at the surface. For example, all mechanical components that undergo sliding or rolling contact are subject to some degree of wear. Typical of such components are bearings, gears, seals, guides, piston rings, splines, brakes, and clutches. Wear of these components may range from mild polishing type attrition to rapid and severe removal of material with accompanying surface roughening.

The terms used to classify wear on the basis of controlling mechanism are adhesion, delamination, fretting, abrasion, erosion, impact, surface fatigue, corrosive wear, diffusive wear and electric contact wear. Wear can also be categorized on the consideration of motions and the bodies involved in the process. Fig. 2.1 groups together various schemes connecting the various motions with basic mechanisms involved in the wear processes.

An alternative scheme of classification is phenomenological in character and simple descriptive terms like sliding, rolling, impact, wet/dry and

lubricated/unlubricated, based on the simple observation of the wear system, are used. The phenomenological approach is based on a macroscopic description of the appearance of worn surfaces, for example scuffing, rubbing and fretting.

The rate of material loss is a relative term. It can be defined as weight or volume loss per unit time or since the sliding speed is often kept constant, the wear rate is expressed as mass or volume removed per unit sliding distance.

2.2 WEAR THEORIES AND COEFFICIENTS FOR DIFFERENT TYPES OF WEAR

For quantitative analysis of wear rates various equations have been developed. The majority of these have the general form based on the first relationship derived by Holm [10] and later, by Archard [11] for a sliding situation (adhesion wear). It considers that the wear volume is a linear function of sliding distance at constant sliding speed and that the volume-rate in wear is proportional to the applied load. Further developments show that the load effect is considered to be proportional to the true area of contact, and the depth of material removed is assumed to be proportional to the radius of the contact circle.

$$V = K \frac{F_N}{H} l \tag{2.1}$$

where V is the volume of wear, F_N is the applied normal force, $H = p_m$ is the hardness or yield strength of the softer surface and l is the sliding distance. The equation may be expressed in the form

$$W = \frac{V}{A} = K \frac{F_N}{H A} l \qquad (2.2)$$

where W is the depth of wear, and A is the area of contact.

The parameter K present in the wear equation allows for the fact that wear does not result from every encounter of asperities during sliding. Thus, K, the wear coefficient is a proportionality number and may be interpreted as the probability of producing a wear particle at any given asperity encounter [12]. In some cases, K may also include a shape factor for the particles, e.g. hemispherical or other particle shapes.

The various wear equations for different forms of wear are given as follows :

Adhesive wear :[11,13]

$$V = K\rho \frac{F_N}{H} l \qquad (2.3)$$

where $\rho = \frac{1}{3}$

Abrasive wear :[13]

$$V = K \rho \frac{F_N}{H} l \qquad (2.4)$$

where $\rho = \frac{a \cot\theta}{\pi}$

$a = 1$ to 2

Delamination wear :[14]

$$V = K \rho \frac{F_N}{H} l \qquad (2.5)$$

where $\rho = \frac{h_1}{P_1} + \frac{\kappa h_2}{P_2}$

κ is a constant

h is the thickness of layer

P is the critical plastic displacement

subscripts 1,2 denote two contacting parts

Oxidation wear :[15]

$$V = K_{oxid} \frac{F_N}{H} l \qquad (2.6)$$

where $K_{oxid} = \frac{\beta_1 e^{-(Q_p/RT)}}{(f\eta_o\rho_o)^2 v}$

$\beta_1 e^{-(Q_p/RT)}$ is the exponential oxidation constant

β_1, Q_p are the constants for given material

R is the universal gas constant

T is the temperature

f is the fraction of oxide which is oxygen

η_o is the critical oxide thickness

ρ_o is the average density of the oxide

v is the velocity of sliding

Fatigue wear :[16]

$$V = K_{fatigue} \frac{F_N}{H} l \qquad (2.7)$$

(for plastic contact)

where $K_{fatigue} = \frac{0.18\,\alpha'}{n_1}\left(\frac{x}{R_1}\right)$

α' is the ratio of nominal area to frictional area of contact

$n_1 = (\varepsilon_{p1}/\varepsilon_{e1})^{t'}$

ε_{p1} is the plastic strain

ε_{e1} is the effective strain

t is the fatigue curve exponent power

x is the depth of penetration

R_1 is radius of curvature of asperity

Erosive wear :[17]

$$V = K\,\rho\frac{F_N}{H} l \qquad (2.8)$$

where $\rho = mv^2/6\,l$

m is the mass of the particle

v is the impact velocity

The wear coefficient for oxidation wear and fatigue wear are having specific values, the primary focus is around the four types of wear which has the following general equation :

$$V = K\,\rho\frac{F_N}{H} l \qquad (2.9)$$

where K is the wear coefficient

ρ is a constant.

The wear coefficient is related to the wear rate as the following (using $l = vt$;where v is the velocity and t is the time.]

$$dV / dl = K \rho \frac{F_N}{H} = K \rho \frac{F_N}{H} v = dV/dt \qquad (2.10)$$

If ρ, F_N, and H are nominally constant, the studying K is equivalent to studying wear rate.

These wear coefficients K, may be obtained from laboratory tests and from field data. Rabinowicz [17] used several examples to illustrate that for any particular wear problem or wear design, the wear coefficient K may be used :

(1) to estimate wear life of some sliding systems, i.e. estimate V / l from published K values knowing the material used and the other operating conditions.

(2) to determine the type of wear in a system by comparing the calculated K value with field or experimentally obtained K values.

(3) to determine the proper material and lubrication system to be used in a system, given the maximum allowable wear rate, the life expectancy of the system and the loading condition.

(4) to determine the type of motion causing wear.

(5) to compute the stress distribution in composite systems.

The most important thing which Rabinowicz [18] has pointed out is that there is a considerable scatter observed in the values of wear coefficient K (Fig. 2.2). A typical set of values of K are given in Table 2.1.

2.3 VARIABLES AFFECTING WEAR

The variety of variables influencing all the wear mechanisms can be classified into the following groups :

(a) Material variables such as composition, grain size, modulus, thermal conductivity, degree of work hardening, hardness etc.

(b) Design variables such as shape, loading, type of motion, roughness, vibration, cycle time, etc.

(c) Environmental variables such as temperature, humidity, atmosphere, contamination, etc.

(d) Lubrication variables such as type of lubricant, lubricant stability type of fluid lubricant, etc.

2.4 STATISTICAL ANALYSIS OF WEAR COEFFICIENT

The wear coefficient K behave as a random variable Fig. 2.2 due to the factors such as scatter in applied load, sliding velocity, temperature, tribological conditions, and surface finish of the contact surfaces. Wallbridge and Dowson [19] have investigated the wear rates of several different combinations of materials and tried to assess the distribution of wear factors. All the materials studied by them showed a log-normal distribution of wear factors. The data of

group 1 (ultrahigh molecular weight polyethylene) and group 8 (ultrahigh molecular weight polyethylene) of the above reference were analysed. The various probability functions of groups 1 and 6 are shown in the Figs. 2.4 and 2.4. Fig. 2.5 shows a representation of the of logarithms of the wear coefficient for group 1 and 6 plotted on the normal probability paper. The straight line demonstrates log normal distribution of K. Wear coefficients are not always lognormally distributed. The data by Shahab [20] demonstrate that the wear coefficients of Archard's law are normally distributed. [Fig. 2.6]

2.5 RELIABILITY ANALYSIS OF WEAR

The basic structure of the equation of the wear damage is

$$W(t) = K \rho \frac{F_N}{H} l \tag{2.11}$$

The sliding distance can written as

The wear rate eq (2.11) can be modified by substituting $l = vt$, as follows

$$W(t) = \mathbf{K}\left[\frac{\rho F_N v}{H} t\right] \qquad t \in \mathbf{T} \tag{2.12}$$

$$W(t) = \mathbf{K}\omega t \tag{2.13}$$

where $\omega = \left[\frac{\rho F_N v}{H}\right]$

The eq (2.13) is identical to the eq (1.11) of Chapter 1 with $D_i = 0$ and $r = K\omega$. This leads to a two parameter inverted normal reliability model [Sec 1.8.3] for the failure criteria $W(t) = W_f$. The parameters of the reliability model

are given as follows :

$$\hat{c} = \frac{D_1}{\omega\, E[K]}$$

$$\hat{\alpha} = \frac{V[K\omega]}{[E\{K\omega\}]^2} = \frac{\omega^2 V[K]}{\omega^2[E\{K\}]^2} = \frac{V[K]}{[E[K]]^2}$$

The corresponding equations eq (1.50) and (1.51) also be modified accordingly. The underlying assumption is that **K** is normally distributed with mean E(**K**) and variance V(**K**) respectively.

In the case of wear rates investigated by Wallbridge and Downson [19] for various combination of materials, the wear coefficient **K** has been demonstrated as lognormal distribution which means **T** is inverted lognormal with the following parameters :

$$\hat{C}_1 = \frac{1}{M}\left[\sum_{i=1}^{M} \ln t_i\right]^{-1} \tag{2.14}$$

$$\hat{\alpha}_1 = \left\{\frac{1}{M}\sum_{i=1}^{M}\left[1 - \frac{\hat{C}_1}{\ln t_i}\right]^2\right\} \tag{2.15}$$

Reliability of a Machine Element subjected to wear :

As an example of wear related reliability analysis consider a machine element subjected to the linear wear process $W(t) = W_i + rt$ following parameters : (see .pp 148-151 of [21]).

$W_i = 10\,\mu m$; $E(W_i) = 0$; $\sigma(W_i) = 1\mu m$;

$E(r) = 2x10^{-2}\,\mu m/h$ $\sigma(r) = 2.77x10^{-3}\,\mu m/h.$

$$C = \left[\frac{W_i - E(D_i)}{E(r)}\right] = 500\ hr$$

$$\alpha = \frac{V(r)}{[E(r)]^2} = 0.0192$$

$$\beta = \frac{V(W_i)}{[E(r)]^2} = 2500\ hr^2$$

Figs. 2.7 to 2.9 shows the three parameter Bernstein reliability, probability density and hazard function of machine element.

Reliability of a Sheet Metal Cutting Dies :

In a sheet metal cutting operation, the burr generated on the workpiece edges is a reflection of the wear of sheet metal cutting dies. Thus if burr is considered as the manifestation of damage (indicating the wear of die) then the experimental evidence support the validity of the random linear growth pattern [Fig. 1.3]. Fig. 1.3 represents the data from Metals Handbook [22] for blanking operations, for D2 tool steel and for TI and M2 HSS steel. The data shows a considerable scatter and linear trend. Each realization in Fig. 1.3 was fitted with

a straight line using linear regression technique. Collection of such straight lines were used to estimate the parameters of the Bernstein model (Sec 1.8.1 Chapter 1) by selecting suitable level of critical damage as the failure criteria. Fig. 2.10 shows the reliability function as well as the actual time to failure data for both types of steels at specified critical damage level. Fig. 2.11 and 2.12 shows probability density function and hazard function for both types of tool steels. The time to failure data is plotted [F(T) vs 1/T] on the normal probability paper. The straight line demonstrates the validity of the inverted normal distribution as shown in Fig. 2.13. The two parameter inverted normal distribution fits better than the three parameter Bernstein model, for both of the tool steels. This discrepancy can be explained by considering the fact that while fitting straight lines to each data realization, we have introduced more than the actual amount of dispersion of initial damage and have also altered the average value of the initial damage. This has slightly distorted the parameters of the three parameter model when estimated from damage function.

Reliability of Aircraft Splines :

Kececioglu and Koharcheck [23] developed empirical mathematical models based on the experimental research conducted on aircraft splines which provide equations for predicting the reliability when spline tooth wear is the failure mode. The model hypothesized by them is of the type $y = mx + b$ and the values of m and b are obtained by minimizing the sum of the squared differences of actual and predicted values by using the least square method of

regression analysis. The data given is in the form of a range (an envelope of lower and upper limits of wear realizations) with mean and standard deviation as a function of time. (Table 3 and Table 4 of the above reference). The underlying damage model is assumed to be of the type $W(t) = W_i + rt$. Based on the assumption the data is further analysed to calculate the parameters of the for a three parameter Bernstein distribution by utilizing the information about means and variance for the wear growth on type 2 splines operating unlubricated at 250°F in dry air and in JP-5G fuel. Figs. 2.14 to 2.16 shows the various probability functions of the two type of splines at the specific damage level. Table 2.4 shows the comparison of results obtained by Kececioglu and Koharcheck [23] using directly the empirical model, and the results obtained by using Bernstein distribution for the various cases mentioned in the above reference. As can be seen from the Table 2.4 the Bernstein distribution provides an excellent results without going to the detailed approach of Kececioglu and Koharcheck [23].

Reliability of Coated Surfaces :

Chow [24] have reported an investigation on the wear behavior of various types of coatings. The data of Chow [24] for two groups are shown in Figs. 2.17 and 2.18. There is a considerable scatter in the data even in the carefully controlled laboratory conditions. Based on the linearity of the wear growth and assuming normality for W_i and r a three parameter Bernstein model is hypothesized. Fig. 2.19 shows the reliability function along with the actual time

to failure data at specific critical damage level for different groups of coatings. Fig. 2.20 and 2.21 shows the respective probability density functions and hazard functions of these groups of coatings. The time to failure data is plotted [F(T) vs 1/T] on the normal probability paper. The straight fit line demonstrates the validity of the inverted normal distribution as shown in Fig. 2.22. The two parameter inverted normal distribution fits better than the three parameter Bernstein model as shown in the Fig. 2.19.

Reliability of Machine Surfaces of metals subjected to linear random wear process :

A typical data set from Shahab [20] is shown in Fig. 2.23. A two parameter inverted normal model is hypothesized. The model parameters are estimated from the damage functions for different critical damage levels and the resulting probability functions are given in Figs. 2.24, 2.25.and 2.26. In the reliability model actual time to failure data, as well as the empirically fitted model [i.e., by plotting on a normal paper and estimating the parameters from the graph or by using maximum likelihood estimators eqs (1.50) and (1.51)] is also plotted [Fig. 2.24].

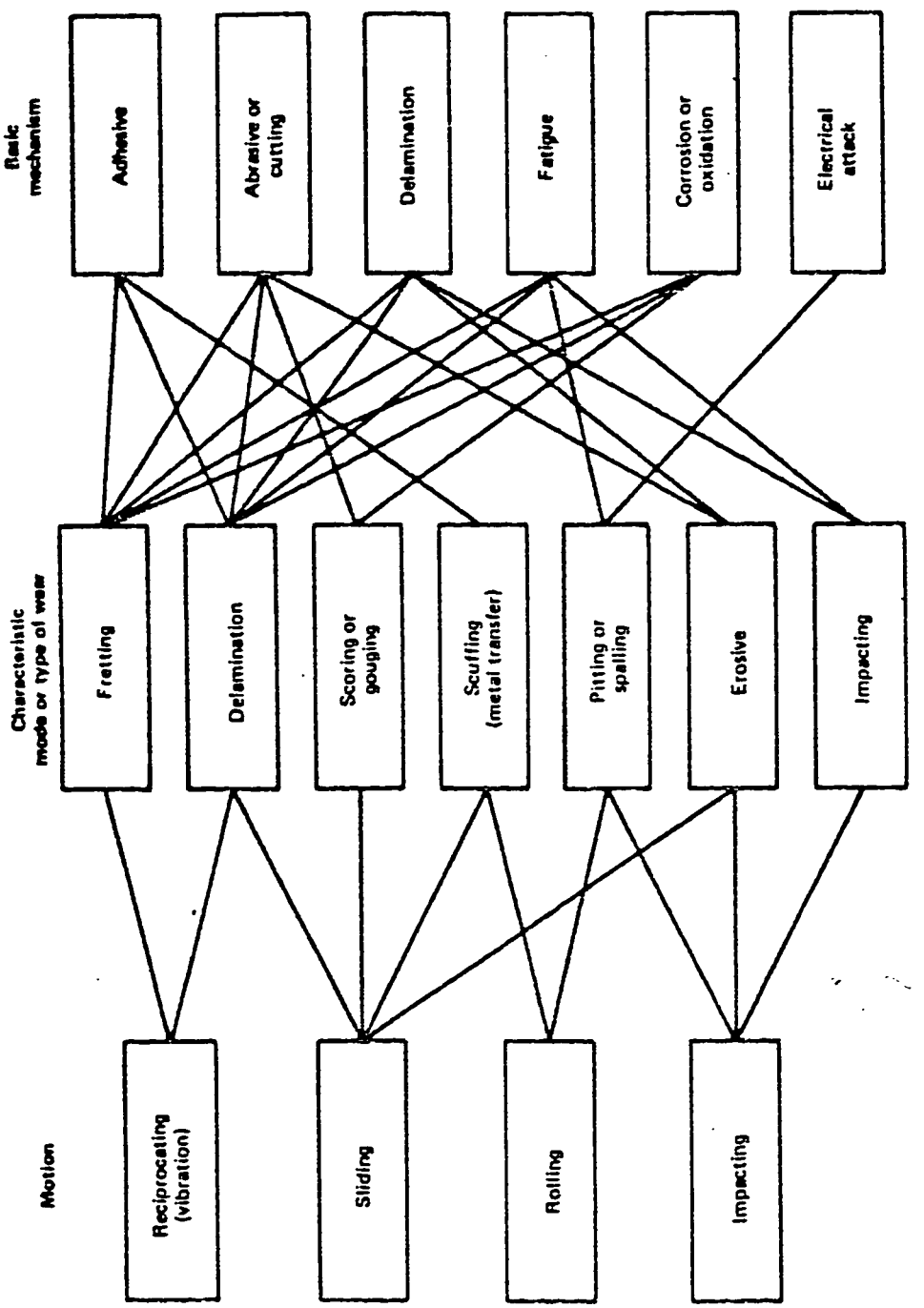

Fig. 2.1 Classification of wear

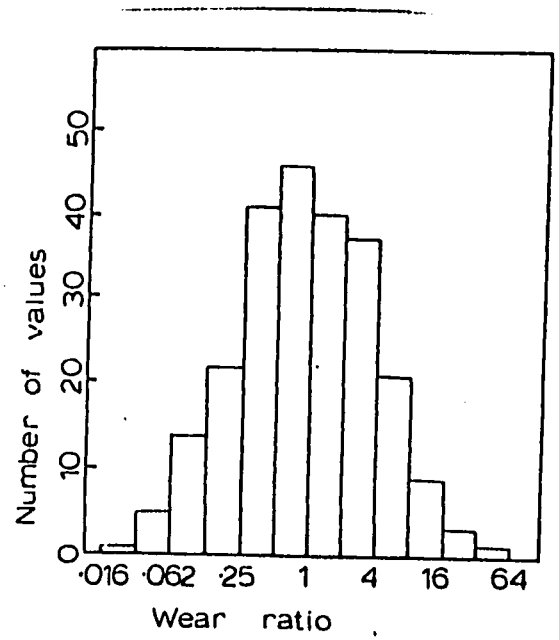

Fig. 2.2 Histogram of the (wear coefficient measured)/(wear coefficient tabulated) values for 243 diverse adhesive wear data [18].

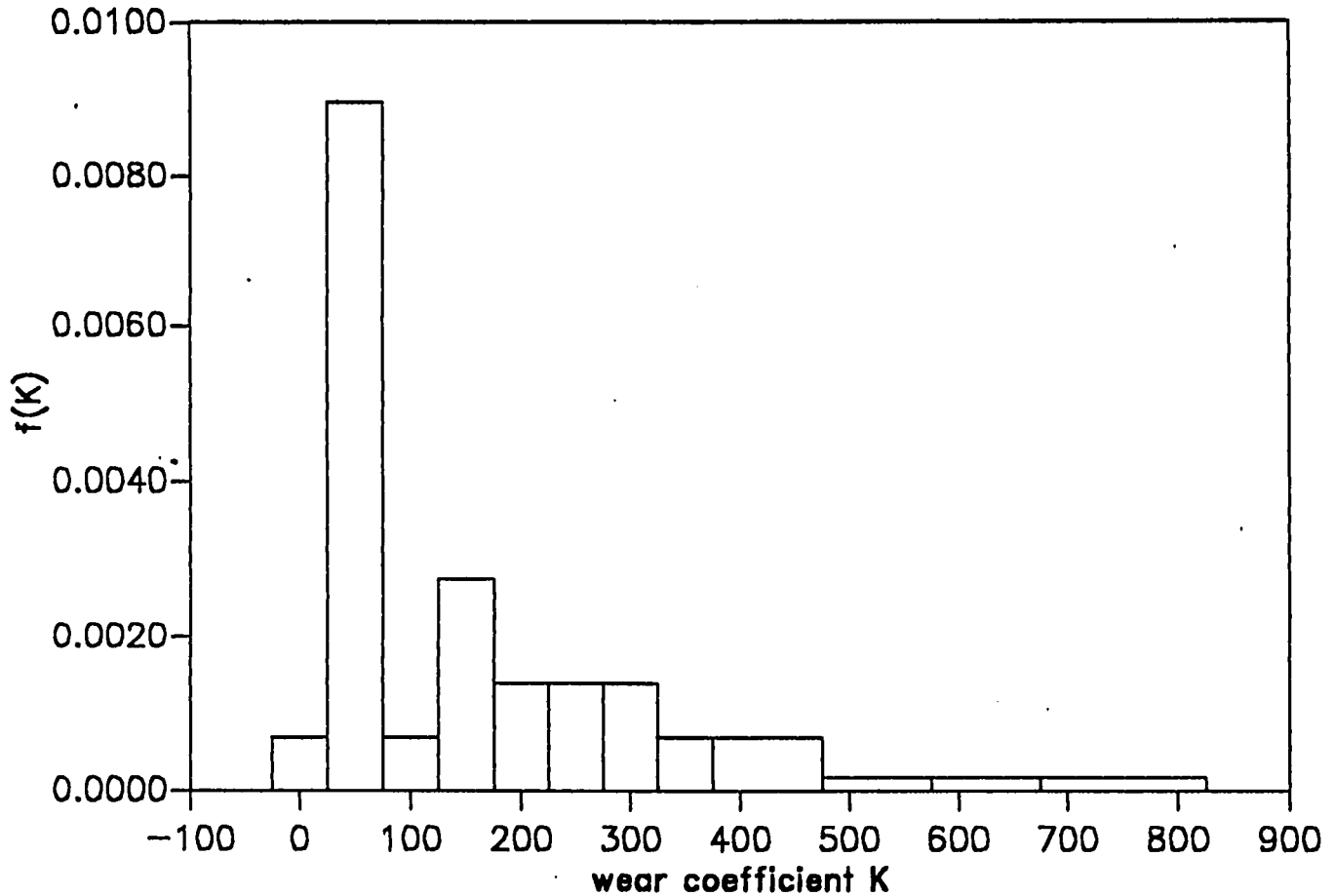

Fig. 2.3 Probability density function of log-normal distribution for polymer of group I (Ultrahigh molecular weight polyethelene) [19].

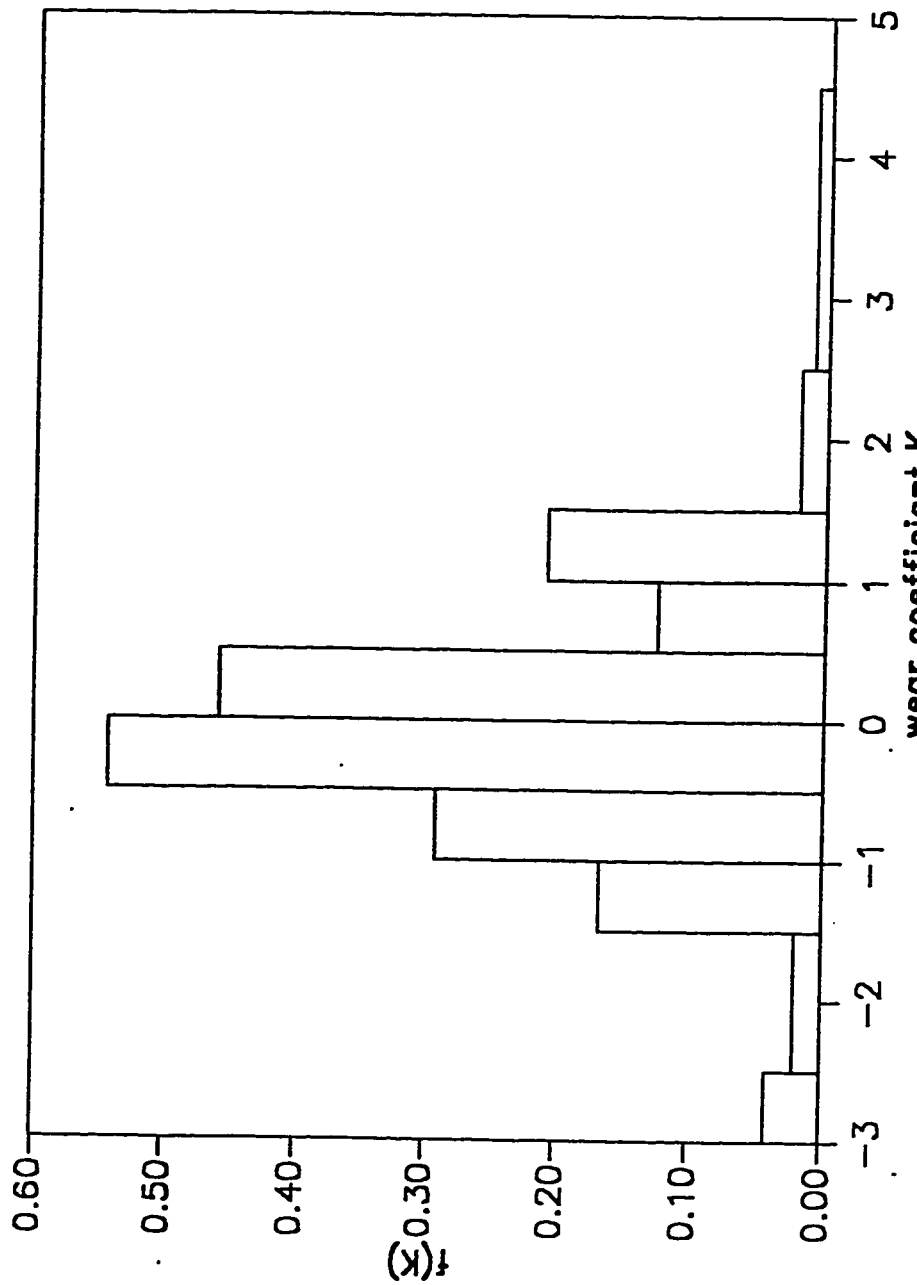

Fig. 2.4 Probability density function of log-normal distribution for polymer of group 6 (Ultrahigh molecular weight polyethelene) [19].

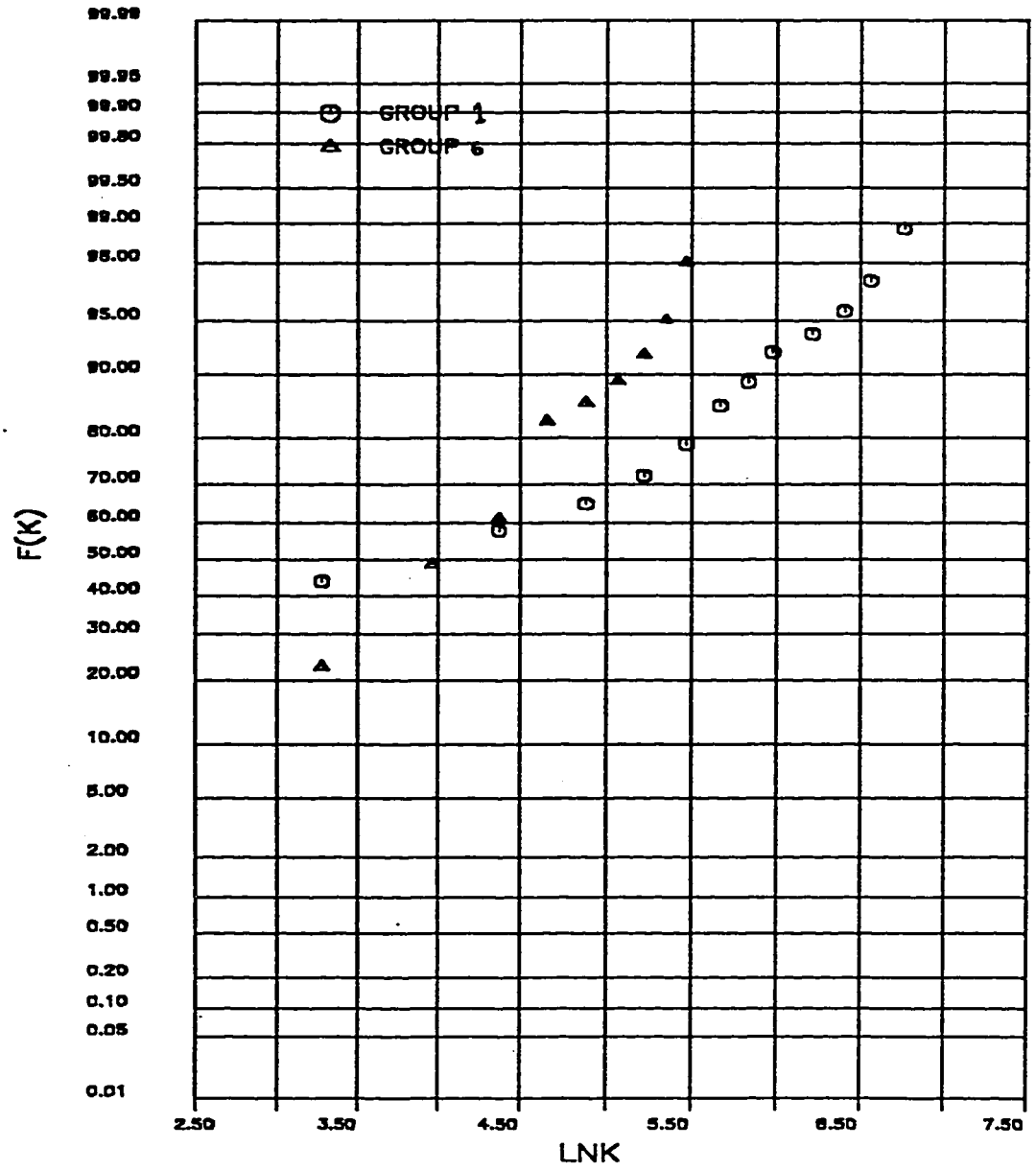

Fig. 2.5 Log-normal distribution of wear coefficients for polymer groups 1 and 6 [19].

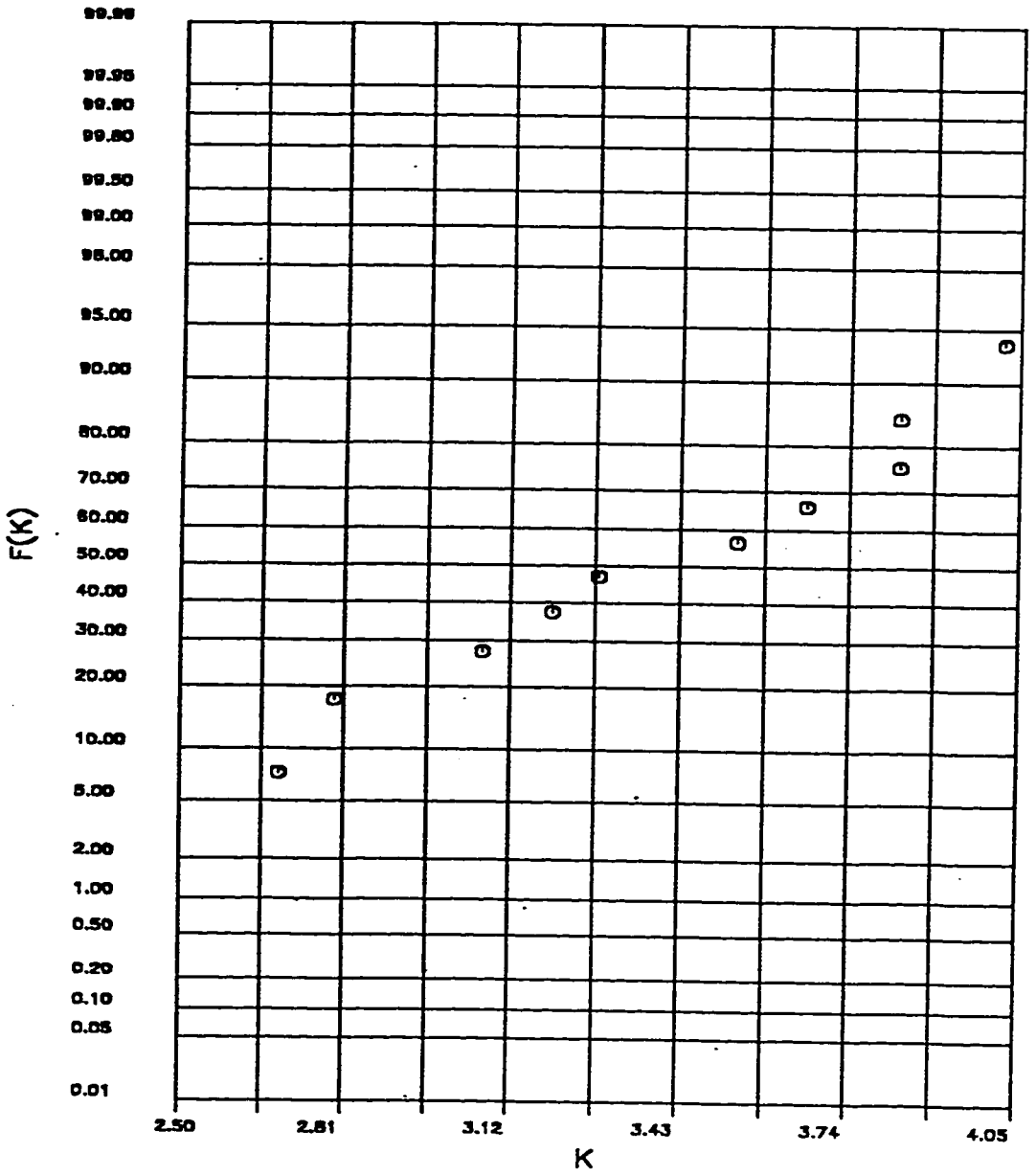

Fig. 2.6 Normal distribution of wear coefficients [20].

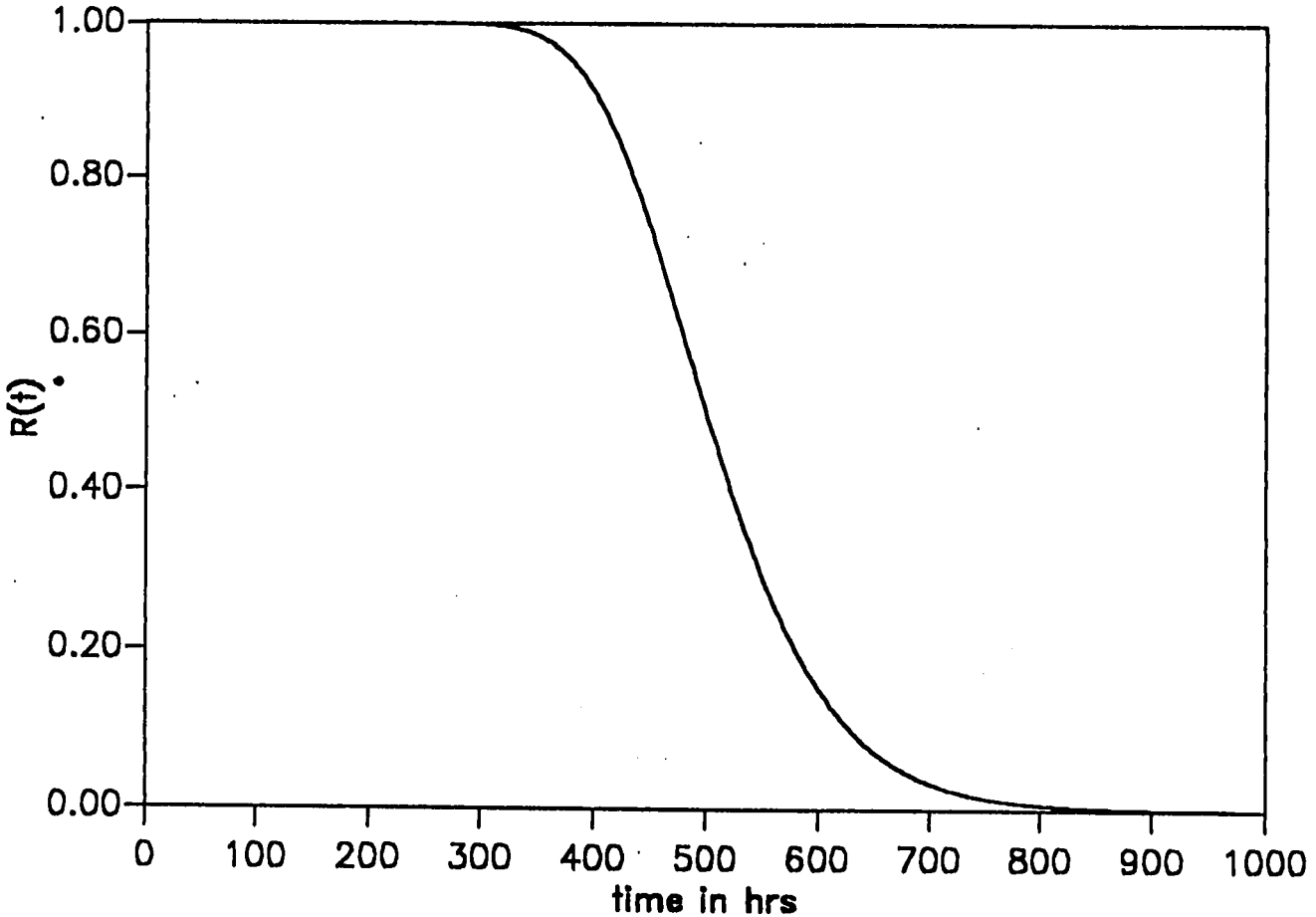

Fig. 2.7 Reliability function for three parameter Bernstein distribution of machine elements subjected to wearout failures. Parameters of the model are
$D_1 = 10\ \mu$ m, c = 500 hrs, $\alpha = 0.0192$, $\beta = 2500$ hr^2 [21].

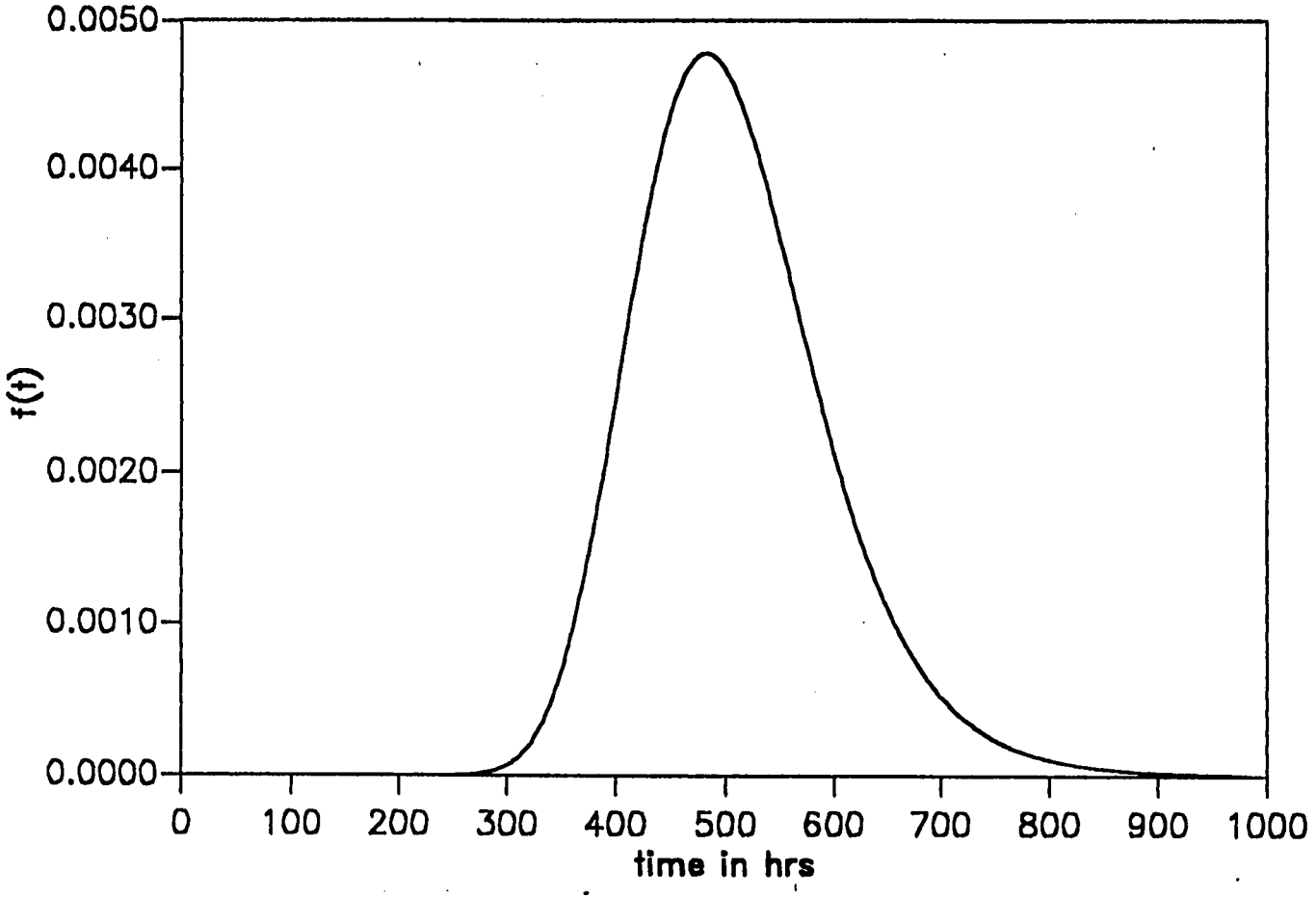

Fig. 2.8 Probability density function for three parameter Bernstein distribution of machine elements subjected to wearout failures. Parameters of the model are $D_1 = 10\ \mu$ m, $c = 500$ hrs, $\alpha = 0.0192$, $\beta = 2500$ hr^2 [21].

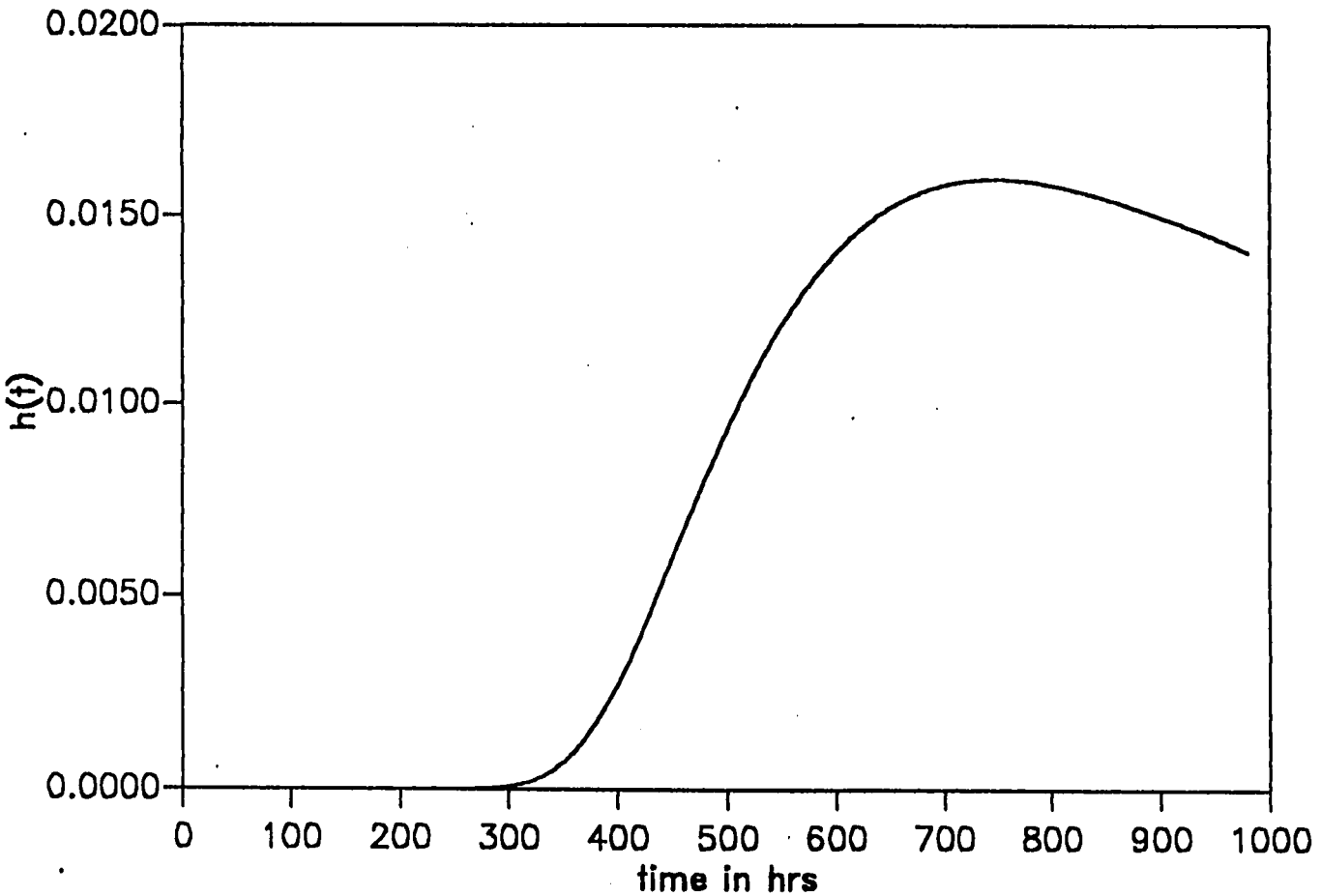

Fig. 2.9 Hazard function for three parameter Bernstein distribution of machine elements subjected to wearout failures. Parameters of the model are
$D_1 = 10\ \mu$ m, c = 500 hrs, $\alpha = 0.0192$, $\beta = 2500$ hr^2 [21].

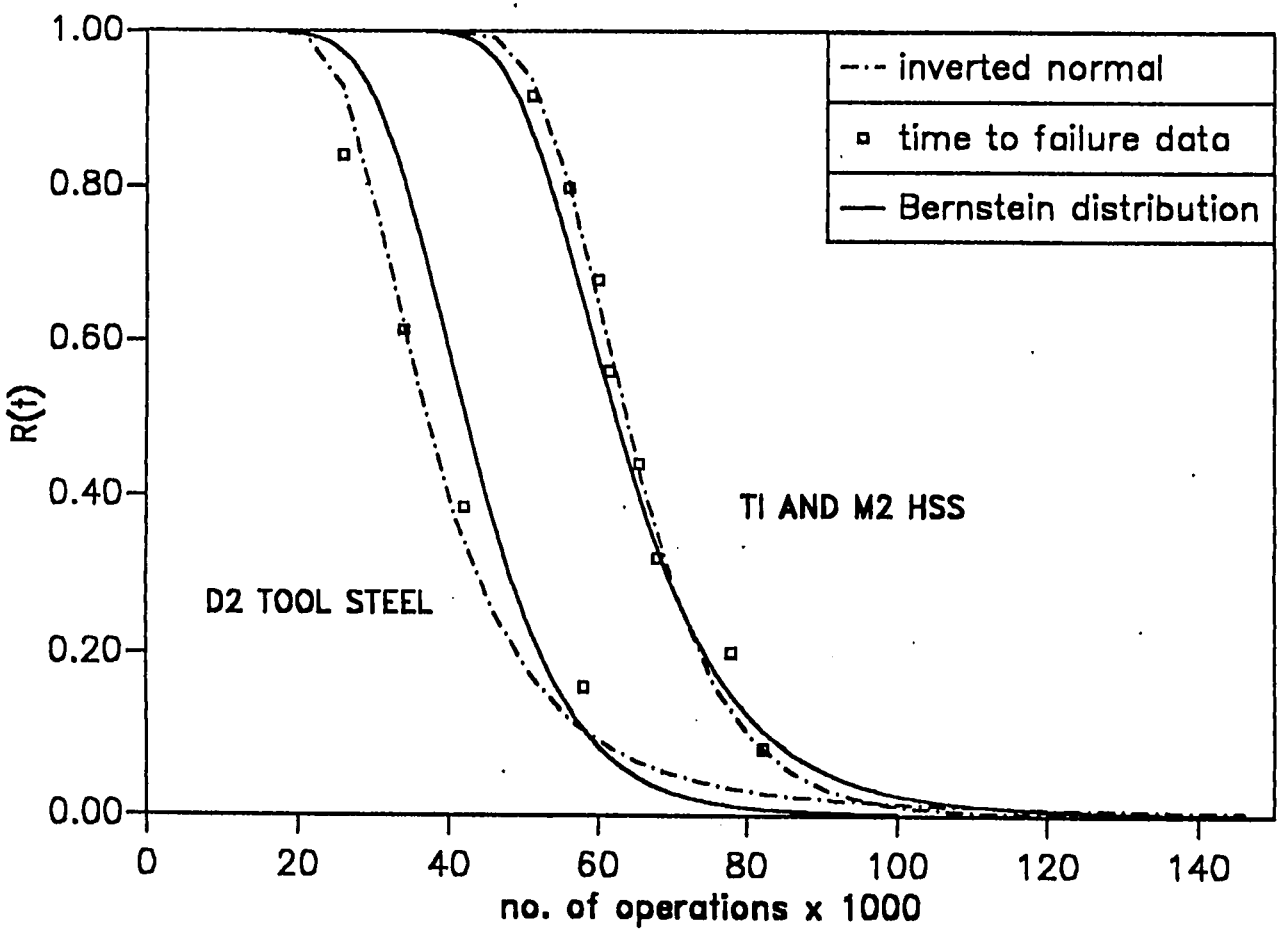

Fig. 2.10 Reliability function for three parameter Bernstein distribution obtained from damage function with actual time to failure data and empirically fitted inverted normal distribution for blanking dies at critical damage level Data from Ref [22]. [See Table 2.2 for distribution parameters].

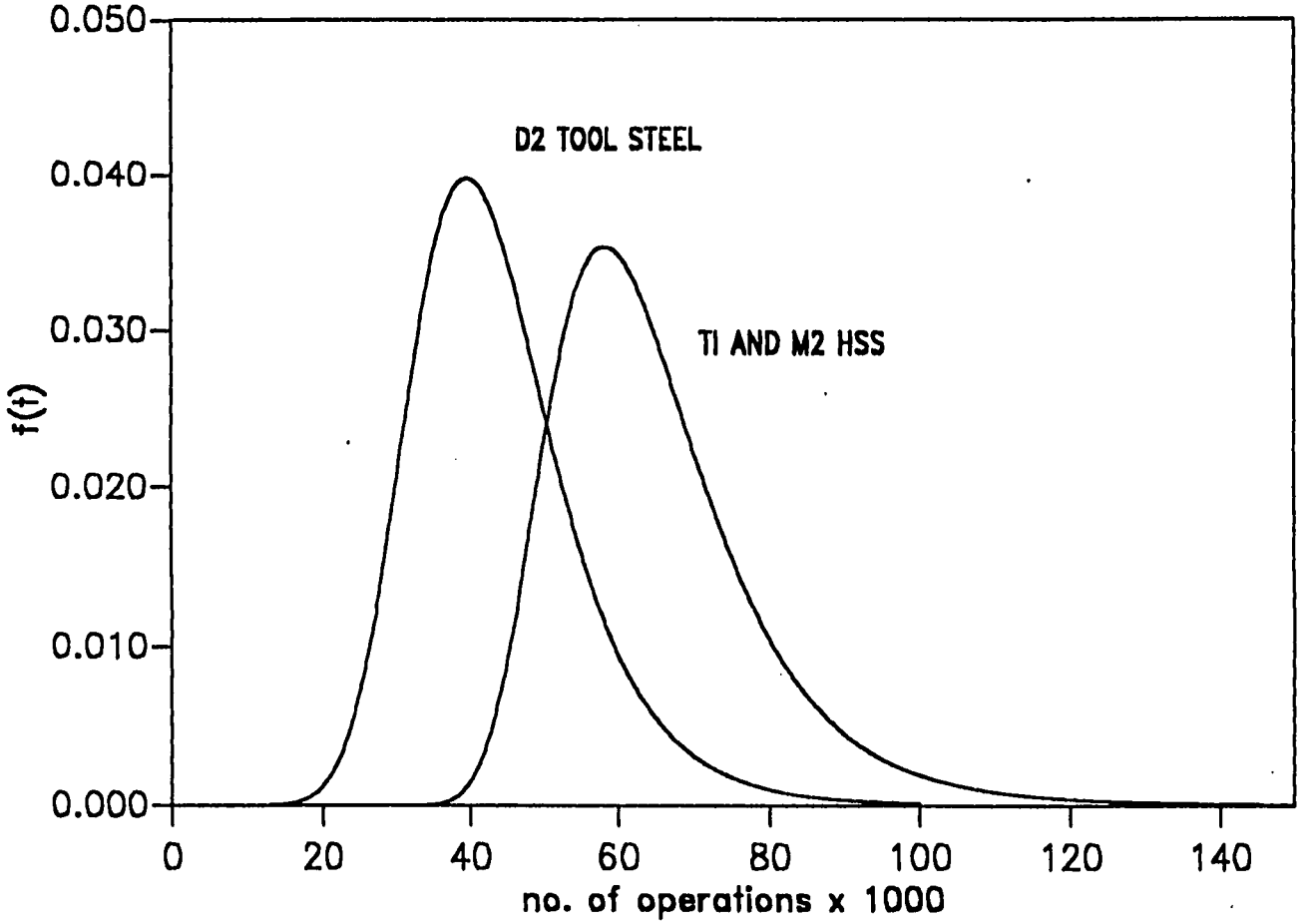

Fig. 2.11 Probability density function for three parameter Bernstein distribution obtained from damage function for blanking dies at critical damage level Data from Ref [22]. [See Table 2.2 for distribution parameters].

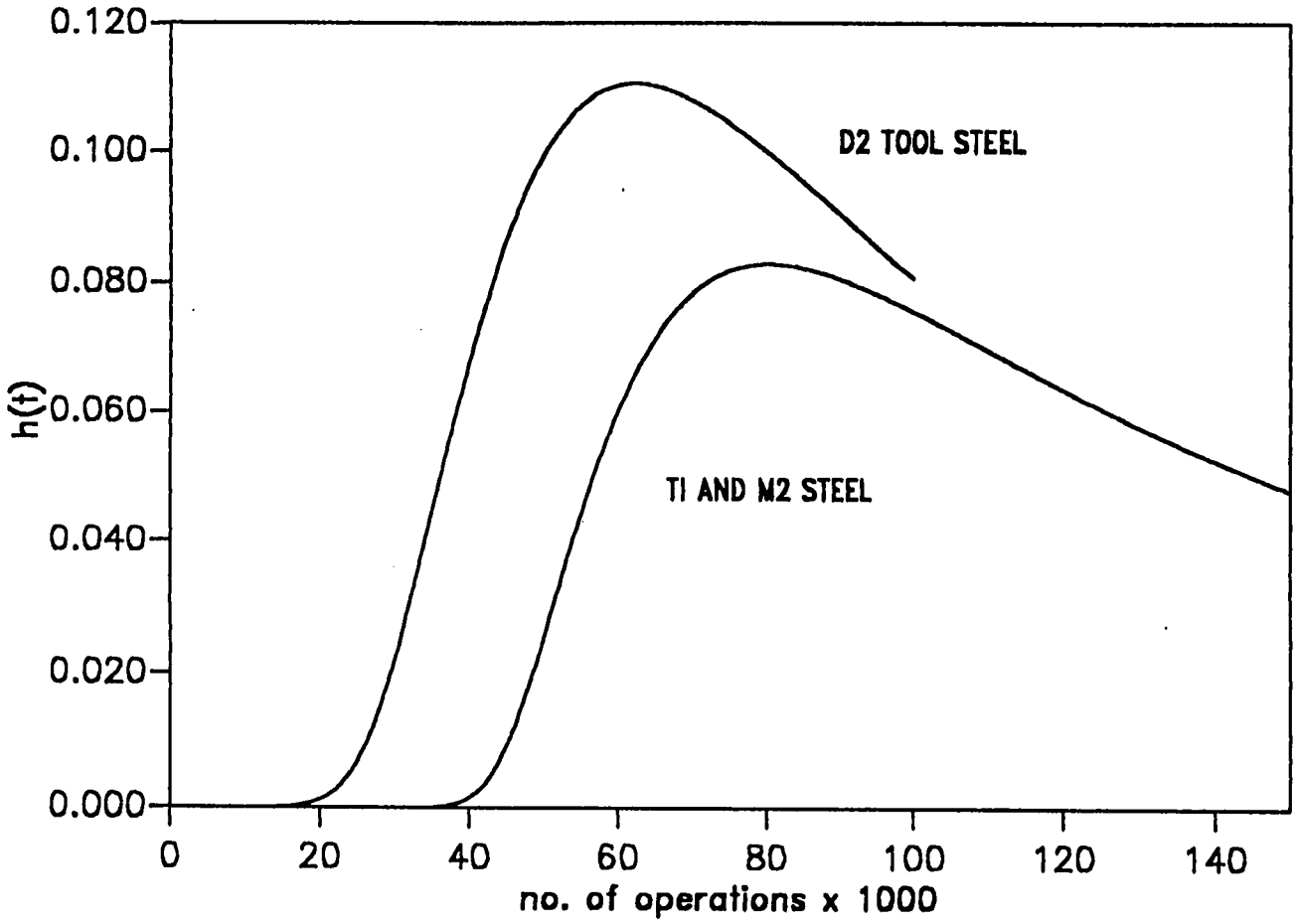

Fig. 2.12 Hazard function for three parameter Bernstein distribution obtained from damage function for blanking dies at critical damage level Data from Ref [22]. [See Table 2.2 for distribution parameters].

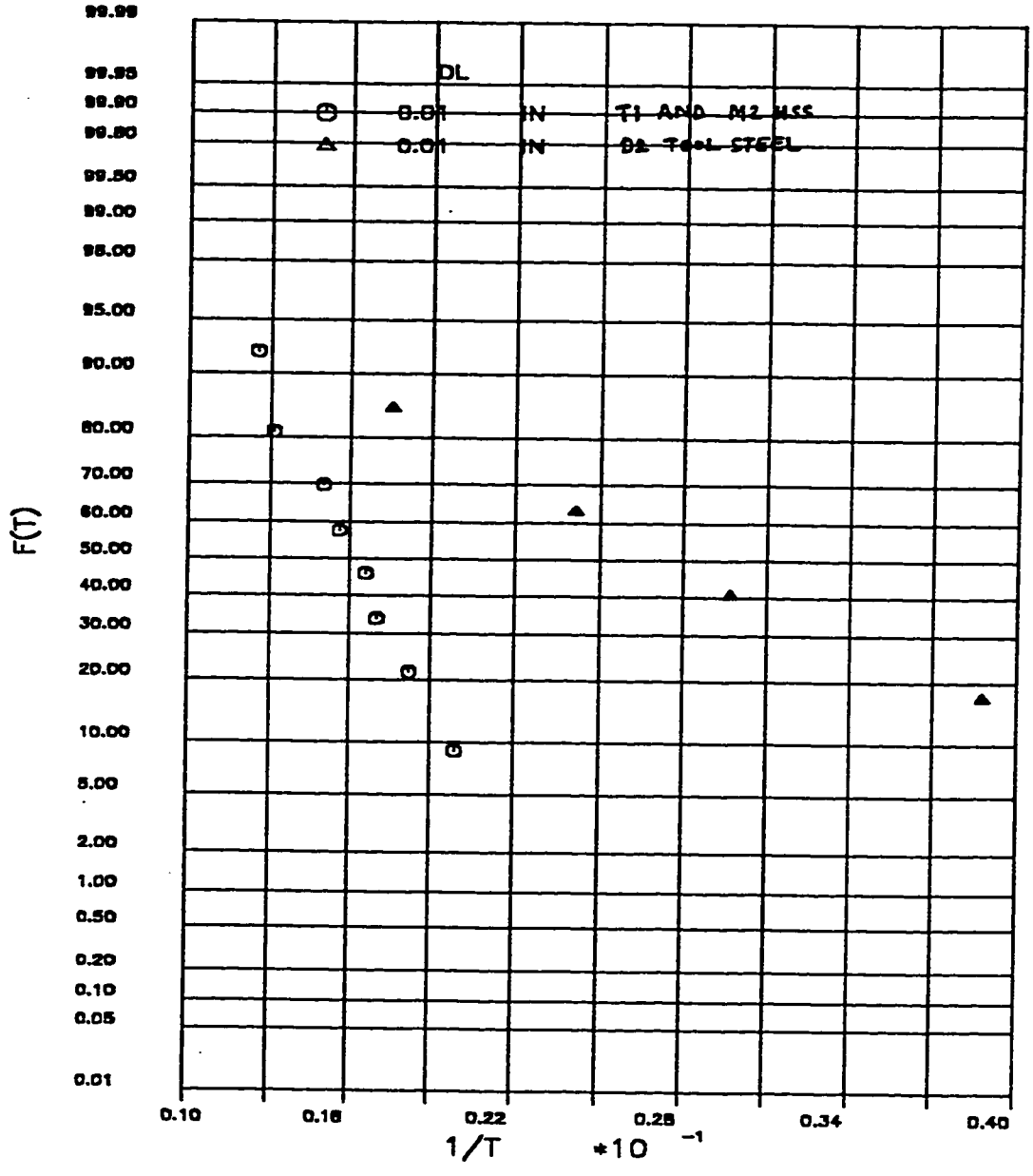

Fig. 2.13 Inverted normal distribution of time to failure of blanking dies at critical damage level for TI AND M2 HSS and D2 TOOL STEEL . Data from Ref [22].

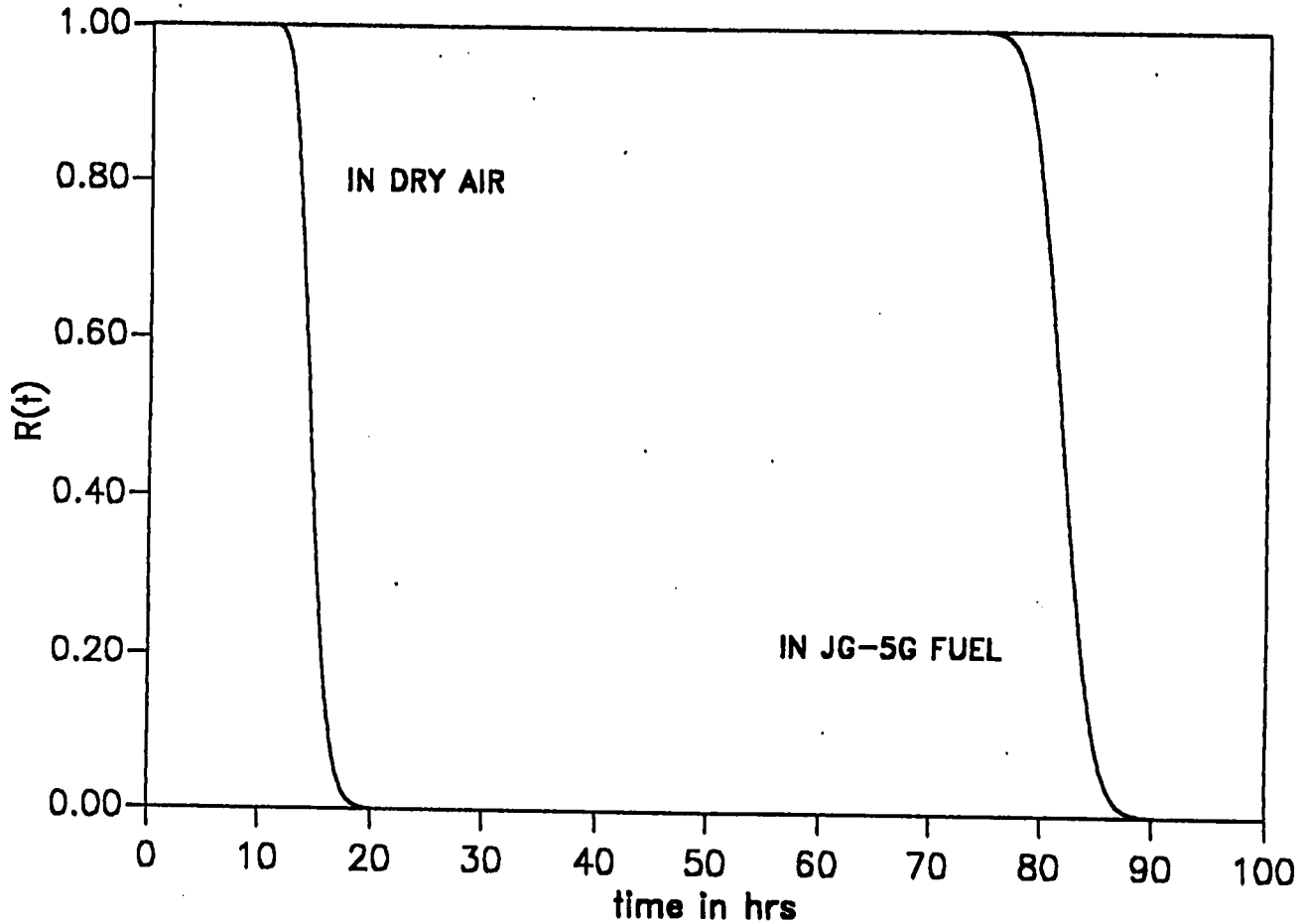

Fig. 2.14 Reliability function for three parameter Bernstein distribution of Type 2 spline at critical damage level. Data from Ref [23]. [See Table 2.3 for distribution parameters].

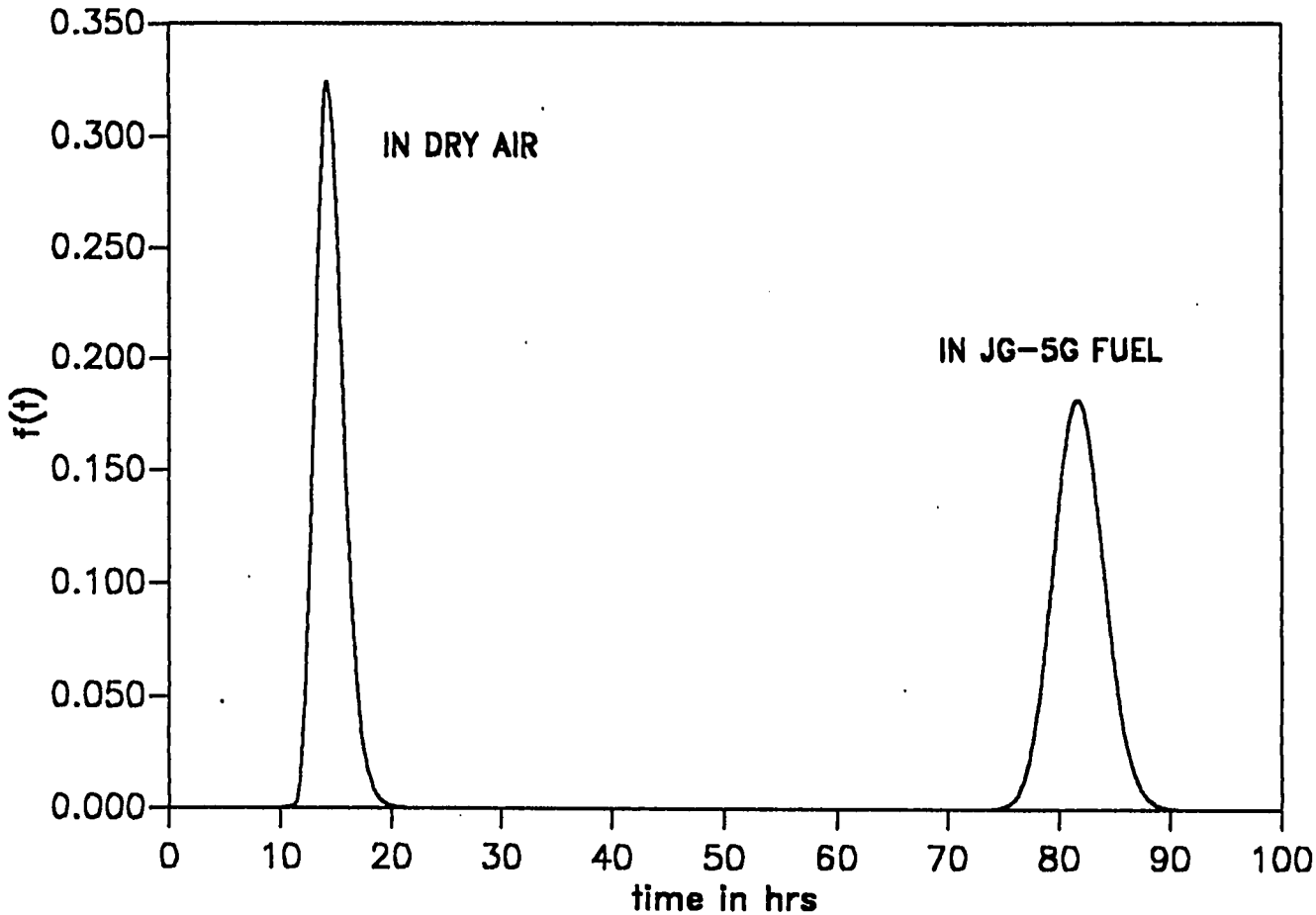

Fig. 2.15 Probability density function for three parameter Bernstein distribution of Type 2 spline at critical damage level. Data from Ref [23]. [See Table 2.3 for distribution parameters].

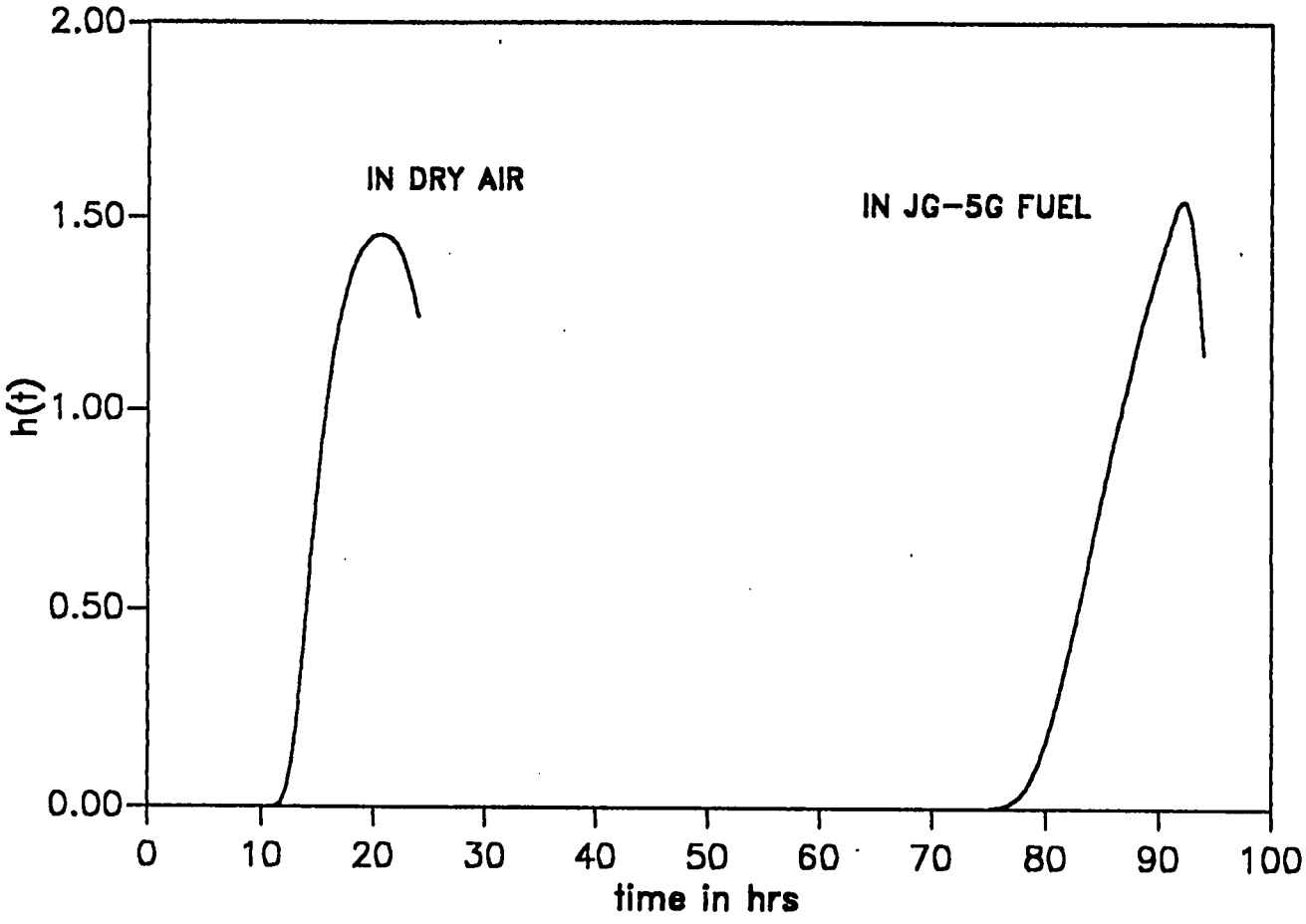

Fig. 2.16 Hazard function for three parameter Bernstein distribution of Type 2 spline at critical damage level. Data from Ref [23]. [See Table 2.3 for distribution parameters].

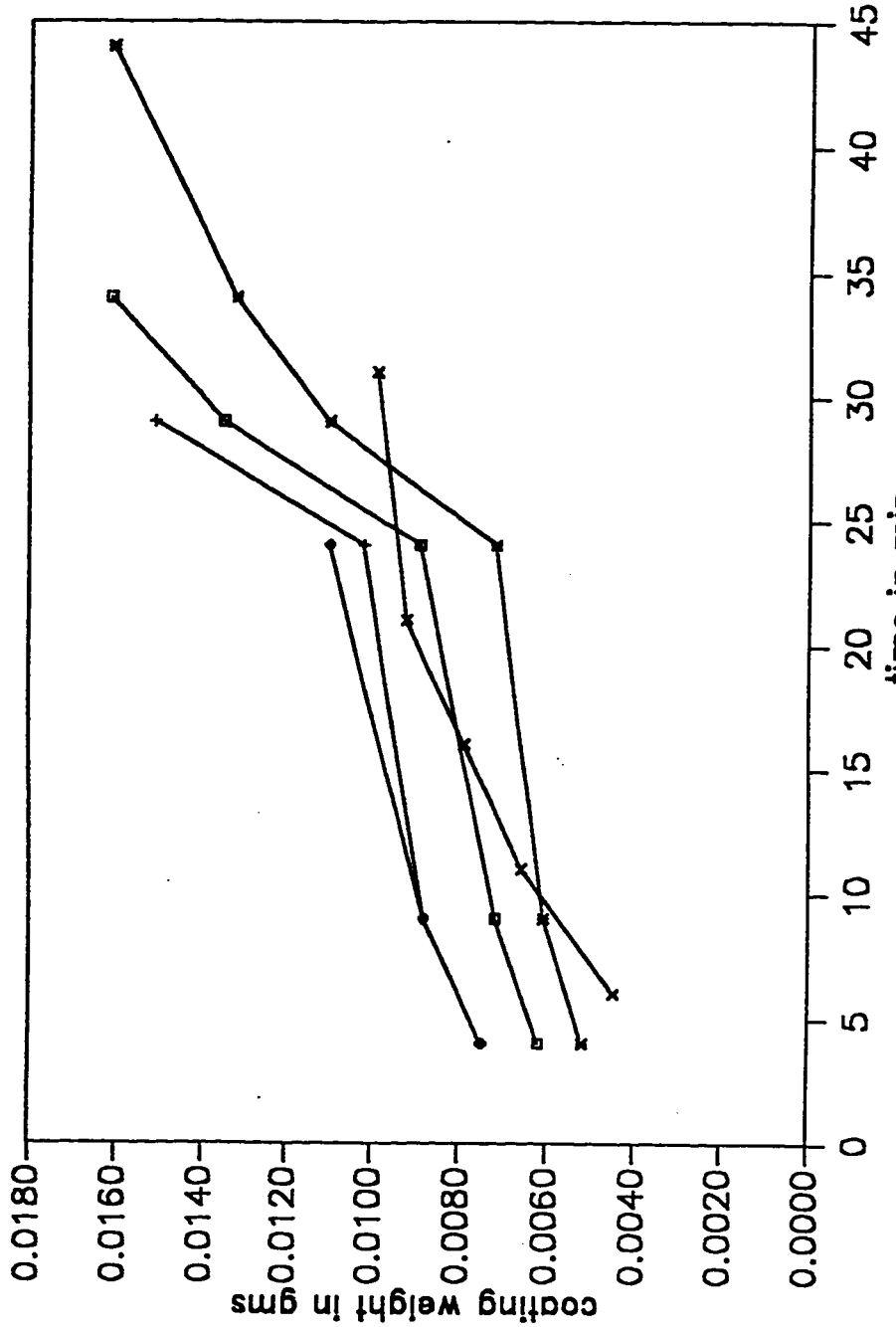

Fig. 2.17 Linear sample functions of coated surfaces of group 2 [24].

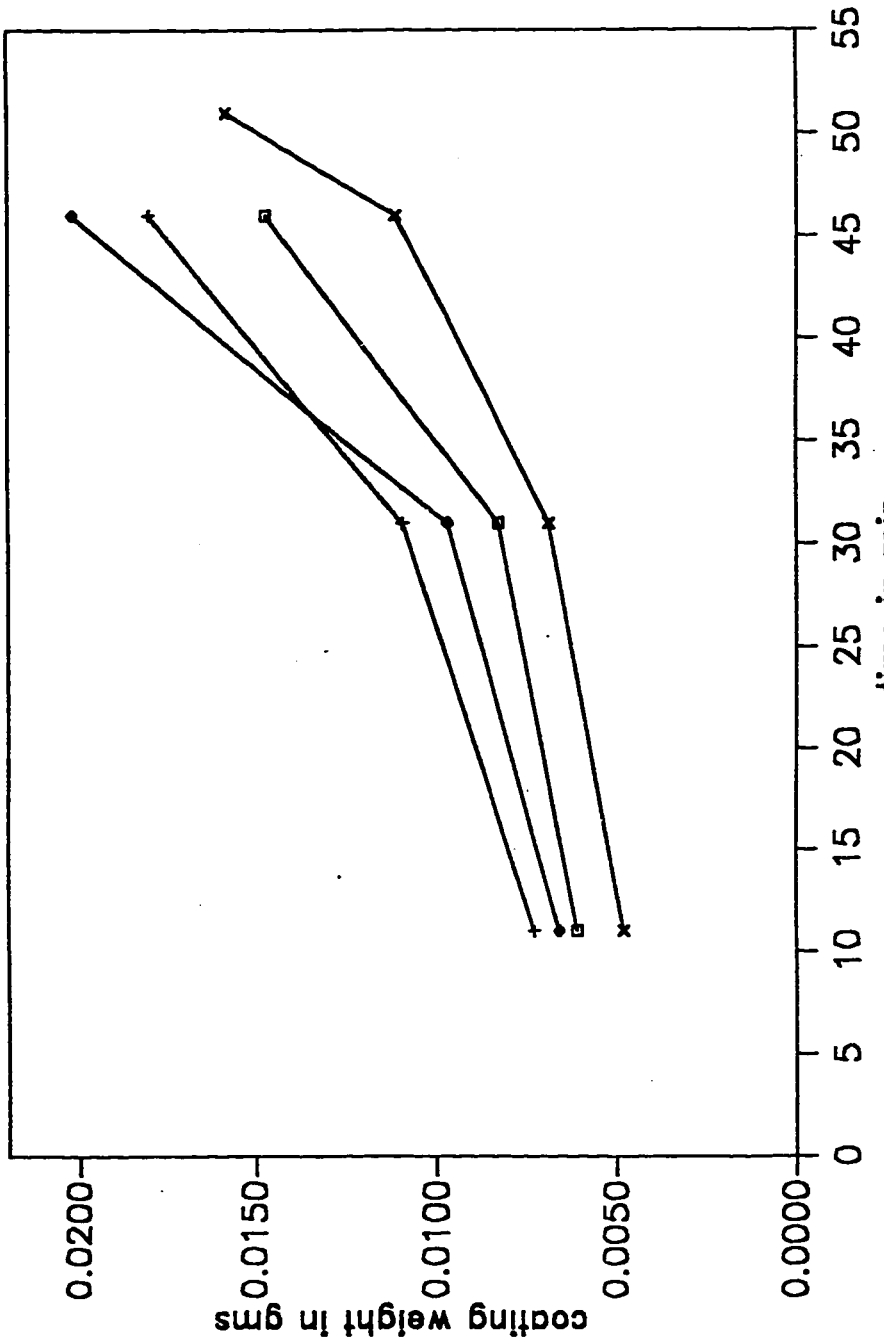

Fig. 2.18 Linear sample functions of coated surfaces of group 3 [24].

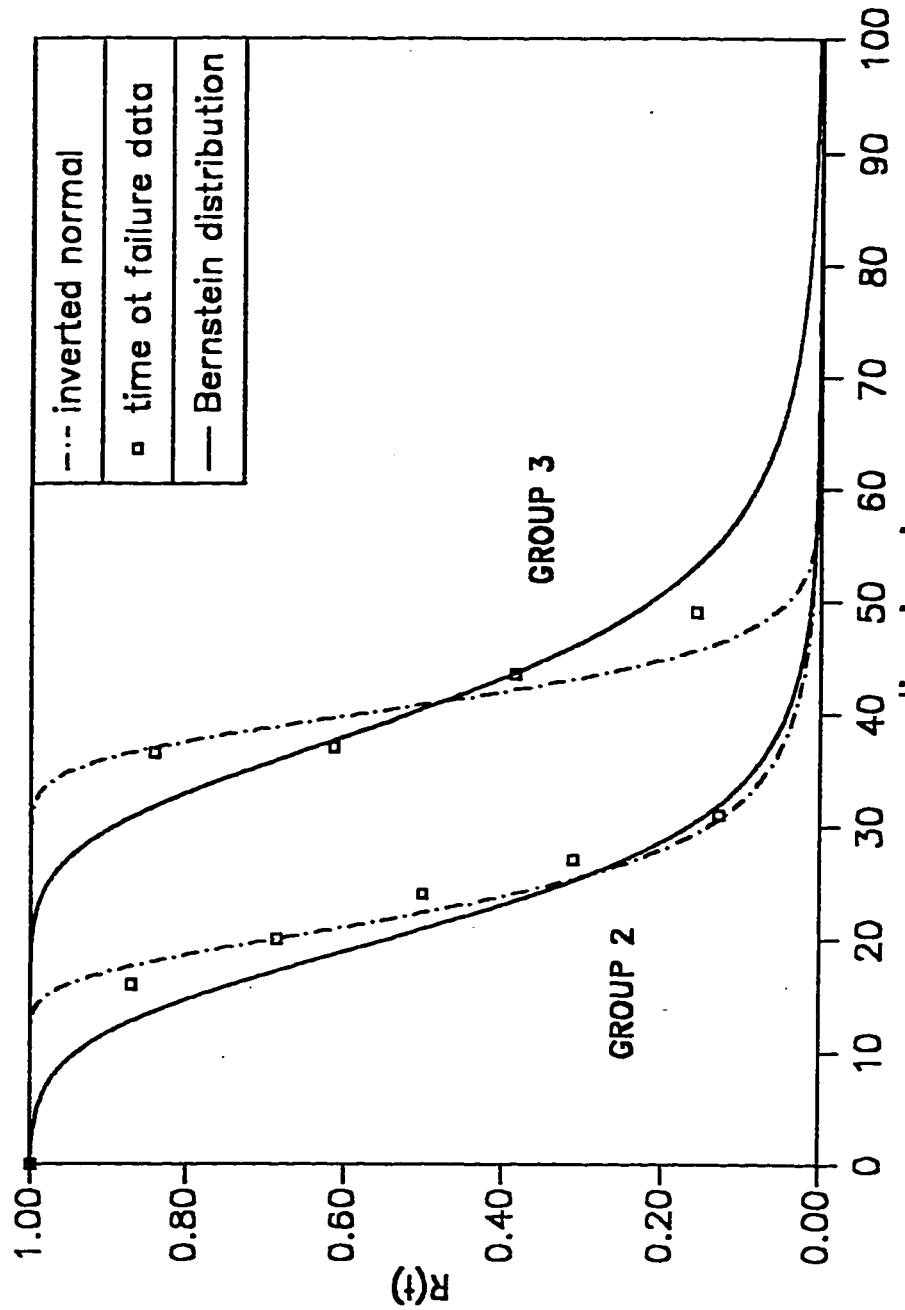

Fig. 2.19 Reliability function for three parameter Bernstein distribution obtained from damage function with actual time to failure data and empirically fitted inverted normal distribution for coating weight at critical damage level for groups 2 and 3. Data from Ref [24]. [See Table 2.5 for distribution parameters].

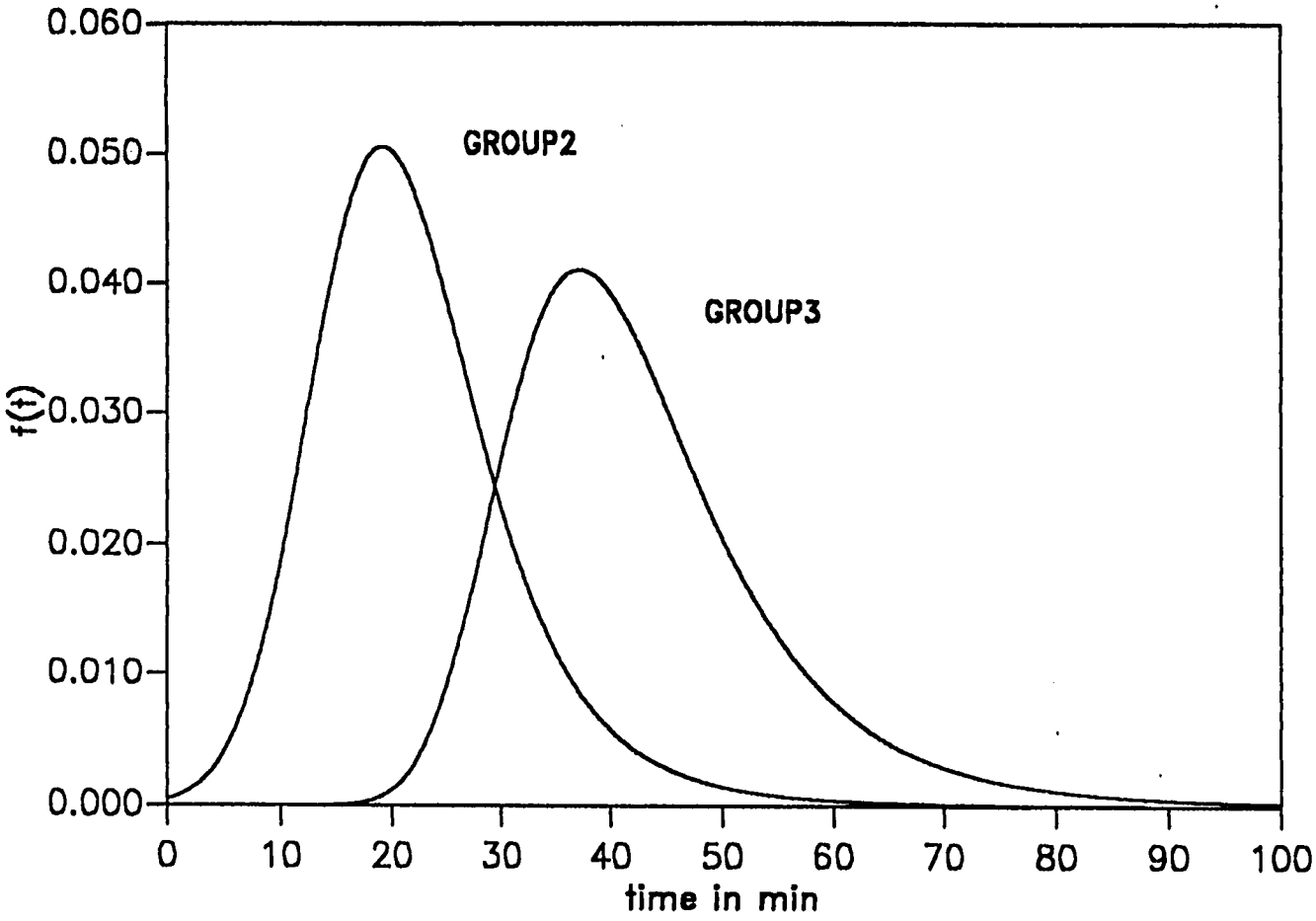

Fig. 2.20 Probability density function for three parameter Bernstein distribution obtained from damage function for coating weight at critical damage level for groups 2 and 3. Data from Ref [24]. [See Table 2.5 for distribution parameters].

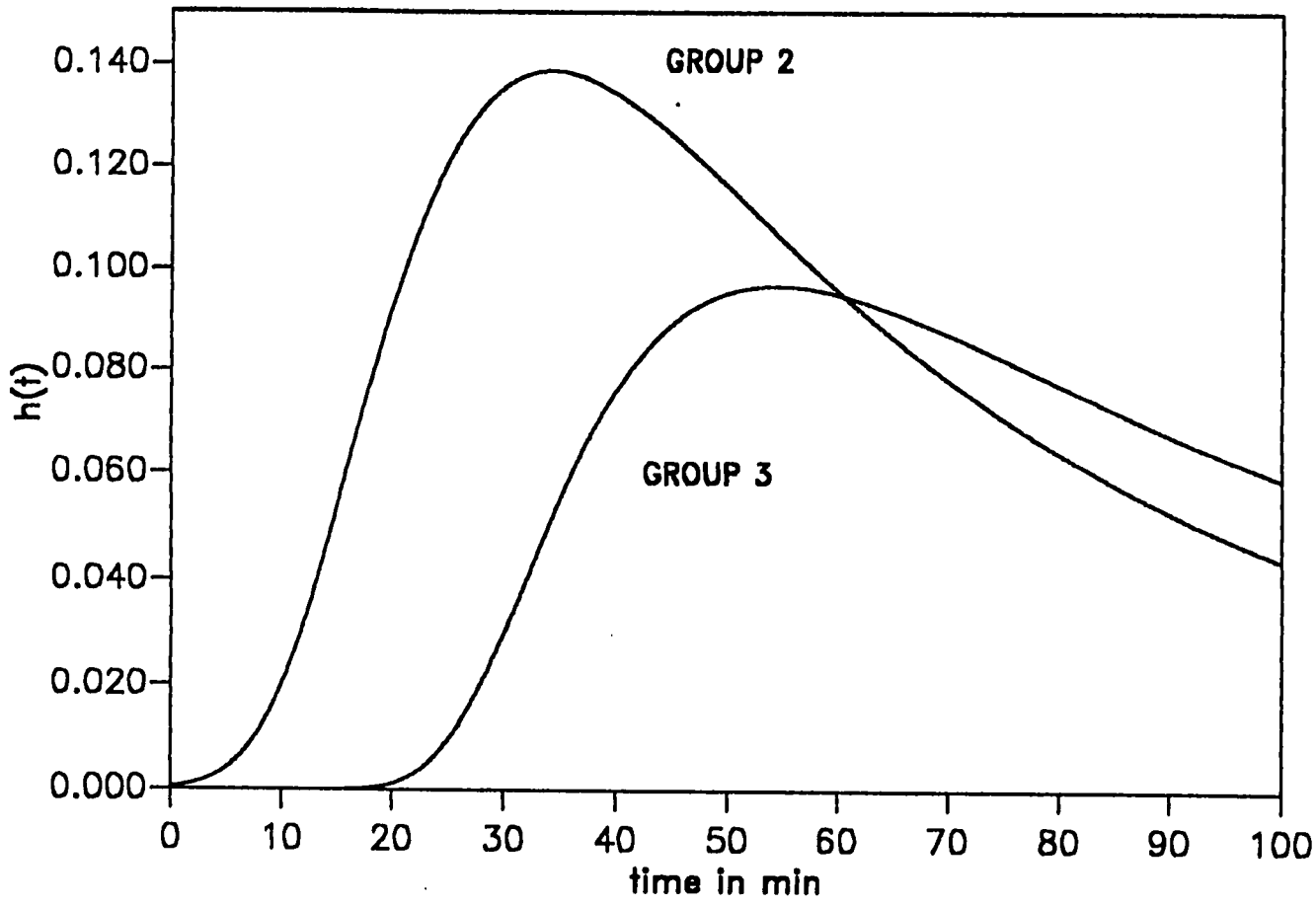

Fig. 2.21 Hazard function for three parameter Bernstein distribution obtained from damage function for coating weight at critical damage level for groups 2 and 3. Data from Ref [24]. [See Table 2.5 for distribution parameters].

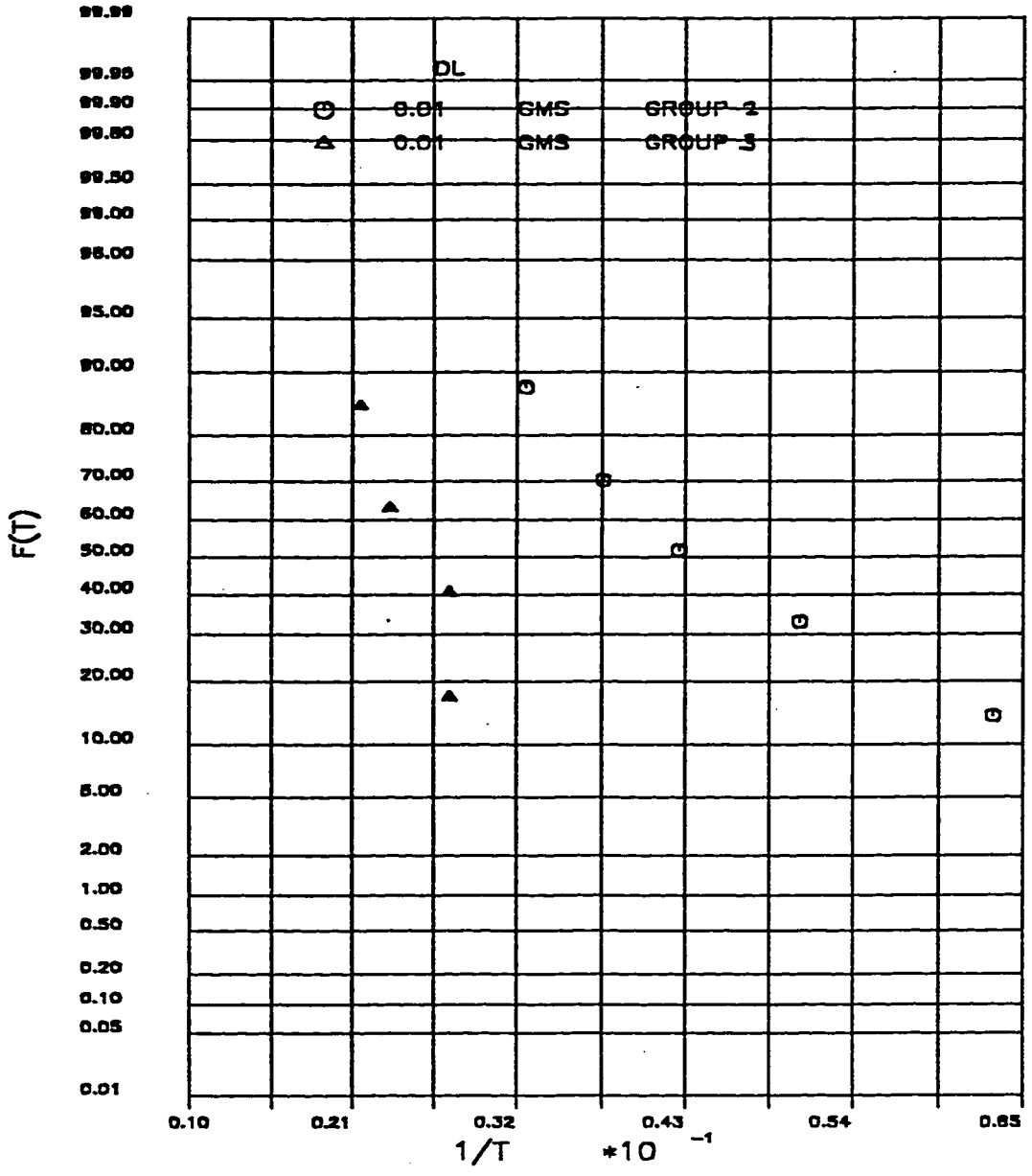

Fig. 2.22 Inverted normal distribution of time to failure for coating weight at critical damage level for groups 2 and 3. Data from Ref [24].

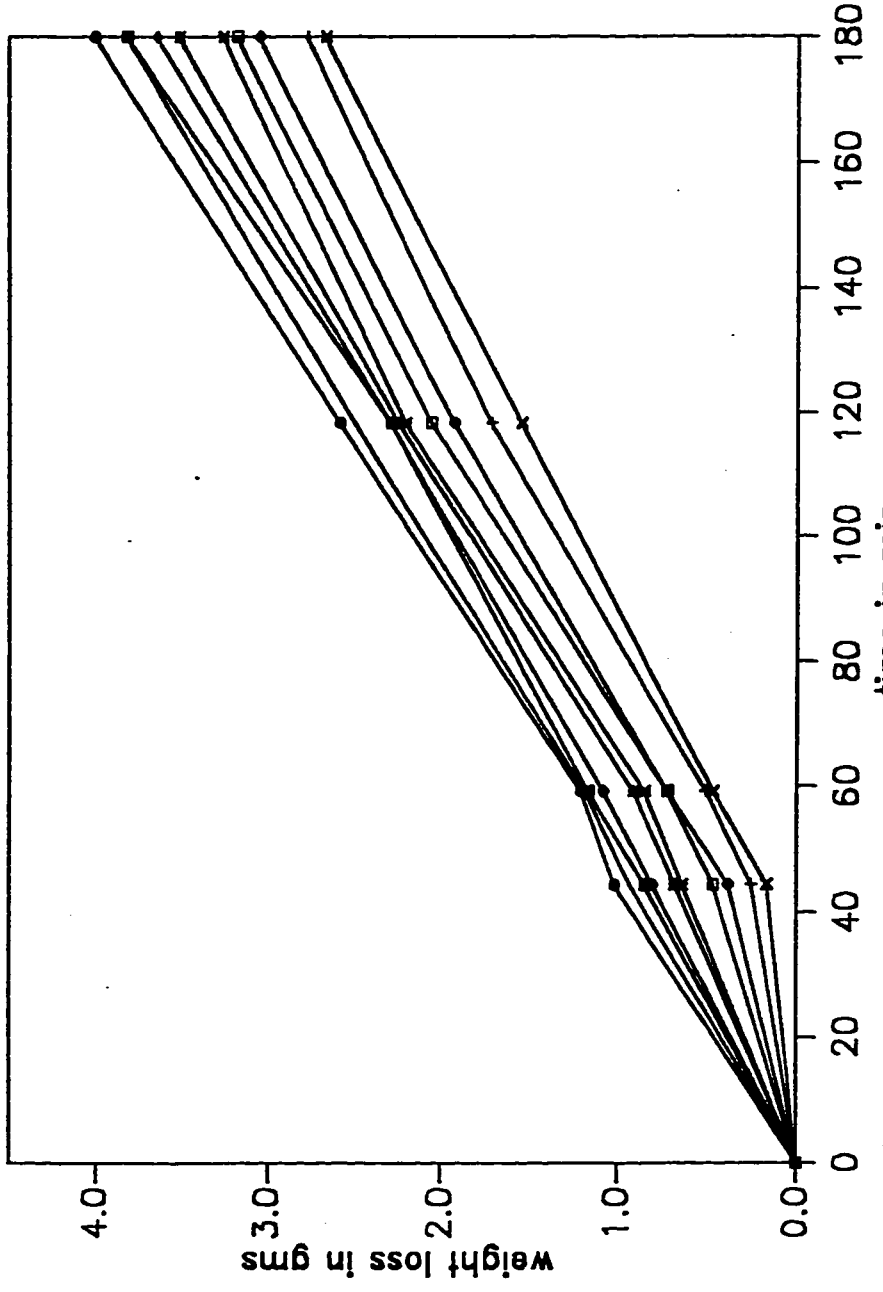

Fig. 2.23 Sample functions of linear wear [20].

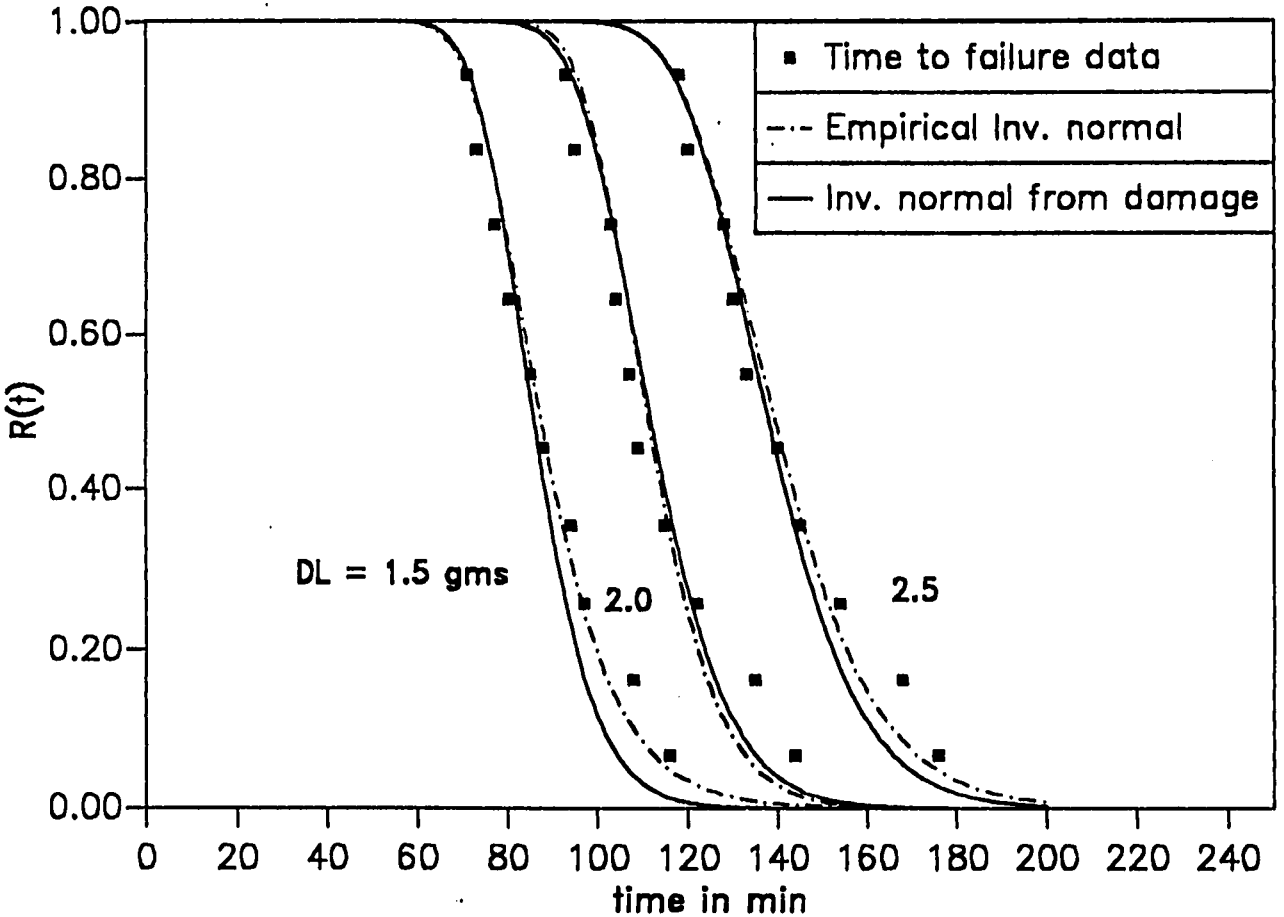

Fig. 2.24 Reliability function for two parameter Inverted normal distribution obtained from damage function with actual time to failure data and empirically fitted inverted normal distribution for wear at different critical damage levels. Data from Ref [20]. [See Table 2.6 for distribution parameters].

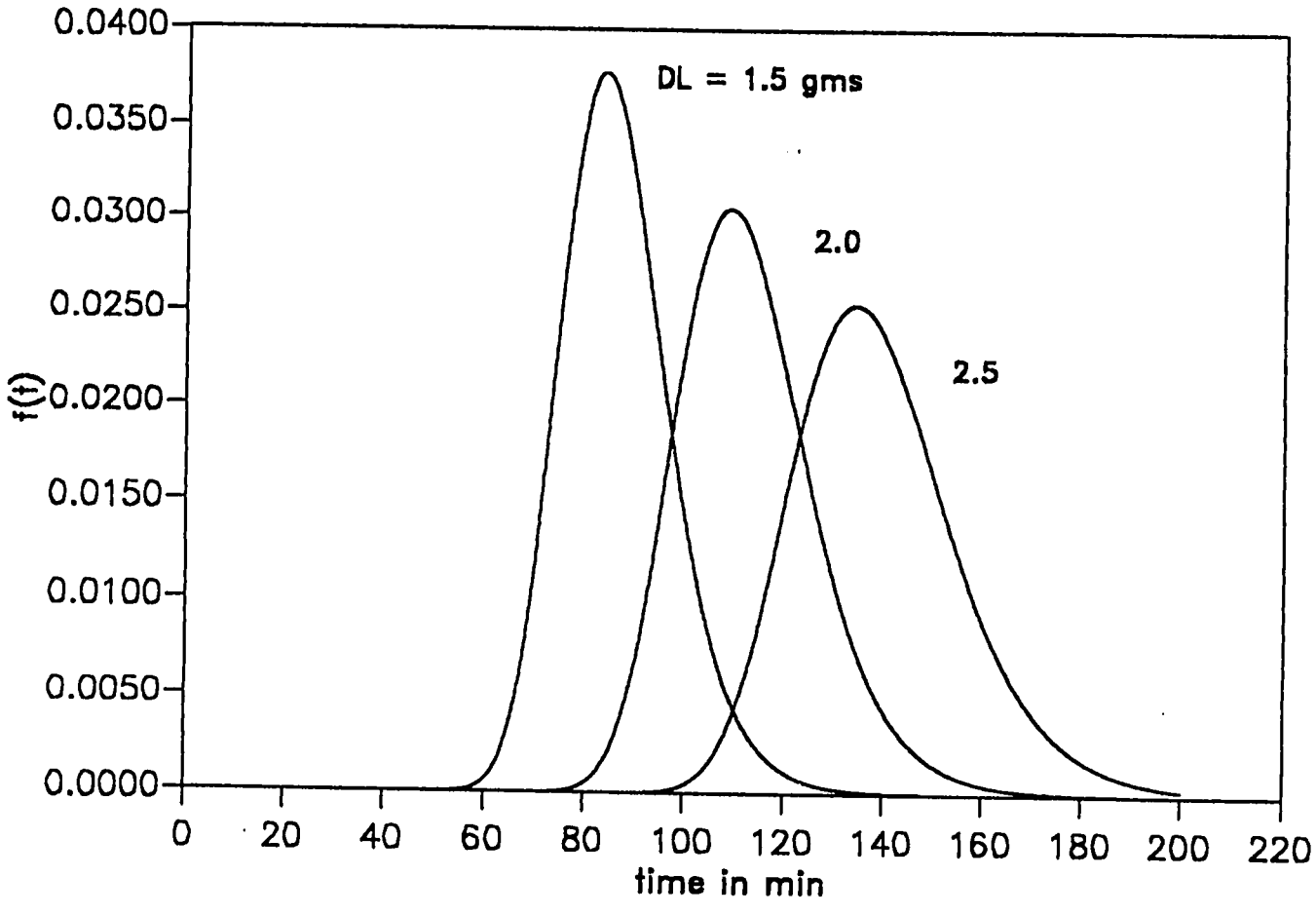

Fig. 2.25 Probability density function for two parameter Inverted normal distribution obtained from damage function for wear at different critical damage levels. Data from Ref [20]. [See Table 2.6 for distribution parameters].

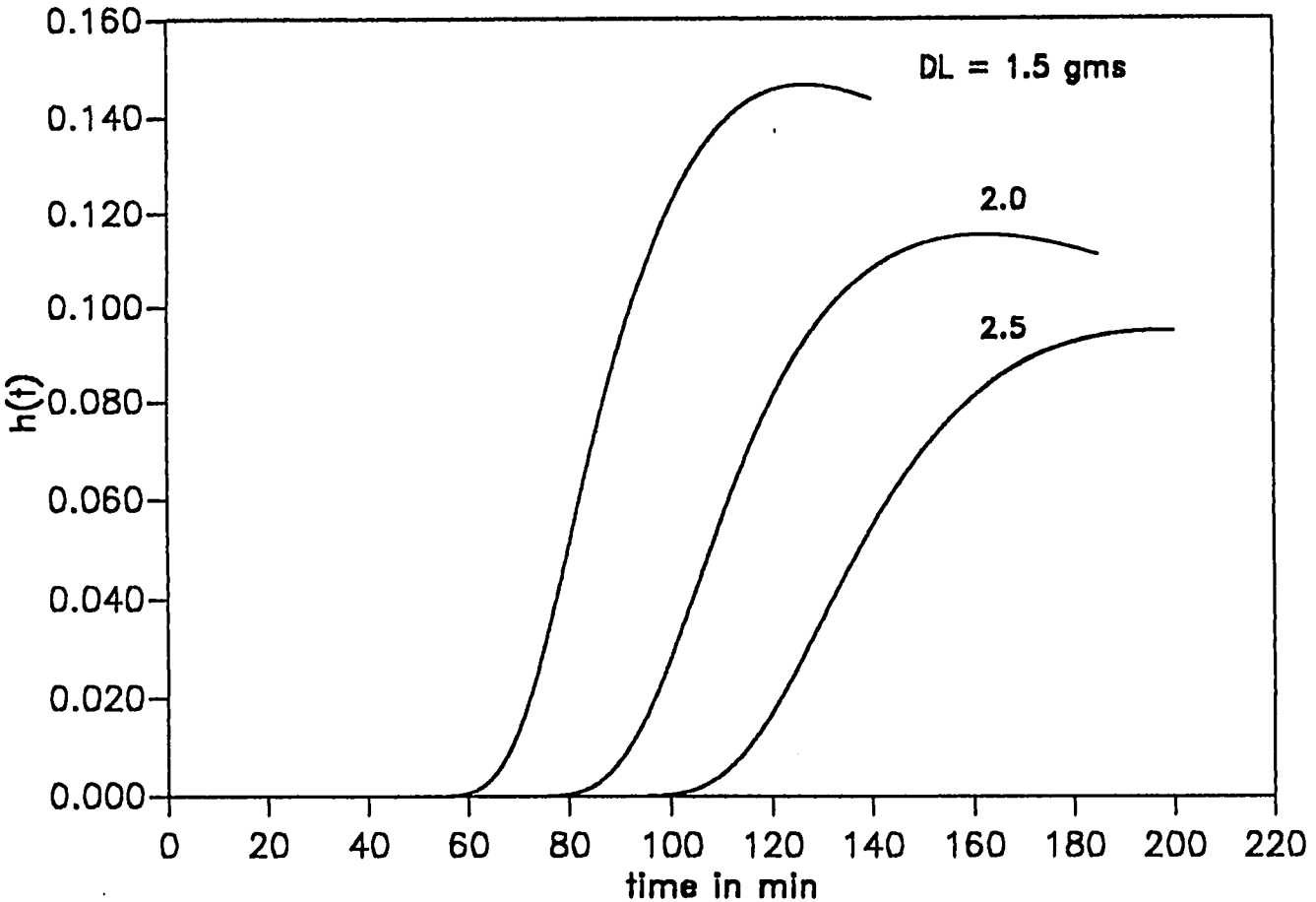

Fig. 2.26 Hazard function for two parameter Inverted normal distribution obtained from damage function for wear at different critical damage levels. Data from Ref [20], [See Table 2.6 for distribution parameters].

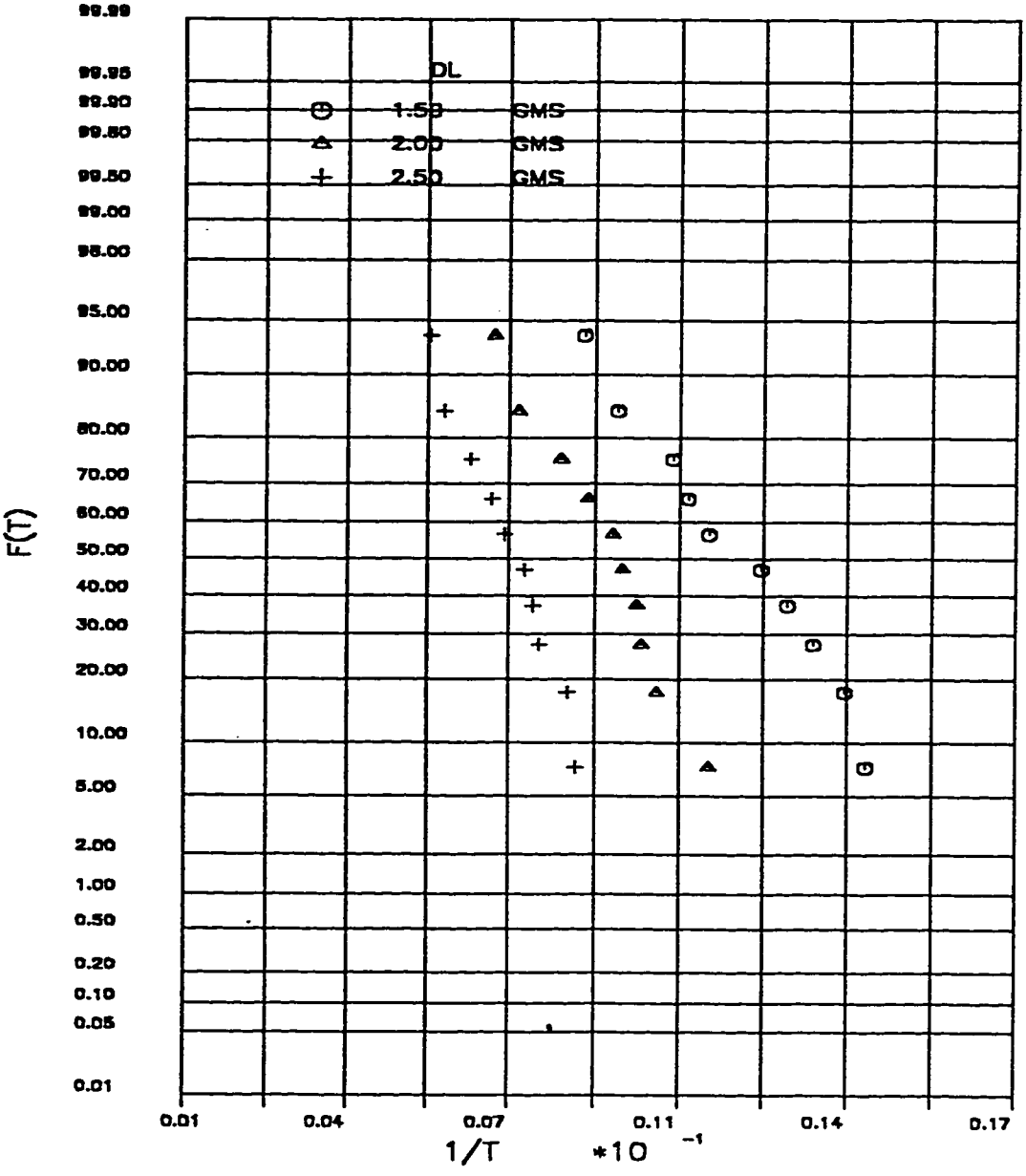

Fig. 2.27 Inverted normal distribution of time to failure of wear at different critical damage levels. Data from Ref [20].

Table 2.1 Range of wear coefficients for sliding wear [25]

Condition	Wear coefficient, K
Metal/metal sliding	
Clean:	
like	5×10^{-3}
unlike	2×10^{-3}
Poorly lubricated:	
like	2×10^{-4}
unlike	2×10^{-4}
Average lubrication:	
like	2×10^{-5}
unlike	2×10^{-5}
Excellent lubrication:	
like	2×10^{-6} to 10^{-7}
unlike	2×10^{-6} to 10^{-7}
Non-metal/metal sliding	
Clean	5×10^{-5}
Poorly lubricated	5×10^{-6}
Average lubrication	5×10^{-6}
Excellent lubrication	2×10^{-6}
Abrasion	
2-body,0 (100 μm) particular	1×10^{-1}
3-body,0 (100 μm) particular	5×10^{-3}
3-body,0 (≤1 μm) particular	10^{-7} to 10^{-4}

Table 2.2 Parameters of the distribution for blanking dies [22].

Fig.	Symbol	Basis	Distribution	Distribution parameters				Material
2.11	———	Damage function	Bernstein model	D_l	c	α	β	TI and M2 HSS
				0.01	62.274	0.037	3.04	
	—·—·—	Time to failure	Inverted normal	D_l	$\hat{c}$		$\hat{\alpha}$	
				0.01	16.77		0.117	
2.11	———	Damage function	Bernstein model	D_l	c	α	β	D2 Tool Steel
				0.01	42.181	0.034	47.73	
	—·—·—·—	Time to failure	Inverted normal	D_l	$\hat{c}$		$\hat{\alpha}$	
				0.01	37.03		0.084	

Table 2.3 Parameters of the distribution for aircraft splines [23].

Fig.	Symbol	Basis	Distribution	Distribution parameters				Type 2
2.14	———	Damage function	Bernstein model	D_1	c	α	β	In dry air
				0.03	14.44	0.0075	0.0035	
2.14	———	Damage function	Bernstein model	D_1	c	α	β	JP - 5G
				0.03	81.73	0.0007	0.0158	

Table 2.4 Relaibility comparison of empirical model and Bernstein model for aircraft splines

Cases	Empirical model [23]	Bernstein model
1	0.986	0.988
2	0.0	0.0
3	0.9989	0.999
4	0.981	0.990
5.1	1.0	1.0
5.2	1.0	0.999

Table 2.5 Parameters of the distribution for coating surfaces [24].

Fig.	Symbol	Basis	Distribution	Distribution parameters				Group
2.11	———	Damage function	Bernstein model	D_1	c	α	β	2
				0.01	20.917	0.049	44.69	
	—·—·—·—	Time to failure	Inverted normal	D_1	$\hat{c}$		$\hat{\alpha}$	
				0.01	22.37		0.057	
2.11	———	Damage function	Bernstein model	D_1	c	α	β	3
				0.014	40.414	0.047	30.61	
	—·—·—·—	Time to failure	Inverted normal	D_1	$\hat{c}$		$\hat{\alpha}$	
				0.014	40.82		0.011	

Table 2.6 Parameters of the distribution for wear [20]

Fig.	Symbol	Basis	Distribution	Distribution parameters		
2.24	———	Damage function	Inverted normal	D_1	c	α
				1.50 2.00 2.50	85.45 111.44 137.44	0.012 0.012 0.012
	—·—·—	Time to failure	Inverted normal	D_1	$\hat{c}$	$\hat{\alpha}$
				1.50 2.00 2.50	87.05 110.99 138.93	0.023 0.012 0.016

CHAPTER 3

3. CORROSION AND OXIDATION

3.1 INTRODUCTION

Corrosion is one of the principal causes of failure for many engineering systems of the present day world. Corrosion causes loss of production, plant shut down, loss of appearance, contamination of product, effects on safety and reliability, and complete failure of the system. Estimates of annual cost of corrosion in U.S. was attributed as high as 30 billion dollars [26]. *Corrosion is defined as the degradation of a material because of its reaction with environment.*

The type of corrosion, its rate and the extent to which it progresses are influenced by the nature, composition and uniformity of the environment and the metal surface that is in contact with that environment. These factors does not remain constant as corrosion progress, but are affected by externally imposed changes and by changes that occur as a direct consequence of the corrosion process itself. Processing and fabrication operations such as grinding, forming, cold working etc., produce changes in metal parts to varying degree and affect their susceptibility to general and localized corrosion. Corrosion can penetrate the wall thickness resulting into leakage of a container, pipe or a tube, which can be viewed as failure in many cases. There are different forms of

corrosion, out of which *stress corrosion cracking* is the most severe followed by *pitting* in view of their destructive and insidious nature.

Let us look at the process of propagation of corrosion inside a metal. The metal consists of elementary volumes the properties of which have random variations. In particular, their resistivity to penetration of corrosion varies randomly. Corrosion begins at the surface and proceeds from volume to volume. When corrosion reaches a given region in the metal, it acquires a certain rate of propagation depending on the properties of that region. Since these properties are random, the rate of corrosion is also random. This rate of corrosion will undergo random changes as it proceeds form one region to the next. Thus, although the external conditions (the corroding medium) remain nominally unchanged, the rate of corrosion is subject to random variations resulting into sample functions such as discussed in Chapter 1.

3.2 STRESS CORROSION CRACKING

3.2.1 INTRODUCTION

When certain metal alloys are exposed to a corrosive environment, while at the sametime they are subjected to an appreciable, continuously maintained, tensile stress, rapid structural failure can occur as a result of stress corrosion. This phenomenon is known as stress corrosion cracking (SCC) and is characterized by a brittle type failure in a material that is otherwise ductile. To define the degree of stress corrosion susceptibility of a material thoroughly, a

complete stress-life curve must be determined, However, as this is expensive and time-consuming, stress corrosion tests are often made at a single applied stress, and materials are compared on the basis of the life obtained. The sources of high local stresses during manufacturing include thermal processing, stress raisers, surface finishing and fabrication techniques.

3.2.2 MECHANISM OF SCC

Although SCC represents a major corrosion problem, its mechanism is not well understood. The main reason for this is the complex interplay of metal, interface and environmental factors. A pit, trench or other discontinuity on the surface of the metal acts as stress raiser. Stress concentration at the tip of the notch increases tremendously as the radius of notch decreases. Once the crack has initiated, it starts propagating with a small radius. Plastic deformation occur in the region immediately preceding the crack tip because of high stresses. The combined action of stress and corrosion helps crack propagation, ultimately leading to a failure.

The parameter of time in SCC is important since the major physical damage occurs during the later stages. Initially the rate of crack movement is slow, but as cracking progresses the cross sectional area of the specimen decreases and the applied stress increases. As a result, the rate of crack movement increases with crack depth until rupture occurs.

Staehle [27] demonstrated that the crack growth on iron base alloys will

follow a logarithmic relationship with time.

3.2.3 STOCHASTIC NATURE OF SCC

The SCC is a time dependent mechanism which can eventually lead to a sudden failure of the material in a specific environment The initiation and propagation of a stress corrosion crack is influenced by factors such as applied stress, strain rate, electrochemical potential, operating temperatures, metallurgical characteristics and surface defects etc. The surface defects are experienced by geometrical discontinuities which facilitates to produce cracks due to residual or applied stress. Recent developments in fracture mechanics, electrochemistry and metallurgy have contributed to a better understanding of the phenomenon and have provide a quantitative basis for predicting the failure life. It should be emphasized however that these approaches are deterministic but in the reality the variables or factors causing the SCC random in nature, therefore statistical and probabilistic interpretations of the SCC process. This was earlier pointed out by Evans [28] by highlighting the intrisinic statistical and probabilistic nature of localized corrosion.

3.2.4 RELIABILITY EVALUATION OF COMPONENTS SUBJECTED TO SCC

Generally, a laboratory accelerated test for determining susceptibility to SCC uses severe conditions such as higher applied stress, higher temperature and higher concentration of aggressive solutions than that of actual service

conditions, in order to minimize the testing time. Such severe conditions are useful for collecting valuable information in a short time, but may not provide reliable data concerning the long term performance, especially for failure life estimation, because the mechanism operating on short term basis may not always be identical to that of the long term performance in service. Furthermore, the failure life of SCC, when measured under well controlled conditions, has shown large scatter, but its statistical nature or distribution at a specified limit of crack length has rarely been studied. Booth and Tucker [29] tried to fit several distributions to time to failure data, including normal, lognormal and extreme value distributions, for an Al-5% Mg alloy and concluded that the lognormal distribution fitted best. The lognormal time to failure distribution has also been reported for type 310SS/ $MgCl_2$ [30], for 7475 Al alloy/3% NaCl [31]. Harshbarger et al. [32] have pointed out the importance of weibull distribution for evaluating SCC failure time. The weibull distribution for time to failure has been found to characterize the materials such as 2014 Al alloys/5% Nacl [33], type 304 sensitized SS/BWR simulated water [34]. Strecker et.al, [35] found an exponential distribution of failure time with hydrogen-induced cracking in 0.95 C steel.

Based on the investigation reported in ref [29,30,31] the damage model $D(t) = D_i(t) + r\,\mathrm{Int}$ can be postulated to characterize the time dependent behavior of SCC. Using this model the data from Kaneko and Simenz [36] was analysed, which shows a considerable scatter in the crack growth for aluminium

alloys. The data is actually given in the form of range of crack growth with respect to time. Fig. 3.1 shows the same data (material 7075-T6) when plotted on a log scale. The the growth rate law is assumed to be of the type $D(\tau) = D_i(0) + r \ln(\tau)$, where $\tau = t - t_o$ and t_o is the induction time. Assuming a 6σ limit for the total variation in the damage at any time t, the data is further processed. For such type of damage function a three parameter log Bernstein distribution is appropriate (Sec 1.10). Figs. 3.2, 3.3, and 3.4 shows the reliability, probability density function and hazard function for different critical damage limits.

Hines and Jones [37] conducted SCC experiments on different types of Cr-Ni austenitic steels. There is a considerable scatter in time to fracture of the replicate specimens of the same material at the same applied stress level. The data is given in the form of logarithmic time. Time to fracture or failures are given at specific stress level. Since the information about damage law is not available we can assume as a first approximation that the damage function is of the type $D(t) = r\ln t$, which leads to an inverted lognormal model (Sec 1.9.2). To check the accuracy of assumption the inverted lognormal model need to be validated from direct time to failure data. The time to data is plotted on the normal probability paper [F(T) vs 1/lnT] for different steel materials as shown in Figs. 3.5 to 3.9. An approximate straight line behavior of these values demonstrates the validity of the inverted log-normal distribution. and underlying assumption about the damage function. The parameters

$\log_e T_M(c_i)$ and $\hat{\alpha}_i$ are calculated using eqs. (1.50) and (1.51). Fig.. 3.10 and 3.11 shows the variation of c_i and α_i with respect to stress σ.

3.3 PITTING

3.3.1 INTRODUCTION

Pitting is an important type of localized attack that results in the form of sharp tiny holes in the metal known as 'pits.' It is one of the most insidious forms of corrosion and causes failure by perforation while producing only a small amount of weight loss on the metal. A large number of small pits on generally uncorroded surface may not be detected by visual inspection or laboratory tests, and their potential for damage may be underestimated. It is also difficult to have quantitative knowledge of the pitting, because of the varying depth and distribution of pits over the surface. The cause for pitting may be the inclusions in the matrix of alloy, local mechanical damage or chemical breakdown of surface film, particles of debris, oxygen depletion beneath non-protective films of corrosion product etc. Sometimes the pits require several months to show up in actual service. Pitting is particularly vicious because it is a localized and intense form of corrosion and failures often occur with extreme suddenness. The dominant factors influencing the pitting are metallurgical, chemical (i.e., chemical composition) and operational (i.e.,velocity, temperature).

3.3.2 MECHANISM OF PITTING

Pitting is divided into two stages. First one, is the pit initiation, and second one, is the pit propagation. The pit initiation mechanism is based on several theories. The mechanical differences such as scratches, rough surfaces, impurities, grain boundaries are favorable sites for pit formation. Once pit is initiated it penetrates through the metal. The rate of penetration depends upon the environment. The growth of pit is observed on horizontal surface in the direction of gravity, whereas surroundings are often unaffected. When a pit has reached a stable stage, it penetrates the metal at an increasing rate by an autocatalytic process and propagates to the maximum depth.

3.3.3 STATISTICAL ANALYSIS OF PITTING

The use of probability concepts in describing corrosion phenomenon was first introduced by Evans, Mears and Queanna [38]. Aziz and Godard [39] demonstrated the importance of specimen area, by experimentally verifying that the probability of pitting increases with the area metal exposed. Summerson et.al [40] also used statistical approach to analyze pit depths in aluminium material. Rosenfled [41] derived a statistical distribution of pit depths for 28 Cu-9Ni-Ti steel. Flaks [42] recommended the lognormal distribution as plausible statistical model of pit depth. Aziz [43], Eldredge [44], Ishikawa et.al [45] and Karkosh et.al [46] presented extreme value model for the deepest pits. Sheikh et.al [9] presented the stochastic characterization of the growth of deepest pits on an exposed surface and developed corresponding reliability models.

As seen from the literature that the pit depth growth has logarithmic relationship with time and at any instant of time the deepest pit $\mathbf{D}_{max}(t)$ is extreme value distributed [43,44,45,46] $\tilde{\mathbf{D}}_{max}(t)$ is the characteristic value of $\mathbf{D}_{max}(t)$ which correspond to $F[D_{max}(t)] = 0.37$. This can be easily shown for a Type I extreme value model.

$$P[\mathbf{D}(t) < \tilde{D}_{max}(t)] = \exp\{-\exp(0)\} = 0.37$$

The characteristic pit depth versus lnt is shown in Fig. 3.12 which demonstrates the validity of $\tilde{\mathbf{D}}(t) = \tilde{D}(1) + r\ln t$ which is the same model as discussed in Sec 1.11. eq (1.93). From the eq (1.93) the time to failure T can be calculated for different critical damage levels D_l Fig. 3.13 shows that the slopes r, the value of is constant for different realizations of maximum pit depth growth process. After knowing r γ can be determined using $r = \alpha(t)r$, which is $\approx \alpha r$ (when α is the asymptotic values of $\alpha(t)$) is the shape parameter of the weibull model, the various probability functions can be calculated from the eqs (1.81), (1.82), (1.83) and are shown in the Figs. 3.14 to 3.16. along with the time to failure data which is shown on the reliability curves. The validity of the weibull model is also checked directly by plotting the time to failure data on a weibull probability paper as shown in Fig. 3.17. Both the approaches give approximately same values of $\gamma \approx 3.1$. Therefore both the damage function based reliability model (as described in Sec 1.11 of Chapter 1) or direct time to failure analysis based reliability model are shown to be weibull distribution for the pitting corrosion process and further reinforce the accuracy of the mathematical formulation of Sec 1.11.

In some cases the pit depth shows a power law relation with respect to time. Crews [4] validated that log-normal distribution can be used to estimate the service life for such cases. The behavior shows logarithmic relationship $D(t) = D_i t^B$ (Sec 1.9. of Chapter 1). The data represents only one realization of the process. By linear regression analysis an estimate of the variance (or standard deviation $\sigma D(t)$ of the process can be made if the following assumptions are invoked about the characteristics of the underlying damage function

(a) $\ln D(t) = \ln D_i + B \ln t$

(b) $V(\ln B) = 0$ i.e., $\alpha_1 = 0$

(c) scatter is bounded in $\pm 3\sigma$ D(t) limits

Under these conditions the two parameter log-normal model is valid. The parameters of the model can be established using eqs (1.69), (1.70) and (1.71). Figs. 3.18 to 3.20 shows various probability functions at different critical damage levels.

However if the assumption (b) is not valid and rather $V(\ln D_i) = 0$ i.e., $\beta_1 = 0$ then the inverted log-normal model will be valid (Sec 1.9.2 of Chapter 1). Taking $\alpha_1 = 0.2$, various probability functions are shown in Figs. 3.18, 3.19, and 3.21. By comparing these curves one can see that inverted lognormal model is conservative to predict the reliable life in this case. Thus if the data is extremely limited then inverted lognormal reliability model should be preferred.

3.4 OXIDATION

3.4.1 INTRODUCTION

Oxidation, which is the terminology used in gas/metal reactions refers to the formation of oxide scales. It can occur in oxygen, air, carbon dioxide, or steam, or in more complex industrial atmospheres containing significant quantities of these gases. The growth of the scales (i.e. corrosion rate) is determined by numerous metallurgical and environmental parameters and the properties of the scales themselves.

There are several ways of measuring the extent of oxidation. Measurement of weight changes per unit area in a given time is a popular procedure. It should be noted that, unless the scale detach off, oxidation is accompanied by weight gain. Because some of the scale can be lost by spalling, some researchers prefer to report the attack as weight loss. A metalographic technique used in laboratory to determine the extent of oxidation measures the amount of metal loss.

3.4.2 MECHANISM OF OXIDATION

A clean reactive metal surface exposed to oxygen follows the sequence (i) adsorption of oxygen (ii) formation of oxide nuclei (iii) growth of continuous oxide film. Because the free energy of adsorption of atomic oxygen exceeds the free energy of dissociation of oxygen, the first formed adsorbed film consists of atomic oxygen. Continued exposure to low pressure oxygen is followed by

adsorption or oxygen molecules on metal atoms exposed through the first adsorbed layer. Since the second layer of oxygen is bonded less energetically than the first layer, it is adsorbed without dissociation of its atoms. Oxide formation nucleates at the surface sites where multi-layer adsorption is favoured, such as at surface vacancies, ledges and other imperfections. When conditions are favorable, oxide nuclei form relatively suddenly at specific sites of the surface aided by rapid surface diffusion of M and O ions. Since the amount of adsorbed oxygen on the site increases with oxygen pressure, more sites are affected, so that the density of nuclei increases. Since multilayer adsorption decreases at elevated temperatures, density of nuclei decreases with increase in the temperature. Nuclei grow rapidly to a certain thickness, then more rapidly in a lateral direction rather than vertical. Sometimes the growth of thick continuous oxide film is controlled by transfer of electrons from metal to oxide or by migration of metal ions in a strong electric field set up by negatively charged oxygen absorbed on the oxide surface. When the continuous film reaches a thickness level, diffusion of ions through the oxide will become rate controlling factor. Eventually, at a critical thickness, the stresses set up in the oxide may cause it to crack and detach (called spalling) and the oxidation rate increases irregularly.

3.4.3 KINETICS OF OXIDATION

The most important parameter of metal oxidation from an engineering point of view is the reaction rate. Since the oxide reaction product is generally

retained on the metal surface, the rate of oxidation is generally measured and expressed as weight gain per unit area. Oxidation of various metals under various condition follows various rate laws [47] :

(a) $W = k_1 t$

(b) $W = \sqrt{k_2 t}$

(c) $W = k_3 t^{\frac{1}{3}}$

(d) $W = k_4 \log(ct + a)$

(e) $W = k_5 + k_6 t$

(f) $W = k_7 + k_8 \ln t$

(g) $W = k_9 t^b$

where W is the amount (weight) of oxide formed

t is the exposure time

a,b,c, k_i, i = 1,2,3,...,9 are constants with respect to time.

The first four rate laws applies for oxidation at high temperatures, where as (e), (f), (g), will apply at atmospheric temperature (atmospheric corrosion). Since the constants are affected by a number of factors involved in the oxidation process which strictly may not be identical from specimen to specimen, they are found to be random in nature, as a consequence the weight gain function follow the typical pattern of sample functions as discussed in Chapter 1.

Drazic and Vascic [48] performed accelerated atmospheric corrosion tests

on Cr-Mo steels on long term basis. The behavior shows linear relationship as seen in Sec 1.8.1 of Chapter 1. Data for analysis is again in the form of a single realization (from Fig. 3 of [48]). If it is assumed to follow the damage function $D(t) = D_i + rt$ the three parameter Bernstein model will be valid. However due to lack of replicate data, we can analyze it under the following two assumptions

(a) $E(D_i)=0$ or constant and $V(D_i)=0$ which means inverted normal is valid

(b) $E(r)=0$ and $V(r)=0$ which means normal model is valid.

The values of $E(D_i)$, $V(D_i)$, $E(r)$, and $V(r)$ are estimated from the linear regression performed on the data. Figs. 3.22 to 3.25 shows reliability, probability density and hazard functions for both the models. The inverted normal model is more conservative. Therefore in the absence of adequate data this model may be preffered.

Legault and Pearson [49] evaluated atmospheric corrosion on aluminized steel panels exposed in both industrial and marine environments and have proposed the general kinetic relationship as $W(t) = K\, t^N$. The above data given in Table 1 of [49] is further analyzed, in view of the proposed mathematical structure of Chapter 1 (Sec 1.9). The damage model representing the data lead to a three parameter Log Bernstein reliability model. Fig. 3.26 shows the reliability function along with the experimental time to failure data at different critical damage levels. Figs. 3.27 and 3.28 represents the probability density function and hazard function. Considering the possibility of distortion in

estimating the three parameters of log Bernstein model by regression equation to each realization, it was decided to check also the two parameter inverted lognormal model directly using the time to failure data by plotting [F(T) vs 1/lnT] on a normal probability paper. The straight line in Fig. 3.29 indicate that the time to failure infact is inverted log-normal distribution. This is also observed in the reliability curve for the inverted lognormal model when superimposed on the log Bernstein model as shown in Fig. 3.26.

Data from Table 4 of [49] represents $D(t) = D_i + r \ln t$ type of model. This type of damage model also leads to the three parameter log Bernstein reliability model as shown in Sec 1.10. Fig. 3.30 shows the reliability function in comparison with the experimental time to failure data at different critical damage levels. Figs. 3.31 and 3.32 represents the probability density function and hazard function. The data is also validated for a two parameter inverted lognormal model by plotting on the normal probability paper. The straight line in Fig. 3.33 [F(T) vs 1/lnT] indicate that inverted log-normal distribution is quite acceptable. The reliability curve for the inverted lognormal model fits slightly better when superimposed on the reliability curve of log Bernstein model as shown in Fig. 3.30. Again the discrepancy can be attributed to introduction of extra amount of initial damage and scatter due to the regression analysis performed on each realization.

The various rate laws of oxidation (a), (b), (c) as mentioned in the previous section generally represents the damage model of Sec 1.9 of Chapter 1.

3.4.4 GENERAL MODEL OF OXIDATION (INCLUDING THE TEMPERATURE EFFECT)

Dunn [50] mentioned that for an oxide film which undergoes no phase change the influence of temperature on oxidation rate is given by the relationship

$$\frac{dW_o}{dt} = A' e^{-Q/RT} \tag{3.1}$$

Integrating the above equation we get

$$W^o = A' e^{-Q/RT} \tag{3.2}$$

where W_o is the oxidation rate

T is the absolute temperature

A' and Q are constants.

In general we can rewrite eq (3.2) as

$$W_o = \varphi(t)\, e^{-Q/RT}$$

where $\varphi(t)$ is the function of time.

Therefore the various rate laws can be modified as :

(1) $W_o(t) = (\alpha_o + \beta_o t)\, e^{-Q/RT}$ (3.3)

(2) $W_o(t) = (\alpha_o + \beta_o \log t)\, e^{-Q/RT}$ (3.4)

(3) $W_o(t) = (\alpha_o\, t^{\beta_o})\, e^{-Q/RT}$ (3.5)

(4) $W_o(t) = (\alpha_o\, t)\, e^{-Q/RT}$ (3.6)

$$(5) \quad W_o(t) = (\alpha_o t^{\frac{1}{2}})\, e^{-Q/RT} \tag{3.7}$$

Taking data from Vernon et.al., [51] for zinc (from Fig. 7 in ref [51]) these above models were analyzed by multiple linear regression technique. By comparing the residual errors the best model of all was observed to be

$$W_o(t) = (\alpha_o t^{\beta_o})\, e^{-Q/RT}$$

By substituting the values of parameters the model is given by

$$W_o(t) = 4.794\, t^{0.338}\, e^{-3074.68/RT}$$

Assuming α_o as fixed, β_o as normally distributed and the damage level criterion as D_l, the following relationship will hold :

$$P[W_o(t) < D_l] = P[\ln \{W_o(t)\} < D_l]$$

$$= P(\ln T > \ln t) = P(T > t) = R(t)$$

Here T is the random variable which is expressed as

$$\ln T = \frac{\ln W_l - \alpha_o}{\beta_o}$$

This leads to the eq (1.61) of Chapter 1. α_o is treated as fixed, because it will result into a more conservative reliability model i.e., a two parameter inverted log-normal distribution (Sec 1.9.2). Fig. 3.34 shows the relationship between $\sqrt{\alpha_l}$ and lnt at different reliable life for fixed W_l and temperature.

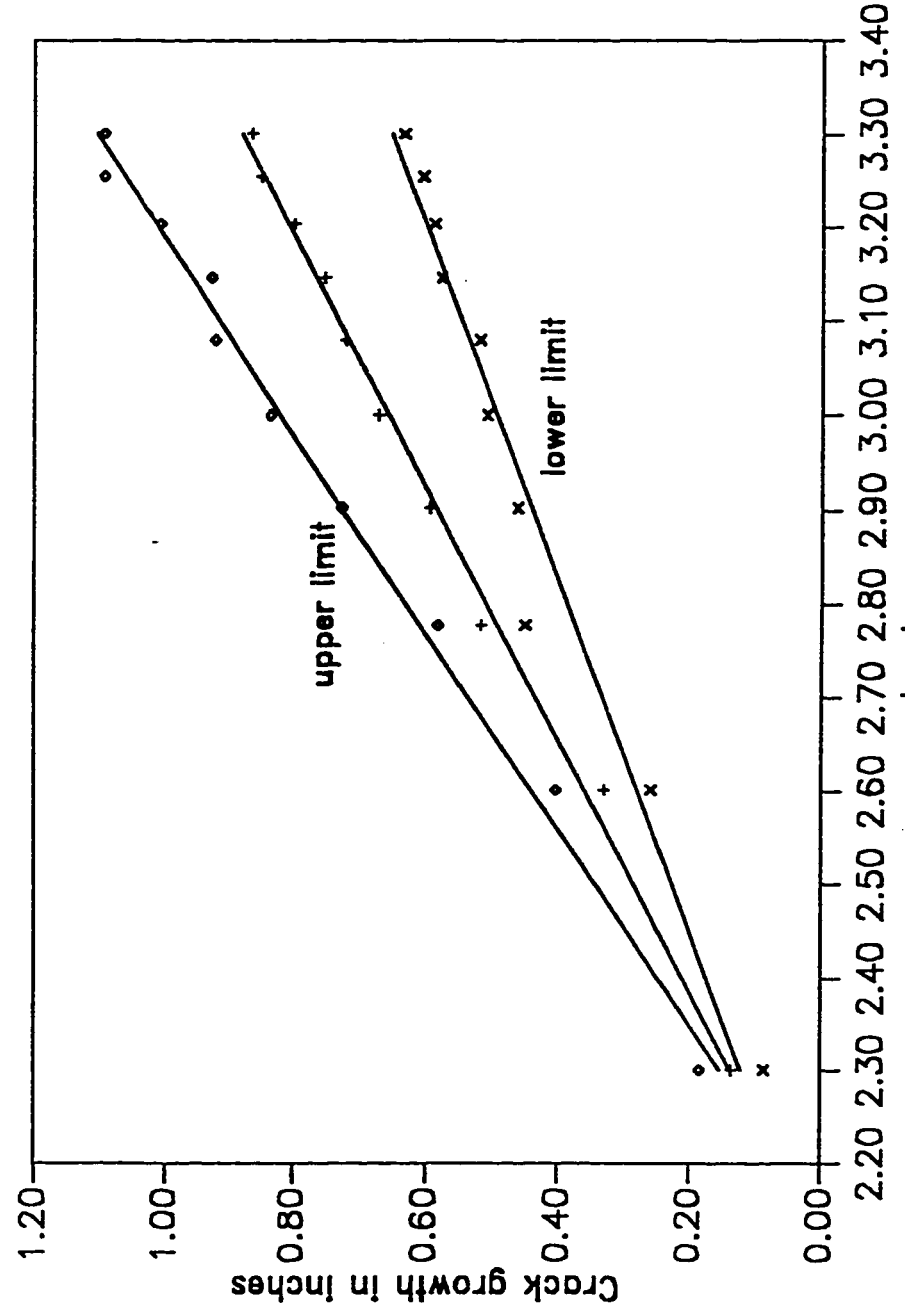

Fig. 3.1 Environmental crack growth as a function of logarithmic time.

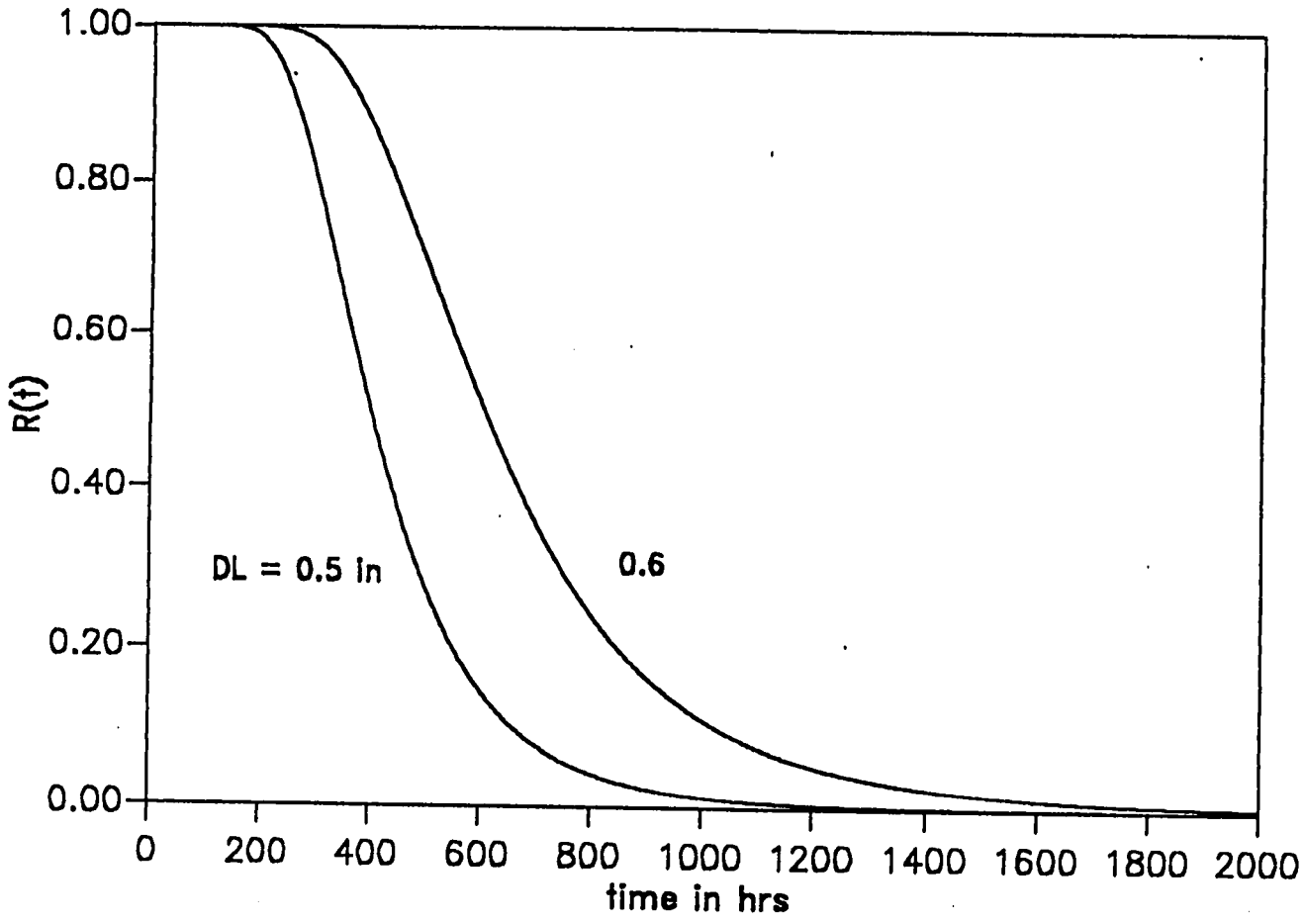

Fig. 3.2 Reliability function for three parameter Log Bernstein distribution obtained from damage function for SCC at different critical crack growth levels. [See Table 3.1 for distribution parameters]. Data from Ref [36].

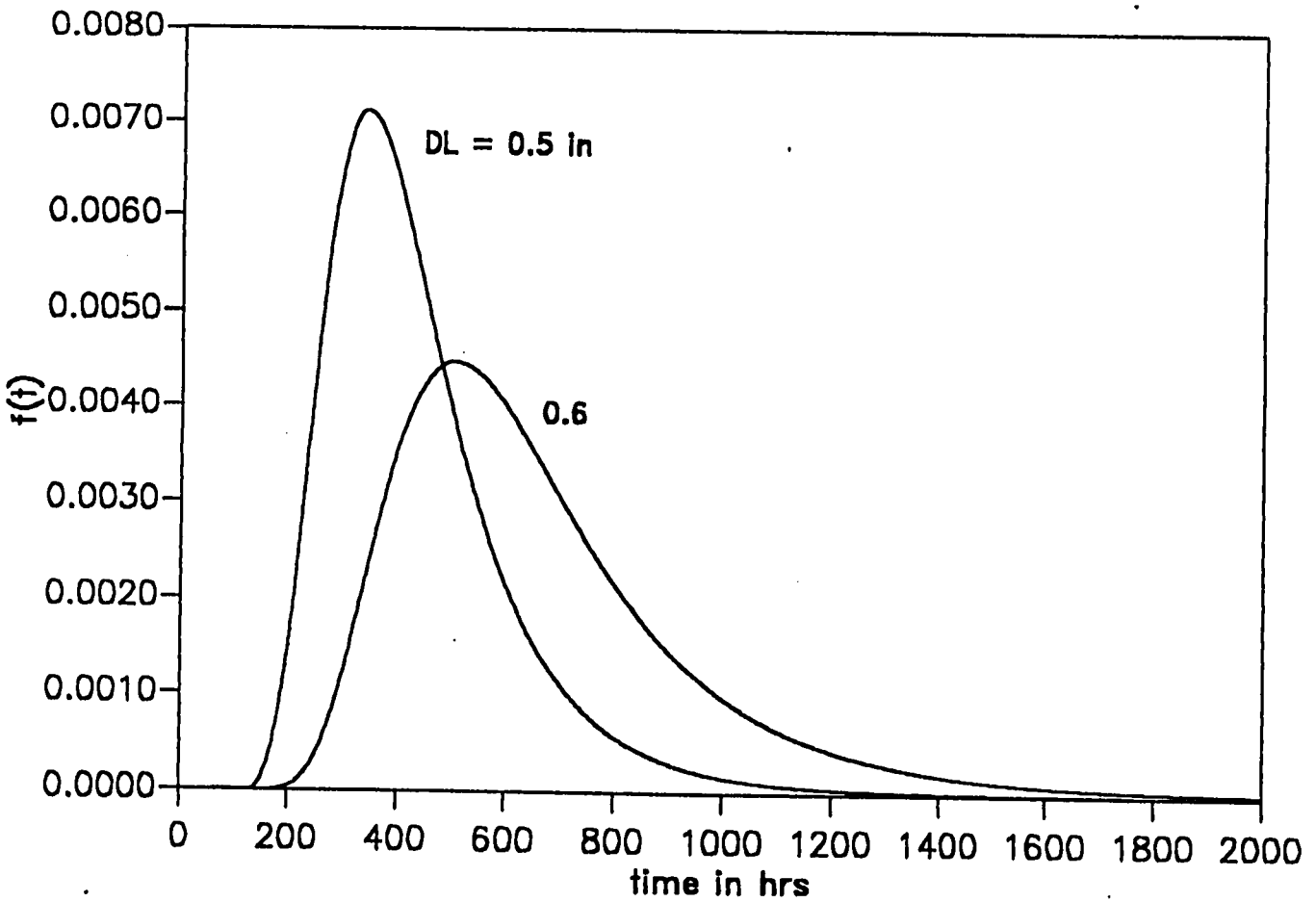

Fig. 3.3 Probability density function for three parameter Log Bernstein distribution obtained from damage function for SCC at different critical crack growth levels. Data from Ref [36]. [See Table 3.1 for distribution parameters].

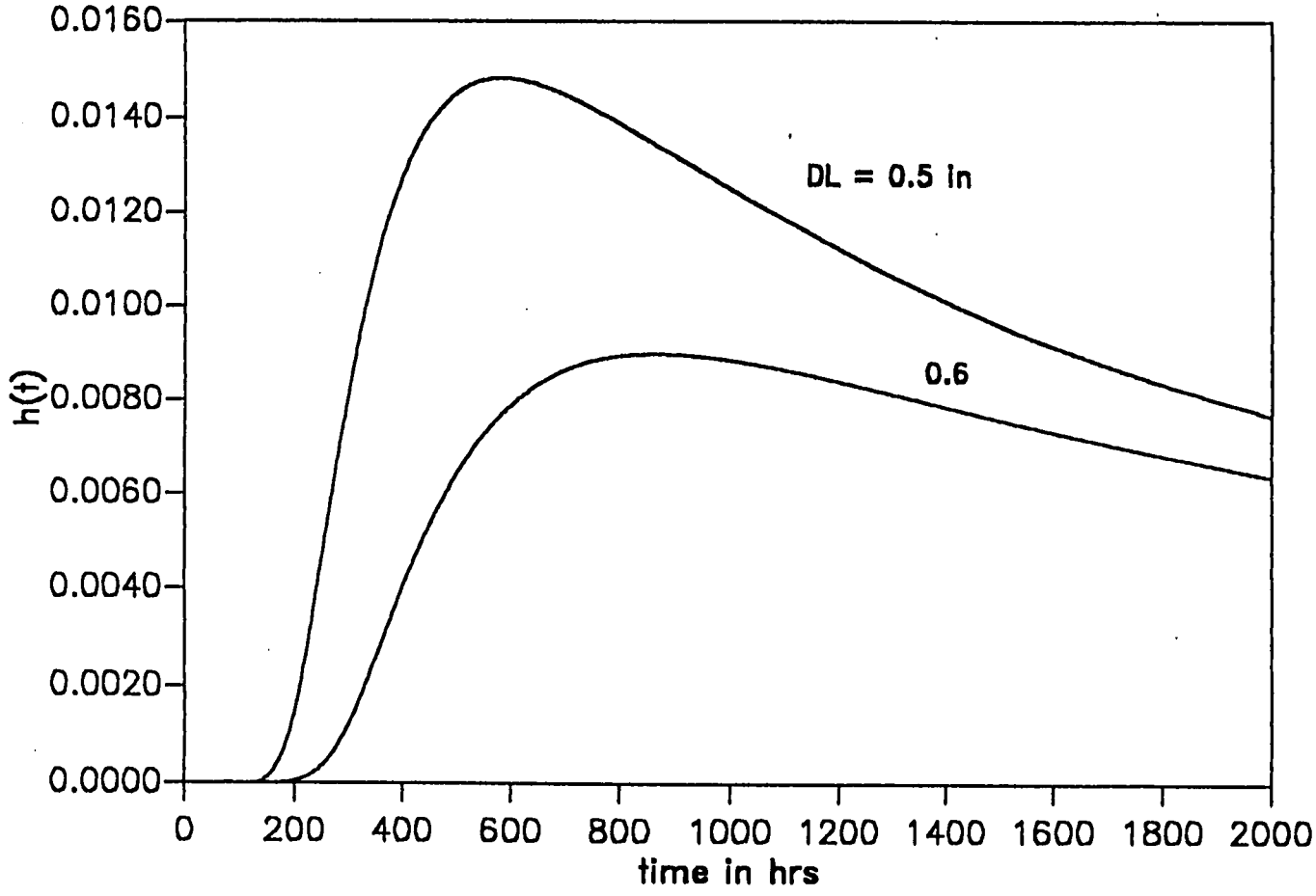

Fig. 3.4 Hazard function for three parameter Log Bernstein distribution obtained from damage function for SCC at different critical crack growth levels. Data from Ref [36]. [See Table 3.1 for distribution parameters].

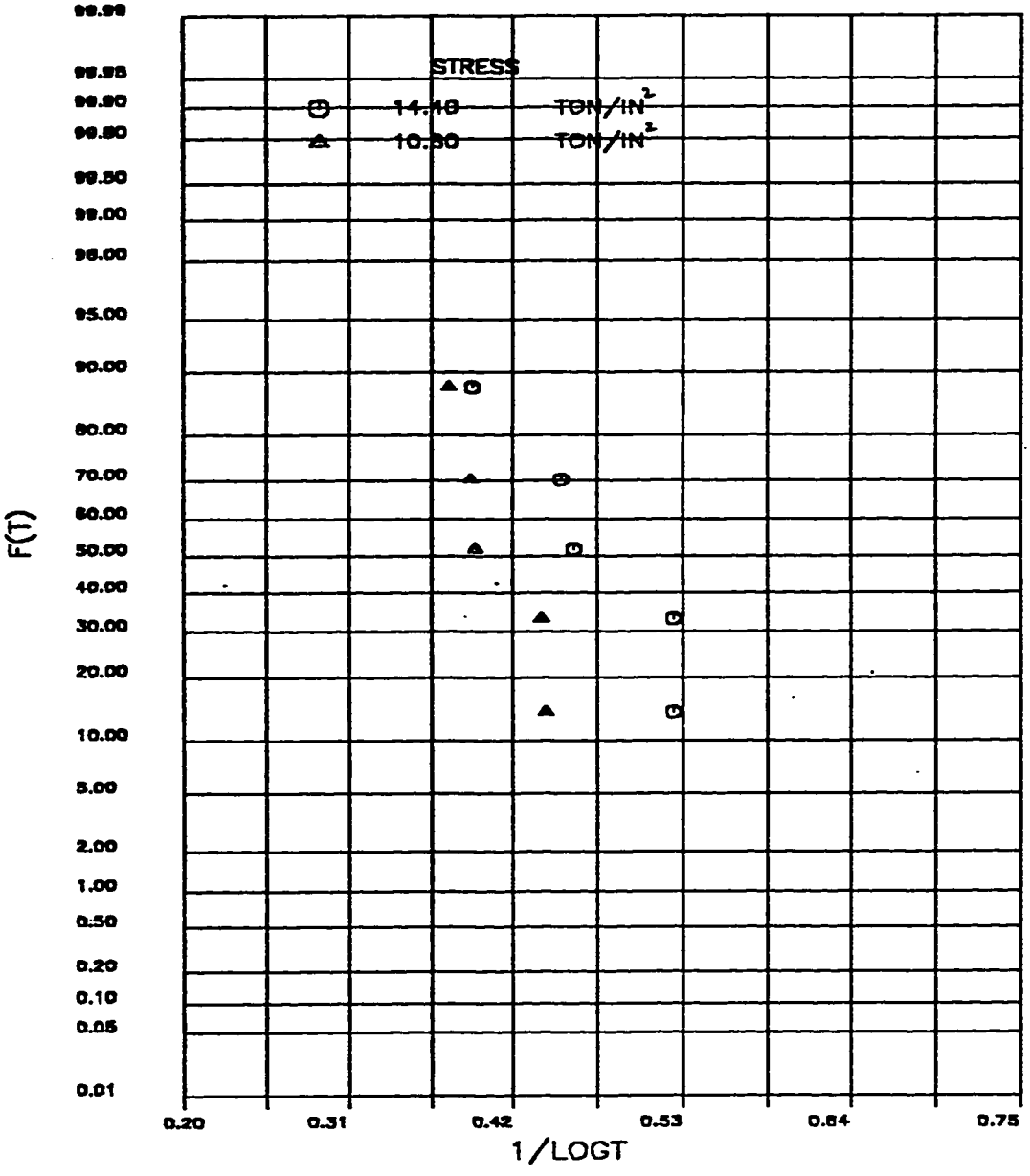

Fig. 3.5 Inverted lognormal distribution for Steel B at different stress levels. Data from Ref [37]. [See Table 3.2 for distribution parameters].

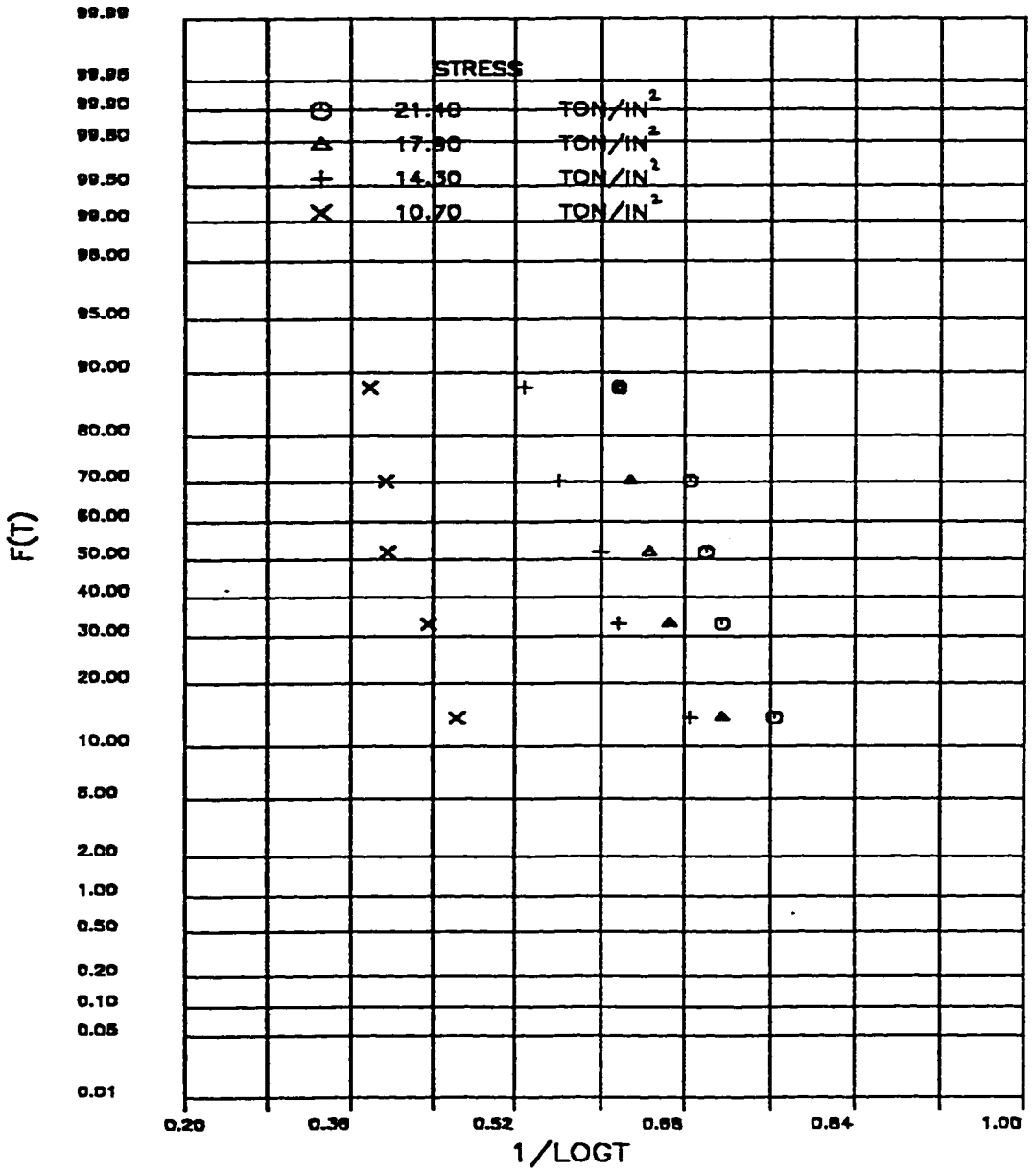

Fig. 3.6 Inverted lognormal distribution for Steel E at different stress levels. Data from Ref [37]. [See Table 3.2 for distribution parameters].

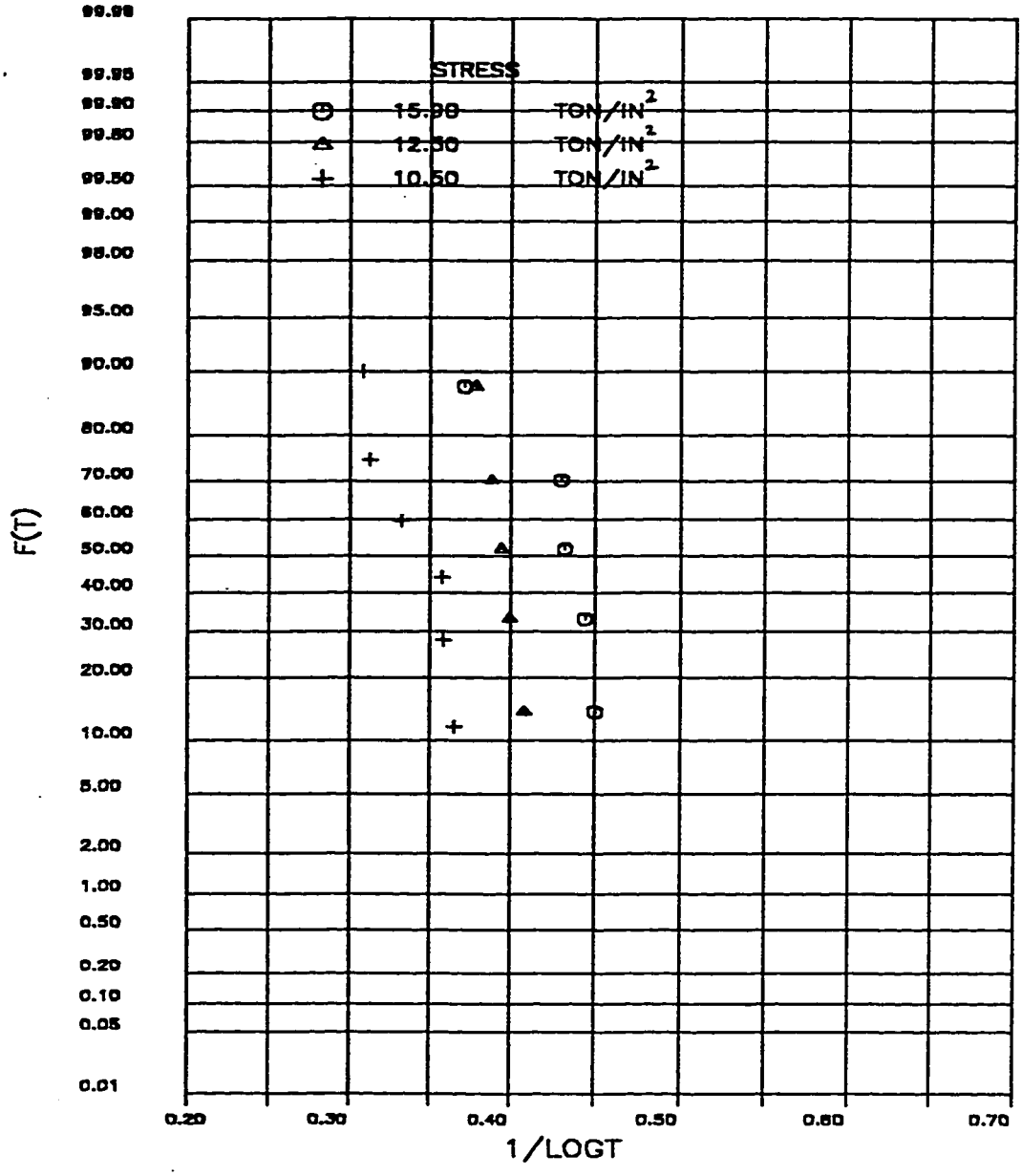

Fig. 3.7 Inverted lognormal distribution for Steel F at different stress levels. Data from Ref [37]. [See Table 3.2 for distribution parameters].

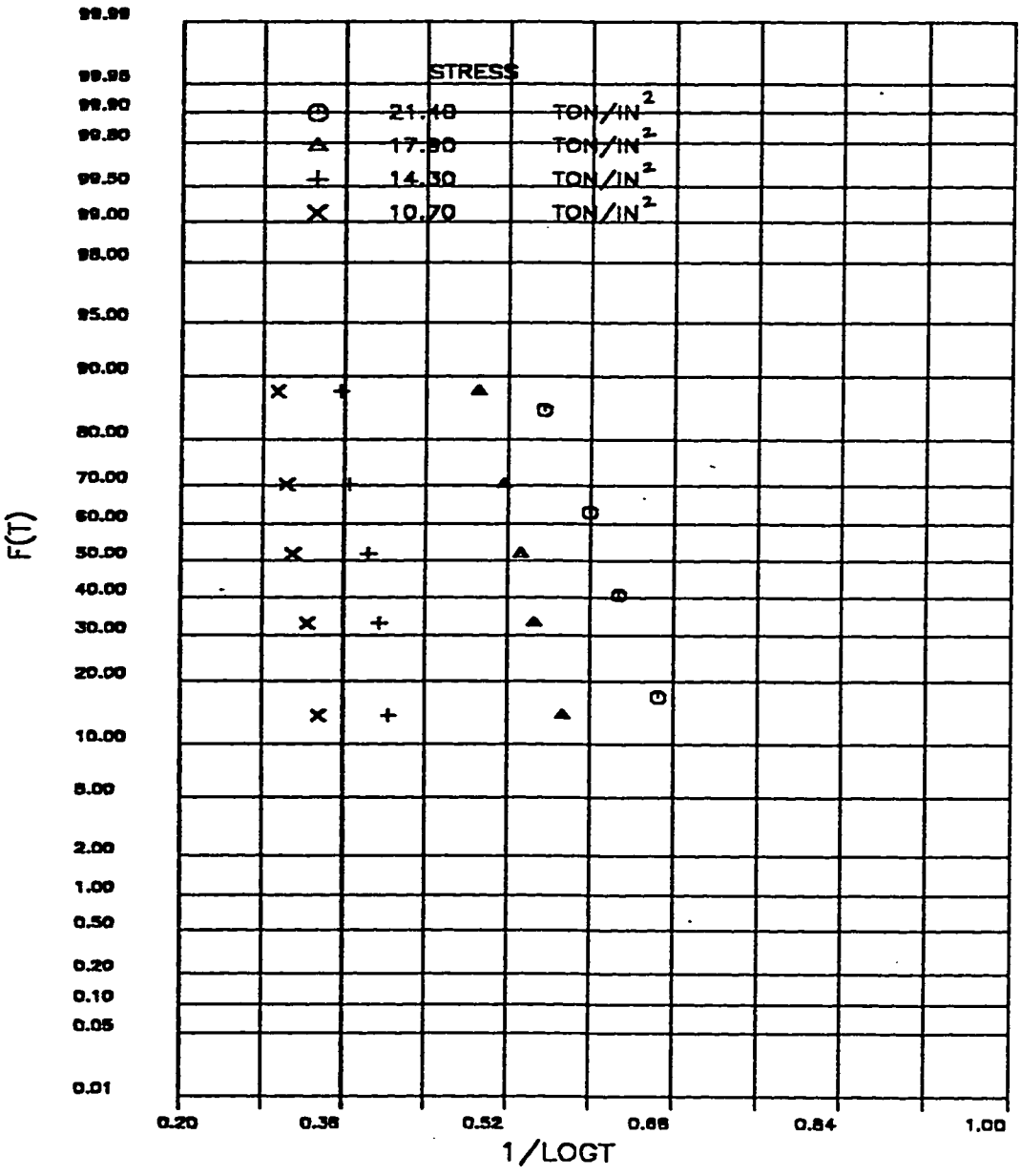

Fig. 3.8 Inverted lognormal distribution for Steel N at different stress levels. Data from Ref [37]. [See Table 3.2 for distribution parameters].

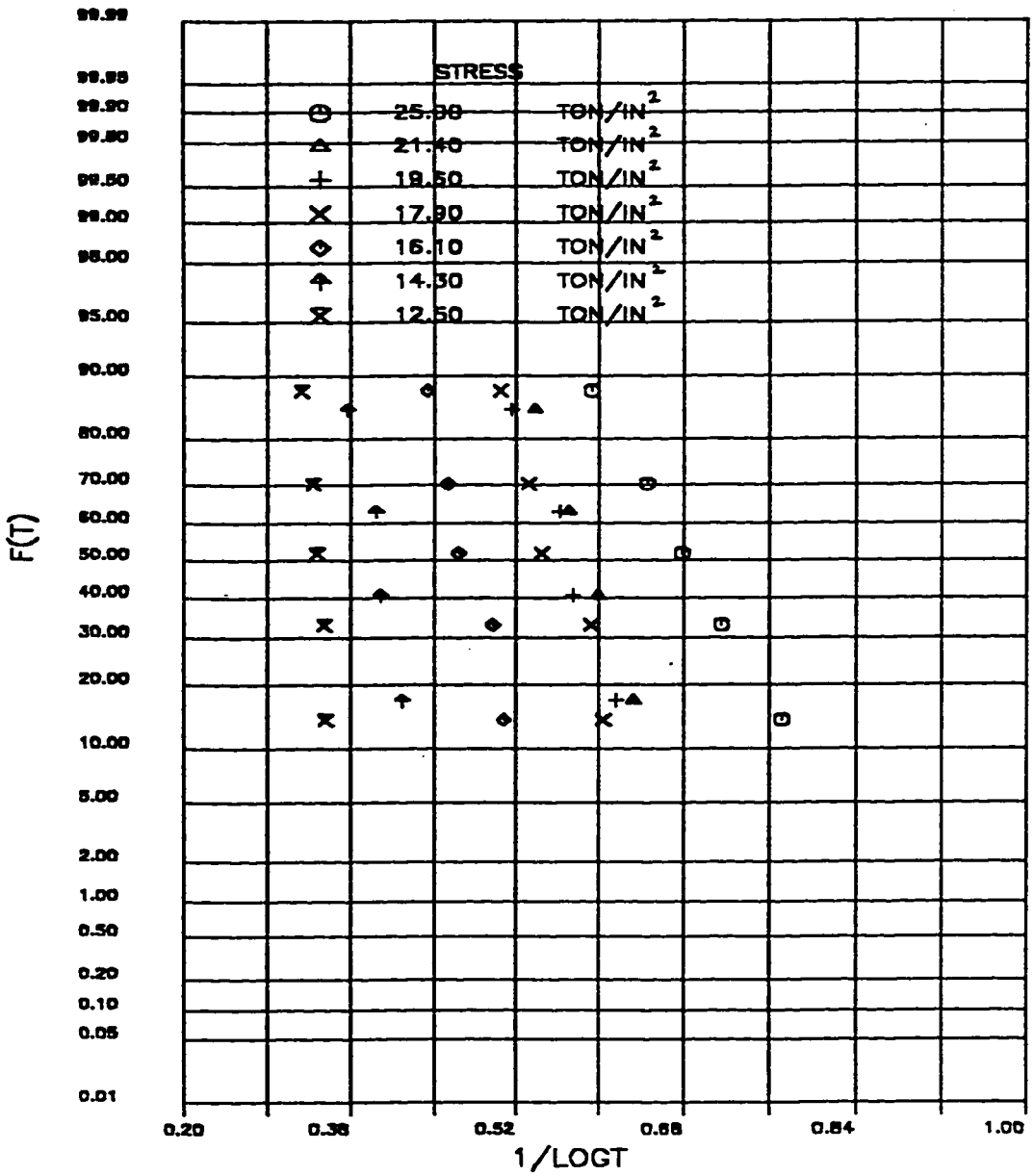

Fig. 3.9 Inverted lognormal distribution for Steel O at different stress levels. Data from Ref [37]. [See Table 3.2 for distribution parameters].

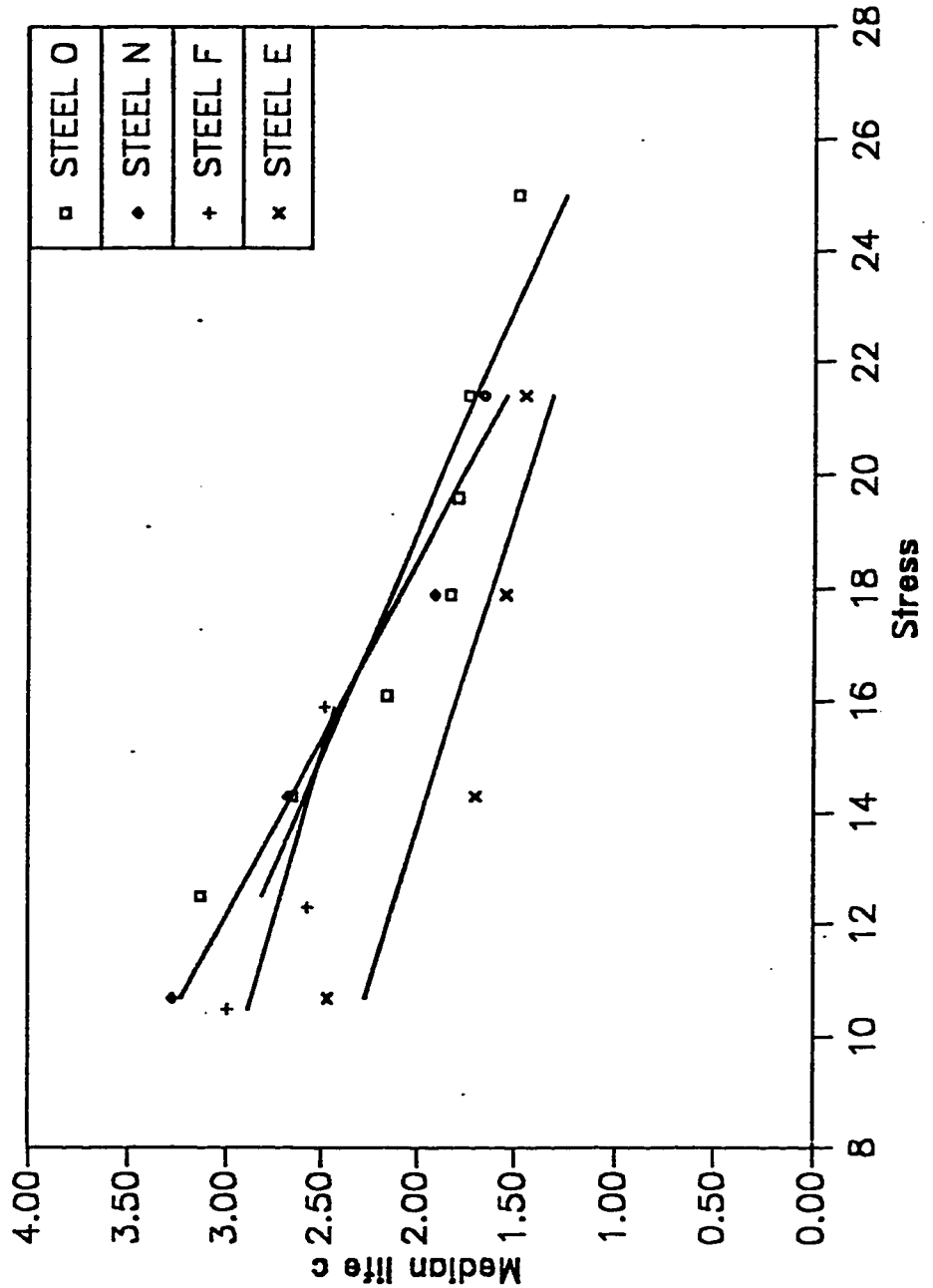

Fig. 3.10 Variation of median life c with stress for different Steels.

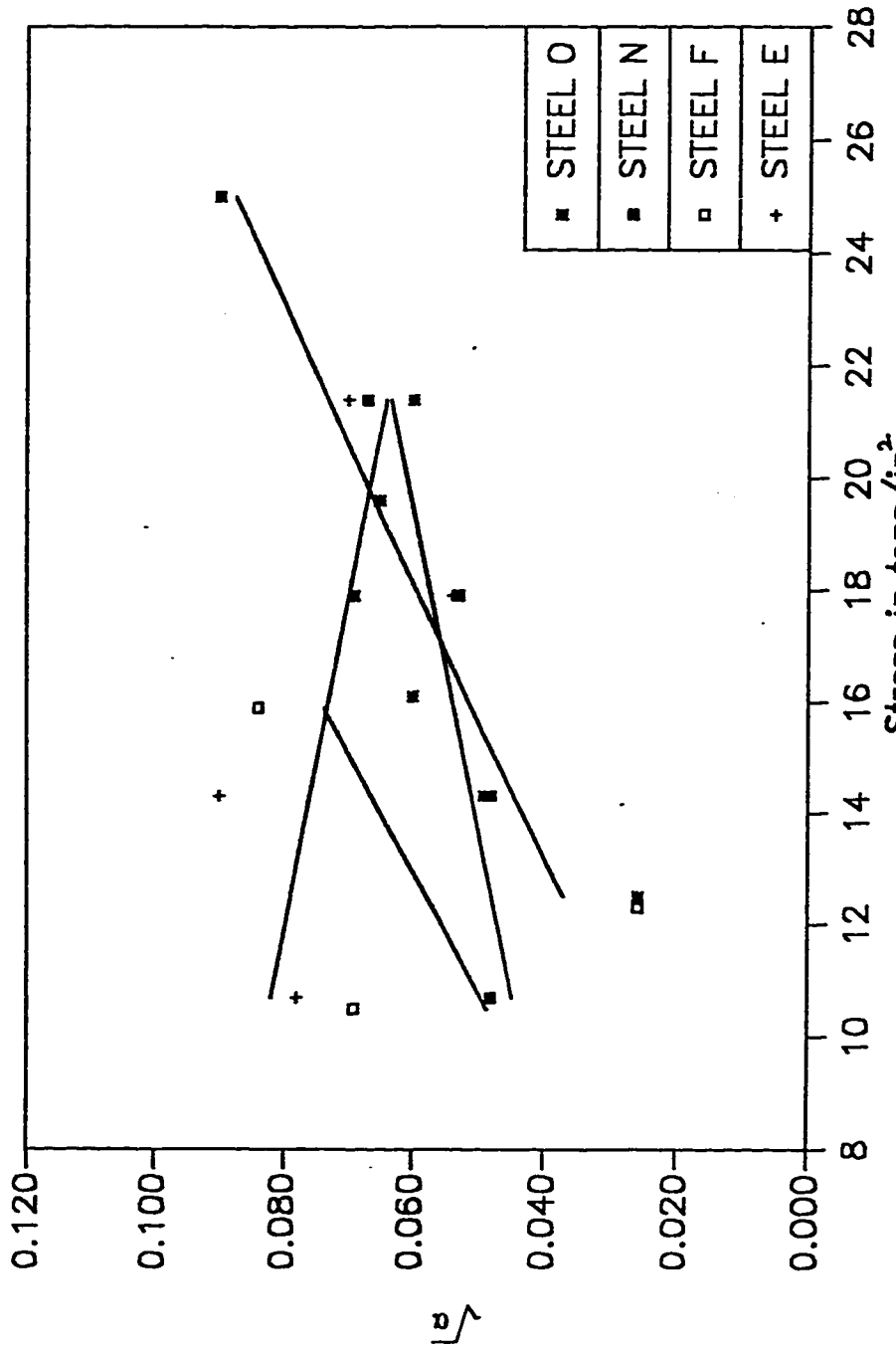

Fig. 3.11 Variation of scatter parameter $\sqrt{\alpha}$ with stress for different Steels.

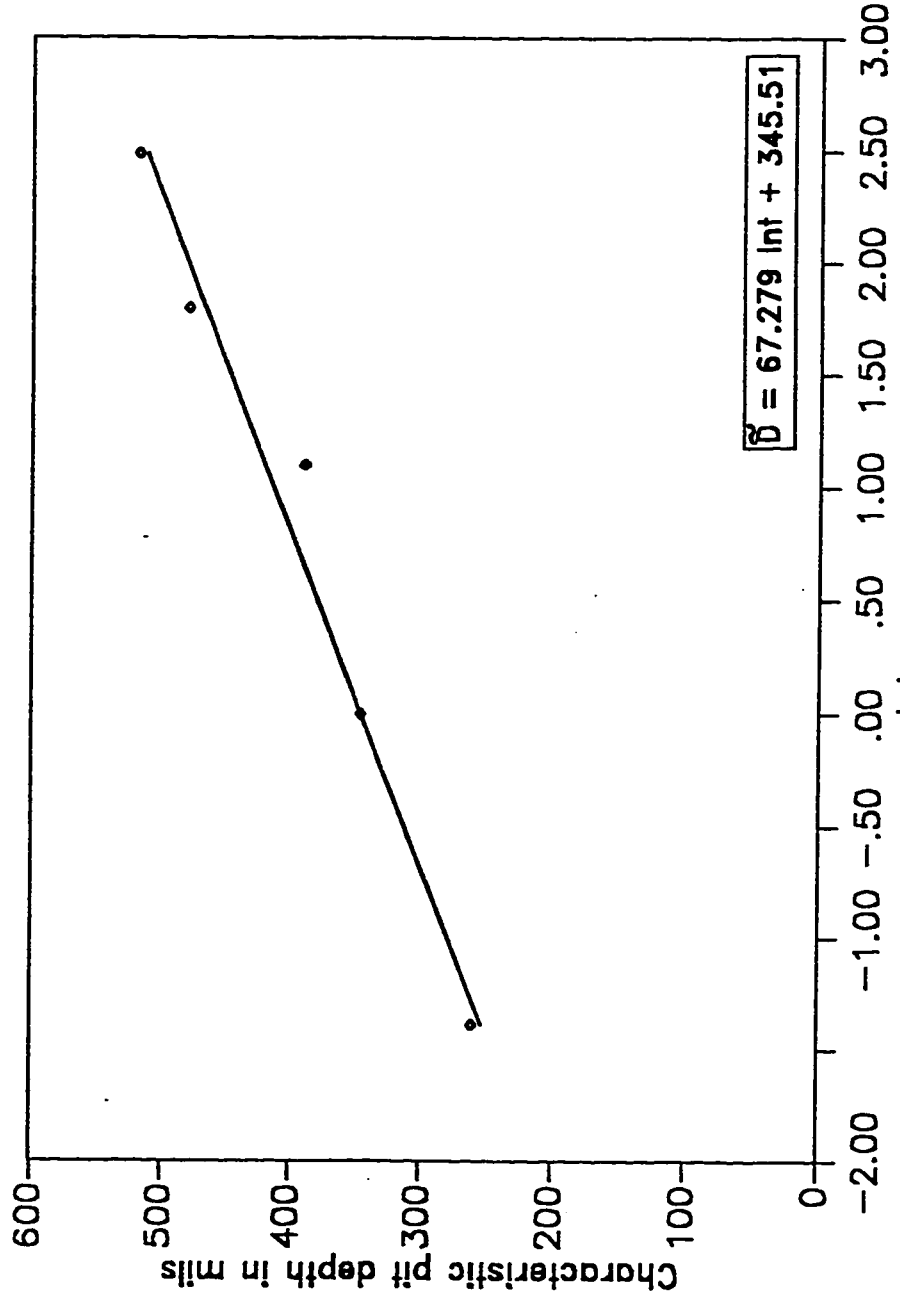

Fig. 3.12 Characteristic pit depth versus logarithmic time. Data from Ref [43].

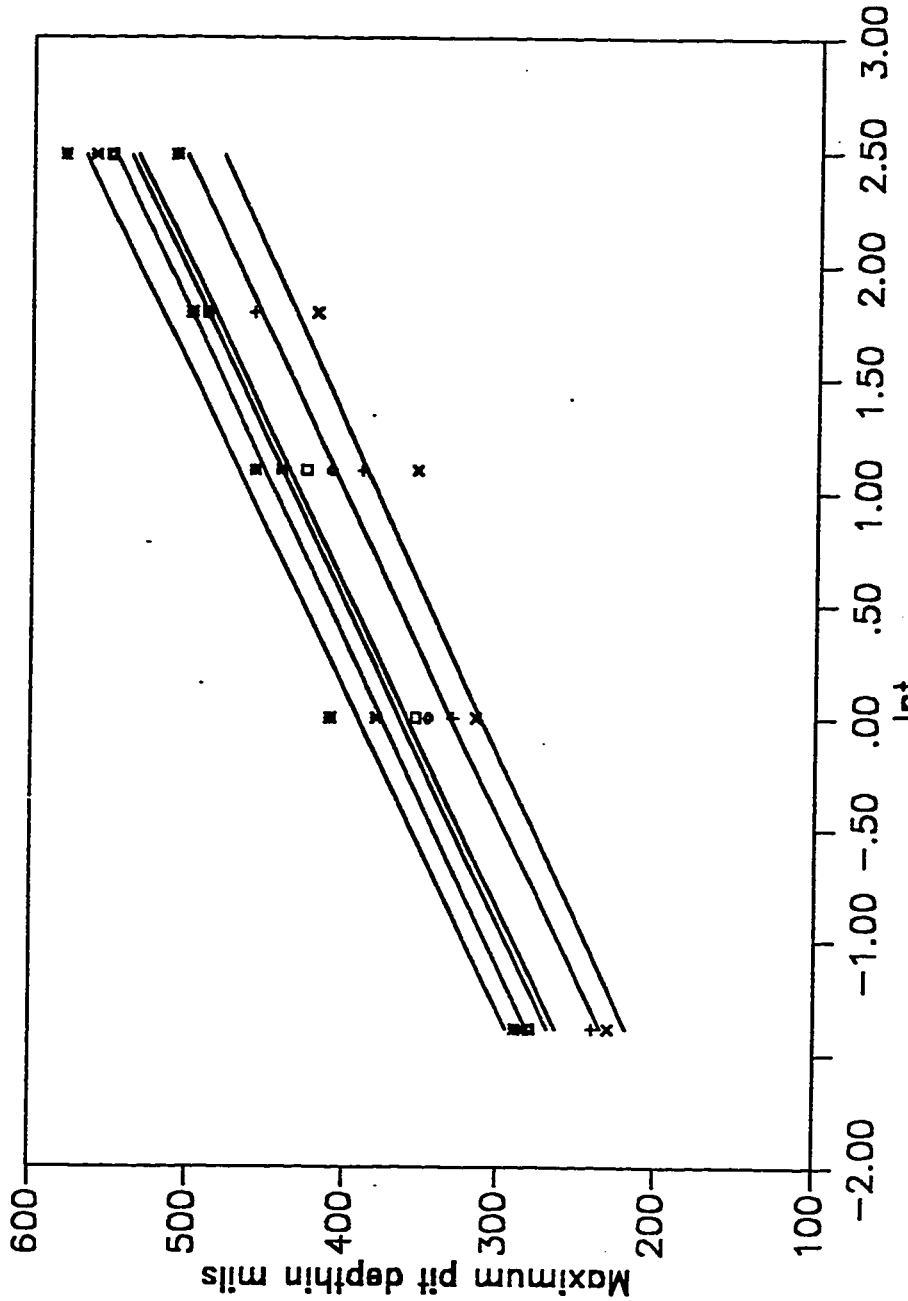

Fig. 3.13 Variation of maximum pit depth and logarithmic time. Data from Ref [43].

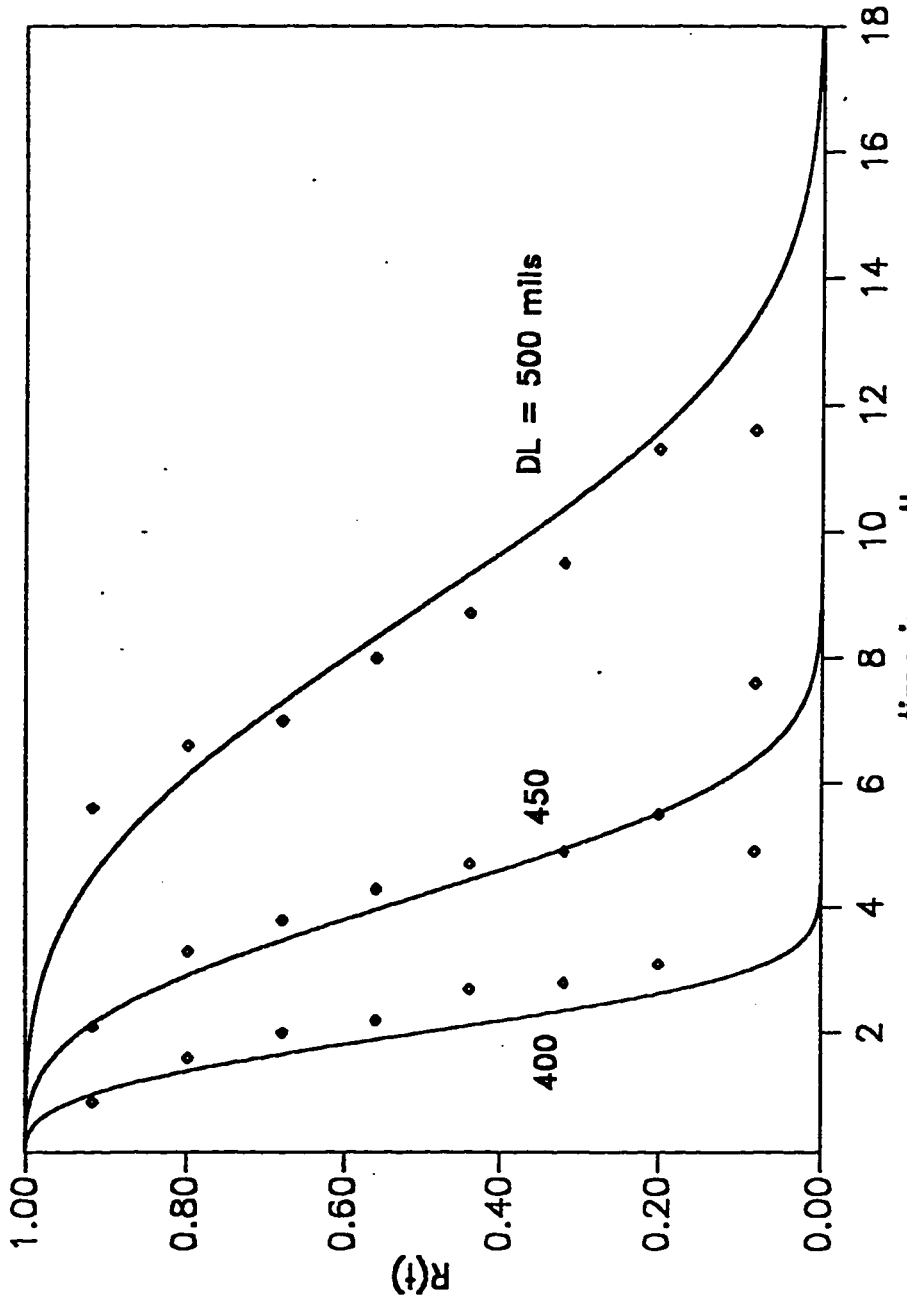

Fig. 3.14 Reliability function of Weibull distribution obtained from damage function with time to failure data for pitting at different critical damage levels. Data from Ref [43]. [See Table 3.3 for distribution parameters].

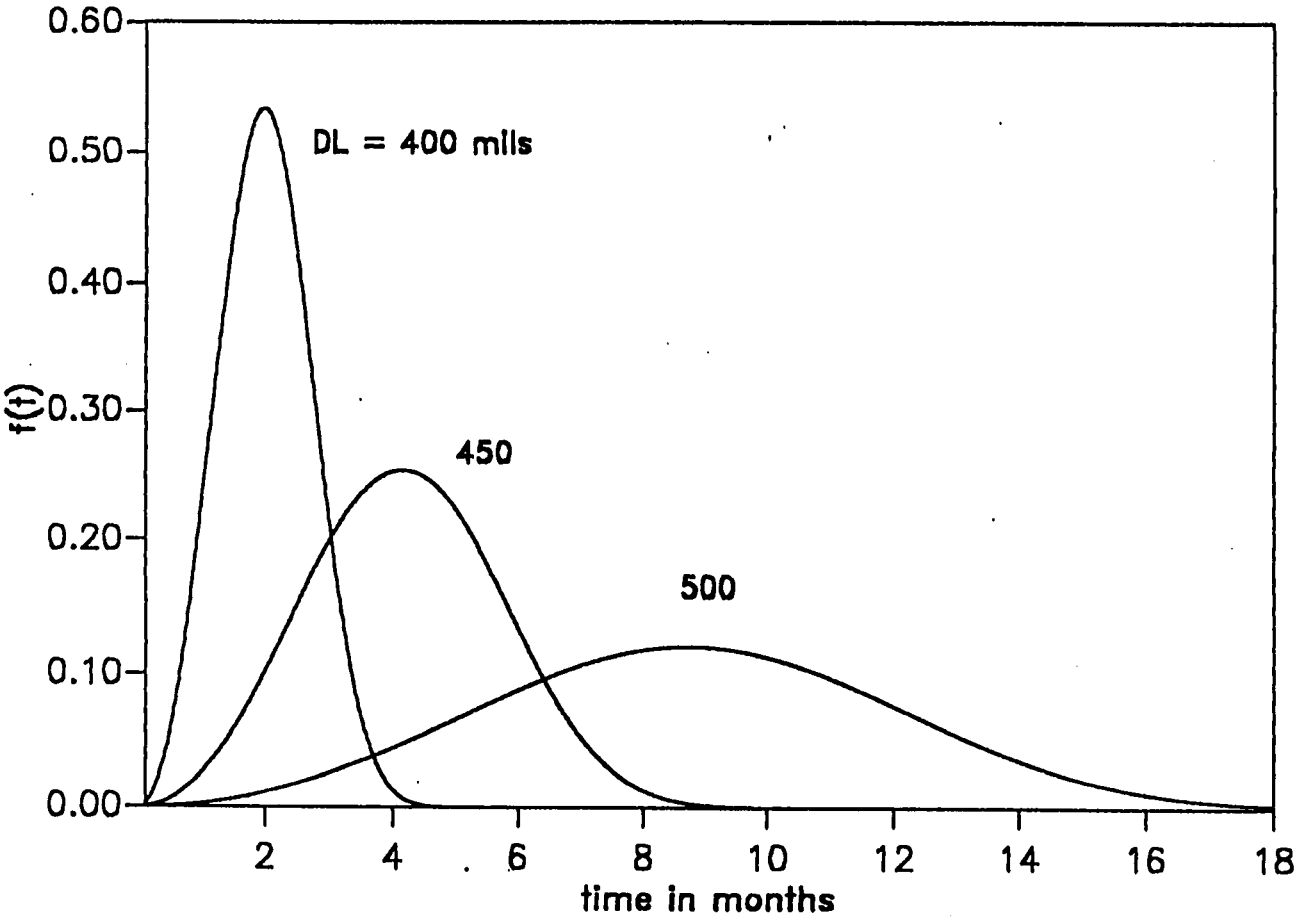

Fig. 3.15 Probability density function of Weibull distribution obtained from damage function for pitting at different critical damage levels. Data from Ref [43]. [See Table 3.3 for distribution parameters].

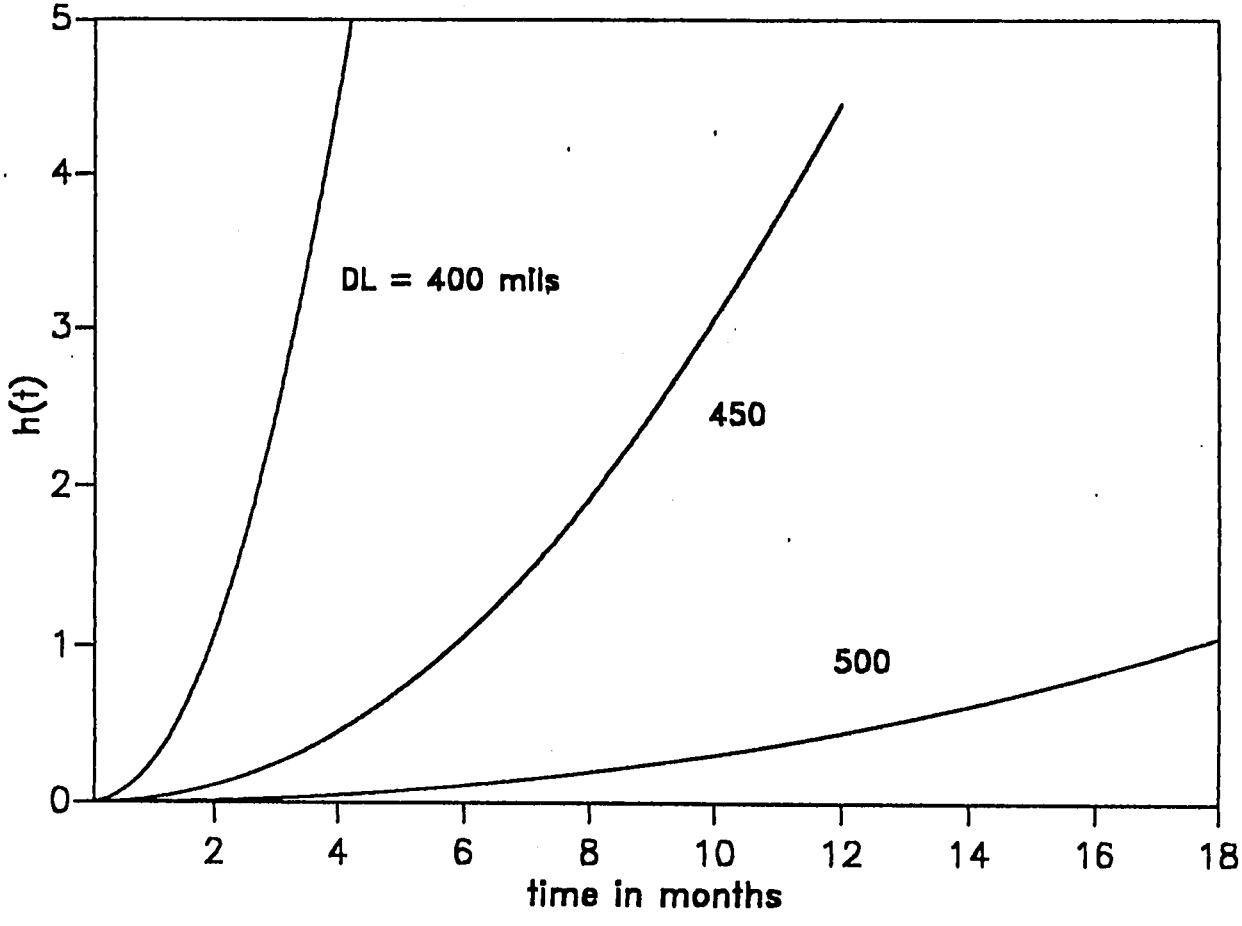

Fig. 3.16 Hazard function of Weibull distribution obtained from damage function for pitting at different critical damage levels. Data from Ref [43]. [See Table 3.3 for distribution parameters].

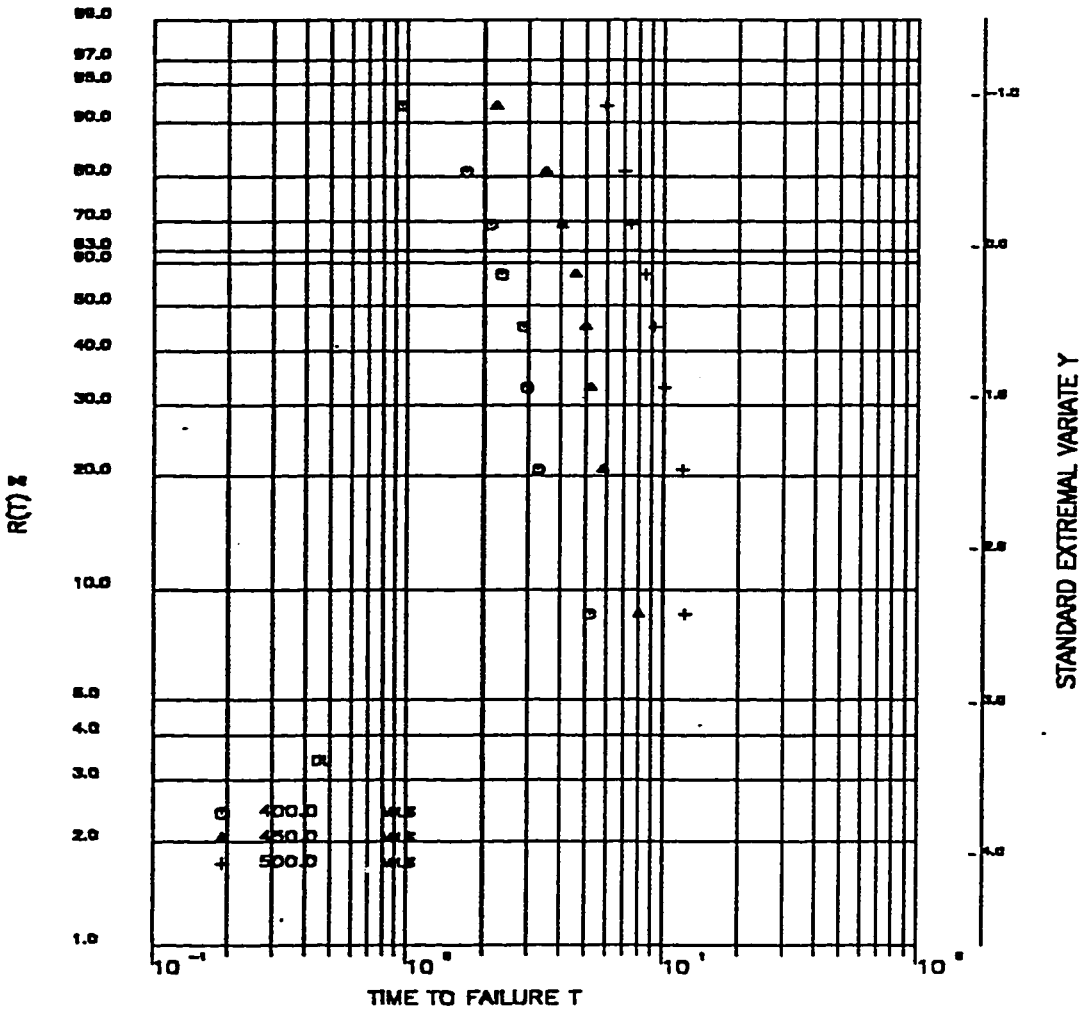

Fig. 3.17 Weibull distribution for time to failure data at different damage levels for pitting. Data from Ref [43].

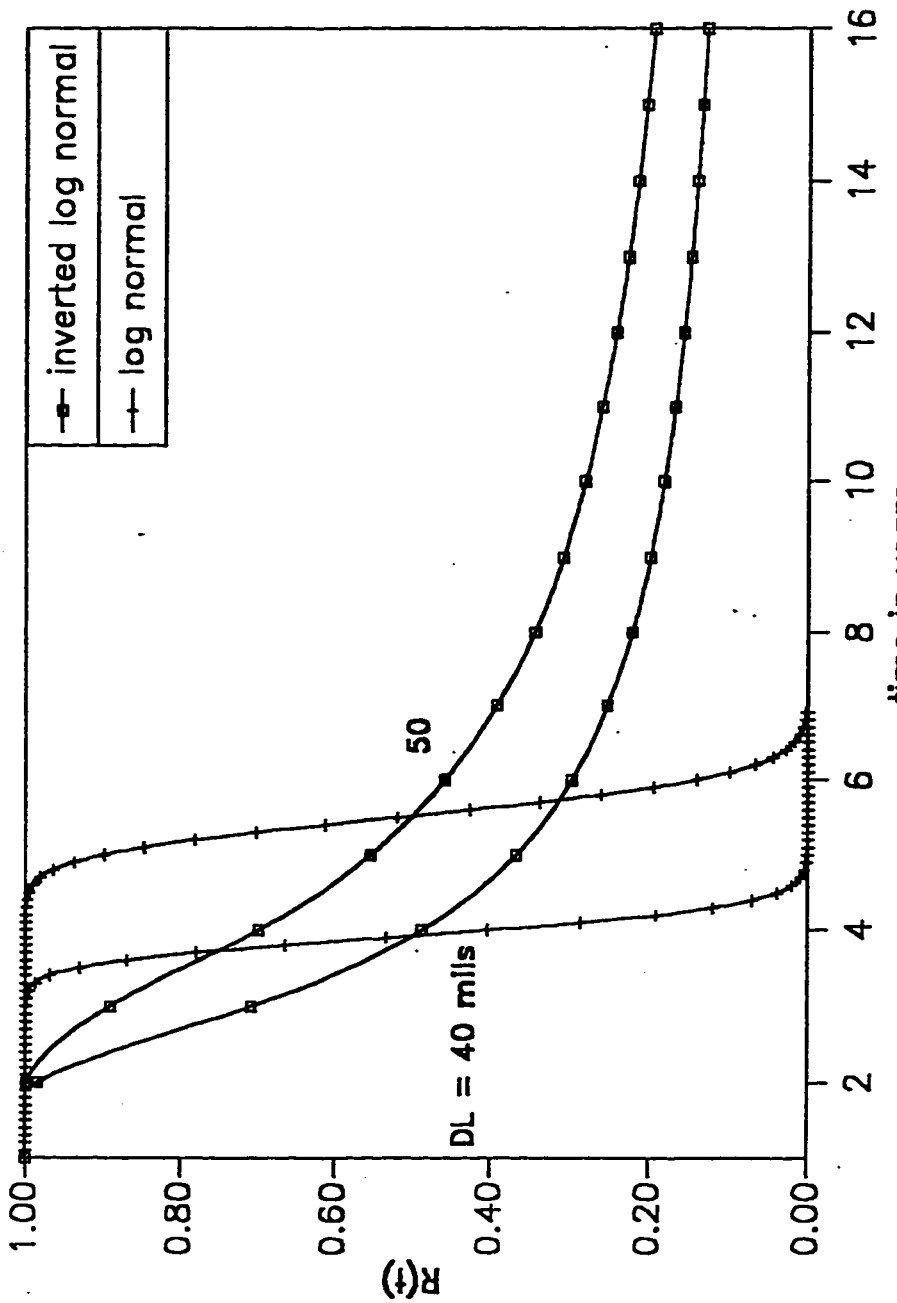

Fig. 3.18 Reliability function of lognormal and inverted lognormal distributions obtained from damage function for oxidation at different critical damage levels. Data from Ref [46]. [See Table 3.4 for distribution parameters].

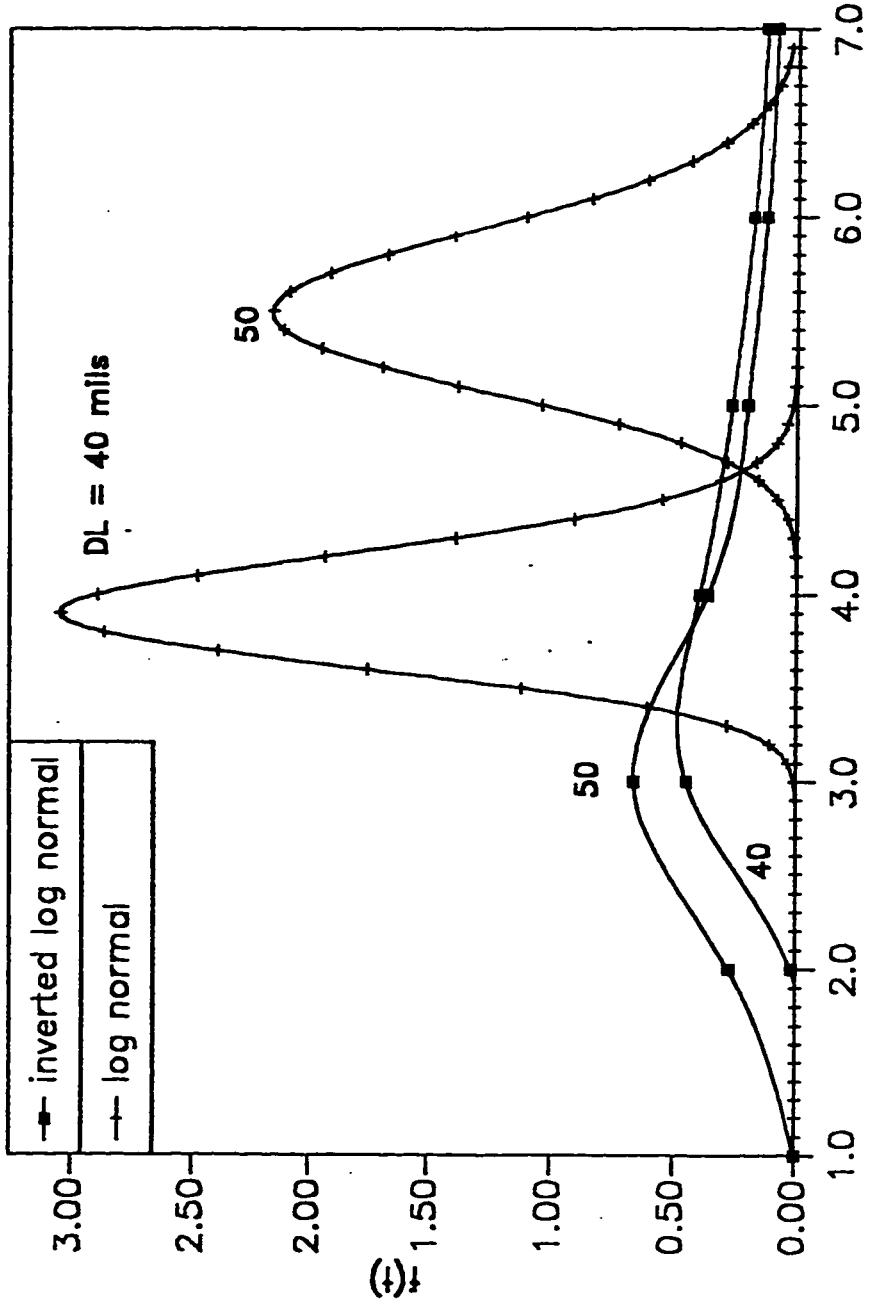

Fig. 3.19 Probability density function of lognormal and inverted lognormal distributions obtained from damage function for oxidation at different critical damage levels. Data from Ref [46]. [See Table 3.4 for distribution parameters].

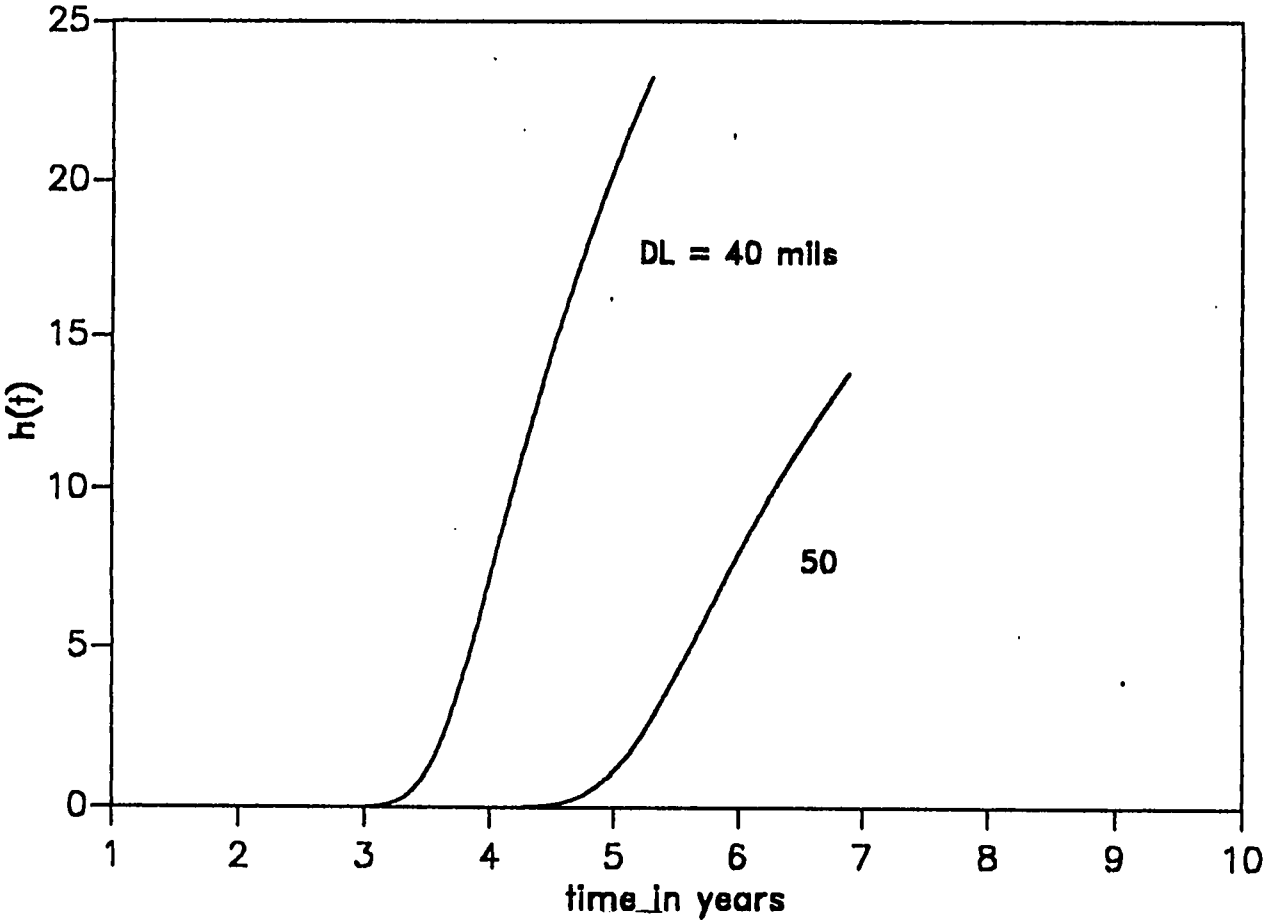

Fig. 3.20 Hazard function of lognormal distribution obtained from damage function for oxidation at different critical damage levels. Data from Ref [46]. [See Table 3.4 for distribution parameters].

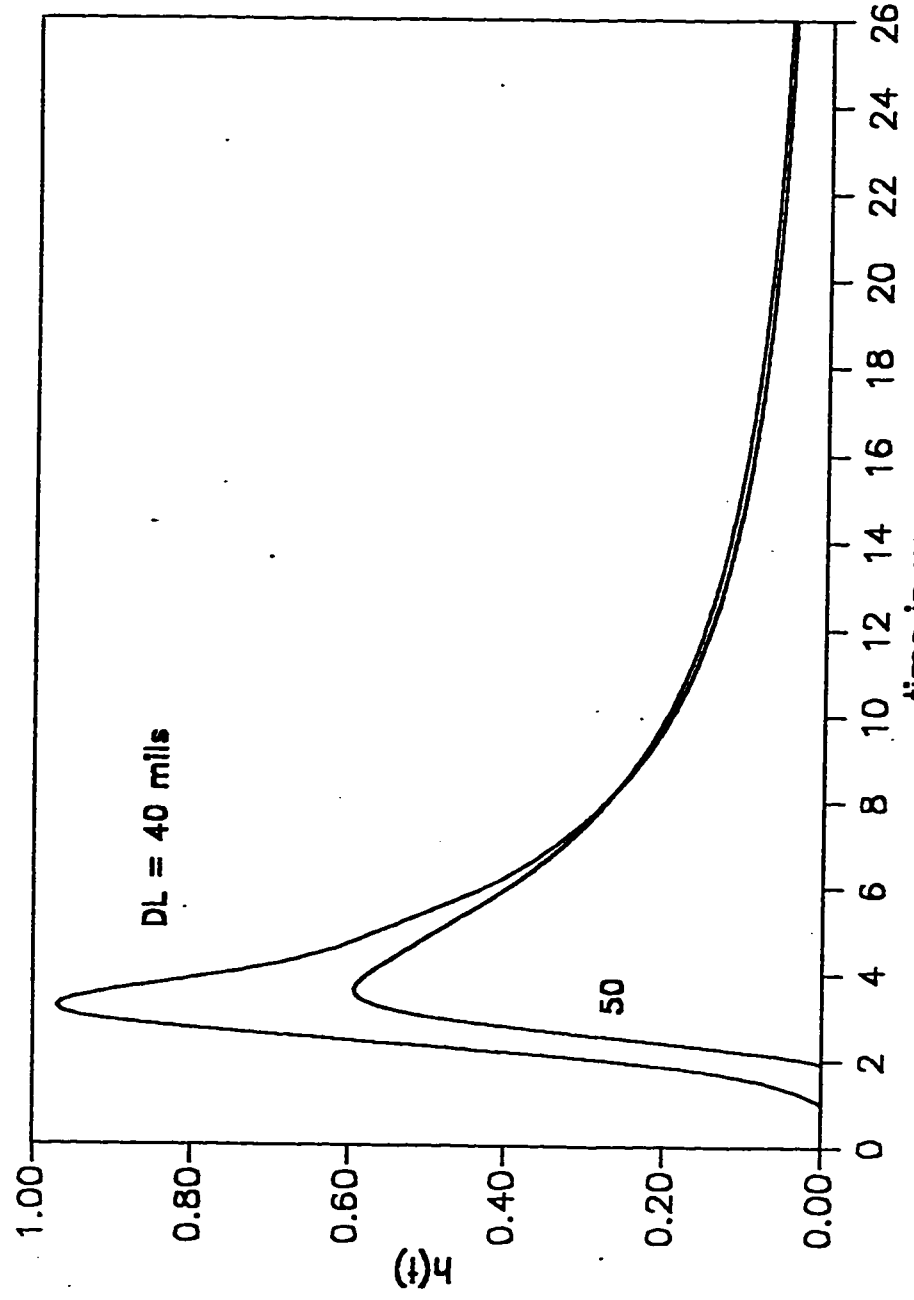

Fig. 3.21 Hazard function of inverted lognormal distribution obtained from damage function for oxidation at different critical damage levels. Data from Ref [46]. [See Table 3.4 for distribution parameters].

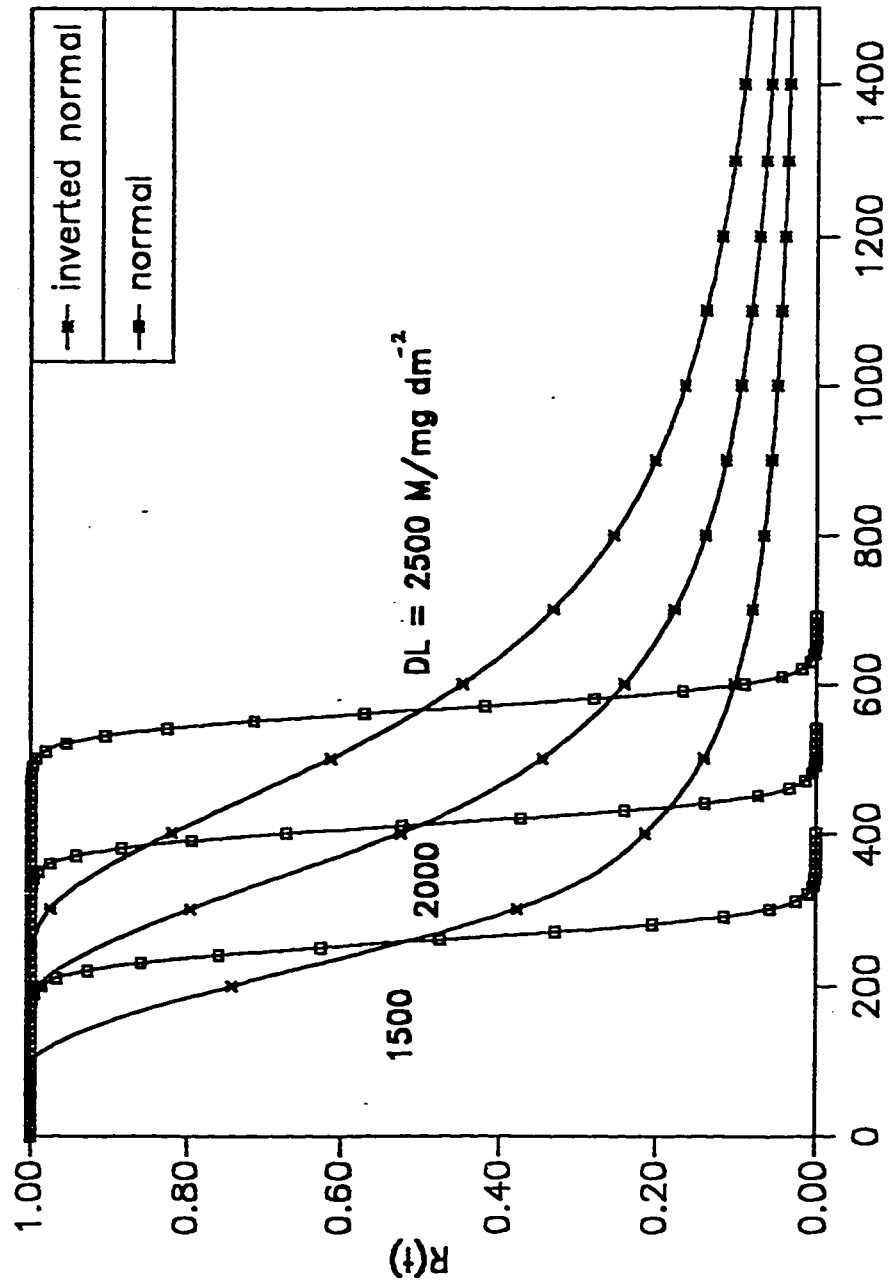

Fig. 3.22 Reliability function of normal and inverted normal distributions obtained from damage function for oxidation at different critical damage levels. Data from Ref [48]. [See Table 3.5 for distribution parameters].

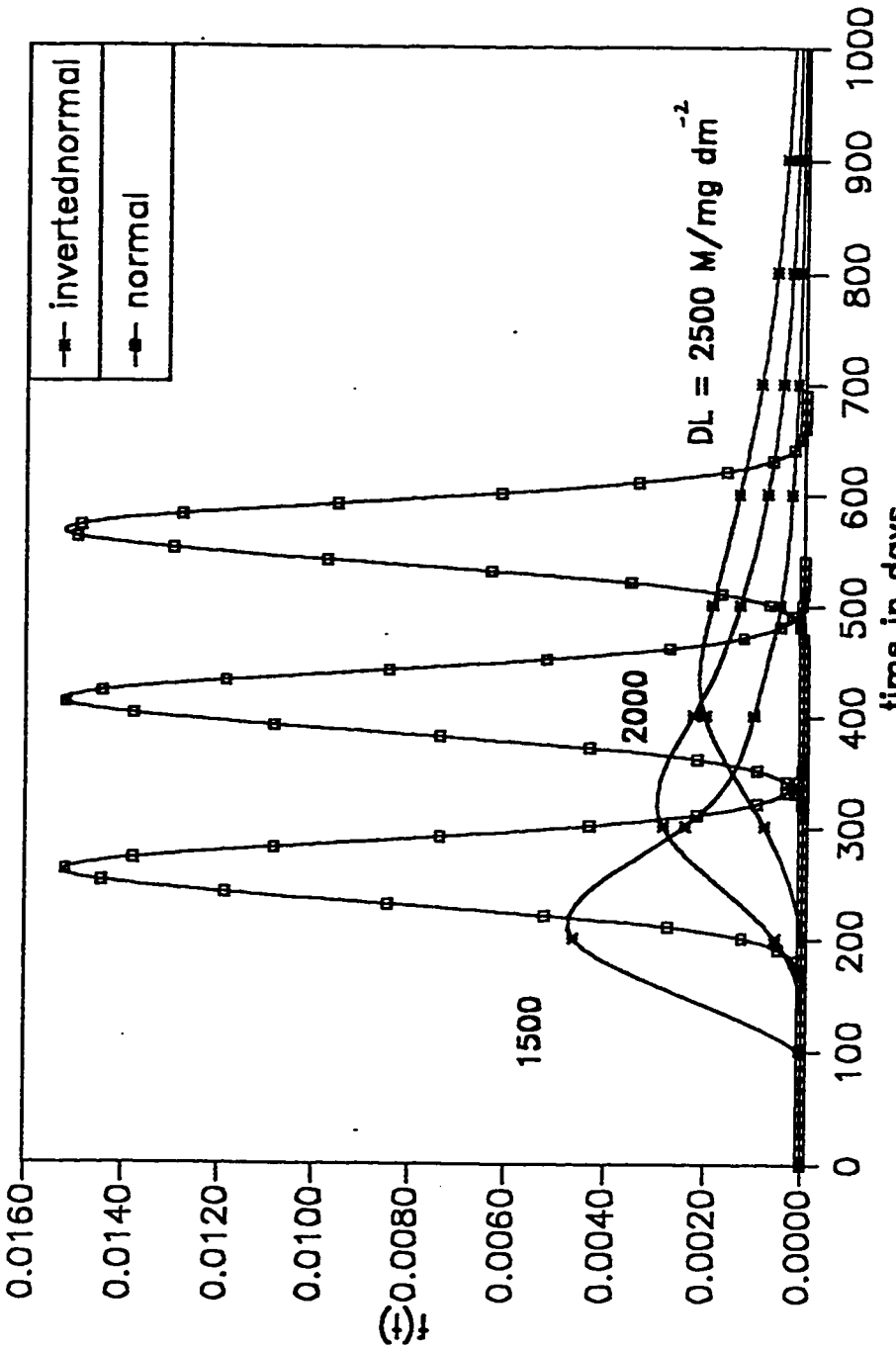

Fig. 3.23 Probability density function of normal and inverted normal distributions obtained from damage function for oxidation at different critical damage levels. Data from Ref [48]. [See Table 3.5 for distribution parameters].

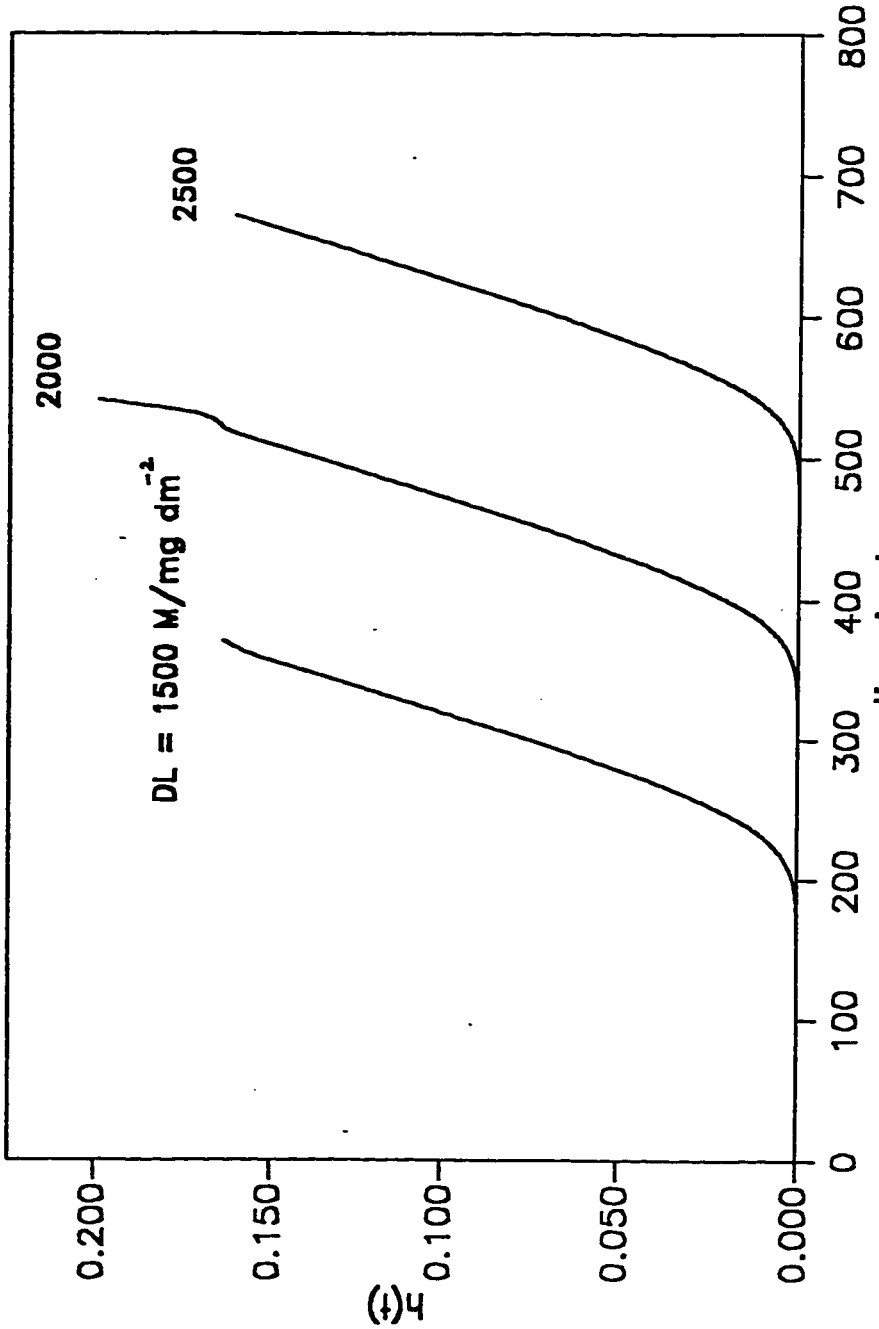

Fig. 3.24 Hazard function of normal distributions obtained from damage function for oxidation at different critical damage levels. Data from Ref [48]. [See Table 3.5 for distribution parameters].

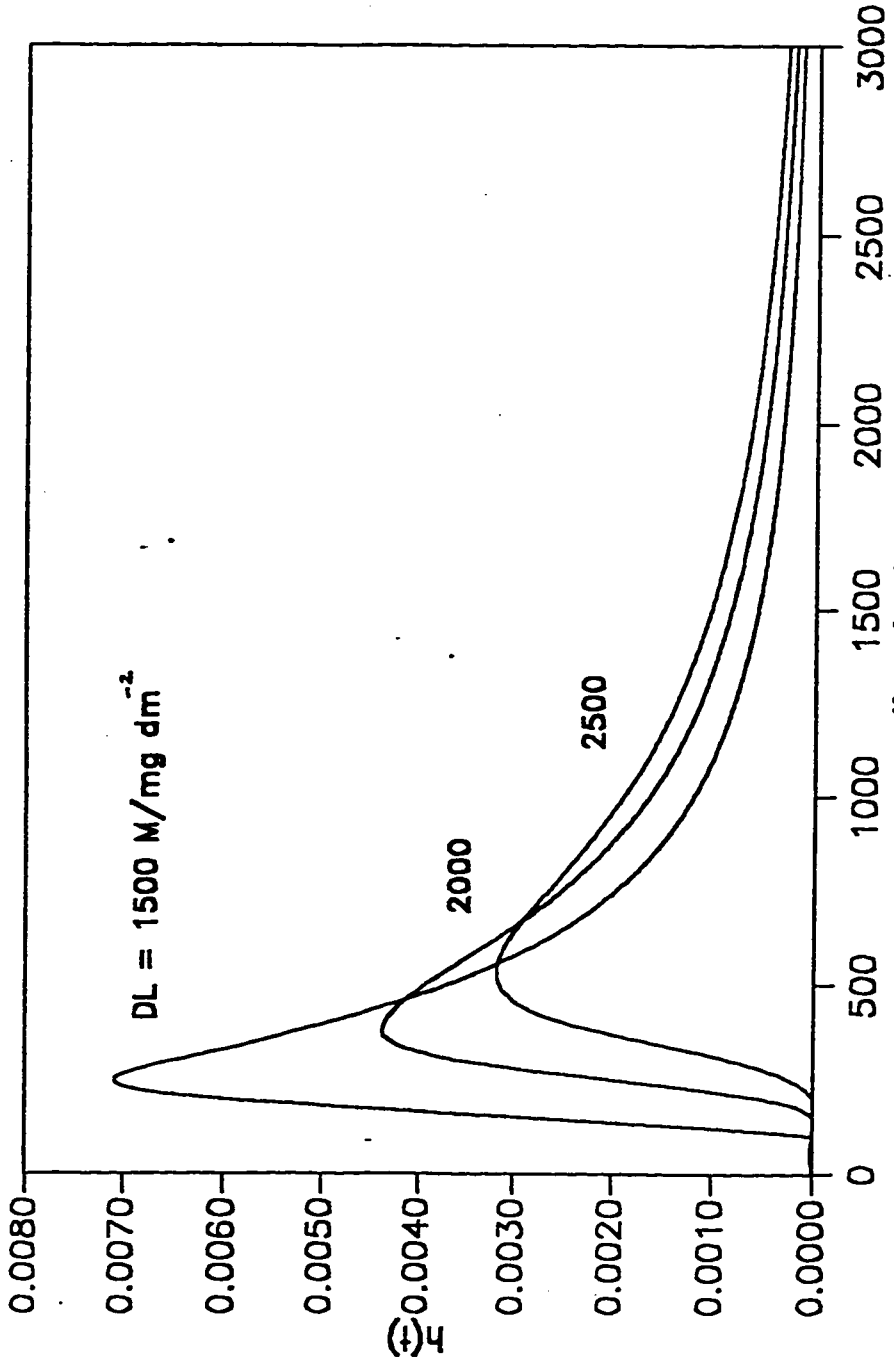

Fig. 3.25 Hazard function of inverted normal distributions obtained from damage function for oxidation at different critical damage levels. Data from Ref [48]. [See Table 3.5 for distribution parameters].

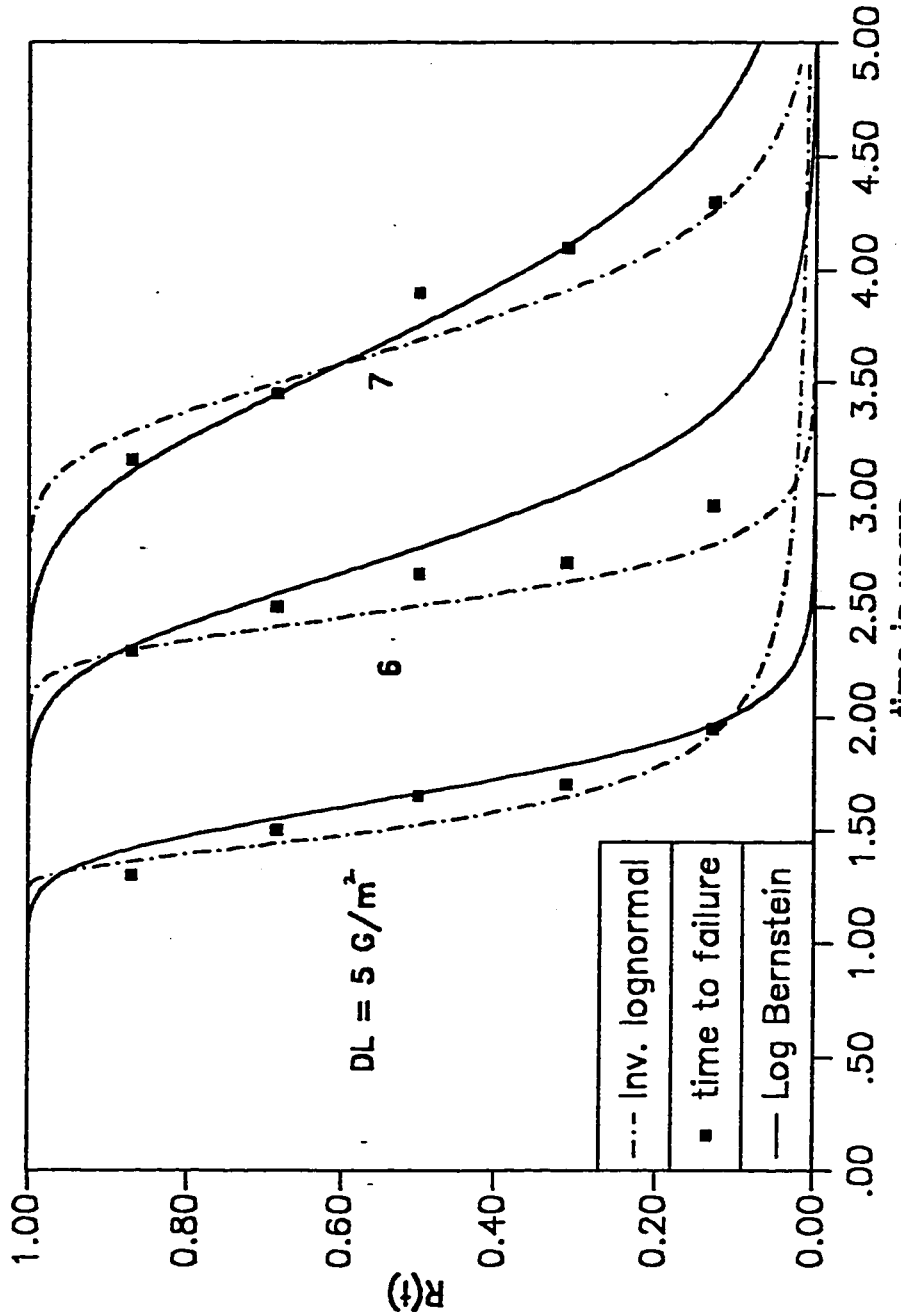

Fig. 3.26 Reliability function for three parameter Log Bernstein distribution obtained from damage function with actual time to failure data and empirically fitted inverted lognormal distribution for oxidation at different critical damage levels. Data from [49]. [See Table 3.6 for distribution parameters].

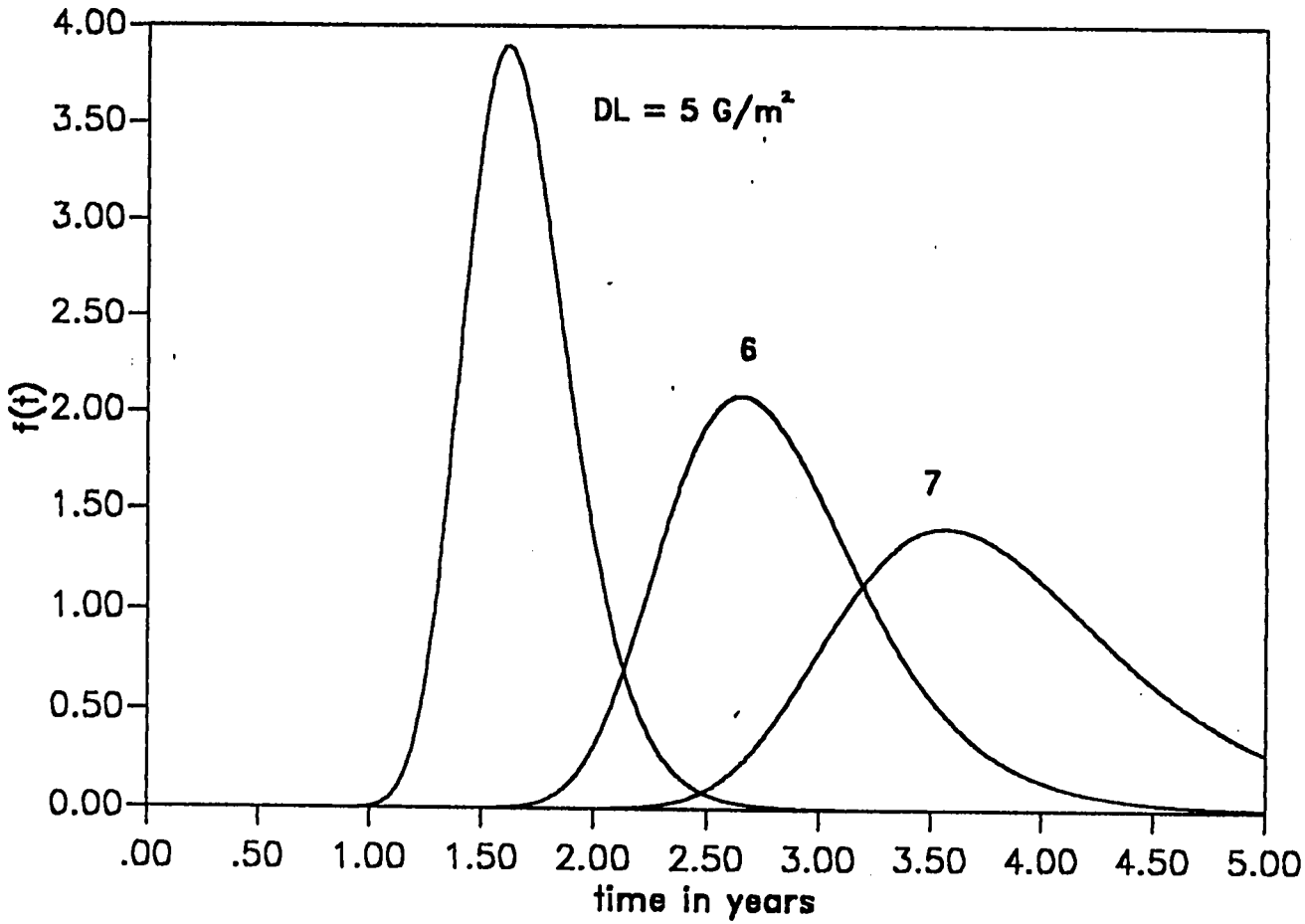

Fig. 3.27 Probability density function for three parameter Log Bernstein distribution obtained from damage function for oxidation at different critical damage levels. Data from [49]. [See Table 3.6 for distribution parameters].

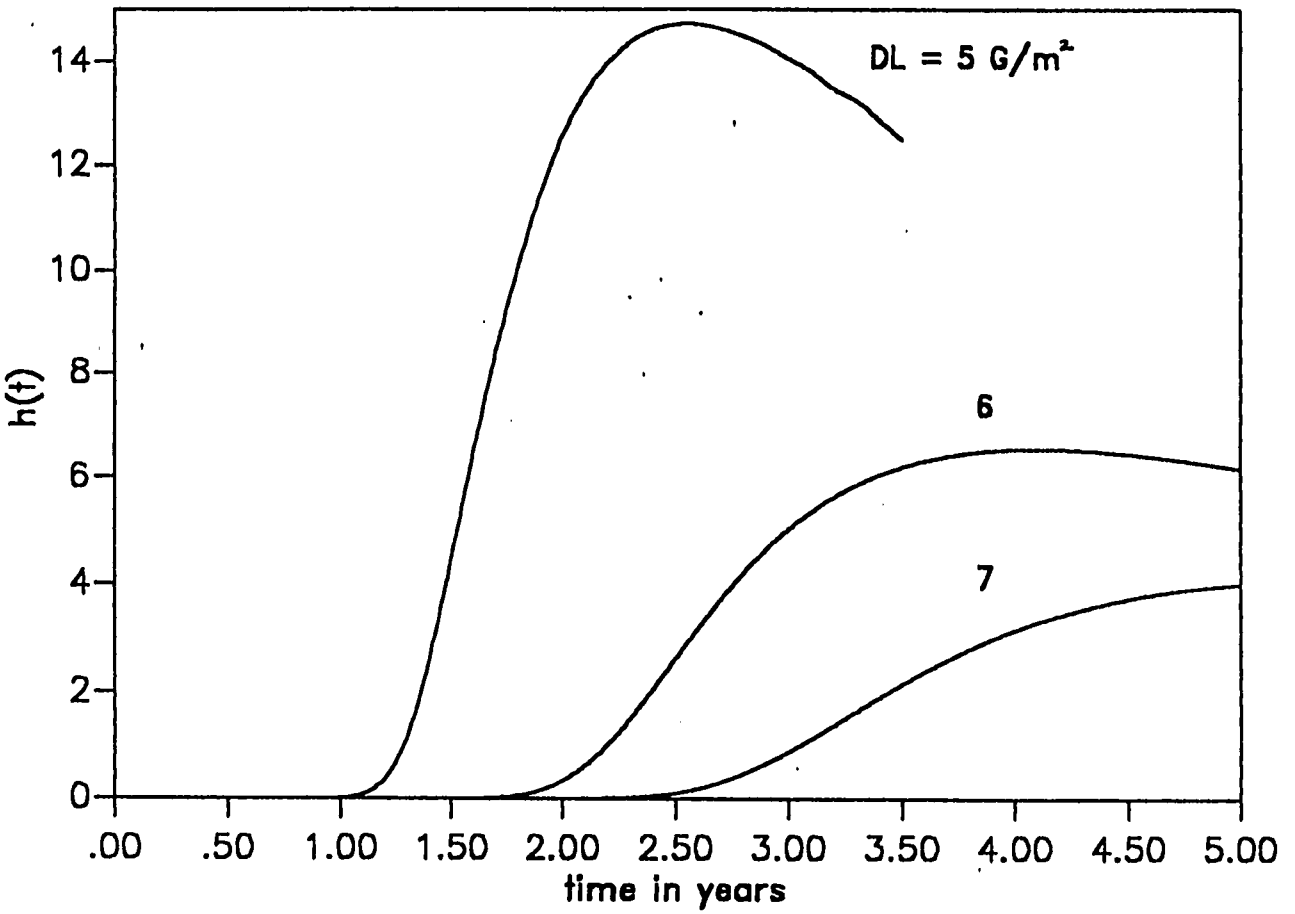

Fig. 3.28 Hazard function for three parameter Log Bernstein distribution obtained from damage function for oxidation at different critical damage levels. Data from [49]. [See Table 3.6 for distribution parameters].

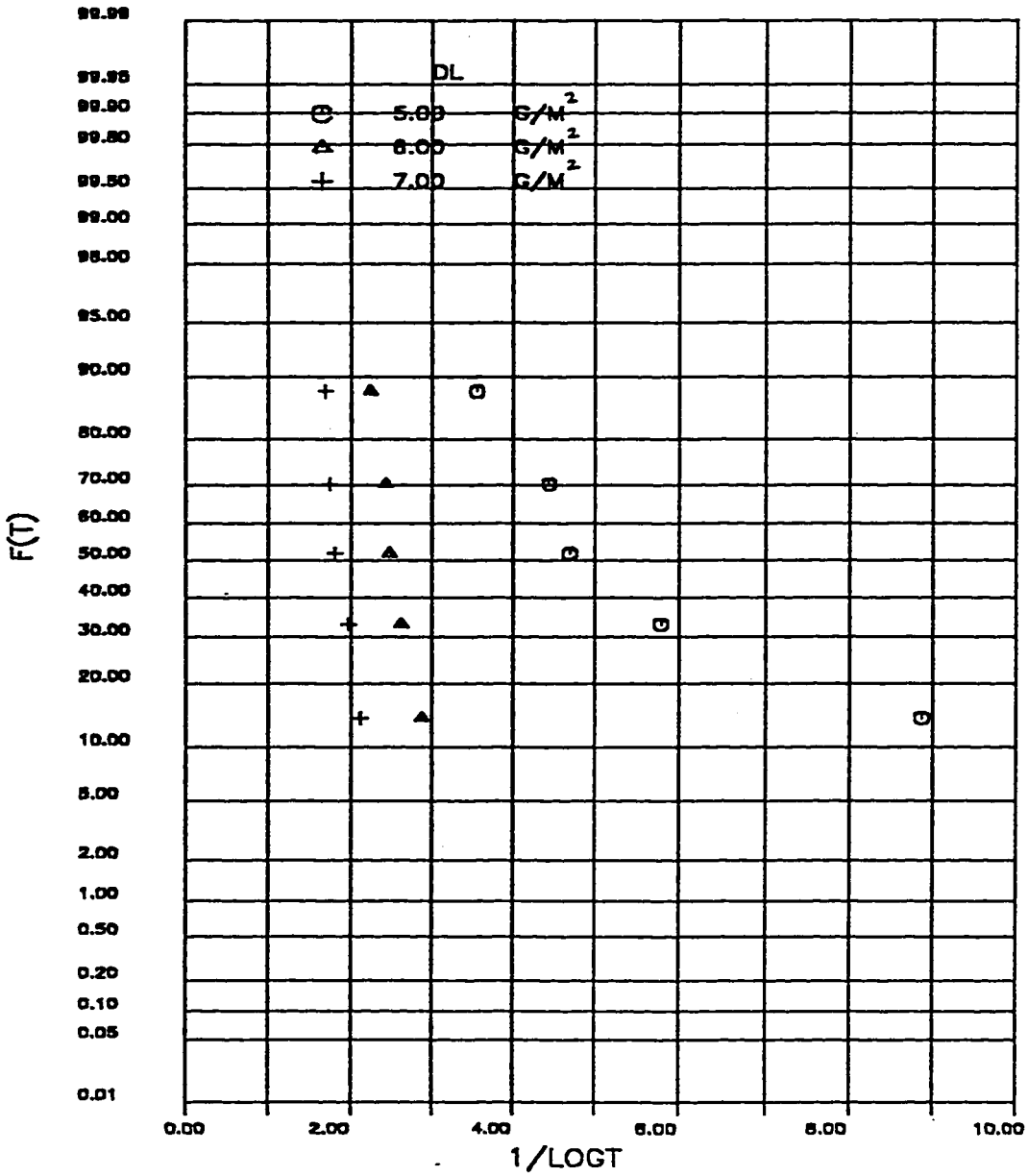

Fig. 3.29 Inverted lognormal distribution of time to failure data for oxidation at different critical damage levels. Time in years. Data from [49].

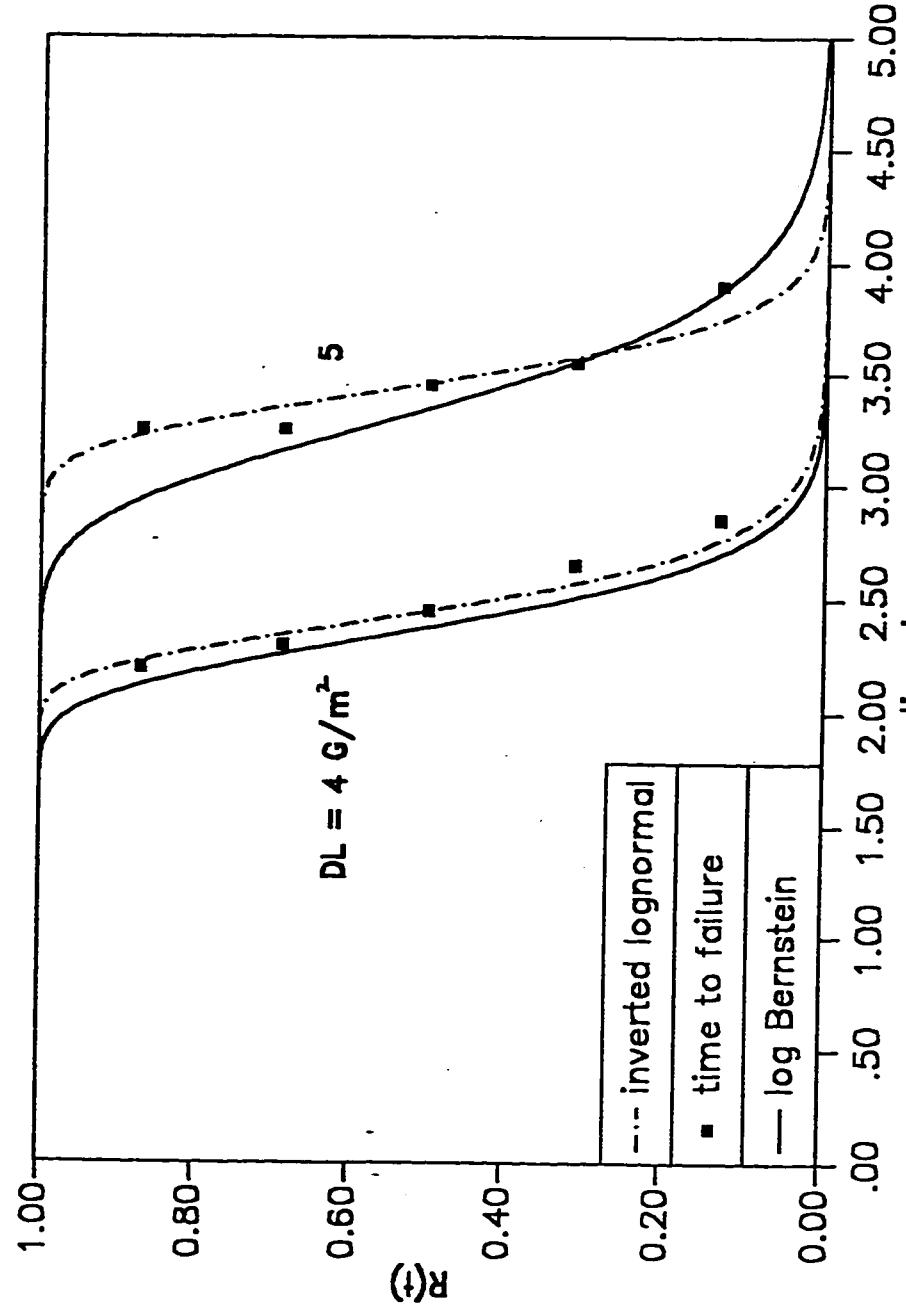

Fig. 3.30 Reliability function for three parameter Log Bernstein distribution obtained from damage function with actual time to failure data and empirically fitted inverted lognormal distribution for oxidation at different critical damage levels. Data from [49]. [See Table 3.7 for distribution parameters].

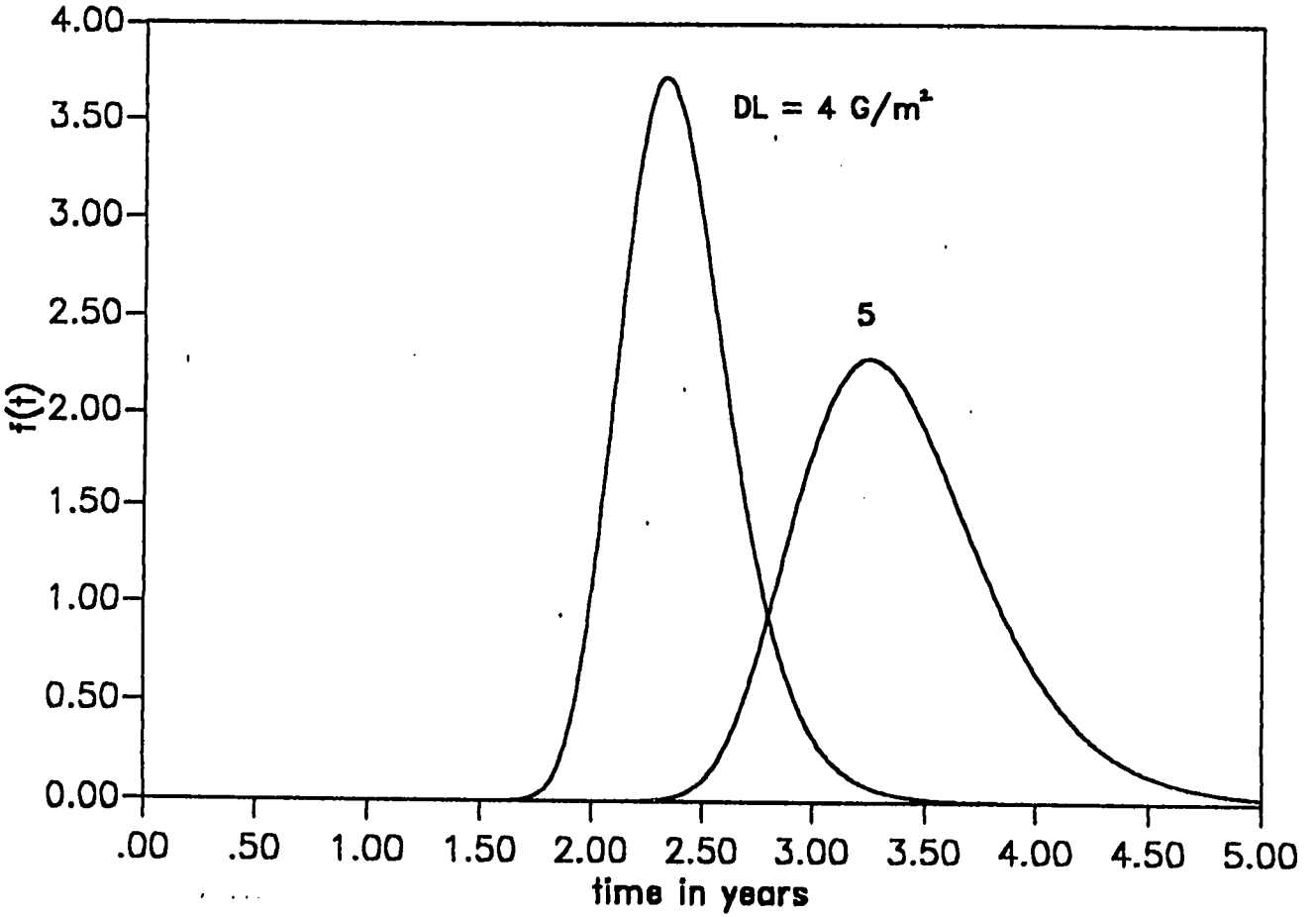

Fig. 3.31 Probability density function for three parameter Log Bernstein distribution obtained from damage function for oxidation at different critical damage levels. Data from [49]. [See Table 3.7 for distribution parameters].

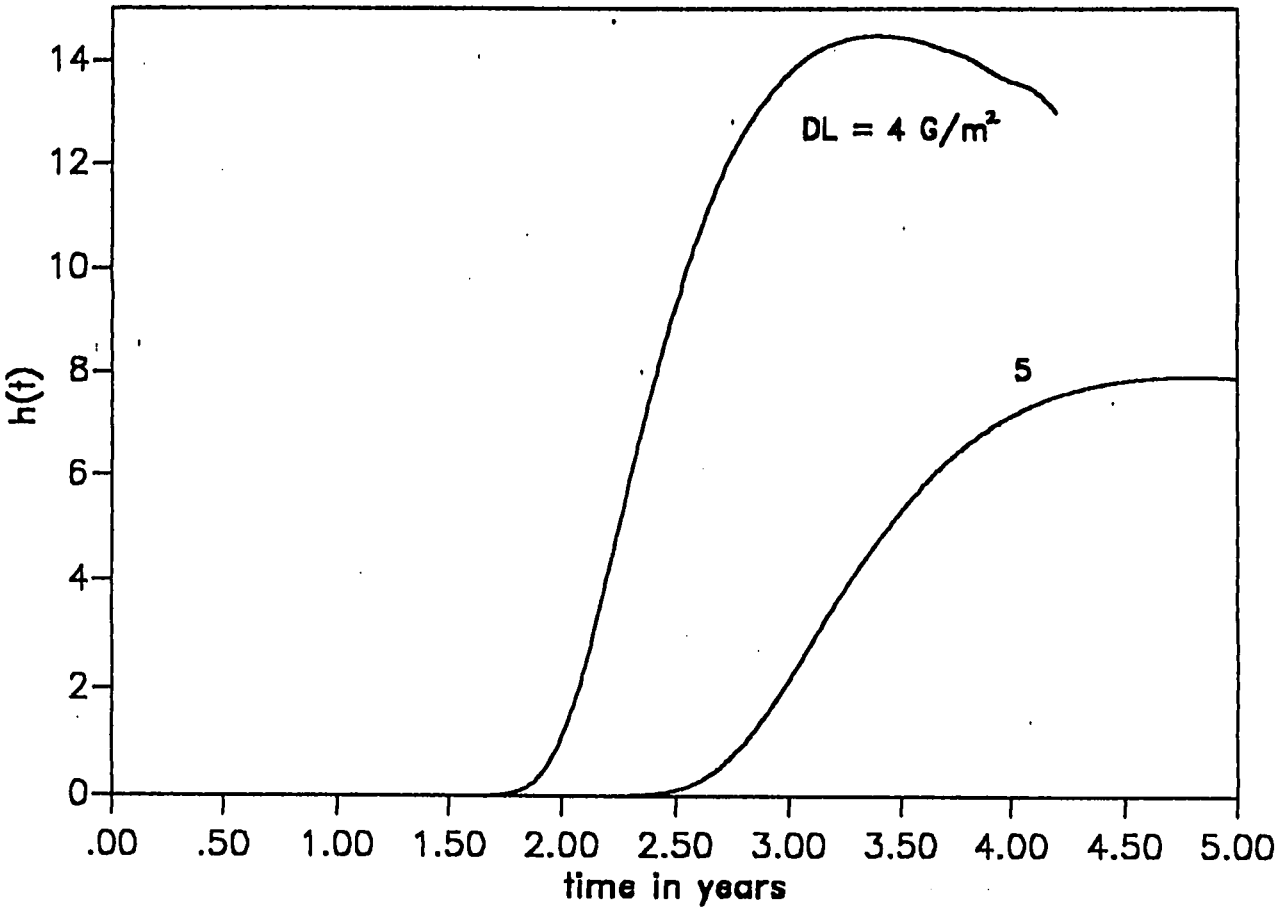

Fig. 3.32 Hazard function for three parameter Log Bernstein distribution obtained from damage function for oxidation at different critical damage levels. Data from [49]. [See Table 3.7 for distribution parameters].

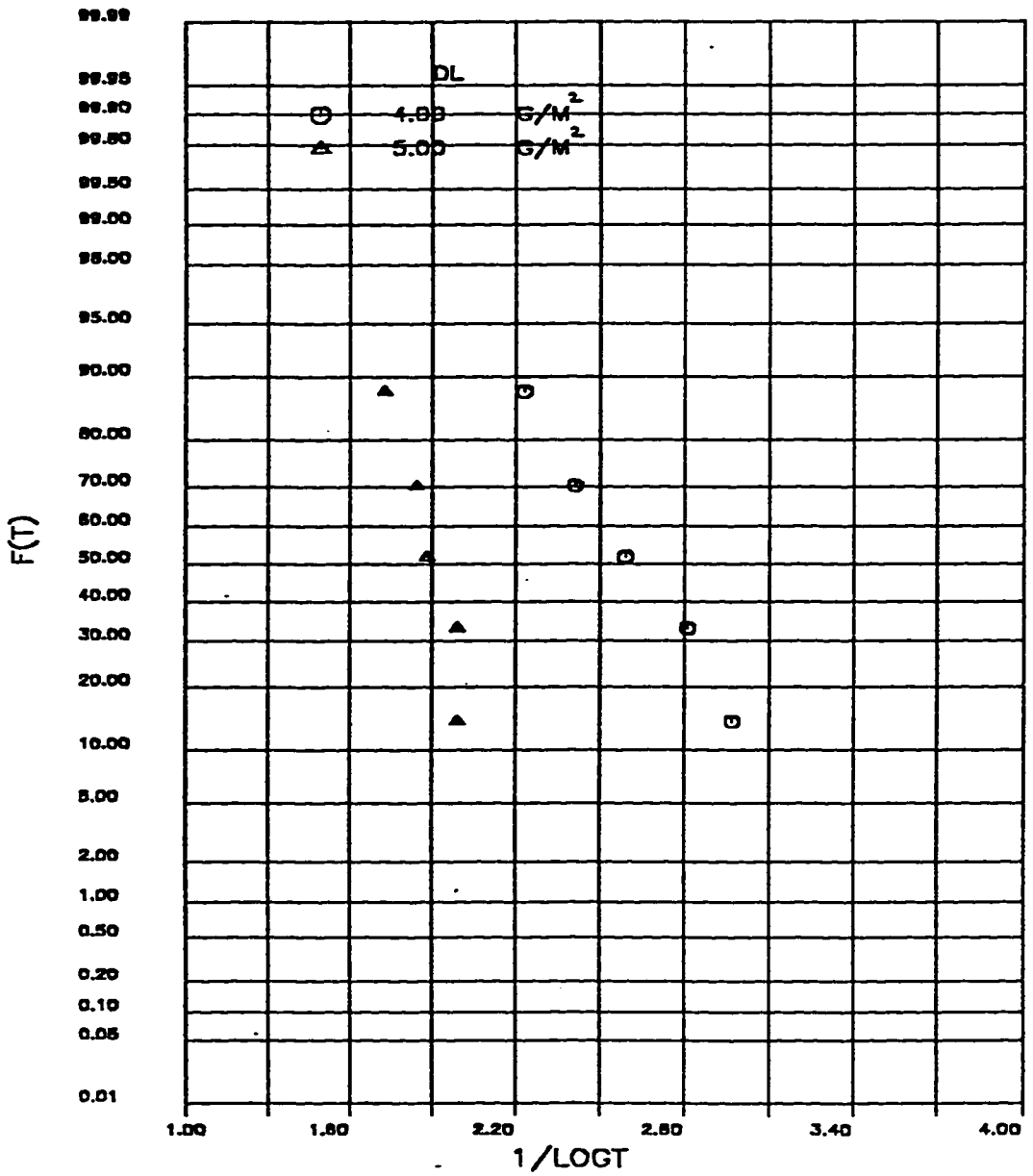

Fig. 3.33 Inverted lognormal distribution of time to failure data for oxidation at different critical damage levels. Time in years. Data from [49].

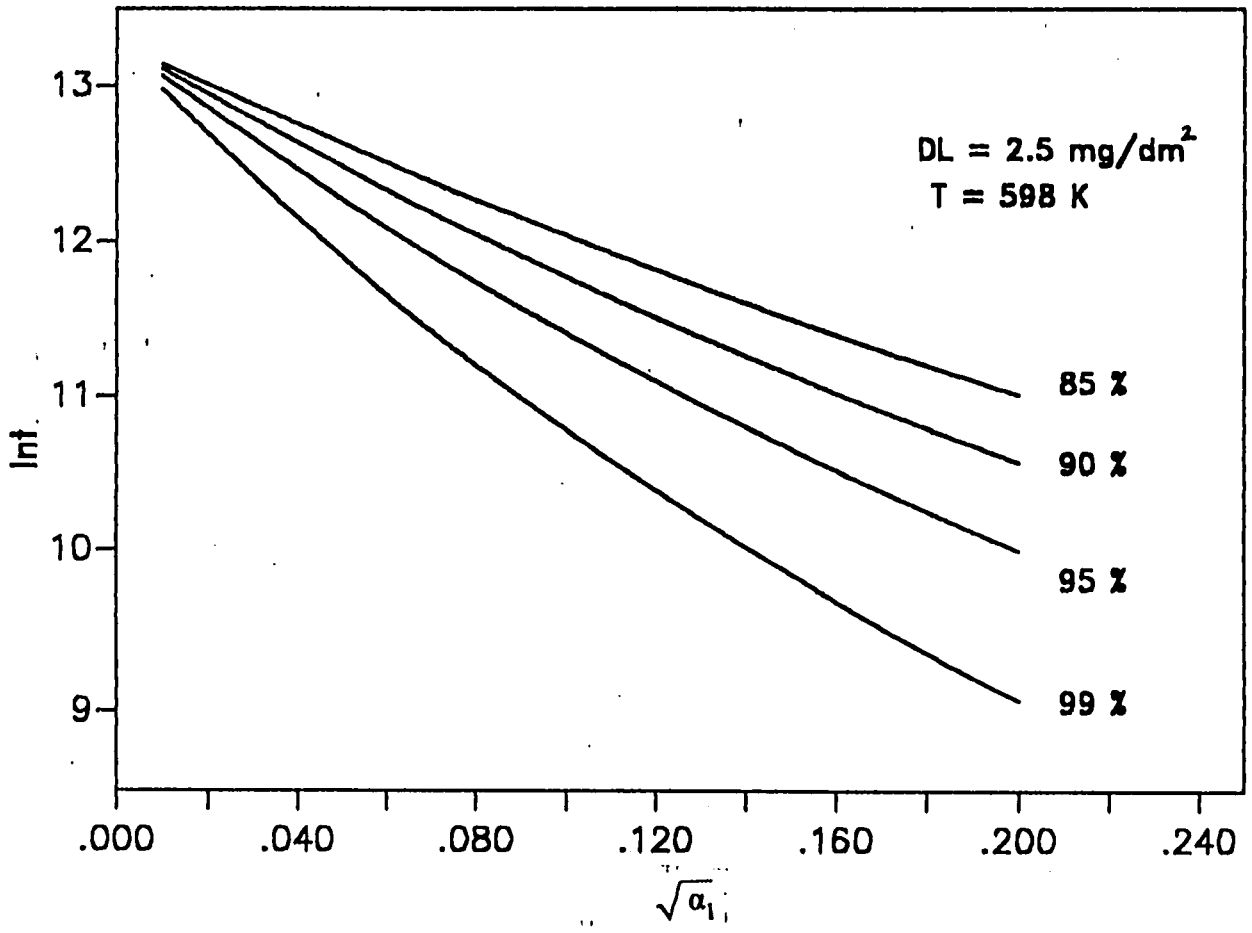

Fig. 3.34 Variation of scatter parameter $\sqrt{\alpha_1}$ with logarithmic of time for variable reliable life at fixed damage level and temperature.

Table 3.1 Parameters of the distribution for SCC [36]

Fig.	Basis	Distribution	Distribution parameters			
3.2	Damage function	Log Bernstein model	D_1	c	α	β
			0.5 0.6	2.60 2.78	0.0035 0.0035	0.00074 0.00074

Table 3.2 Parameters of the distribution for SCC [37]

Fig.	Basis	Distribution	Stress	Distribution parameters	
3.5	Time to failure	Inverted lognormal		$\hat{c}$	$\hat{\alpha}$
			14.4	2.152	0.0113
			10.8	2.481	0.0043
3.6	Time to failure	Inverted lognormal	21.4	1.453	0.0049
			17.9	1.548	0.0029
			14.3	1.698	0.0082
			10.7	2.469	0.0061
3.7	Time to failure	Inverted lognormal	15.9	2.485	0.0070
			12.3	2.575	0.0007
			10.5	2.997	0.0047
3.8	Time to failure	Inverted lognormal	21.4	1.658	0.0045
			17.9	1.911	0.0028
			14.3	2.682	0.0023
			10.7	3.277	0.0023
3.9	Time to failure	Inverted lognormal	25.0	1.487	0.0082
			21.4	1.733	0.0036
			19.6	1.789	0.0042
			17.9	1.826	0.0047
			16.1	2.161	0.0036
			14.3	2.656	0.0024
			12.5	3.132	0.0007

Table 3.3 Parameters of the distribution for Pitting [43]

Fig.	Symbol	Basis	Distribution	Distribution parameter		
3.14	———	Damage function	Weibull	D_i	γ	η
				400	3.1	2.25
				450	3.1	4.73
				500	3.1	9.93

Table 3.4 Parameters of the distribution for Pitting [4]

Fig.	Symbol	Basis	Distribution	Distribution parameters			
3.18	———	Damage function	lognormal	D_1	c_1	α_1	β_1
				40 50	0.594 0.742	0.0 0.0	0.00112 0.00112
3.18	———	Damage function	Inverted lognormal	40 50	0.594 0.742	0.2 0.2	0.0 0.0

Table 3.5 Parameters of the distribution for Oxidation [48]

Fig.	Symbol	Basis	Distribution	Distribution parameters			
3.22	———	Damage function	normal	D_1	c	α	β
				1500	259.42	0.0	688.297
				2000	412.56	0.0	688.297
				2500	565.70	0.0	688.297
3.18	———	Damage function	Inverted normal	1500	259.42	0.2	0.0
				2000	412.56	0.2	0.0
				2500	565.70	0.2	0.0

Table 3.6 Parameters of the distribution for Oxidation [49]

Fig.	Symbol	Basis	Distribution	Distribution parameters			
3.26	———	Damage function	Log Bernstein model	D_l	c_l	α_l	β_l
				5 6 7	0.2201 0.4418 0.5744	0.0078 0.0078 0.0078	0.0036 0.0036 0.0036
	—·—·—·—	Time to failure	Inverted lognormal	D_l	$\hat{c}_l$	$\hat{\alpha}_l$	
				5 6 7	0.183 0.399 0.567	0.1000 0.0082 0.0078	

Table 3.7 Parameters of the distribution for Oxidation [49]

Fig.	Symbol	Basis	Distribution	Distribution parameters			
3.30	———	Damage function	Log Bernstein model	D_l	c_l	α_l	β_l
				4 5	0.3759 0.5242	0.0057 0.0057	0.0013 0.0013
	—·—·—·—	Time to failure	Inverted lognormal	D_l	$\hat{c}_l$	$\hat{\alpha}_l$	
				4 5	0.356 0.539	0.0110 0.0029	

CHAPTER 4

FOULING

4.1 INTRODUCTION

The term fouling can be defined as *the deposition of unwanted material on heat transfer equipments which results in an increase in thermal resistance to heat transfer and a subsequent loss of thermal efficiency of the heat transfer equipment.* It should be noted that the growth of the fluid impurities causes the thermal-hydraulic performance of heat transfer equipments to decrease continuously with time. These fluid impurities may be crystals, biological growths, corrosion products, or a combination of these. The deposition of these fluid impurities is a function of the surface temperature, surface material, surface condition, fluid velocity, flow geometry and fluid composition. Different aspects of the deposition process and its characterization are discussed in references [52], [53]. A review of the effects of variables is provided by Suitor et.al [54].

4.2 TYPES OF FOULING PROCESSES

There are several types of basic fouling mechanisms by which the deposition may occur and each of them in general depends upon several variables.

4.2.1 PARTICULATE FOULING

Many streams and particularly cooling water contain suspended solid particles such as rust, clay, dust etc., which can settle upon the heat transfer surface. These deposits, typically do not adhere strongly to the surface and are likely to wash off during the operation. It should be noted that the thicker the deposit becomes, the more likely it is to wash off (in patches) and thus attain some asymptotic average value over a period of time. Particulate fouling is strongly affected by velocity, whereas it is more or less not influenced by the normal operating temperature of the heat transfer surface. However the deposit can 'bake on' to a relatively hot surface and may be difficult to wash off during the service. It should be noted that a comprehensive review of particulate fouling in relation to the Kern and Seaton [6] successful deposition-removal model has been discussed by Gudmudsson [55].

4.2.2 CRYSTALLIZATION FOULING

Certain salts commonly found in natural waters such as calcium sulphate are less soluble in warm water than in cold. If such a stream encounters a heat transfer surface at a temperature greater than the corresponding saturating temperature for dissolved salt, then the salt will crystallize on the surface. Crystallization will begin at hot spots such as scratches and pits, often after considerable induction period, and then spread over the entire surface. The buildup of fouling (or scaling) will continue as long as the surface is in contact with the fluid and has a temperature above saturation. The scale formation is

strong adherent and usually requires vigorous mechanical or chemical treatment to remove it. It should be noted that many salts have quite complex crystallization diagrams, and the crystalline form changes with temperature. This complicates the predictability of crystallization fouling as the temperature inside the scale can frequently change [52], particularly in constant heat flux operations. A systematic study of the scaling characteristics of cooling tower water has been conducted by several researchers [56,57,58].

4.2.3 CHEMICAL REACTION FOULING

This type of fouling mechanism involve primarily physical changes. A common source of fouling on the process stream side are chemical reactions that result in producing a solid phase at or near the heat transfer surface. For example a hot heat transfer surface may cause a thermal degradation of one of the components of process stream, resulting in carbonaceous deposits commonly called 'coke' on the surface. In some process applications a surface may cause polymerization to occur, resulting in tough layer of low-grade plastic or synthetic rubber. These deposits are sometime extremely hard and may require extreme measures as burning off the deposit in order to return the heat exchanger to satisfactory operation level.

In some cases, such as with crude oil, the chemical reaction fouling will be combined with particulate fouling or crystallization fouling. Taborek et.al. [52], Watkinson and Epstein [59], have indicated that most types of process streams produce asymptotic fouling curves, indicating the existence of flow velocity

dependent removal mechanisms or perhaps deposition rate decrease mechanism.

4.2.4 CORROSION PRODUCT FOULING

Corrosion product fouling is due to the chemical reaction of containment materials (including heat transfer surfaces) with the circulating process stream. Somerscales [60] distinguishes between two types of corrosion related fouling. In one type the fouling is a result of corrosion products formed at locations remote from the heat transfer surface, and transported and deposited on the heat transfer surface. Lister [61] has reviewed aspects of this type of ex-situ corrosion fouling. The second type, in-situ corrosion fouling, is due to corrosion products that form and remain at the heat transfer surface.

It should be noted that the roughness of the surface, invariably connected with corrosion, will produce hot spots for crystallization and particle sedimentation. In boiling, the surface roughness due to corrosion can have a nucleation promoting effect which is very sensitive to fouling accumulation.

4.2.5 ORGANIC MATERIAL FOULING

Many cooling water sources such as sea, river, or lake water contain organisms that will attach to heat transfer surfaces and grow with time. These organisms range from algae and micro-organisms (microbial fouling) to macro-organisms such as barnacles (microbial biofouling). It should be noted that only a very thin film of organic material is present, and the heat transfer resistance is high. Biofouling is typically controlled with proper treatment in cooling water

systems. Charackils [62] has conducted extensive study of biofouling and he analyzed the physical, chemical and biological processes that constitute the overall biofouling mechanism.

4.2.6 FREEZING OR SOLIDIFICATION FOULING

In this type of fouling a pure liquid solidifies when it comes in contact with a subcooled heat transfer surface or it may be defined as the deposition of a high melting point constituent of a liquid in contact with a cold heat transfer surface. Although freezing or solidification fouling is known in a number of industrial applications and processes, it is only in the field of ice formation that there has been an attempt to quantify it. The calculation of ice film thickness according to the method suggested [63] is recommended by Bott [64] in a review article on freezing fouling.

4.2.7 COMBINED FOULING

Most fouling processes that occur on a heat transfer surface are the result of a combination of two or more of the types discussed in the above sections. A common example is combination of sedimentation and crystallization fouling in a cooling water systems. It should be noted that most surface waters contain both sediment and calcium carbonates, and the concentration of these components rise as the water is recirculated through the cooling system. It is therefore common to find deposits that are composed of crystals of inverse solubility salts together with finely divided sediments. Bell and Muller [65]

indicated that the behavior of these deposits is intermediate between two limiting cases : the crystals tend to hold the sediment in place, but there are planes of weakness in the structure that fail from time to time and cause the deposit to break off in patches, thus it can attain some asymptotic average value over a period of time.

4.3 MATHEMATICAL MODELS OF FOULING

Various researchers [53,54,6], contributed to develop the analytical basis for predicting the failure of the equipment by fouling using deterministic approaches. The most widely accepted analytical approach have been based on the following material balance equation proposed by Kern and Seaton [6]

$$\frac{dR_f}{dt} = \Phi_d - \Phi_r$$

where dR_f / dt = the net rate of fouling accumulation

Φ_d = the rate of fouling deposition

Φ_r = the rate of fouling removal

From this very basic equation, we can emphasize that the fouling is a complex phenomenon that is affected by many factors. The term Φ_d depend on the type of the fouling mechanism, while Φ_r depends on the adhesive force of the deposit and the shear stress due to the flow velocity. The rate of deposition and the rate of removal have been proposed by various researchers, which can be summarized by the following deterministic fouling growth kinetic models :

(a) Linear fouling [66] $R_f(t) = A + Bt$ (4.1)

(b) Falling rate fouling [53] $R_f(t) = A + B \ln t$ (4.2)

(c) Asymptotic fouling [6] $R_f(t) = R_f^* [1 - e^{-\lambda t}]$ (4.3)

It is frequently observed that there is a delay time between the start of the fouling growth process and the formation of fouling deposits. This period is defined as induction or delay time t_o. The fouling growth models mentioned earlier can be modified to introduce delay time as follows :

(a) $R_f(t) = A + B(t - t_o)$ (4.4)

(b) $R_f(t) = A + B \ln(t - t_o)$ (4.5)

(c) $R_f(t) = R_f^* [1 - e^{-\lambda(t - t_o)}]$ (4.6)

The parameter A represent the initial fouling at time $t=0$, (or $t=t_o$) for linear fouling, and at time $\ln t=0$ (or $t=t_o$) for falling rate fouling. In most of the cases A is zero or negligible.

Both replicate laboratory experiments in the study of these models as well as field investigations have shown considerable scatter in the values of fouling resistance at any time t and vice versa. [66,53,6]. This randomness is due to various factors such as, variations and fluctuations in velocity and temperature around their nominal values, perturbations in the foulant chemistry, metallurgical features of the tube materials, operating and environmental conditions. Thus in reality, fouling phenomena is stochastic in nature, therefore it is more appropriate to investigate the fouling by using statistical /

probabilistic approaches.

4.4 STOCHASTIC CHARACTERIZATION OF FOULING

As mentioned in the above section that the fouling process is a random phenomena, the fouling stochastic growth models corresponding to the deterministic representation of eqs (4.1), (4.2), (4.3) are :

(a) $R_f(t) = A + Bt$ (4.7)

(b) $R_f(t) = A + B \ln t$ (4.8)

(c) $R_f(t) = R_f^* [1 - e^{-\lambda t}]$ (4.9)

where A, B, R_f^* are random variables and $R_f(t)$ is the random fouling process. Random variable A represent the initial amount of fouling and is usually zero (i.e., $\mu(A) = 0, \sigma(A) = 0$).

Morse and Knudsen [56] investigated the scaling behavior of a simulated cooling tower water on a heat transfer surface. The data obtained from fig. 4, of ref [56] shows that sample functions of fouling growth resistance are linear in nature. This data set is further analysed in this section [Fig. 4.1] Based on linearity of the sample function of fouling resistance and normality of A and B, a three parameter Bernstein distribution function is hypothesized to characterize the time to reach a threshold value of $R_f(t) = R_{fl}$. as mentioned in Sec 1.8.1 of Chapter 1. The reliability function along with the observed time to failure (time to reach the threshold value) data at different critical damage levels (fouling resistance R_{fl}) is shown in the Fig. 4.2. Figs. 4.3 and 4.4 shows the respective

probability density function and hazard function. The time to failure data is also plotted [F(T) vs 1/T] on the normal probability paper [Fig. 4.5] The straight line demonstrates the inverted normal distribution is also acceptable model. Both the models are equally fitted well as shown in Fig. 4.2.

Taborek et.al, [53] presented a preliminary, semi-analytical method for predicting cooling tower water fouling. The data of the falling rate fouling is analysed here. When data was plotted on semilog paper it shows linear fit [Fig. 4.6] for each data realization which indicates the validation of eq (4.8). Assuming a log normal distribution for **A, B**, a three parameter log Bernstein model can be proposed for such data. (Sec 1.10). Fig. 4.7 shows the reliability function along with the time to failure data at different critical damage levels. Figs. 4.8 and 4.9 represents the respective probability density and hazard functions. When time to failure is plotted independently on a normal probability paper as F(T) vs 1/lnT, inverted log-normal distribution is also observed to fit the data as shown in the Fig. 4.10. A comparison of three parameter log Bernstein model and inverted lognormal illustrate that the log Bernstein distribution fits better than the two parameter inverted lognormal model [Fig. 4.7]

Dunqi and Knudsen [67] analysed the experimental data of asymptotic fouling on the basis of the change in overall heat transfer coefficient of the fouling test section and determined the parameters λ and R_f^* by regression analysis. In the present investigation using the values of λ and R_f^* the reliability

function is developed by using Monte Carlo simulation technique as described in the Sec 1.12 of Chapter 1. Taking mean of R_f^* as 0.79 ft^2 h °F/Btu and λ as 0.001/day [67], time to failure distribution is developed by assuming different coefficient of variation for R_f^*. The fouling model eq (4.9) is modified by introducing induction time as

$$R_f(t) = R_f^* [1 - e^{-\lambda(t - t_o)}]$$

where t_o is the induction time.

For failure criterion defined as $R_f(t) = R_{fl}$, the equation for time to failure is

$$T = t_o - \frac{1}{\lambda} \ln\left[1 - \frac{R_{fl}}{R_f^*}\right]$$

For Monte Carlo simulation to generate a sample of time to failure t_i, the following equation is used

$$X_i = T_i - t_o = -\frac{1}{\lambda} \ln\left[1 - \frac{R_{fl}}{R_{fl,i}^*}\right]$$

where $R_{fl,i} = \mu(R_{fl,i}^*) + z_i \sigma(R_{fl,i})$

where z_i is the random observation of standardized normal variate. The 10000 values of X_i were obtained and grouped in various frequency. When the cumulative frequency of time to failure is plotted on weibull probability paper a straight line fit is observed, which demonstrate that a three parameter weibull reliability function is valid and $t_o = 0.975\, T_1$, where T_1 is the minimum observation. (Fig. 4.11 to 4.14). The parameters γ and η were obtained as

illustrated in Sec 1.7. Fig. 4.15 and Fig. 4.16 shows the variation of shape γ and scale η parameters with respect to coefficient of variation of the fouling process.

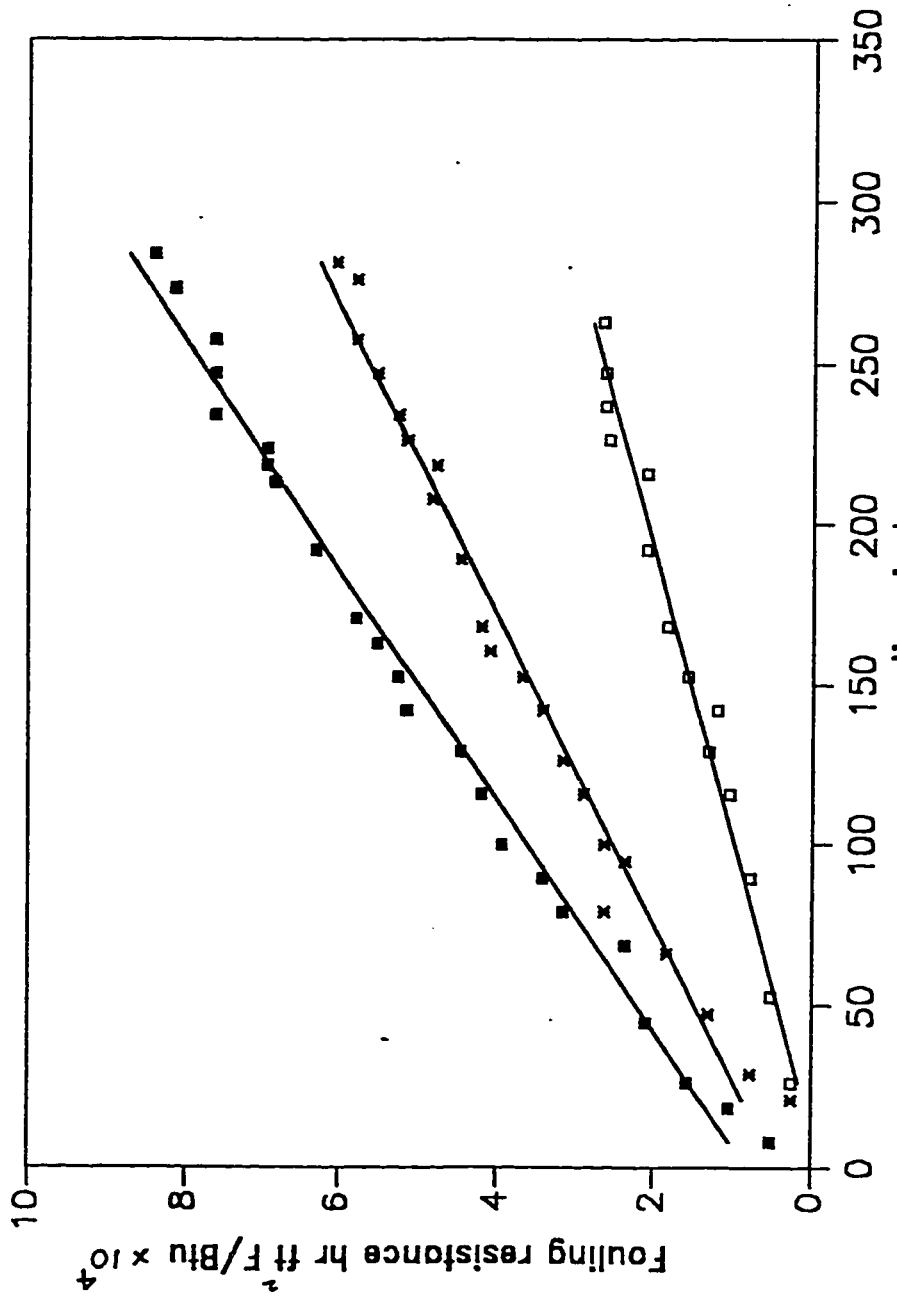

Fig. 4.1 Linear sample functions for fouling process [56].

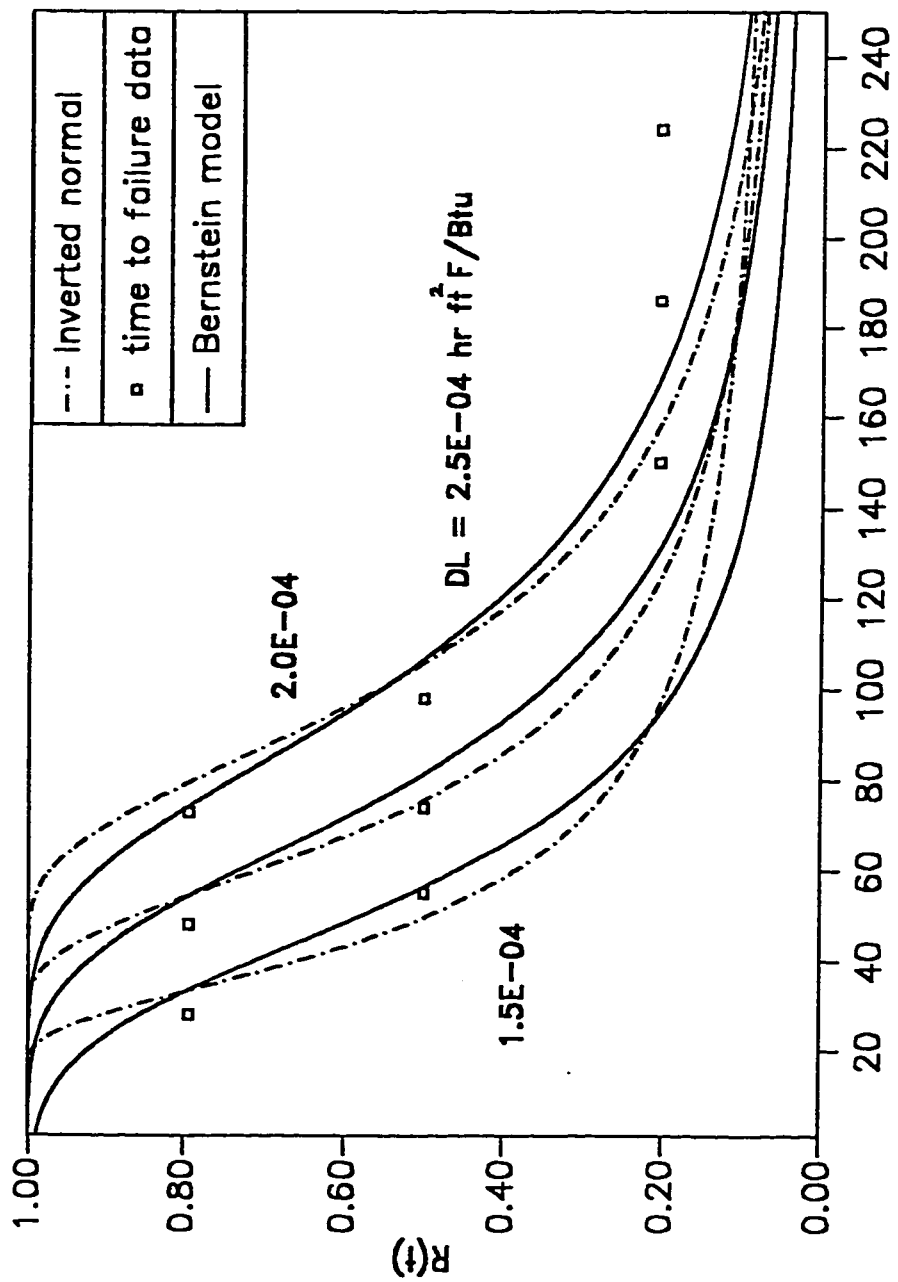

Fig. 4.2 Reliability function for three parameter Bernstein distribution obtained from damage function with actual time to failure data and empirically fitted inverted normal distribution for fouling at different critical damage levels. Data from Ref [56]. [See Table 4.1 for distribution parameters].

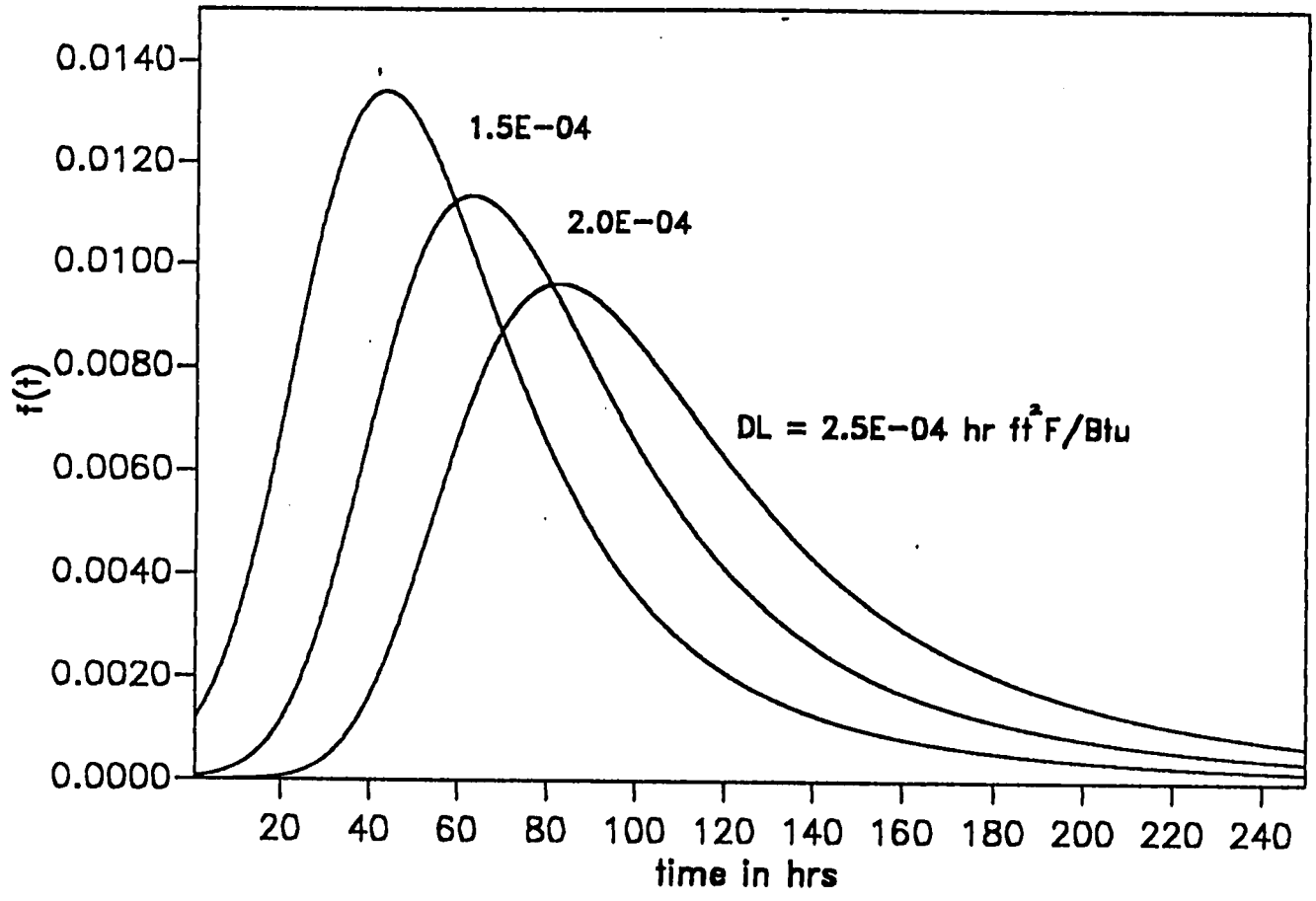

Fig. 4.3 Probability density function for three parameter Bernstein distribution obtained from damage function for fouling at different critical damage levels. Data from Ref [56]. [See Table 4.1 for distribution parameters].

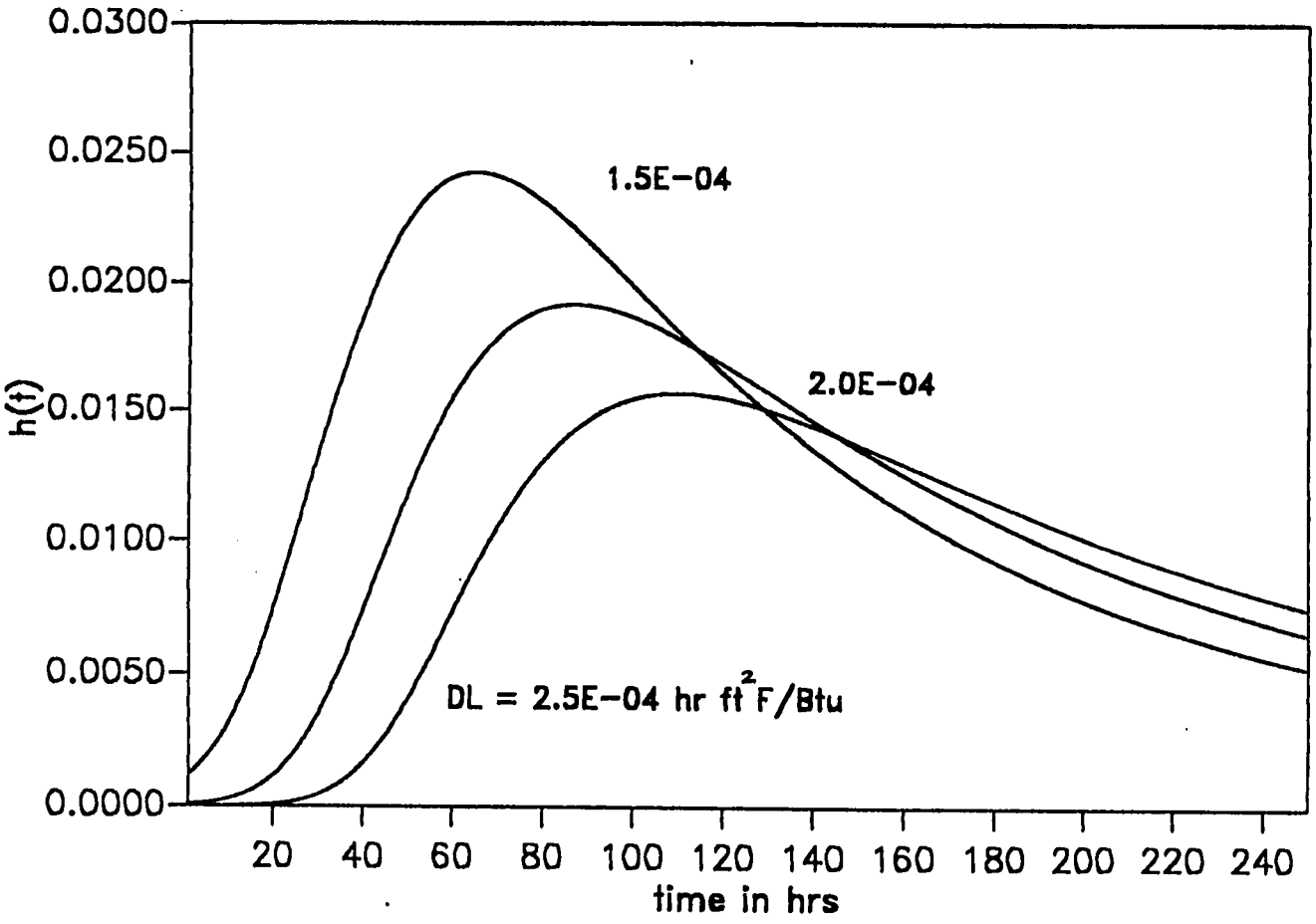

Fig. 4.4 Hazard function for three parameter Bernstein distribution obtained from damage function for fouling at different critical damage levels. Data from Ref [56]. [See Table 4.1 for distribution parameters].

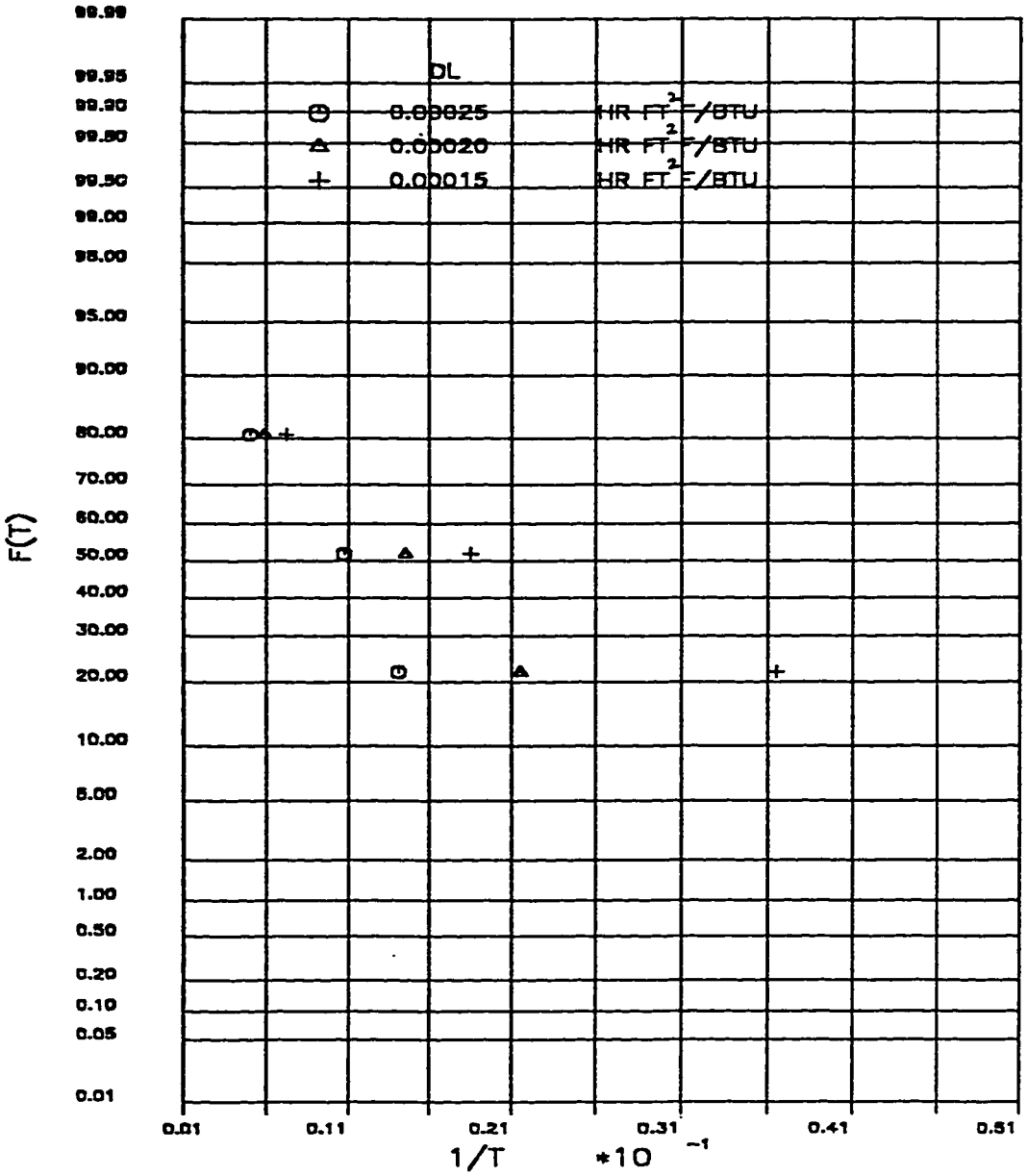

Fig. 4.5 Inverted normal distribution of time to failure data for fouling at different critical damage levels. Data from Ref [56].

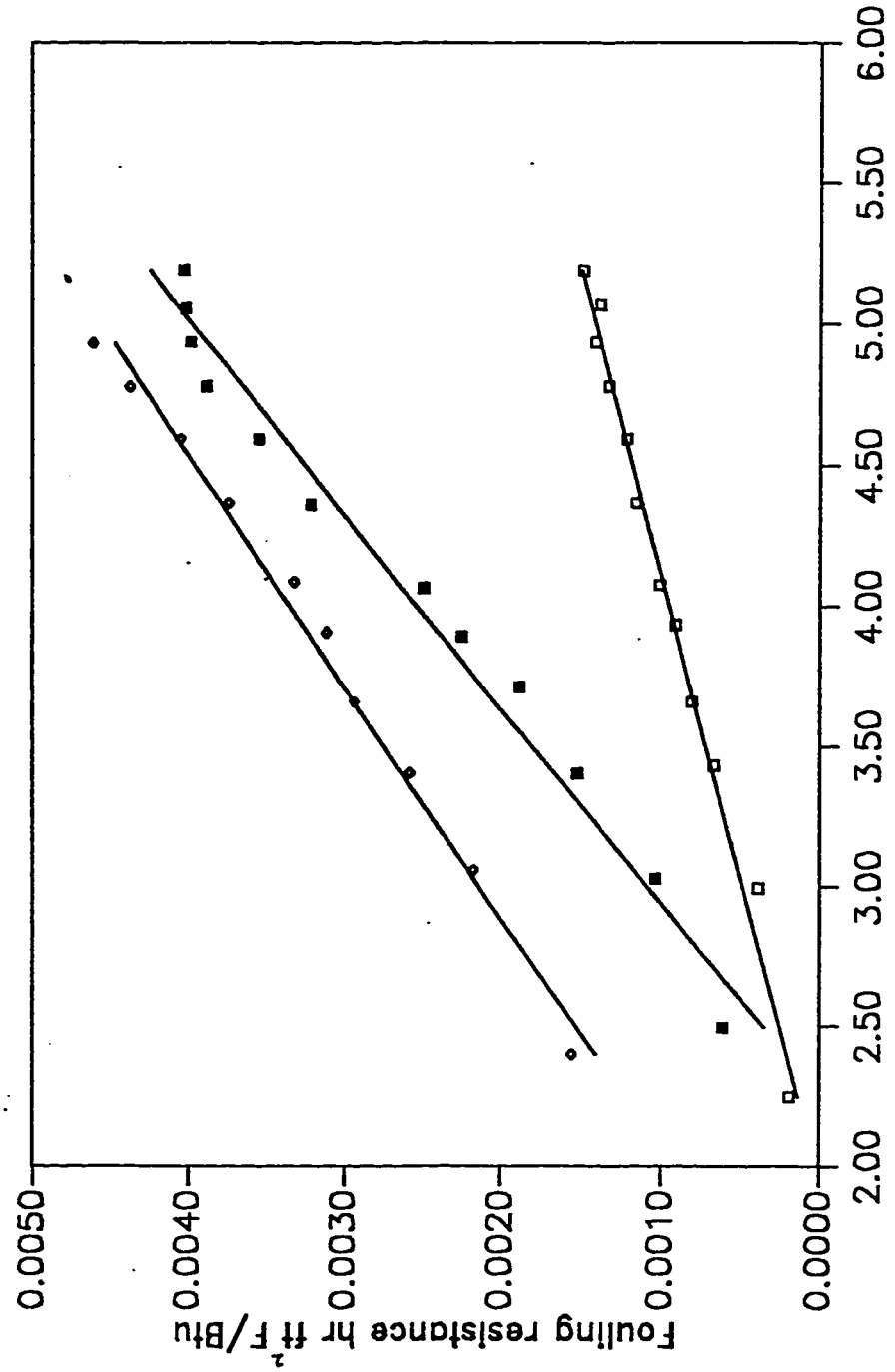

Fig. 4.6 Logarithmic sample functions for fouling process [53].

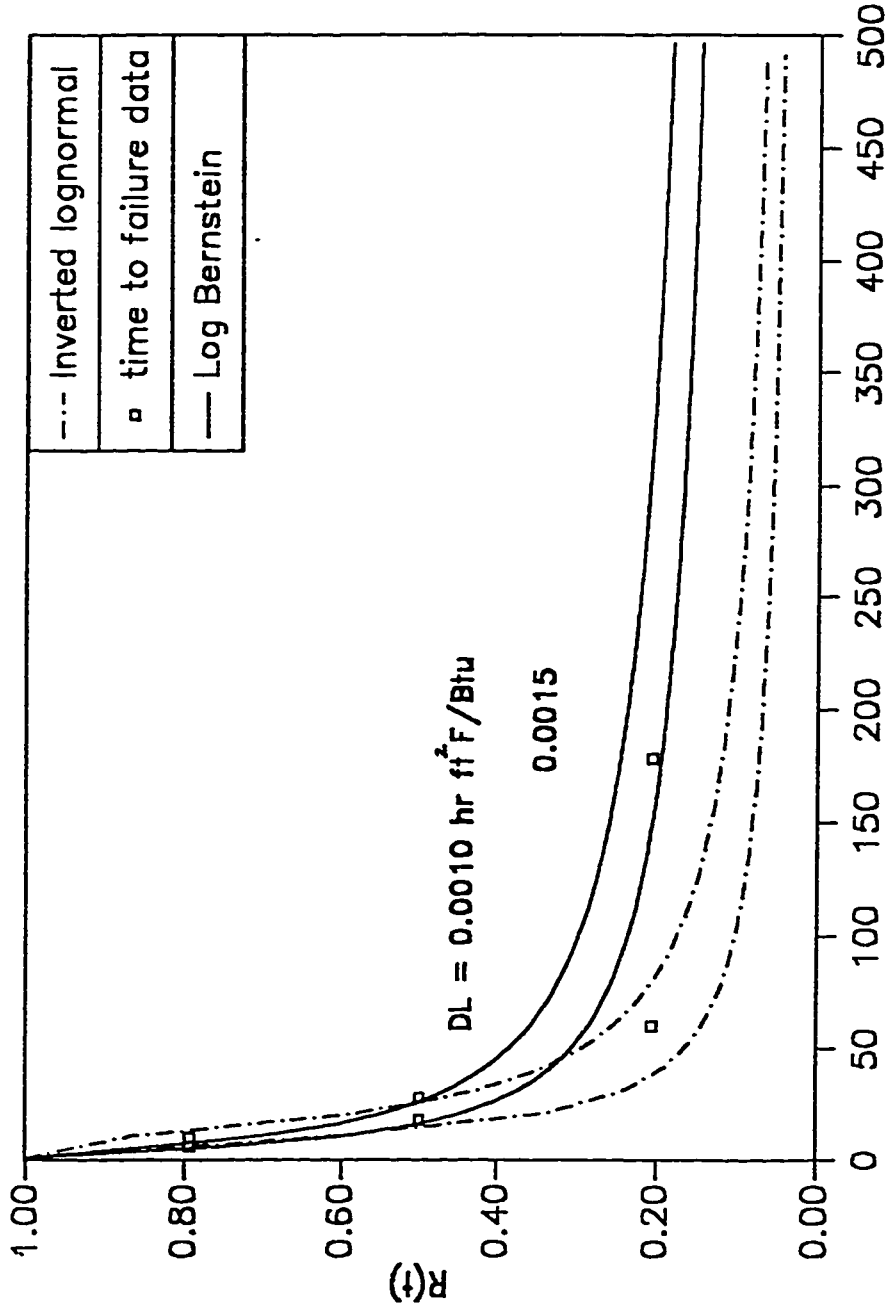

Fig. 4.7 Reliability function for three parameter Log Bernstein distribution obtained from damage function with actual time to failure data and empirically fitted inverted lognormal distribution for fouling at different critical damage levels. Data from Ref [53]. [See Table 4.2 for distribution parameters].

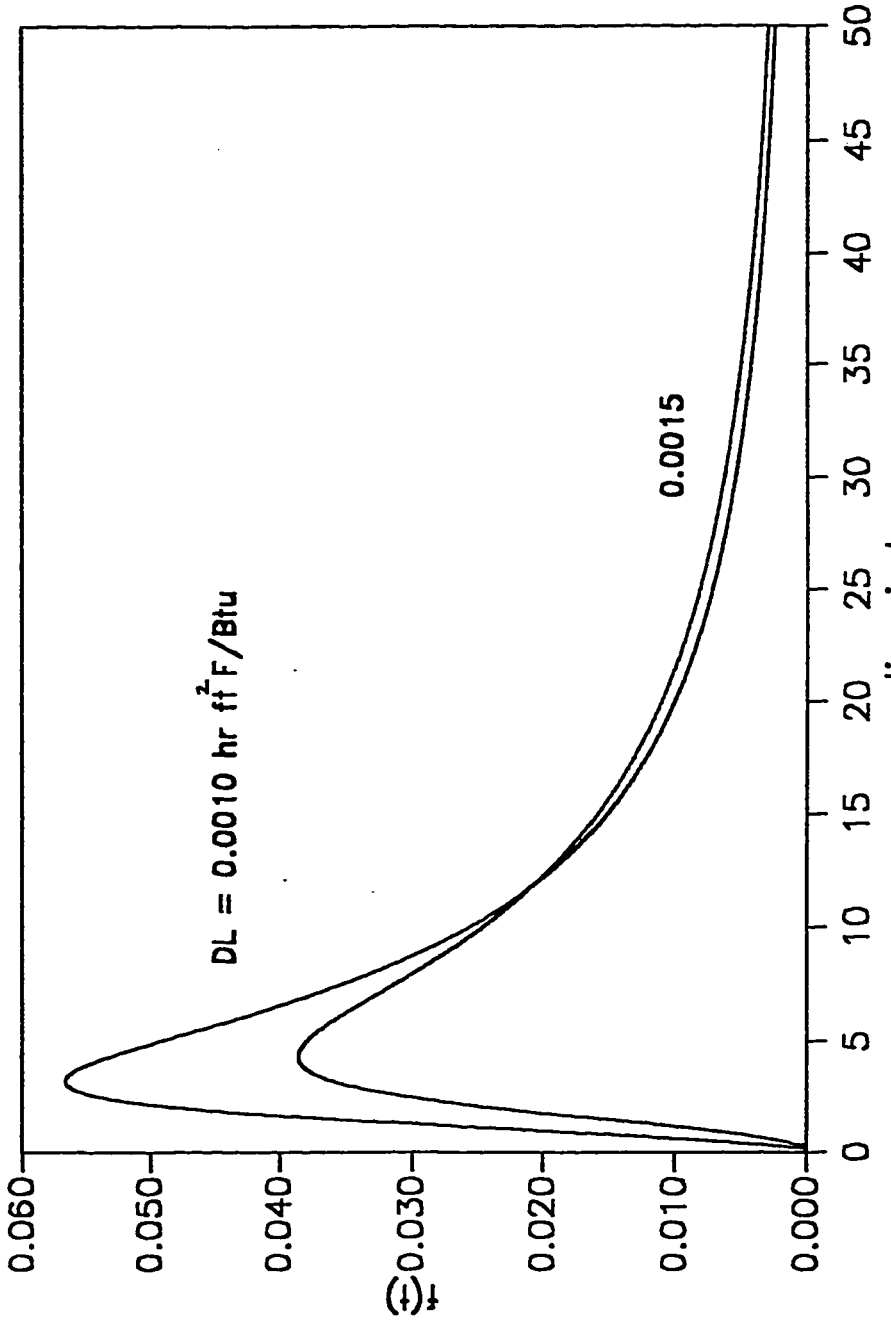

Fig. 4.8 Probability density function for three parameter Log Bernstein distribution obtained from damage function for fouling at different critical damage levels. Data from Ref [53]. [See Table 4.2 for distribution parameters].

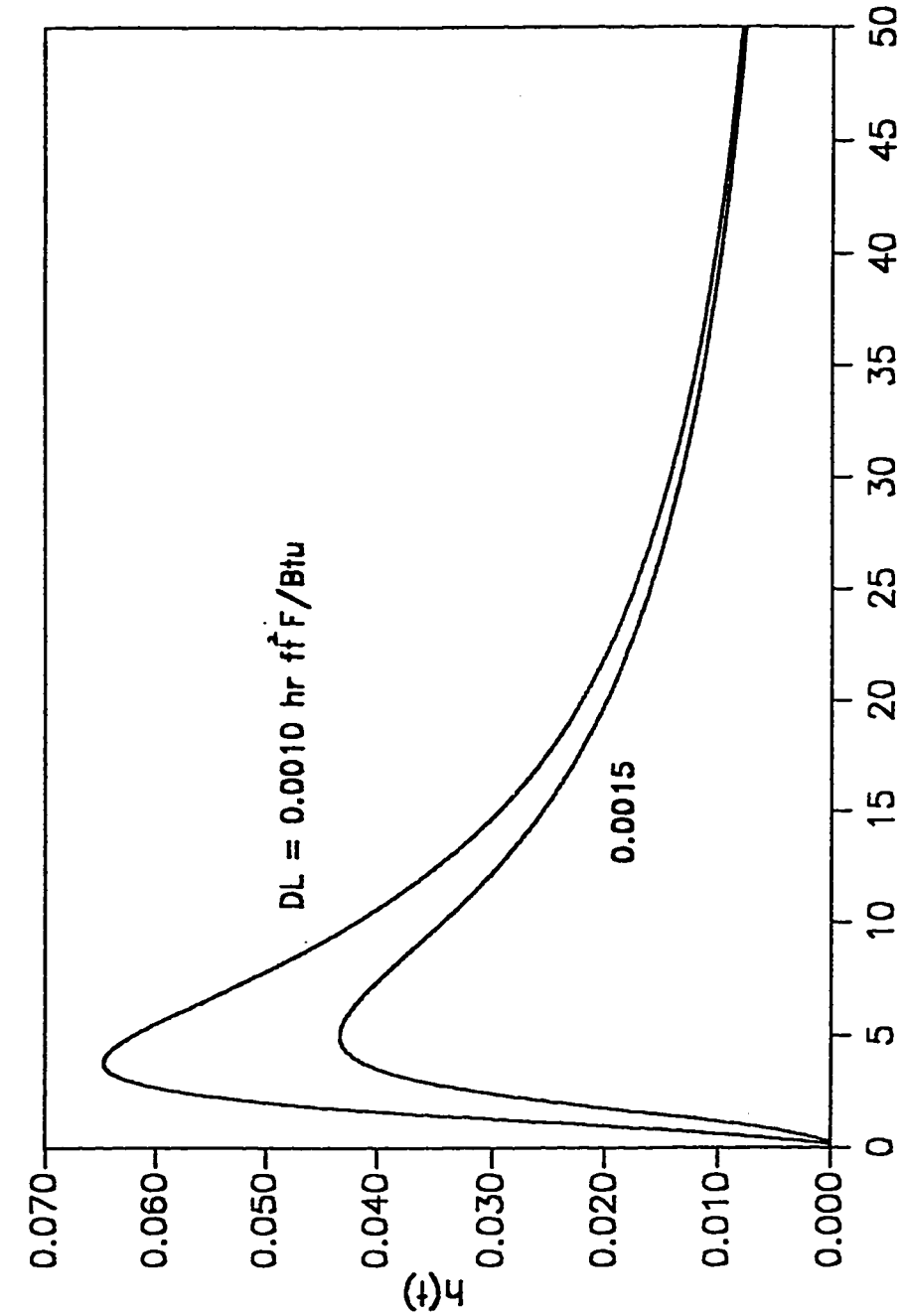

Fig. 4.9 Hazard function for three parameter Log Bernstein distribution obtained from damage function for fouling at different critical damage levels. Data from Ref [53]. [See Table 4.2 for distribution parameters].

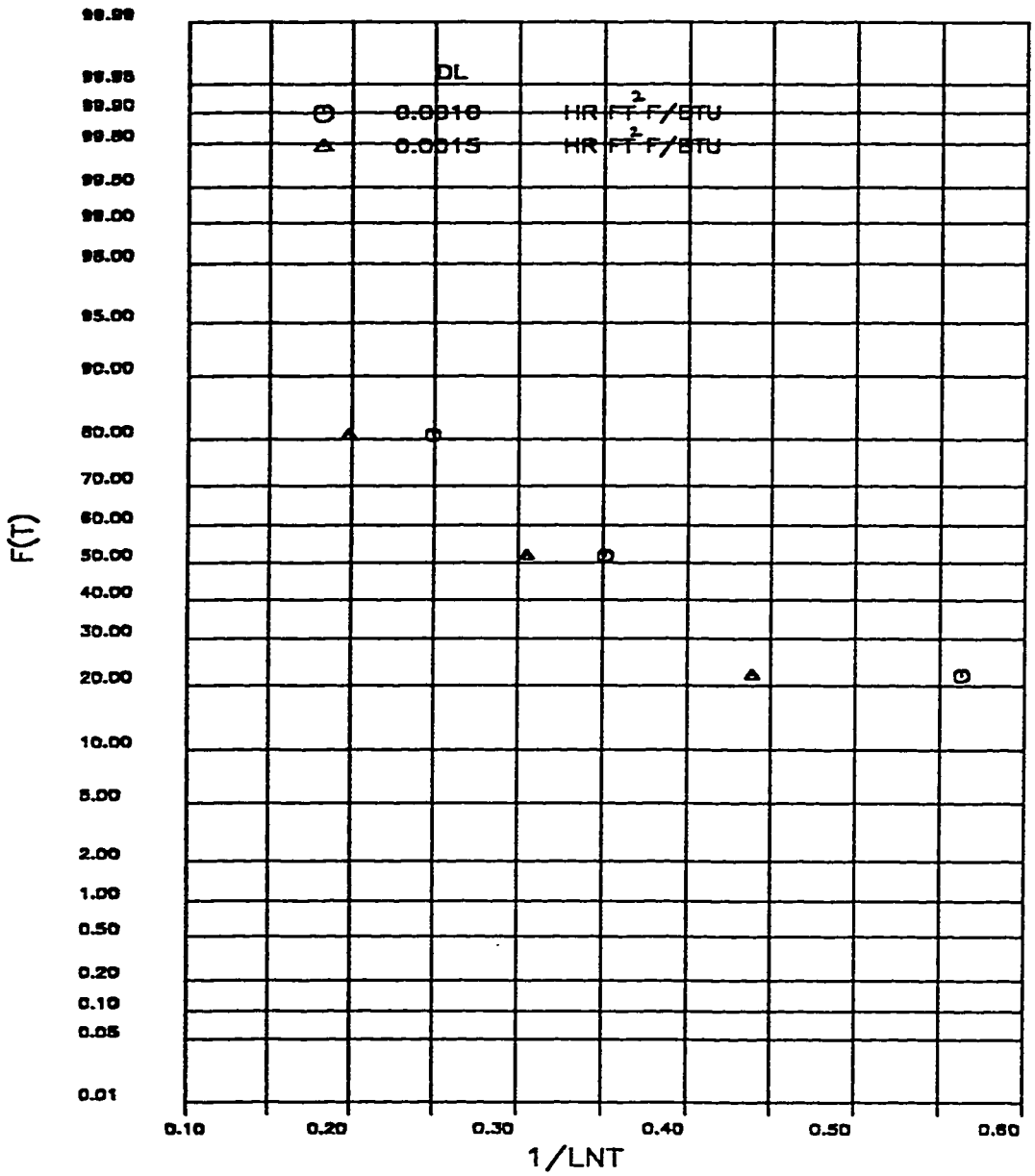

Fig. 4.10 Inverted lognormal distribution of time to failure data for fouling at different critical damage levels. Data from Ref [53].

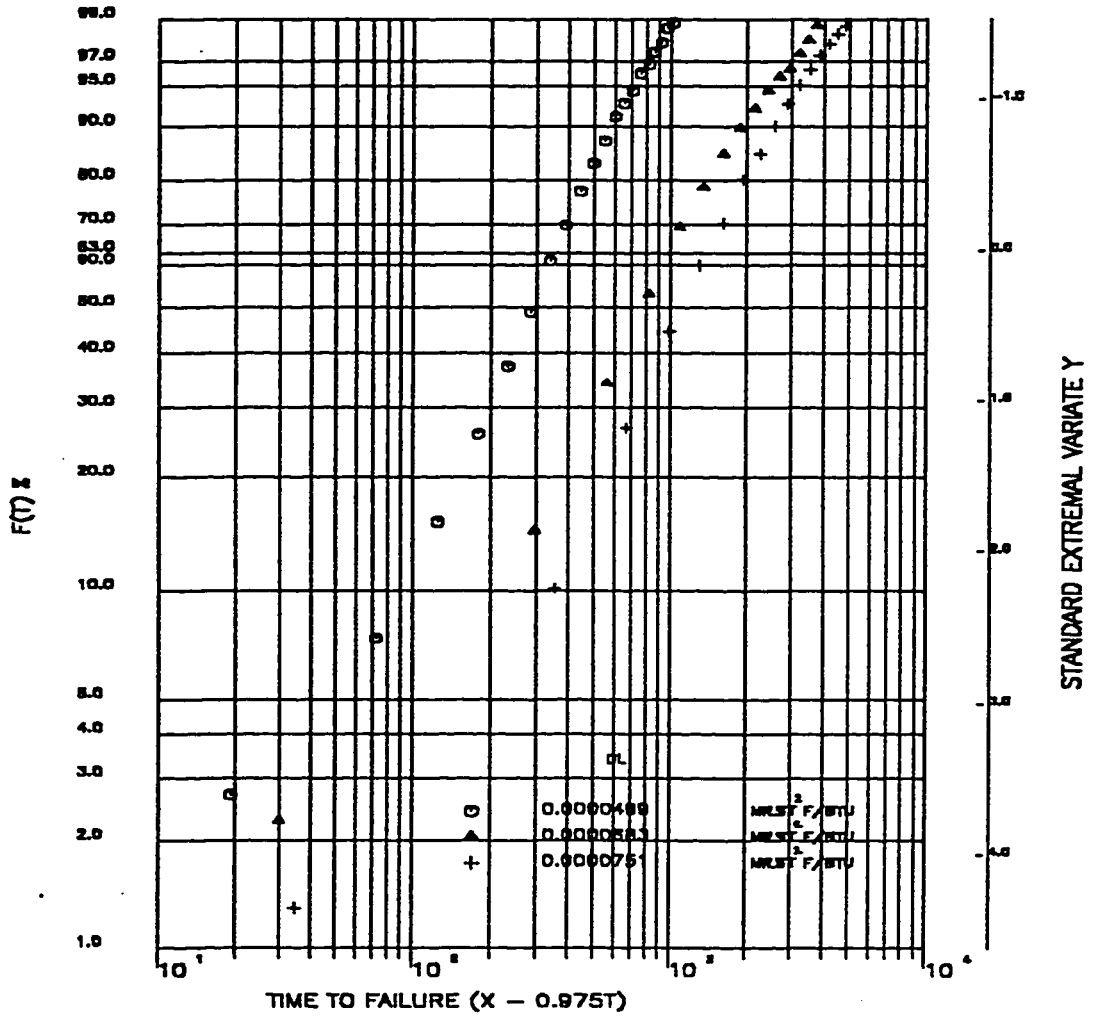

Fig. 4.11 Weibull distribution for coefficient of variation 0.10 for fouling at different critical damage levels.

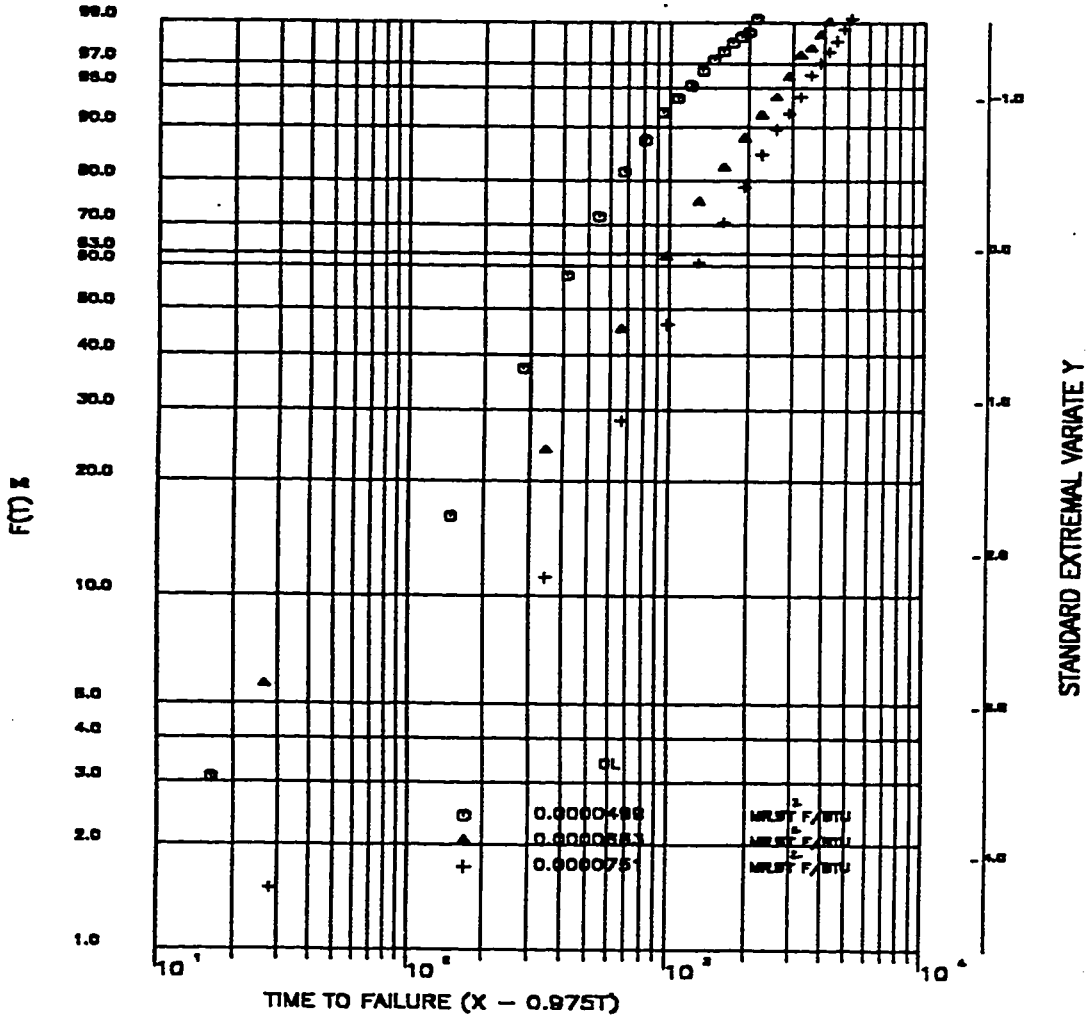

Fig. 4.12 Weibull distribution for coefficient of variation 0.15 for fouling at different critical damage levels.

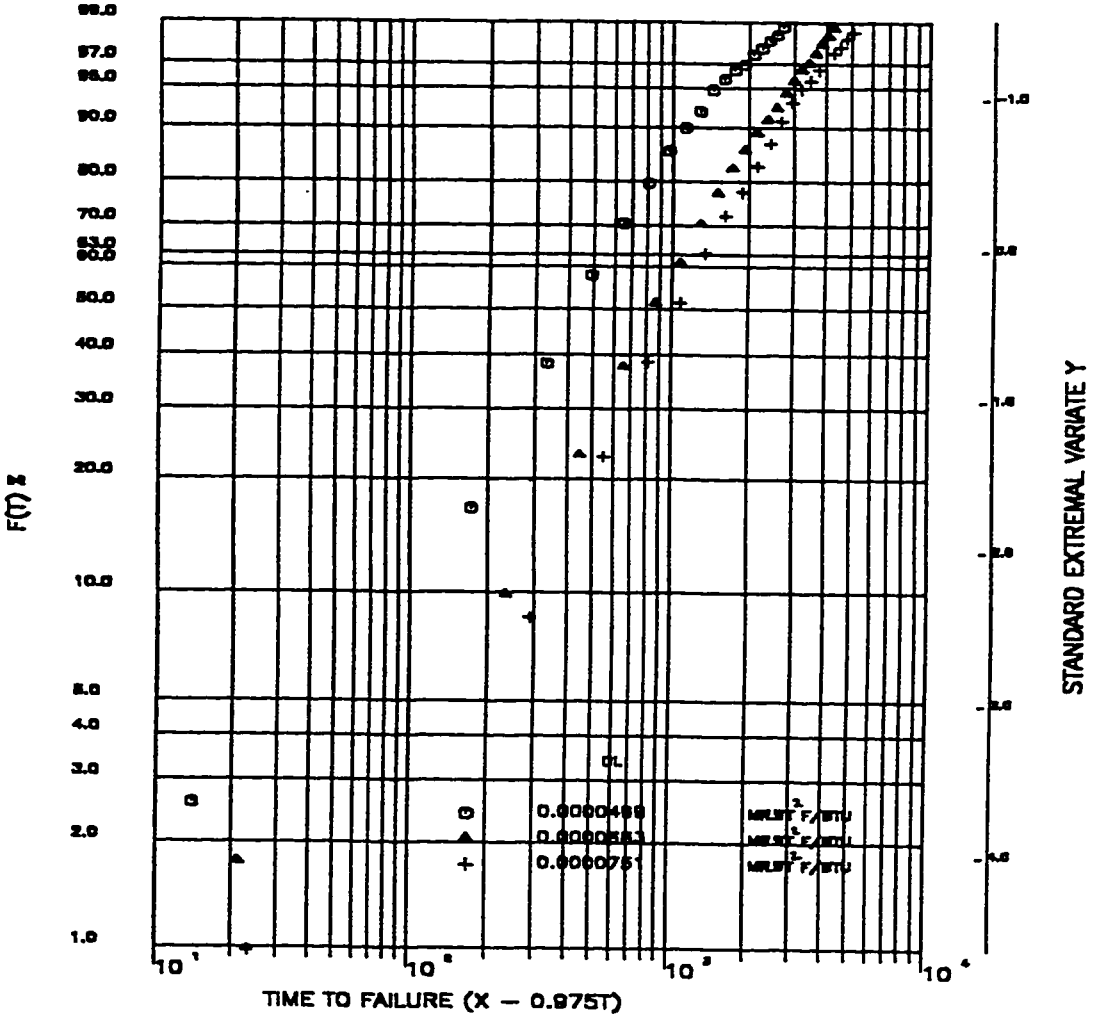

Fig. 4.13 Weibull distribution for coefficient of variation 0.20 for fouling at different critical damage levels.

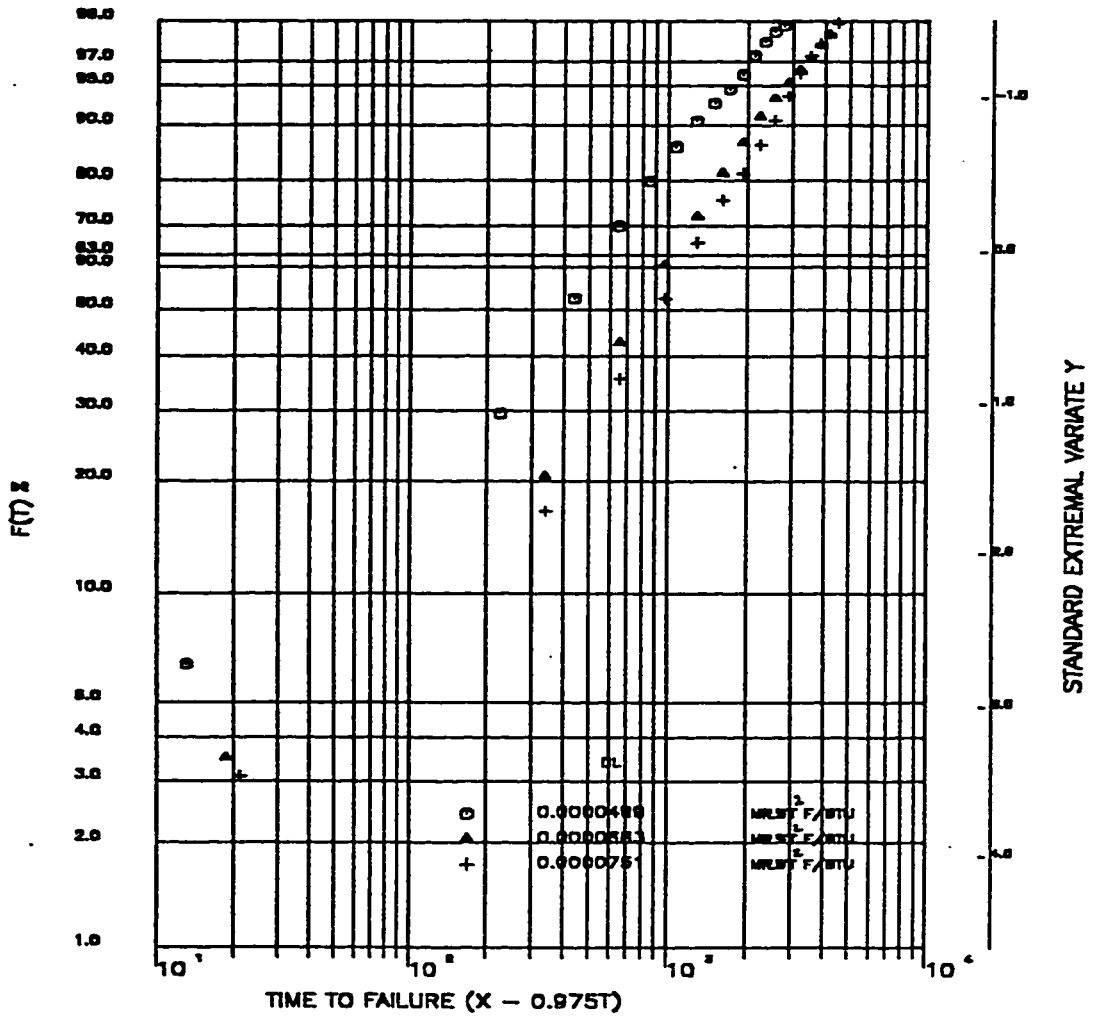

Fig. 4.14 Weibull distribution for coefficient of variation 0.25 for fouling at different critical damage levels.

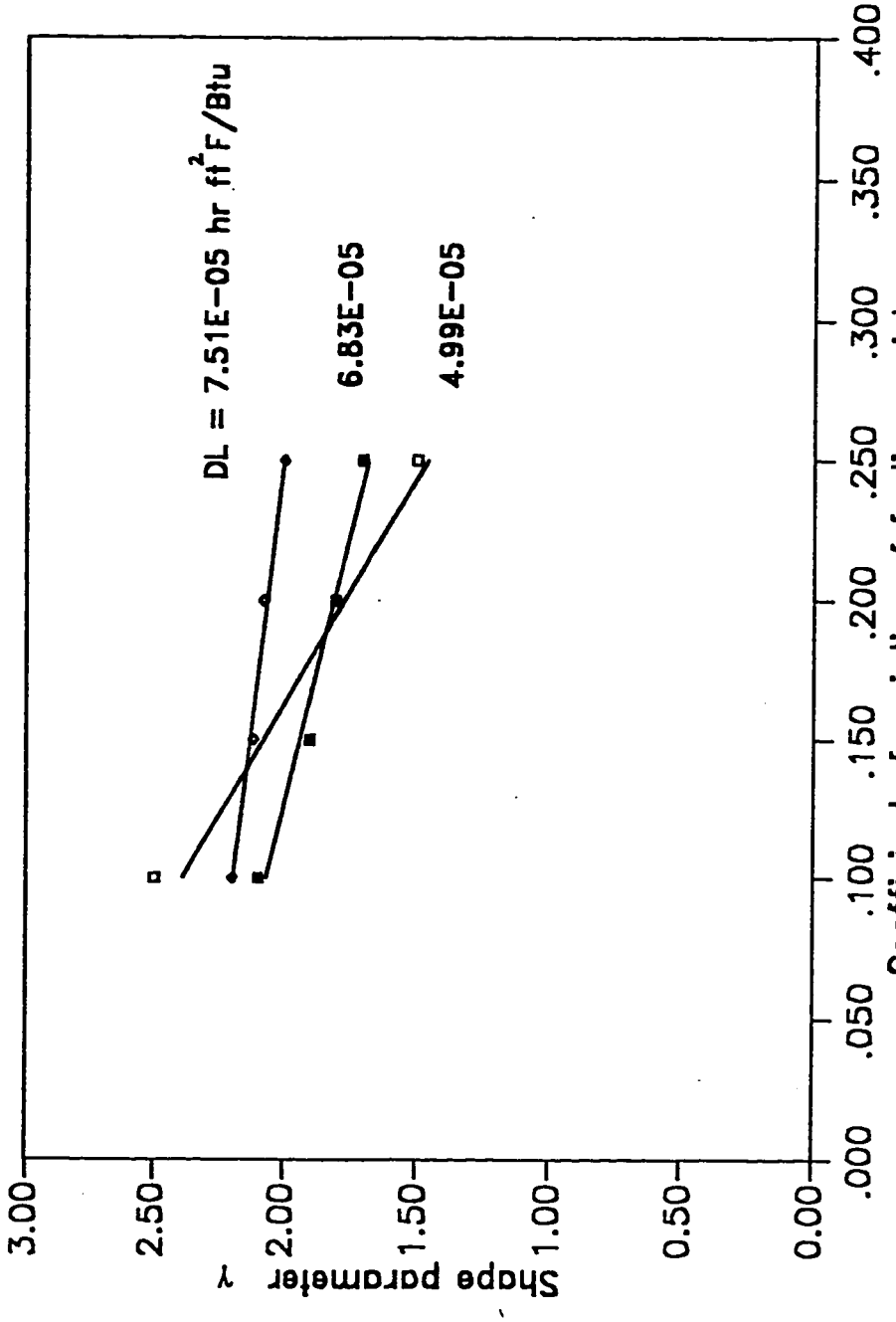

Fig. 4.15 Variation of coefficient of variation with shape parameter γ of weibull model for fouling at different critical damage levels.

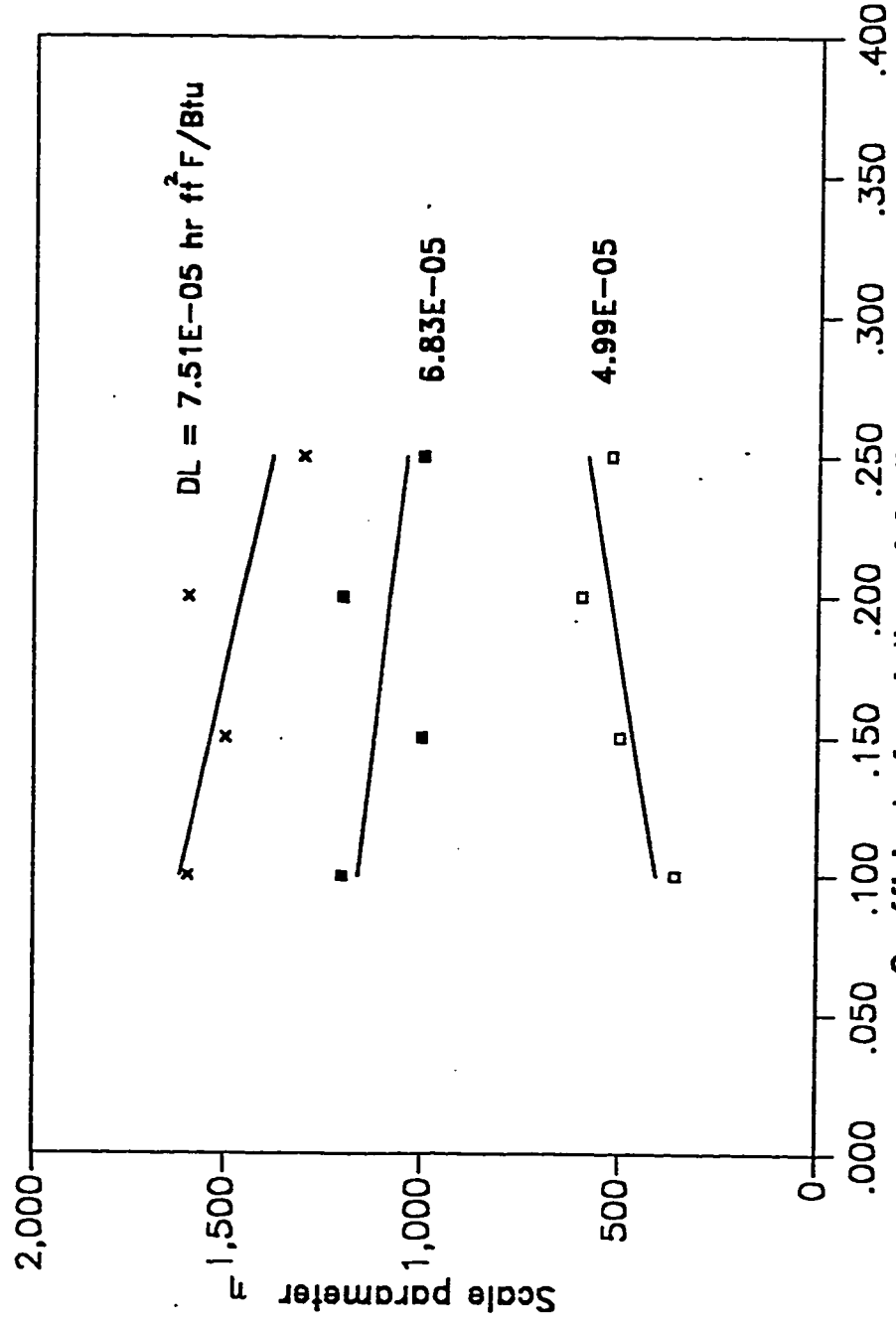

Fig. 4.16 Variation of coefficient of variation with scale parameter η of weibull model for fouling at different critical damage levels.

Table 4.1 Parameters of the distribution for linear fouling [56]

Fig	Symbol	Basis	Distribution	Distribution parameters			
4.2	———	Damage function	Bernstein model	D_l	c	α	β
				1.5E-04 2.0E-04 2.5E-04	56.221 81.362 106.505	0.1795 0.1795 0.1795	572.956 572.956 572.956
	—·—·—·—	Time to failure	Inverted normal	D_l	$\hat{c}$		$\hat{\alpha}$
				1.5E-04 2.0E-04 2.5E-04	49.53 75.58 105.78		0.3490 0.2265 0.1622

Table 4.2 Parameters of the distribution for falling rate fouling [53]

Fig	Symbol	Basis	Distribution	Distribution parameters			
4.7	————	Damage function	Log Bernstein model	D_1	c_1	α_1	β_1
				0.0010 0.0015	2.773 3.254	0.2433 0.2433	1.387 1.387
	—·—·—·—	Time to failure	Inverted lognormal	D_1	$\hat{c}_1$	$\hat{\alpha}_1$	
				0.0010 0.0015	2.613 3.236	0.117 0.102	

CHAPTER 5

CREEP

5.1 INTRODUCTION

During the past several years the creep of metals and alloys has become an increasingly important problem. The main reason for this is that, the designers of industrial installations (thermal, nuclear, chemical etc.) are tending to raise the operating temperatures of structural components as far as possible to increase the thermodynamic efficiency of the system. For a long time the high temperatures were generally associated with steam power plants, oil refineries and chemical plants. The introduction of gas turbine engine, rocket engines and ballistic missile nose cones pose much greater problems, which has been met only by the most ingenious use of the available high temperature materials.

An important characteristic of high temperature strength is that it must always be considered with the time scale. At elevated temperature the service life of a metal component subjected to either vibratory or non-vibratory loading is predictably limited. The principal types of elevated temperature mechanical failures are creep, stress-rupture, low or high cycle fatigue, thermal fatigue etc., and combinations of these as modified by environment. Stress imposed at high temperatures produces a continuous strain in the component or equipment and

results in a phenomenon known as creep. *Creep by definition is a time dependent strain occurring under constant stress (or load) at elevated temperature.* After a period of time creep may terminate in fracture by stress-rupture. The conditions of temperature, stress and time under which creep and stress-rupture failures occur depend on the metal or alloy, its microstructure and the service environment.

5.2 CHARACTERISTICS OF CREEP

As defined earlier the progressive deformation of a material at constant stress and at elevated temperature is known as creep. The creep is usually considered to operate at temperature $\geq 0.4\, T_{Melt}$, where T_{Melt} is the absolute melting temperature of the metal. The creep phenomenon is usually represented by a creep curve. To determine the engineering creep curve of a metal, a constant load is applied to tensile specimen maintained at constant temperature, and the strain (extension) of the specimen is determined as a function of time. Fig. 5.1 illustrates the idealized shape of the creep curve. The slope of this curve $d\varepsilon/dt$ or $\dot{\varepsilon}$ is the **creep rate.** Most creep curves consists of three distinct stages (Fig. 5.1). By the application of load, initial elastic strain results followed by a region of increasing plastic strain at a decreasing strain rate is called first-stage or ***primary creep.*** Following the primary creep is a region of constant rate of plastic strain known as second-stage or ***secondary creep.*** This minimum creep rate (MCR) which is commonly used in research and engineering studies. Secondary creep is essentially a transition phase between primary and tertiary

creep and occupies the major portion of the creep test. On the strain-rate-time curve, this transition zone in creep resistant materials is sufficiently flat so the minimum creep rate is applicable to all of secondary creep. For these materials the minimum creep rate can be empirically The creep rate during this portion is also called the ***minimum creep rate or steady state creep rate.*** Finally, there is a region of drastically increased strain rate with rapid extension to fracture which is known as third-stage or ***tertiary creep.*** related to rupture life.

5.3 INFLUENCE OF STRESS AND TEMPERATURE

The influence of stress and temperature on the creep process is illustrated schematically in Fig. 5.2. and 5.3. Fig. 5.2 shows the increase in creep deformation with increase in stress at a constant temperature, and Fig. 5.3 shows similar influence due to temperature for constant stress.

For the stress and temperature levels generally used in design, creep is a very slow process. If a machine is to be designed to operate for a period of 10 years, for example, it is not feasible to postpone the design until the creep tests for a period of 10 years duration have been performed. For this reason, accelerated life testing of creep (compression of time scale by intensifying the stress and temperature) provide the most practical method to study the creep as a function of time, temperature, and stress. This relationship developed by accelerated life testing approach can be used for extrapolating short time creep data to longer times. Several methods have been proposed in literature to model the creep data for this purpose and two of the most common methods to express

creep data in a most comprehensive form are to plot the data as stress versus Larson-Miller or Manson-Haferd parameter.

5.4 EVALUATION OF CREEP DAMAGE

All materials, creep under the load (stress) at elevated temperatures ($\geq 0.4\ T_{Melt}$). The shape of the creep curve for any material will depend on the temperature of the test and the stress at any time since these are the main factors controlling the work hardening and recovery processes. The rate of steady state creep is a function of σ, T and can be expressed mathematically as:

$$\dot{\varepsilon}_s = f(\sigma,T)$$

Since the creep is a thermally activated diffusion controlled process, the creep rate will increases when the temperature increases (at a constant stress), this is due to the softening processes such as dislocation climb which takes place. Therefore the creep rate is expected to obey an Arrhenius-type equation with characteristic activation energy Q for the rate controlling mechanism i.e.,

$$\dot{\varepsilon}_s = A' e^{-Q/RT} \qquad (5.1)$$

where $\dot{\varepsilon}_s$ is the secondary creep rate, Q is the activation energy, Cal/mole, R is the Universal gas constant, J $mole^{-1}$ K^{-1}, T is the absolute temperature °K and A' is a constant, which is a function of stress σ.

If the stress dependence of the steady-state creep rate is considered over a wide range of stresses at a fixed temperature, then the relationship is expressed

by the Power law equation [68] :

$$\dot{\varepsilon}_s = \beta_1 \sigma^n \tag{5.2}$$

where β_1 and n are constants and σ is the stress. The parameter β_1 is a function of temperature.

The combined effect of stress (sigma) and temperature T on the steady state creep rate can be represented as

$$\dot{\varepsilon}_s = A_o \sigma^n e^{-Q/RT} \tag{5.3}$$

Eq (5.1) and eq (5.2) are special cases of eq (5.3).

5.4.1 PARAMETER METHODS

In practical applications, usually engineers confirm that particular component will withstand usage at elevated temperatures for a particular life time. The interpolation or extrapolation depends on finding a function that has a form.

$$f(\sigma, t_r, T) = \text{constant} \tag{5.4}$$

More typically it is written as

$$f(t_r, T) = P(\sigma) \tag{5.5}$$

5.4.1.1 LARSON-MILLER PARAMETER

One of the well known creep parameter is Larson-Miller Parameter and is based upon the Arrhenius equation [eq(5.1)]. On the basis of experiment it is assumed that the minimum creep rate satisfies [69]

$$t_r \left(\frac{d\varepsilon}{dt}\right)_{min} = \text{constant} \tag{5.6}$$

Combining eq(5.1) and eq(5.6) we get

$$A\, t_r\, e^{-Q/RT} = \text{constant} \tag{5.7}$$

Now it is assumed that Q is a function of stress only, taking the logarithms on both sides give

$$\log t_r + \log(e^{-Q/RT}) = \log C' \tag{5.8}$$

Eq (5.8) becomes

$$\log t_r - 0.4343\left(\frac{Q}{RT}\right) = \log C' = C \tag{5.9}$$

or

$$T(\log t_r + C) = 0.4343\left(\frac{Q}{R}\right) \tag{5.10}$$

$$T(\log t_r + C) = m = f(\sigma) \tag{5.11}$$

where m is a function of stress.

The quantity $T(\log t_r + C) = P_{Lm}$ is known as Larson-Miller parameter, and is a function of stress [eq (5.11)]. Alternatively eq (5.11) can be expressed as follows :

$$\sigma = f^{-1}[P_{Lm}].$$

The value of constant C in Larson-Miller parameter is obtained from the intercept when $\log t_r$ is plotted against 1/T for a constant stress.

5.4.1.2 MANSON-HAFERD PARAMETER

Manson and Haferd also developed their parameter on an empirical grounds but in a slight different manner. They plotted $\log t_r$ as a function of temperature T for a different values of stresses. All these curves (straight lines) at a point having cooridinates and concluded that for a constant stress, the quantity ($\ln t_a$ and T_a) which results into a constant slope at any stress σ this slope is

$$\frac{T - T_a}{\ln t - \ln t_a} \tag{5.12}$$

and is known as Manson-Haferd parameter, and this is a function of stress. T_a and t_a can be interpreted as are material constants different for each material.

The use of Manson-Haferd parameter for extrapolation purposes is the same as was outlined for the case of Larson-Miller parameter. To use Larson-Miller parameter only one constant C need to be determined, where as for Manson-Haferd two constants T_a and t_a need to be determined.

5.5 STATISTICAL ANALYSIS OF CREEP

5.5.1 STOCHASTIC NATURE OF CREEP

To determine the engineering creep curve of a metal, a constant load is applied to a tensile specimen maintained at a constant temperature and the strain of the specimen is determined as a function of time. Although the nature

of the experiment is quiet simple in principle, in practice it requires considerable laboratory equipment.

From the creep test for a certain material, we should expect the same strain or creep rate, if replicates of an experiment were made under same load and temperature conditions. Several lead specimens were tested in laboratory under replicate conditions [70] and the resulting figures of strain versus time (ε vs t), for four different stress levels are shown in Figs. 5.4 to 5.7. These figures show a considerable scatter of creep $\varepsilon = f(\sigma,T,t)$ around the average value, inspite of the fact that experiments are conducted in controlled laboratory conditions. The replicates of the experiments have resulted in a band (enveloping a set of realizations) of an underlying stochastic process of damage instead of a single deterministic curve. This proves that the behavior of the creep is random and need to be characterized using a probabilistic approach.

5.5.2 RELIABILITY MODELLING OF CREEP

Under the conditions of appreciable scatter of the results of creep tests, the use of probabilistic approach ensures a high degree of reliability in evaluating the safe life of the structural elements. Some concepts of statistics on the problems of analyzing creep were discussed in references [71,72]. To analyze the results of heat resistance and creep tests, many criterion have been suggested involving T, t and σ [73]. In many of the cases these criteria are intended to find a single curve but not to give an expression to the complex physical process. The stochastic equations obtained in studies by Samarin [74] predict creep only

during the first two stages, without the allowance of accelerated creep, although that is not of much practical interest. As mentioned earlier that the creep rate remain steady or constant in the secondary zone which contributes substantially to the total strain. Focusing on the region of the secondary creep, we can characterize the creep damage as a linear non-stationary random process which is mathematically expressed as the damage model of Sec 1.8. of Chapter 1.

Figs. 5.4 to 5.7 shows the real sample functions of the random creep process. The study of creep was conducted on lead material under controlled conditions of laboratory [70]. The data shows that the strain in the secondary zone is linear in nature. The data at two different loads are analysed by linear regression analysis performed on each realization. Based on the linearity of the realizations and assuming normality of D_i and **r**, a three parameter Bernstein distribution is hypothesized to characterize the time to failure as mentioned in Sec 1.8.1 of Chapter 1. The reliability function along with time to failure at different critical damage levels (strain limits) for different loads are shown in Figs. 5.8 to 5.11. Figs. 5.12 to 5.15 shows the respective probability density function and hazard function at different critical damage levels for different loads. The time to failure data was also plotted on the normal probability paper as [F(t) vs 1/T] to check the validity of inverted normal distribution by empirical approach. The straight line demonstrates that the inverted normal distribution as shown in Figs. 5.16 and 5.17 at different critical damage levels for different loads, fits slightly better than the three parameter Bernstein

distribution (Figs. 5.8 to 5.11). This discrepancy can be explained by considering the fact that while fitting the regression lines to each data realization, we have introduced more than the actual amount of dispersion of initial damage. This has slightly distorted the parameters of the three parameter model when estimated from damage function. The behavior of median life c, scatter parameter $\sqrt{\alpha}$ as a function of applied stress are illustrated in Fig. 5.18 and 5.19. The resulting equations for steady state creep of lead for strain rate at a fixed temperature are given as follows :

$$\dot{\varepsilon}_{max} = 4.09 \times 10^{-15} \sigma^{12.466}$$

$$\dot{\varepsilon}_{mean} = 3.85 \times 10^{-13} \sigma^{10.196}$$

$$\dot{\varepsilon}_{min} = 3.63 \times 10^{-11} \sigma^{7.9254}$$

and on integrating with respect to time the steady state creep equations for strain can be written as

$$\varepsilon_{max} = 4.09 \times 10^{-15} \sigma^{12.466} t$$

$$\varepsilon_{mean} = 3.85 \times 10^{-13} \sigma^{10.196} t$$

$$\varepsilon_{min} = 3.63 \times 10^{-11} \sigma^{7.9254} t$$

Assuming that the range $\varepsilon_{max} - \varepsilon_{min}$ represent $6\sigma(\varepsilon)$ and for the assumption of normal distribution of ε $[\varepsilon \sim N(\mu(\varepsilon), \sigma(\varepsilon))]$ as illustrated in Fig. 5.20, time to failure can be calculated for any reliability at critical strain limit between the maximum and minimum values of strain. $[P(\varepsilon < \varepsilon_l)]$.

5.5.3 GENERAL MODEL FOR CREEP (INCLUDING THE TEMPERATURE EFFECT)

In predicting the long term characteristics of creep, we need to have the information in terms of the operating temperature and stress. Perlta et.al [75] presented a general method for reliability analysis of creep-rupture data employing the time-temperature concept and using a lognormal model for creep strength. Stepnov et.al [76] used the scatter data of the logarithm of time to failure in relation to the test temperature and stress level for studying the impact of stress and temperature on the characteristics of life dispersion.

In order to develop a versatile reliability model with respect to temperature and stress the real life data from [76] is analysed in view of the mathematical framework of this thesis. Median time to failure at different temperature (or stress) levels are plotted as a function of stress (or temperature) in Fig. 5.21 (or Fig. 5.22). Fig. 5.21 illustrate that the median life decreases with an increase in stress at constant temperature. Fig. 5.22 shows that the median life decreases with an increase in temperature at constant stress. Fig. 5.23 shows that the median life also decreases with the increase in ζ which is the product of stress σ and temperature T.

The LM parameter is given by the expression

$$T(\log t_r + C) = P_{Lm}(\sigma)$$

Following the approach presented by Goldloff [77], the value of constant C in Larson-Miller parameter can be calculated from Fig. 5.24, which is obtained by plotting $\frac{1}{T}$ vs $\log t_m$. In this case the value of C is 18. Fig. 5.25 shows the relationship between stress and LM parameter for the material Ak4-1 [76].

Considering the above data, the following trends or combinations of stress, temperature and product stress and temperature were hypothesized:

a. $\ln t_m = \alpha_0 \frac{1}{T} + \alpha_1 \ln\sigma$

b. $\ln t_m = \alpha_0 T + \alpha_1 \ln\sigma$

c. $\ln t_m = \alpha_0 \frac{1}{T} + \alpha_1 \zeta$

d. $\ln t_m = \alpha_0 T + \alpha_1 \zeta$

e. $\ln t_m = \alpha_0 \frac{1}{T} + \alpha_1 \ln\sigma + \alpha_2 \zeta$

f. $\ln t_m = \alpha_0 T + \alpha_1 \ln\sigma + \alpha_2 \zeta$

The above models were fitted to the matrix of t_m, σ, and T values, using generalized multiple linear regression approach. The results of residual errors (difference between actual and predicted values of t_m) were compared. As a consequence the following two models which were almost equivalent in terms of their residual errors were selected as the best models :

1. $\ln t_m = \alpha_0 \frac{1}{T} + \alpha_1 \ln\sigma + \alpha_2 \zeta$ (5.13)

2. $\ln t_m = \alpha_0 T + \alpha_1 \ln\sigma + \alpha_2 \zeta$ (5.14)

In most of the cases model 1 [eq (5.13)] was observed to be best and it also relates to the creep theory in terms of Arrhenious relationship of temperature with steady state creep.

Assuming that time to failure $t = t_f$ reach a specified critical strain $\varepsilon = \varepsilon_1$ is approximately equal to the time to rupture, t_r. Steady state creep rate model [eq (5.3)] can be expressed as follows :

$$\frac{d\varepsilon}{dt} = A_o \sigma^n e^{-Q/RT} = A_o \sigma^n e^{\xi/T}$$

where $\xi = (-Q/R)$

On integrating we get

$$\varepsilon = (A_o \sigma^n e^{\xi/T})\, t$$

Taking the failure at the fixed critical limit ε_1

$$\varepsilon = \varepsilon_1 = (A_o \sigma^n e^{\xi/T})\, t_f$$

$$t_f = \frac{\varepsilon_1}{A_o} \sigma^{-n} e^{\xi/T} = \theta_o \sigma^{-n} e^{\xi/T} \quad (5.15)$$

where as the regression eq (5.13) will result into the following expression

$$t_r \approx t_f = \theta_o \sigma^{\alpha_1} e^{\xi/T} \varphi(\sigma,T) \quad (5.16)$$

$\varphi(\sigma,T)$ is the additional term which is appearing in the form of a product of stress and temperature in the regression based model. When compared to the conventional model of steady state creep this product term will characterize the joint effect of σ and T due to the interaction of stress and temperature. Fig. 5.26

shows the relationship between the scatter parameter $\sigma_1 = \sigma(\ln T_r)$ which represents coefficient of variation of time to rupture as a function of $\zeta = \sigma T$. The following modle seems to represent that the coefficient of variation

$$\frac{\sigma(t_r)}{\mu(t_r)} = \alpha_3(\sigma T) - \alpha_4$$

Since ε_1 is the maximum permissible strain limit, the possibility of the event $(T_f > t_f)$ is equivalent to the probability of the event $(\varepsilon < \varepsilon_1)$. The probability of the event $(T_f > t_f)$ based on fixed strain can be characterized as a two parameter inverted normal reliability model as described in Sec 1.8.3 of Chapter 1 and further reinforced in Sec 5.5.2. For further verification of the adequacy of inverted normal model to represent the reliable life due to stress rupture the data from ASM Handbook [78] was analysed for time to rupture. The time to rupture data [78] was plotted [F(t) vs 1/T] on the normal probability paper as shown in Fig. 5.27. The resulting straight line demonstrates the validity of inverted normal distribution for various materials such as Rene 41 and M252. The various probability functions for Rene 41 material are shown in Figs. 5.28 to 5.30. This also shows that the assumption that the time to failure t_f is in the neighborhood of time to rupture t_r is valid. Since the time to failure (or time to rupture) has been validated as the inverted normal reliability model, the reliable life for Ak4-1 can be obtained from the following equation :

$$R(t) = P[T_f > t_r] = P[\varepsilon > \varepsilon_1]$$

$$= 1 - \Phi\left\{\frac{t - C}{\sqrt{\alpha t}}\right\}$$

$$= 1 - \Phi\left\{\frac{t - t_m}{\sqrt{\alpha t}}\right\} \tag{5.17}$$

$$= 1 - \Phi\left\{\frac{t - \theta'_o \sigma^{\alpha_1} e^{\alpha_2/T} e^{\alpha_2/(\sigma T)}}{\left[\alpha_3 (\sigma T) - \alpha_4\right] t}\right\} \tag{5.18}$$

$$f(t) = \frac{1}{\sqrt{2\pi}} \frac{\left[\theta'_o \sigma^{\alpha_1} e^{\alpha_2/T} e^{\alpha_2/(\sigma T)}\right]}{\sqrt{\left[\alpha_3 (\sigma T) - \alpha_4\right] t^2}} \exp\left\{\frac{-1}{2}\left[\frac{t - \theta'_o \sigma^{\alpha_1} e^{\alpha_2/T} e^{\alpha_2/(\sigma T)}}{\sqrt{\left[\alpha_3 (\sigma T) - \alpha_4\right] t}}\right]^2\right\} \tag{5.19}$$

$$h(t) = \frac{1}{\sqrt{2\pi}} \frac{\left[\theta'_o \sigma^{\alpha_1} e^{\alpha_2/T} e^{\alpha_2/(\sigma T)}\right]}{\sqrt{\left[\alpha_3 (\sigma T) - \alpha_4\right] t^2}} \frac{\exp\left\{\frac{-1}{2}\left[\frac{t - \theta'_o \sigma^{\alpha_1} e^{\alpha_2/T} e^{\alpha_2/(\sigma T)}}{\sqrt{\left[\alpha_3 (\sigma T) - \alpha_4\right] t}}\right]^2\right\}}{1 - \Phi\left\{\frac{t - \theta'_o \sigma^{\alpha_1} e^{\alpha_2/T} e^{\alpha_2/(\sigma T)}}{\left[\alpha_3 (\sigma T) - \alpha_4\right] t}\right\}} \tag{5.20}$$

The linear regression on the Fig. 5.26 suggest that the following relationship is valid between $\sqrt{\alpha} = \frac{\sigma(t_r)}{\mu(t_r)}$ as $\zeta = \sigma T$.

$$\sqrt{\alpha} = 0.0558\zeta - 0.2020 \tag{5.21}$$

When the estimated values of the parameters $\alpha_o, \alpha_1, \alpha_3$ (obtained as result of regression analysis performed on the matrix of t_m, σ, and T) are substituted in the regression model of eq (5.13) the following relationship is obtained

$$\ln t_m = -45.78 + 9.85 \ln\sigma + 8703.12 \frac{1}{T} - 2.08\,\zeta \qquad (5.22)$$

$$t_m = e^{-45.78 + 9.85 \ln\sigma + 8703.12 \frac{1}{T} - 2.08\,\zeta}$$

By substituting these values [eq (5.21) and (5.22)] in eq (5.17) (or substituting the values of $\theta'_o, \alpha_1, \alpha_2, \alpha_3, \alpha_4$ in eq (5.18)) the reliability function for Ak4-1 at different combination of σ and T can be obtained. Typical curves at different temperatures for fixed stress level are shown in Fig. 5.31.

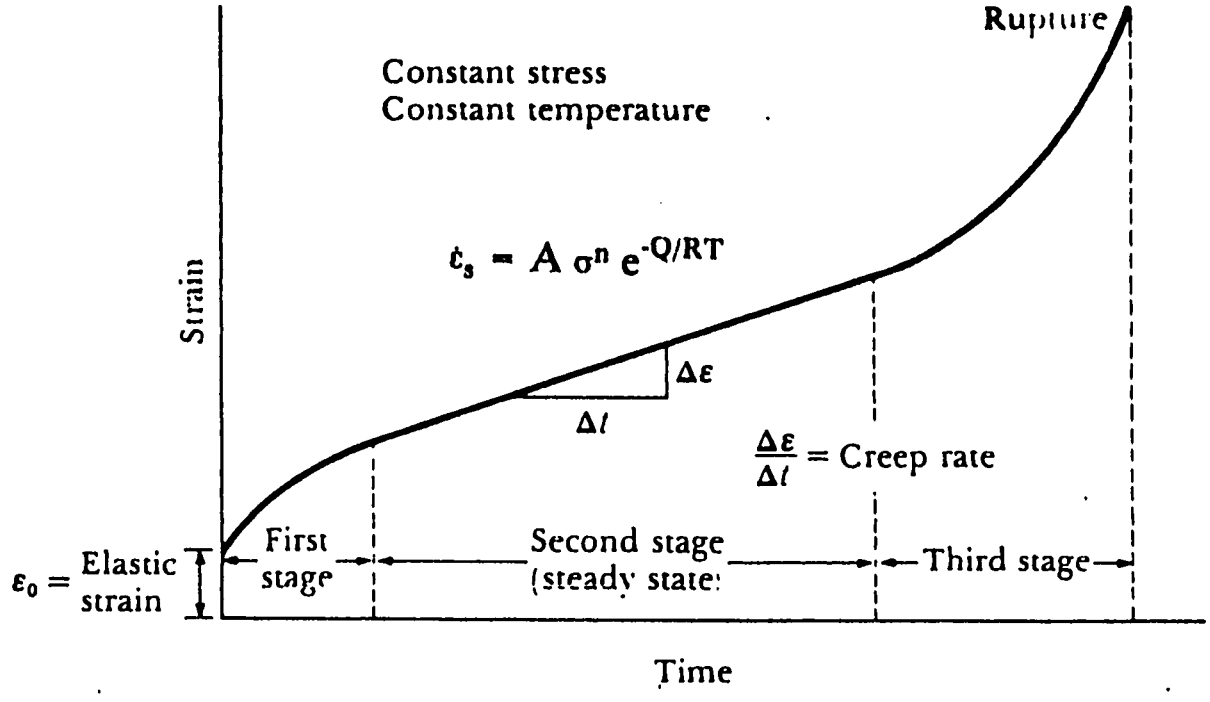

Fig. 5.1 A typical creep curve showing the strain produced as function of time for a constant stress and temperature.

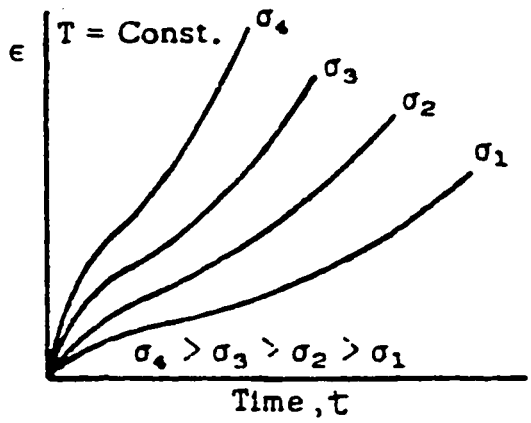

Fig. 5.2 Creep deformation with stress at a constant temperature.

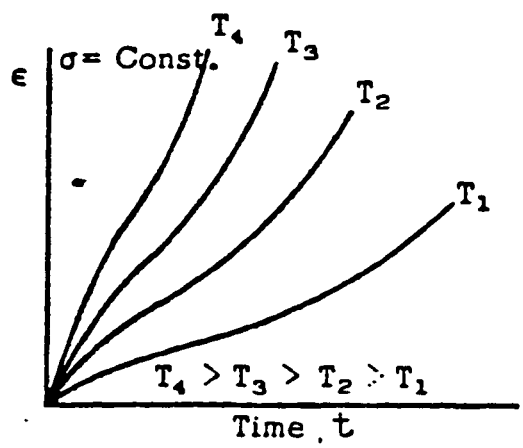

Fig. 5.3 Creep deformation with temperature at a constant stress.

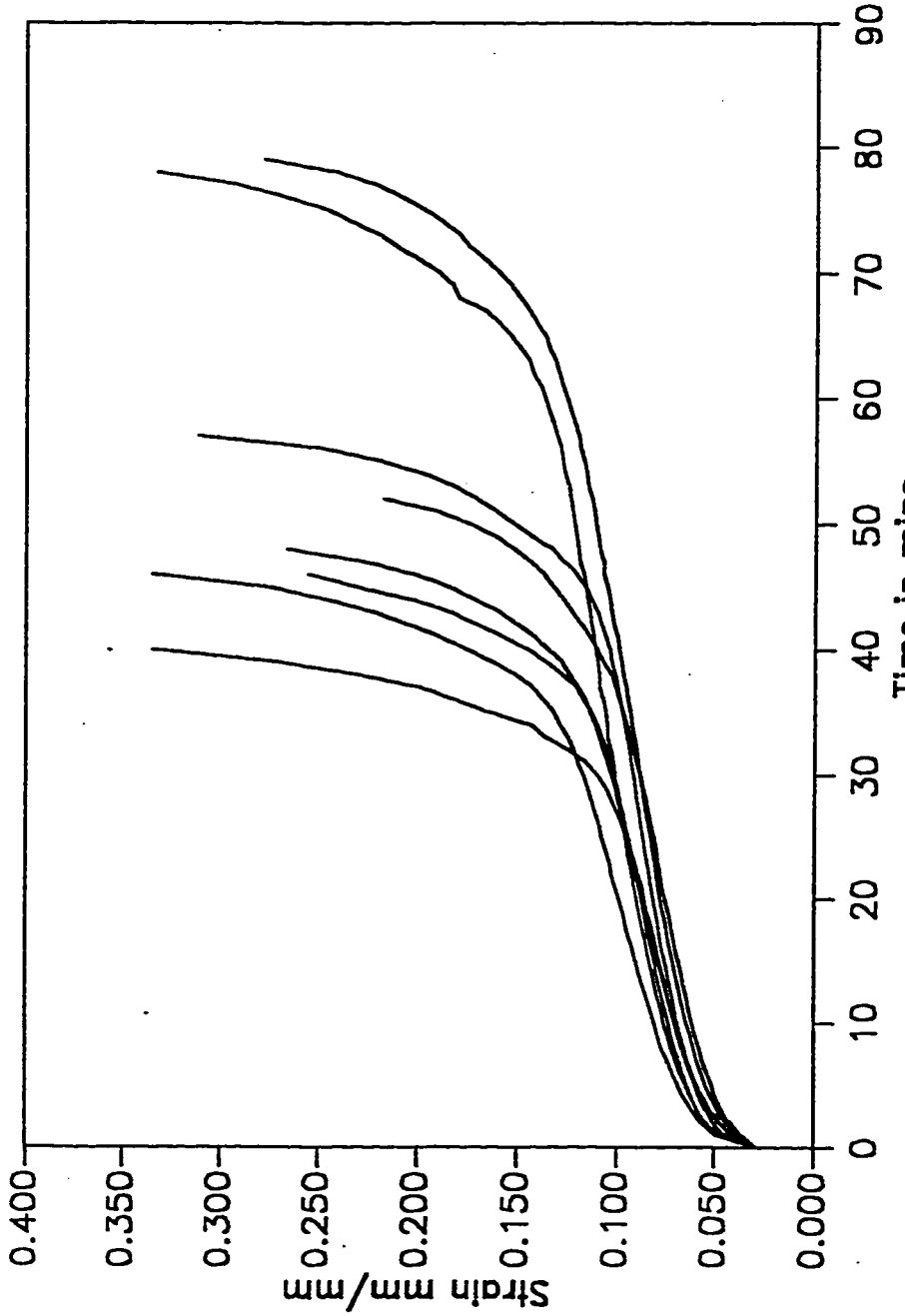

Fig. 5.4 Sample functions for creep of lead at stress 8.6414 N/mm^2 [70].

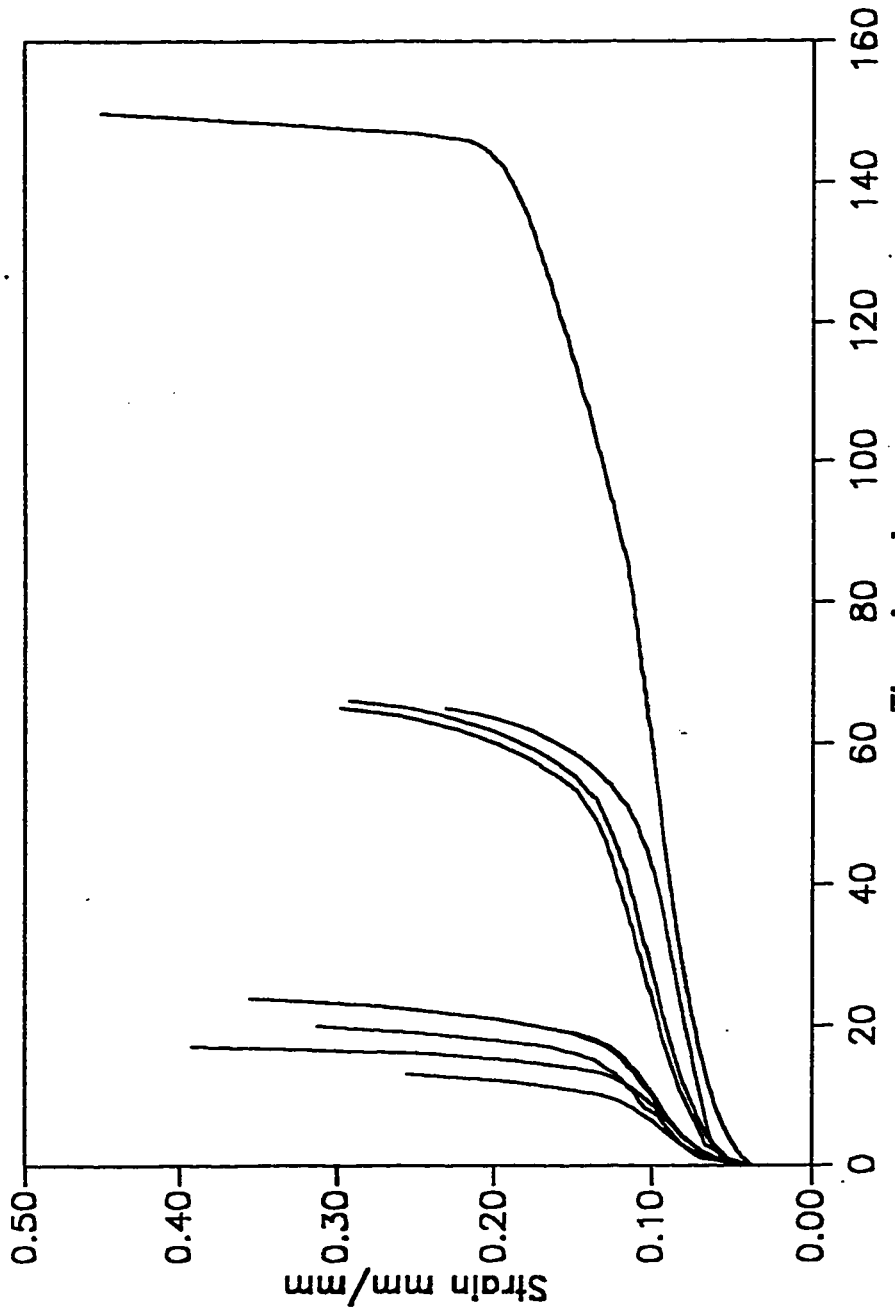

Fig. 5.5 Sample functions for creep of lead at stress 9.5055 N/mm^2 [70].

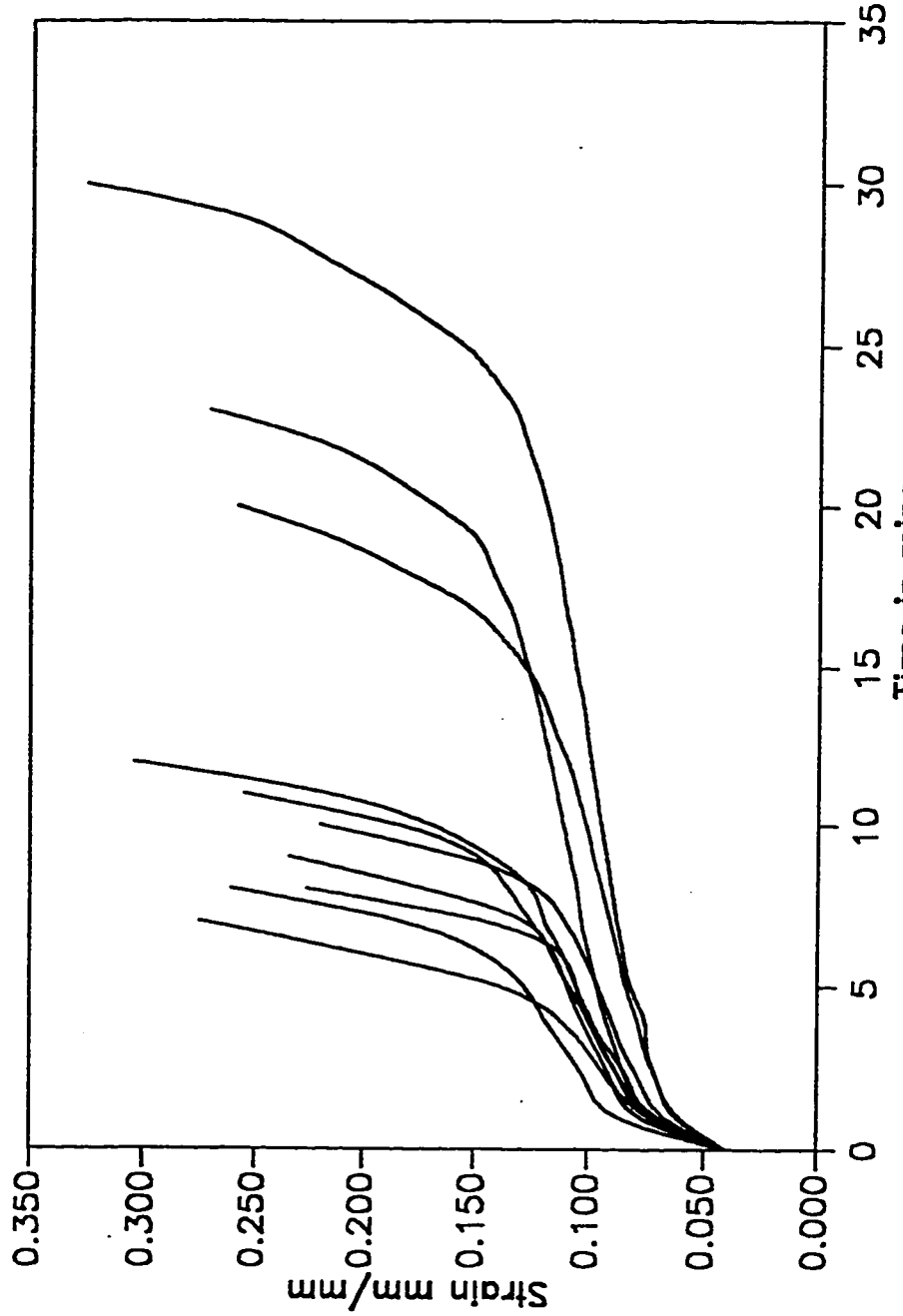

Fig. 5.6 Sample functions for creep of lead at stress 10.3697 N/mm^2 [70].

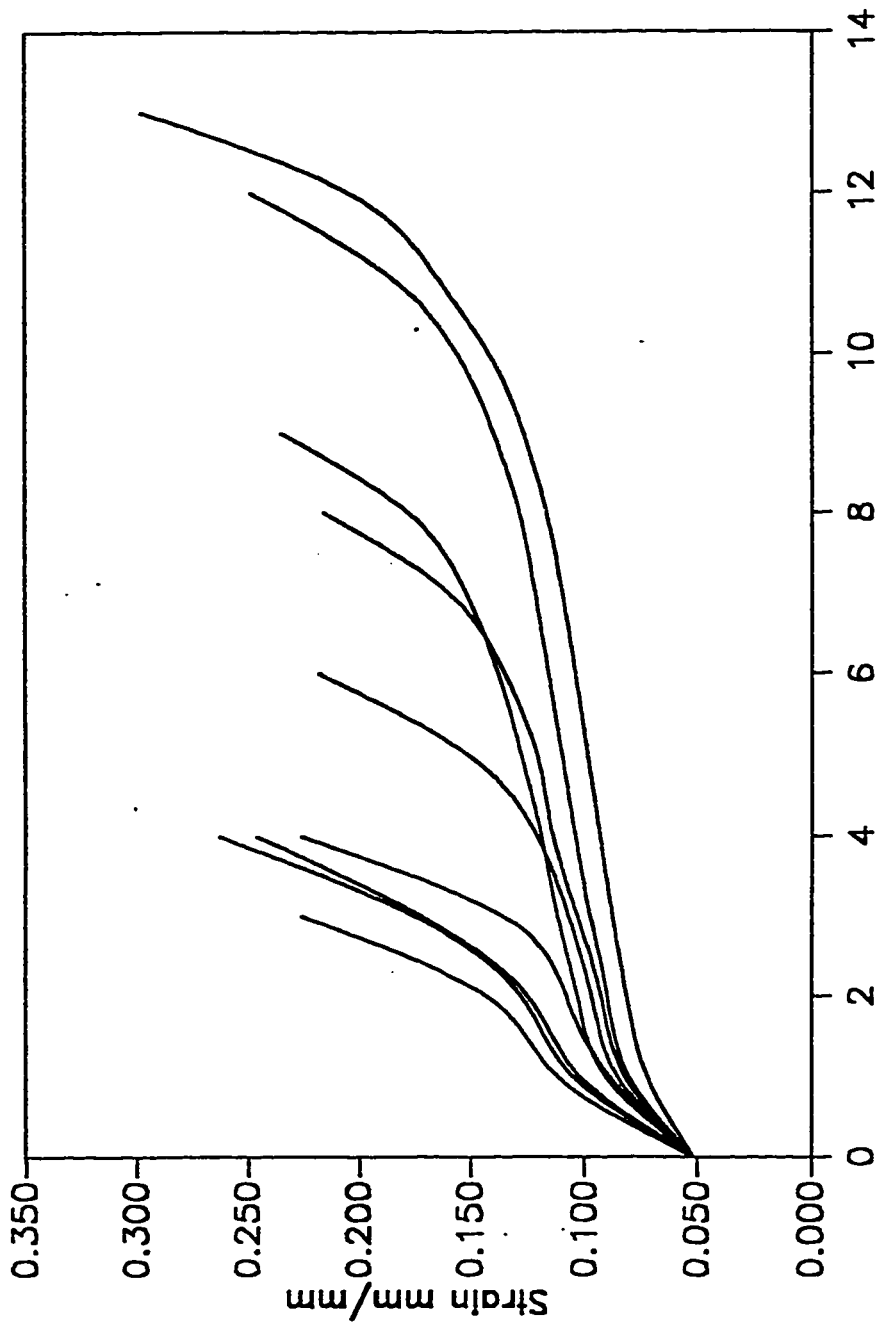

Fig. 5.7 Sample functions for creep of lead at stress 11.2338 N/mm^2 [70].

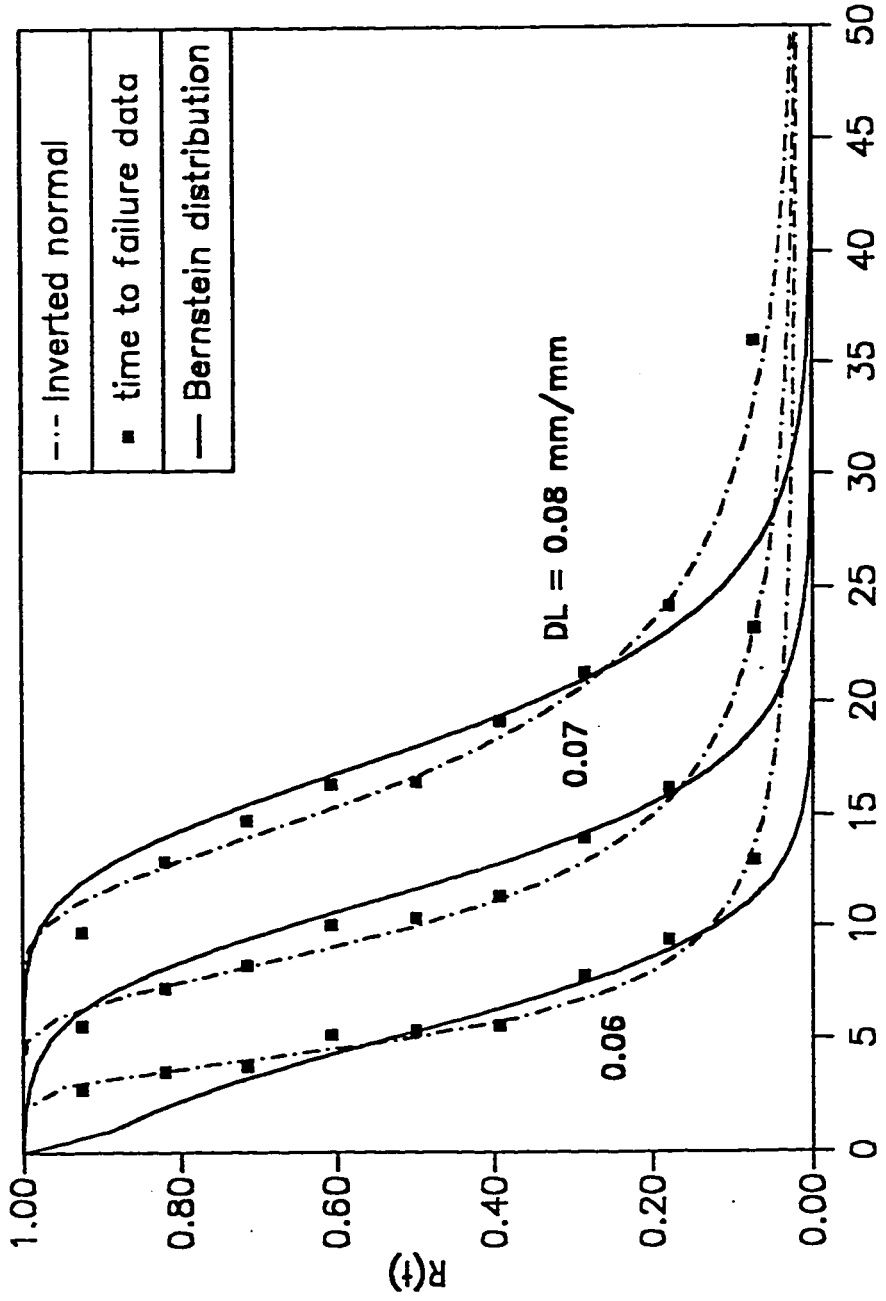

Fig. 5.8 Reliability function for three parameter Bernstein distribution obtained from damage function with actual time to failure data and empirically fitted inverted normal distribution for creep for stress 8.6414 N/mm^2 at different critical damage levels. Data from Ref [70]. [See Table 5.1 for distribution parameters].

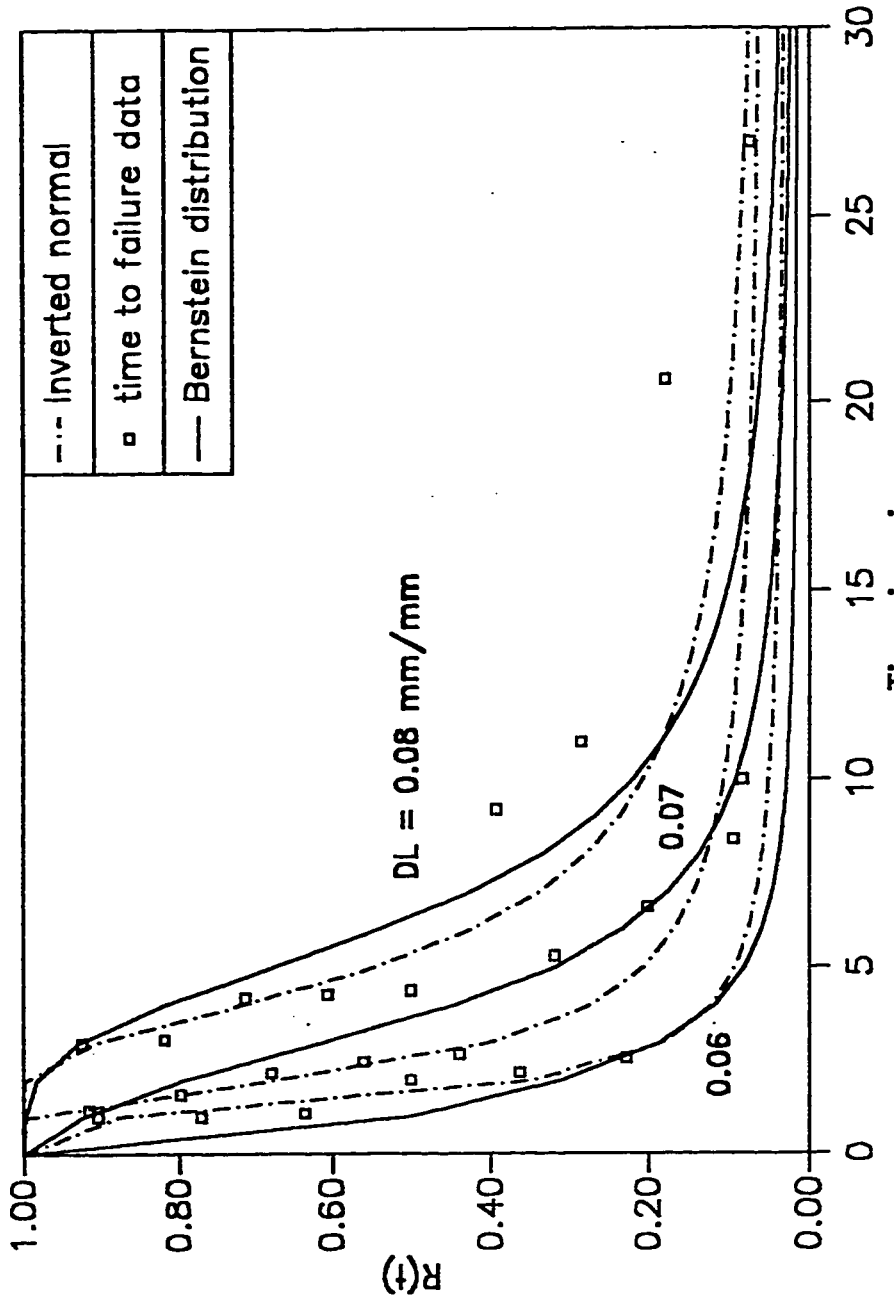

Fig. 5.9 Reliability function for three parameter Bernstein distribution obtained from damage function with actual time to failure data and empirically fitted inverted normal distribution for creep for stress 9.5055 N/mm^2 at different critical damage levels. Data from Ref [70]. [See Table 5.2 for distribution parameters].

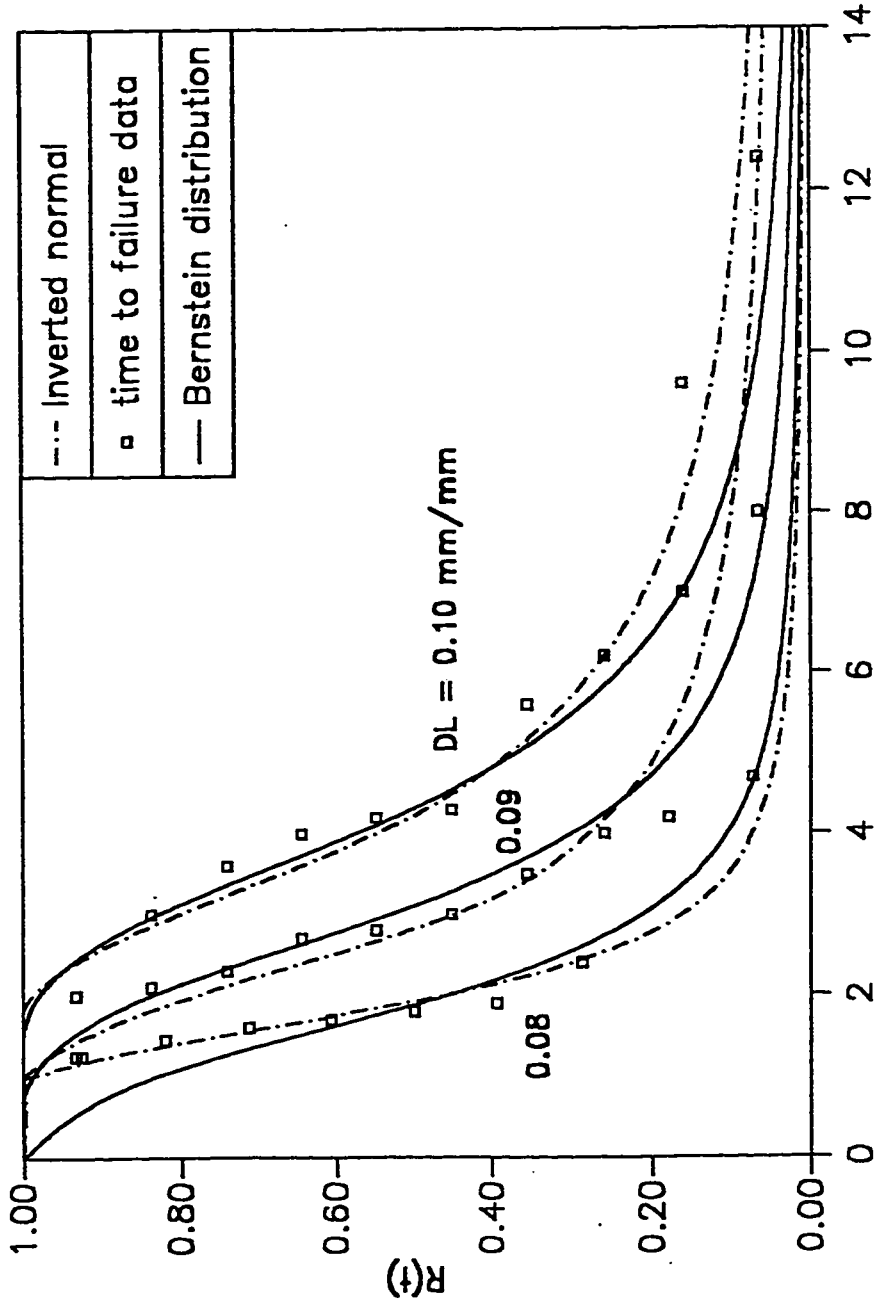

Fig. 5.10 Reliability function for three parameter Bernstein distribution obtained from damage function with actual time to failure data and empirically fitted inverted normal distribution for creep for stress 10.3697 N/mm^2 at different critical damage levels. Data from Ref [70]. [See Table 5.3 for distribution parameters].

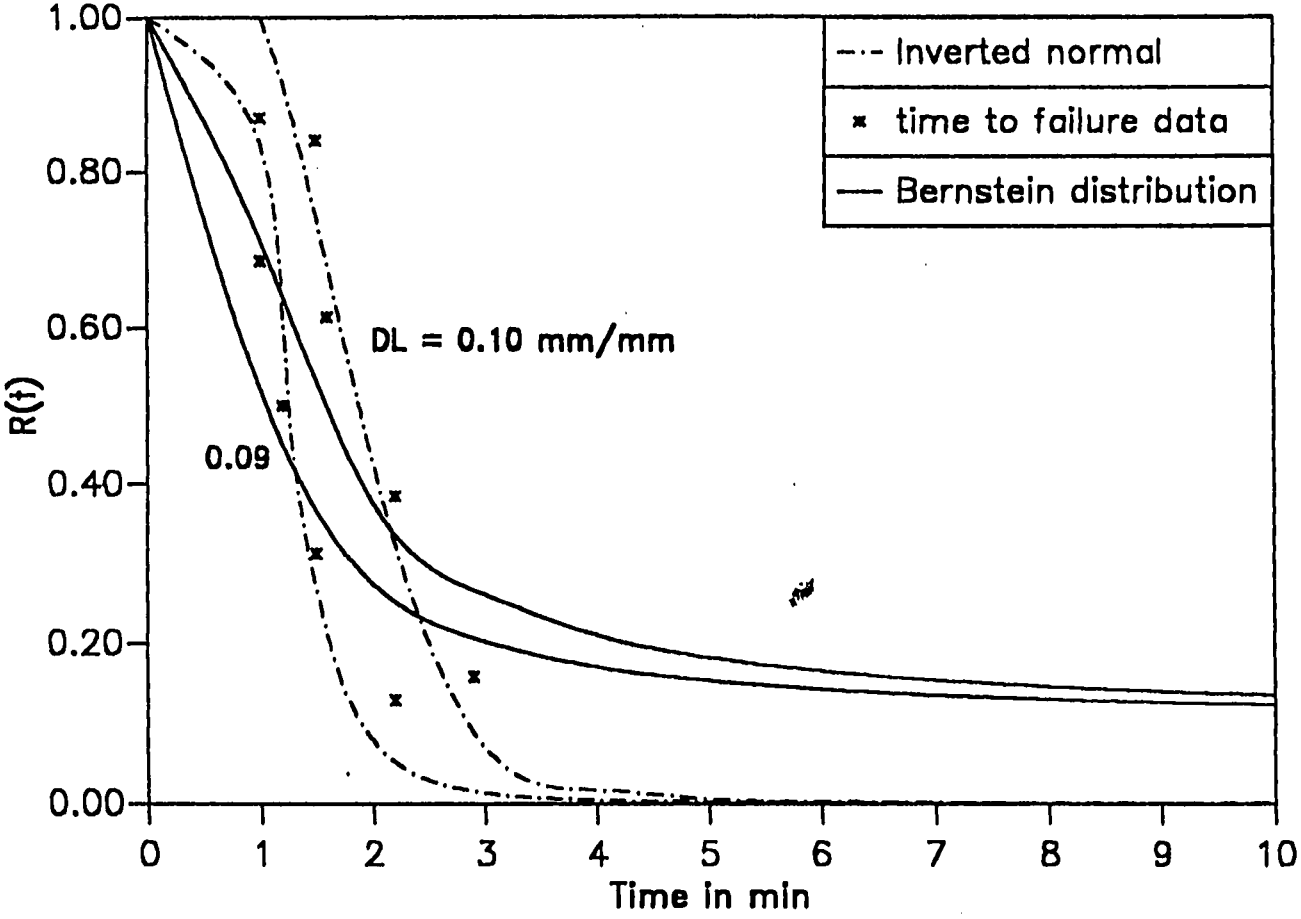

Fig. 5.11 Reliability function for three parameter Bernstein distribution obtained from damage function with actual time to failure data and empirically fitted inverted normal distribution for creep for stress 11.2338 N/mm^2 at different critical damage levels. Data from Ref [70]. [See Table 5.4 for distribution parameters].

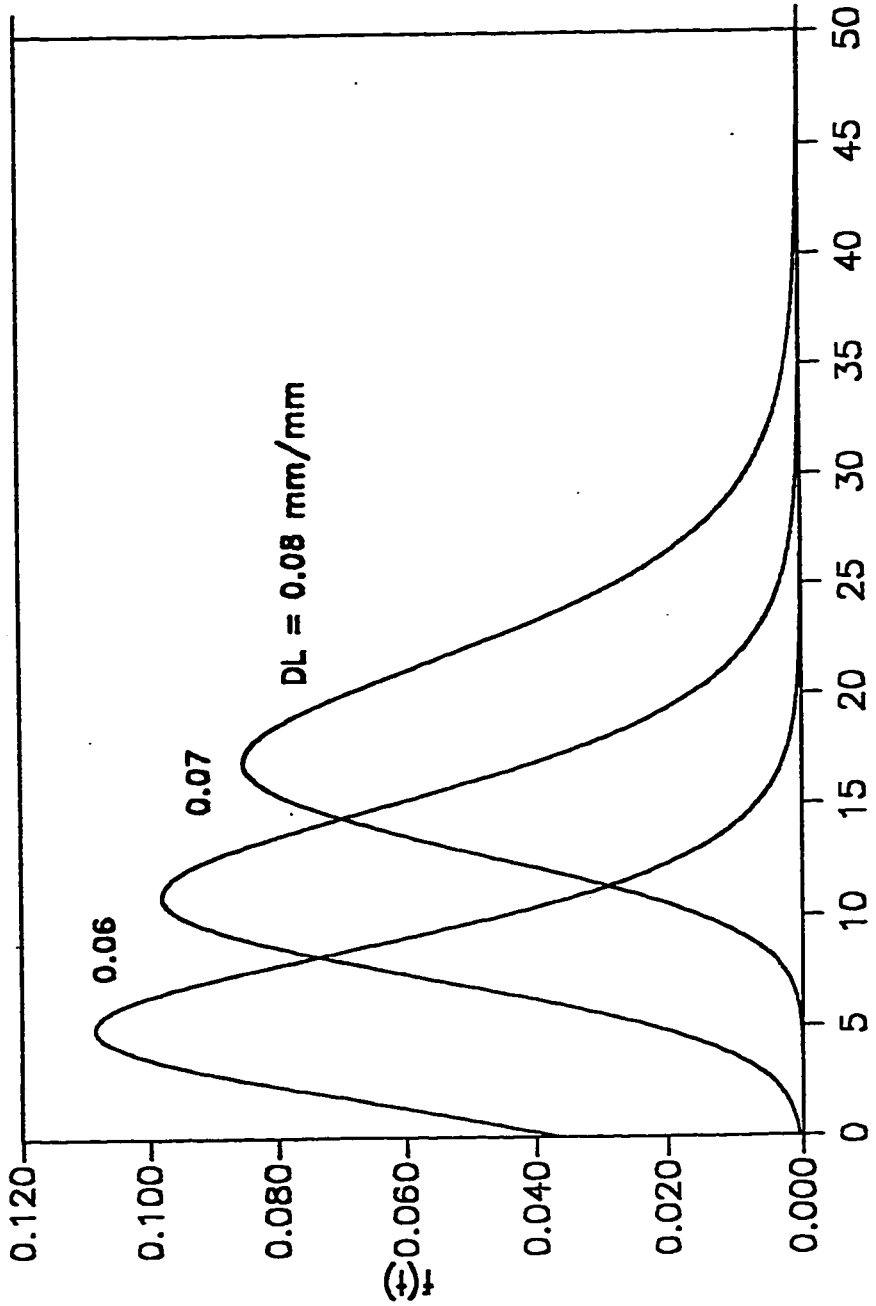

Fig. 5.12 Probability density function for three parameter Bernstein distribution obtained from damage function for creep for stress 8.6414 N/mm^2 at different critical damage levels. Data from Ref [70]. [See Table 5.1 for distribution parameters].

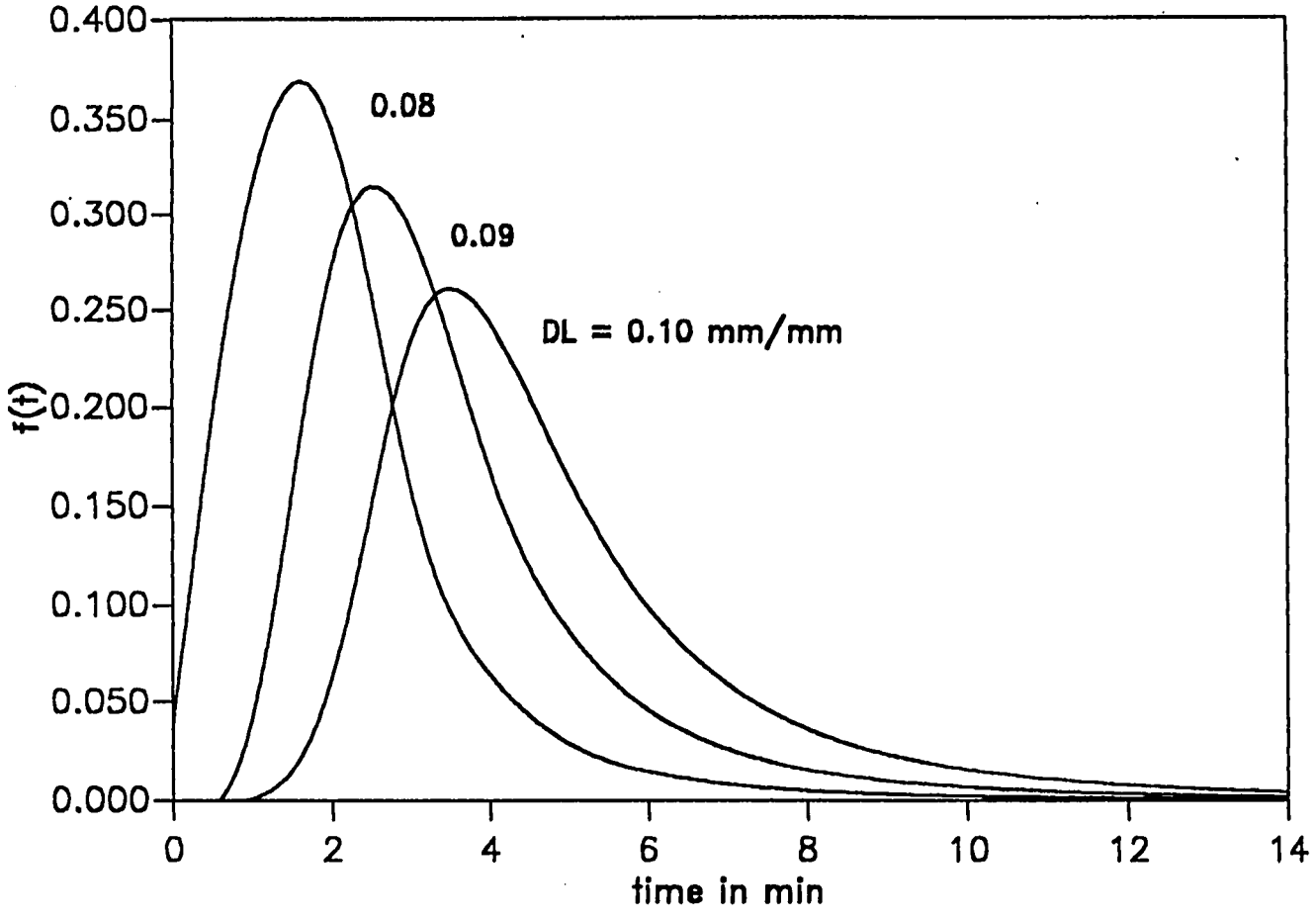

Fig. 5.13 Probability density function for three parameter Bernstein distribution obtained from damage function for creep for stress 10.3697 N/mm^2 at different critical damage levels. Data from Ref [70]. [See Table 5.3 for distribution parameters].

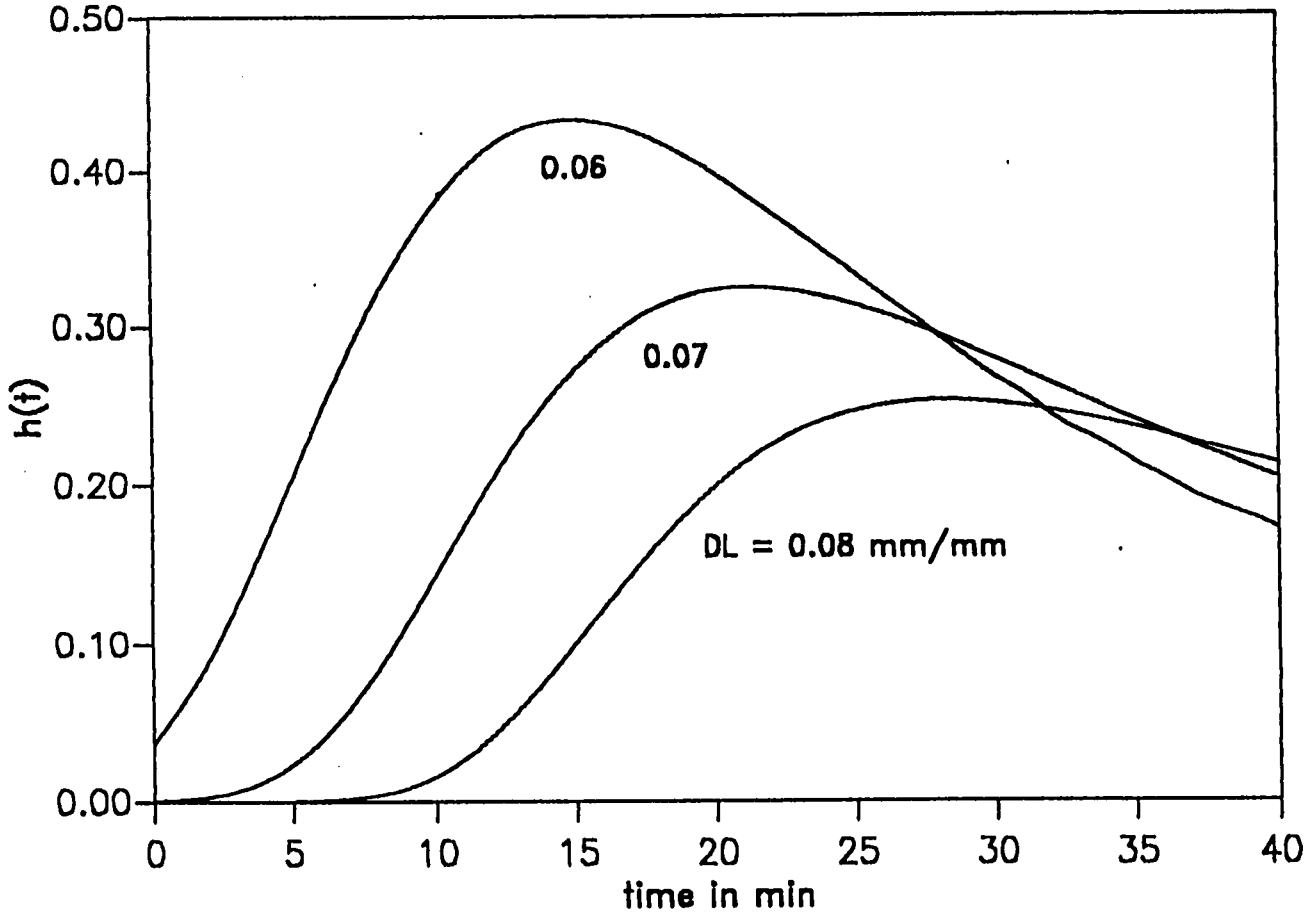

Fig. 5.14 Hazard function for three parameter Bernstein distribution obtained from damage function for creep for stress 8.6414 N/mm^2 at different critical damage levels. Data from Ref [70]. [See Table 5.1 for distribution parameters].

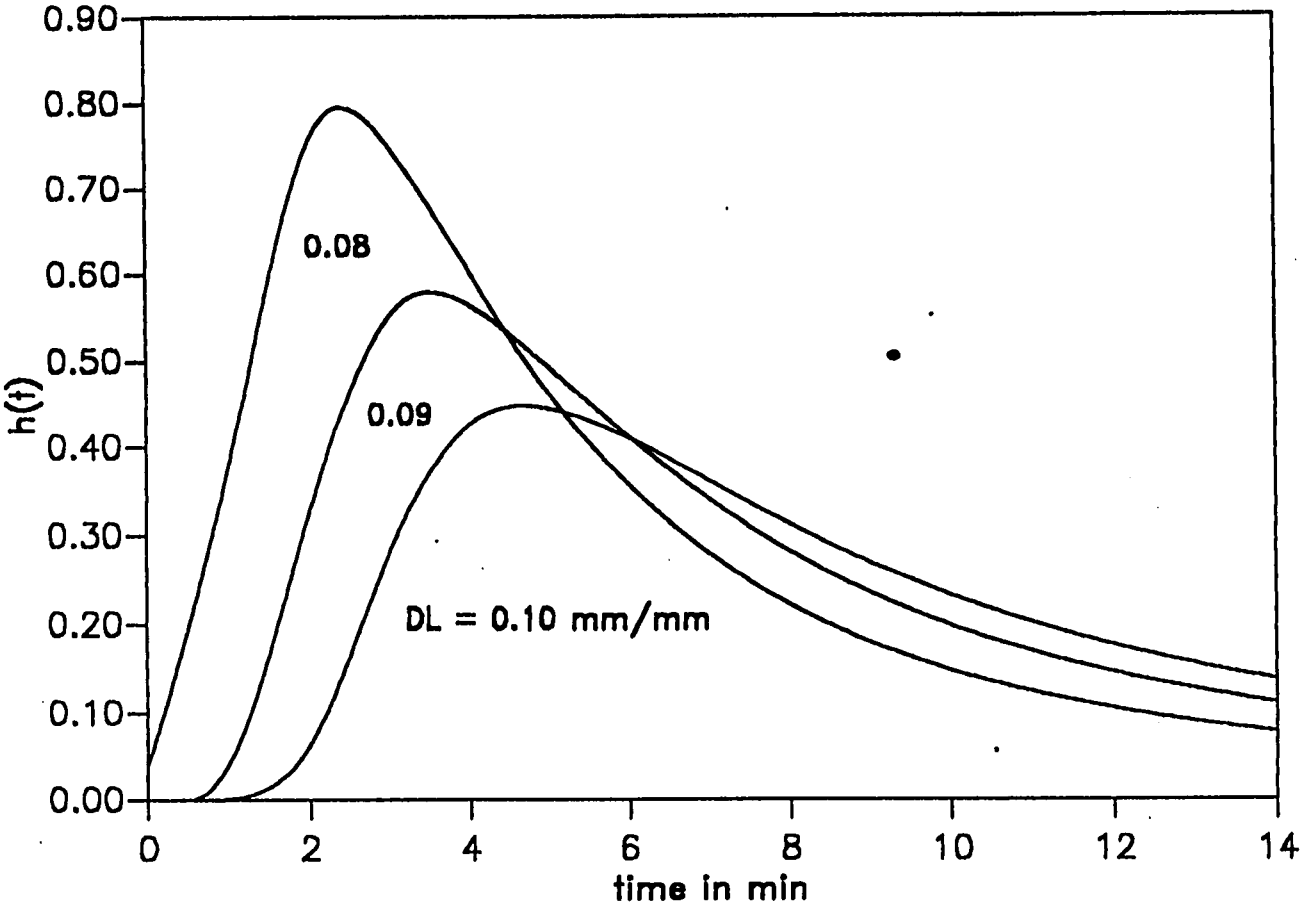

Fig. 5.15 Hazard function for three parameter Bernstein distribution obtained from damage function for creep for stress 10.3697 N/mm^2 at different critical damage levels. Data from Ref [70]. [See Table 5.3 for distribution parameters].

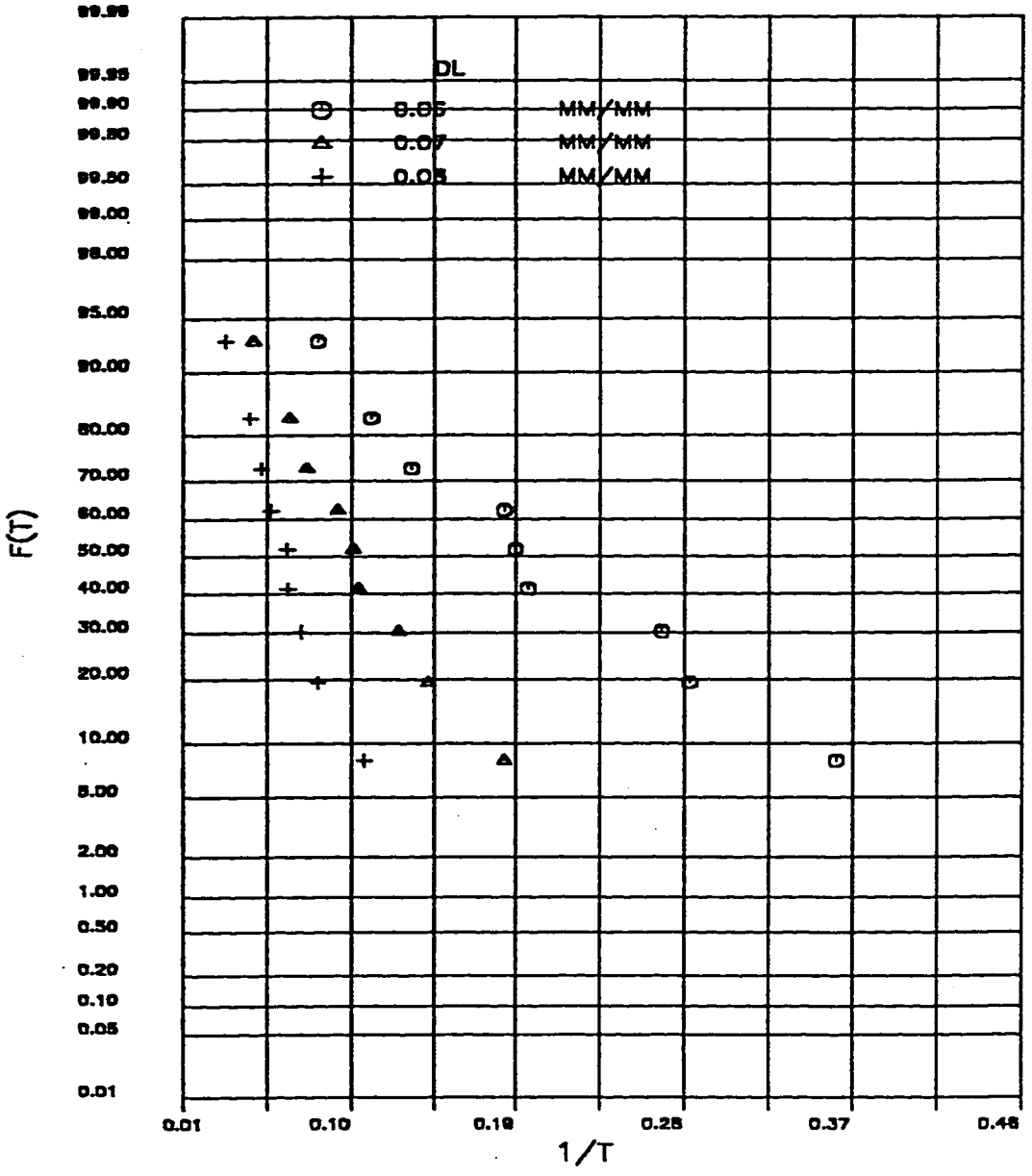

Fig. 5.16 Inverted normal distribution of time to failure data for creep for stress 8.6414 N/mm^2 at different critical damage levels [70].

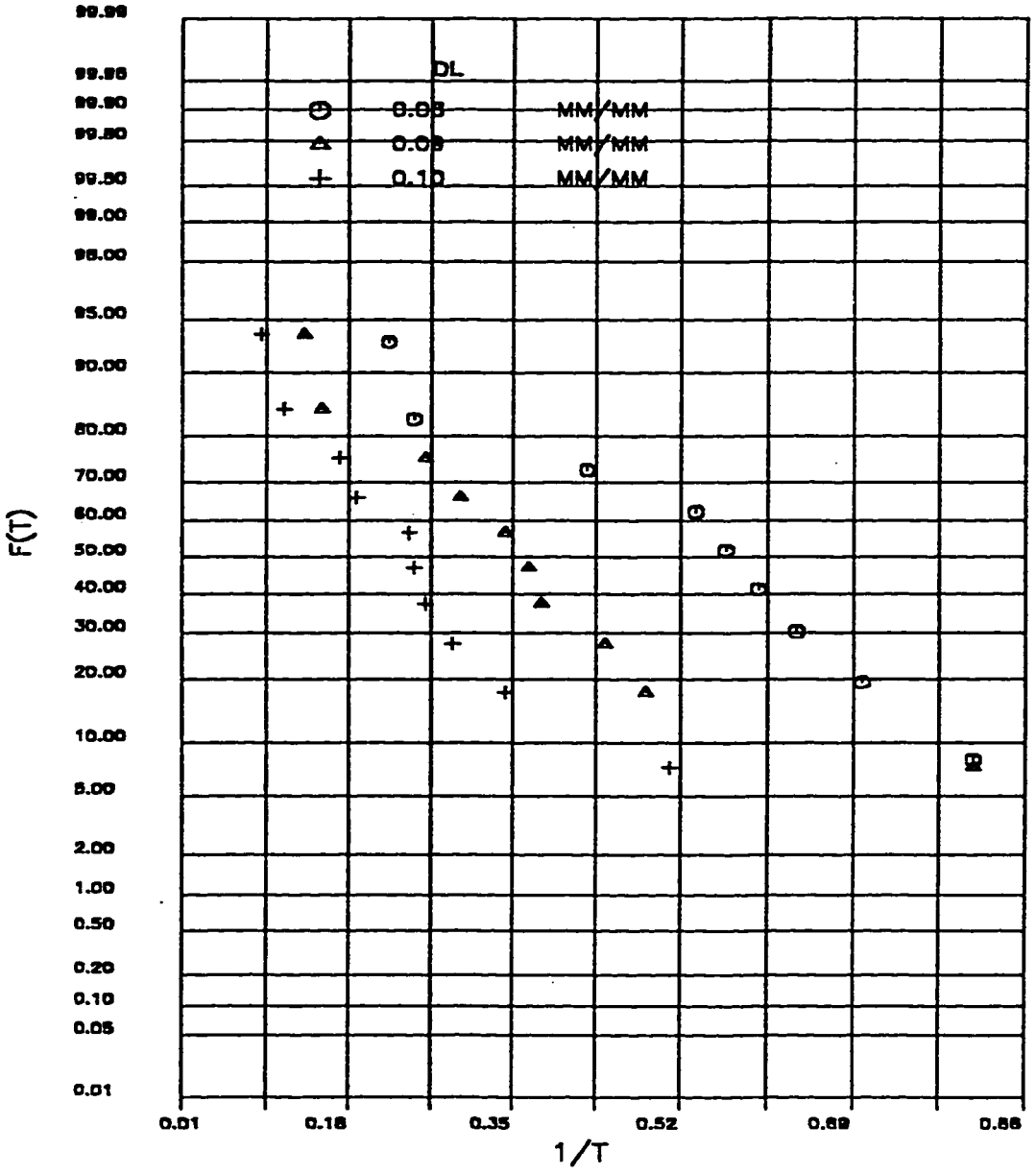

Fig. 5.17 Inverted normal distribution of time to failure data for creep for stress 10.3697 N/mm^2 at different critical damage levels [70].

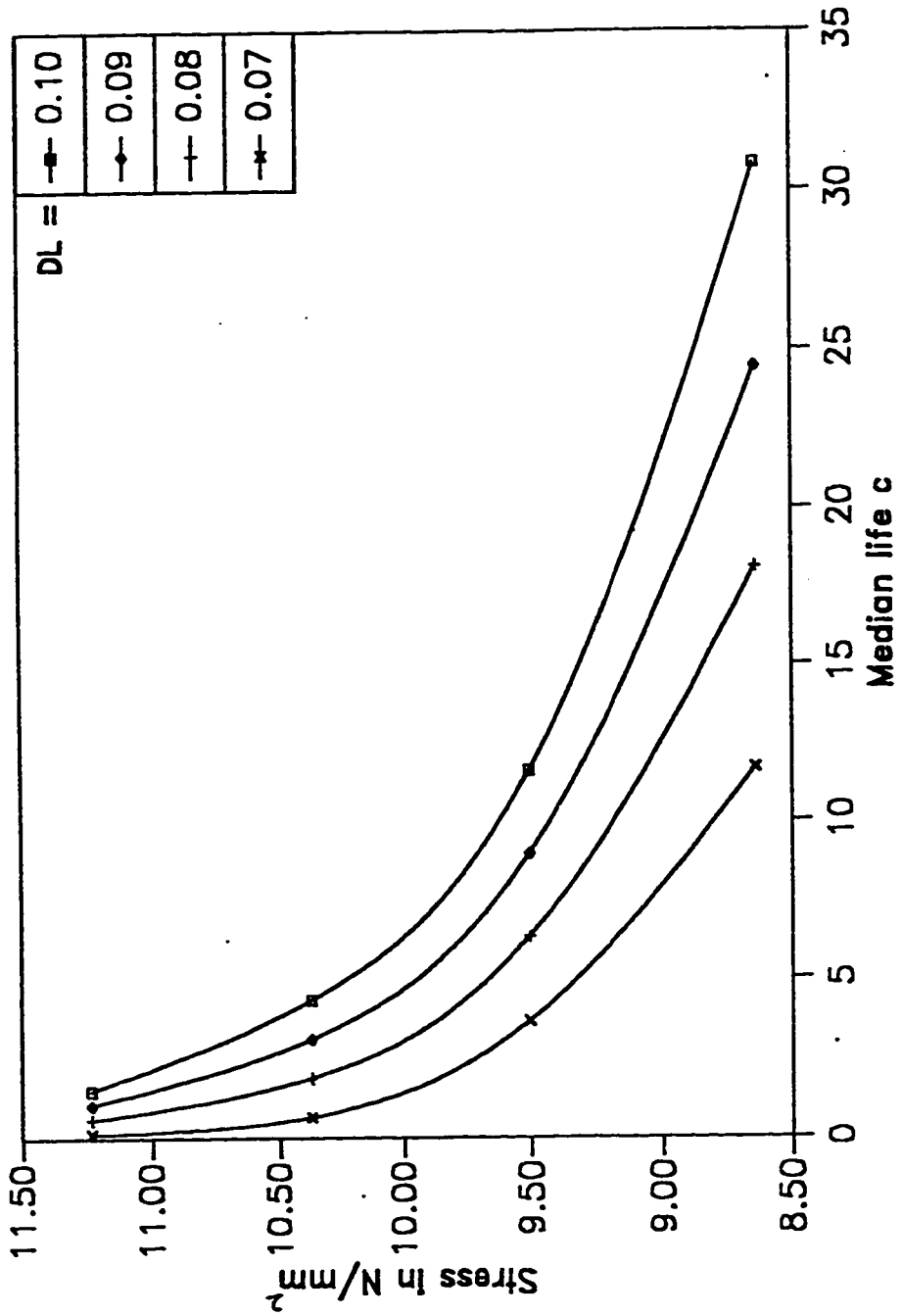

Fig. 5.18 Variation of stress with median life c for creep at different critical damage levels [70].

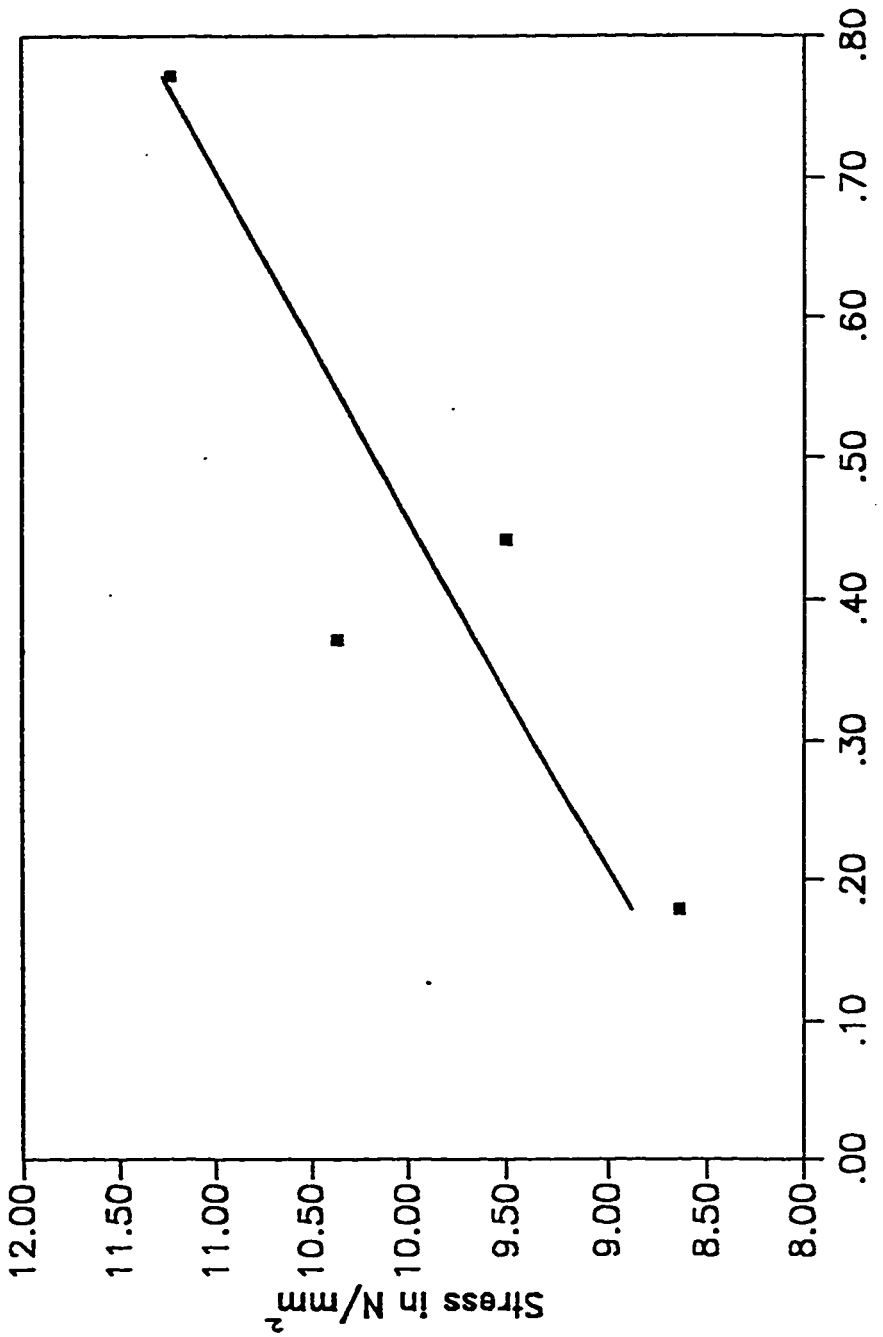

Fig. 5.19 Variation of stress with scatter parameter $\sqrt{\alpha}$ for creep [70].

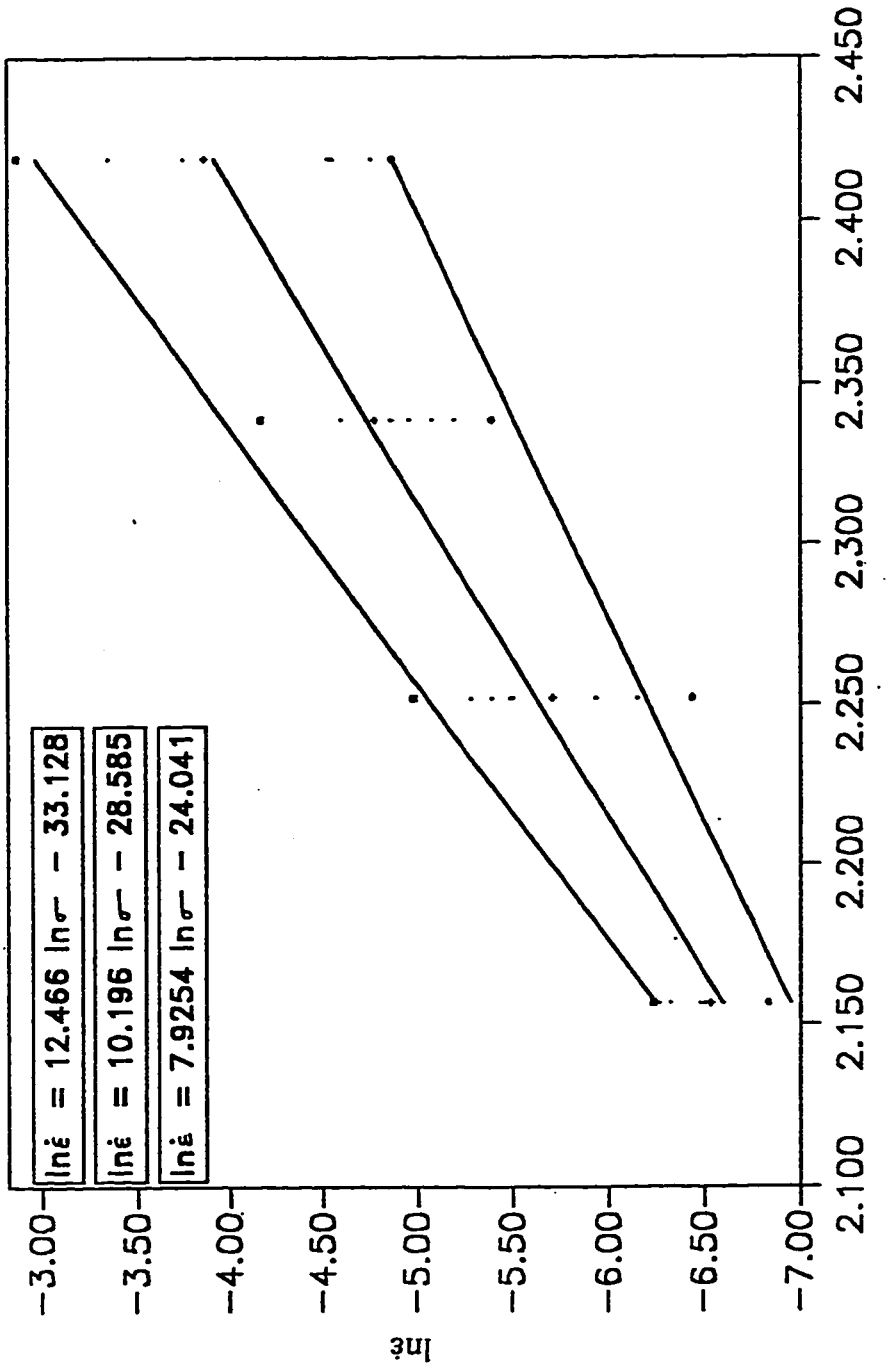

Fig. 5.20 Variation of logarithmic stress and logarithmic strain rate [70].

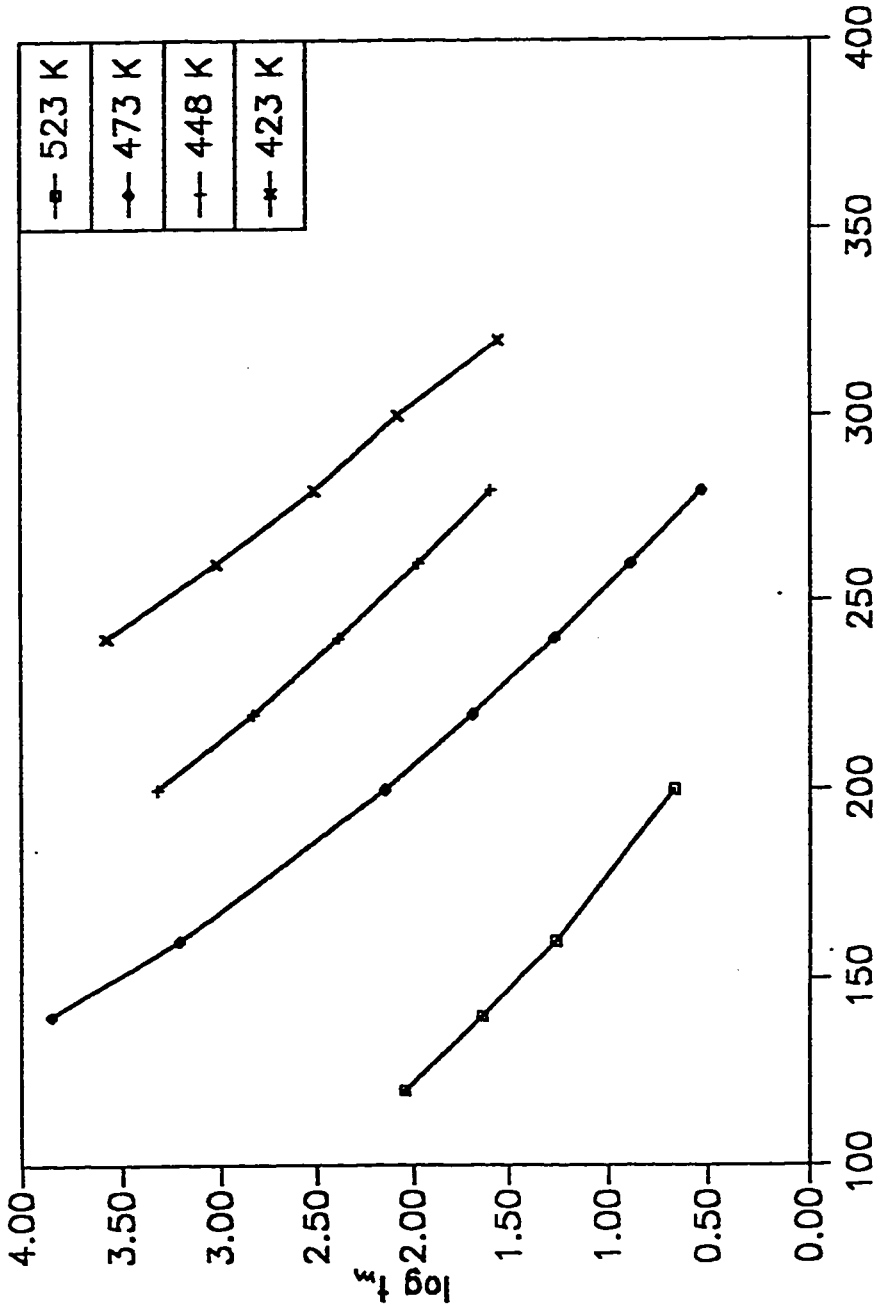

Fig. 5.21 Variation of stress with logarithmic time at different temperatures [76].

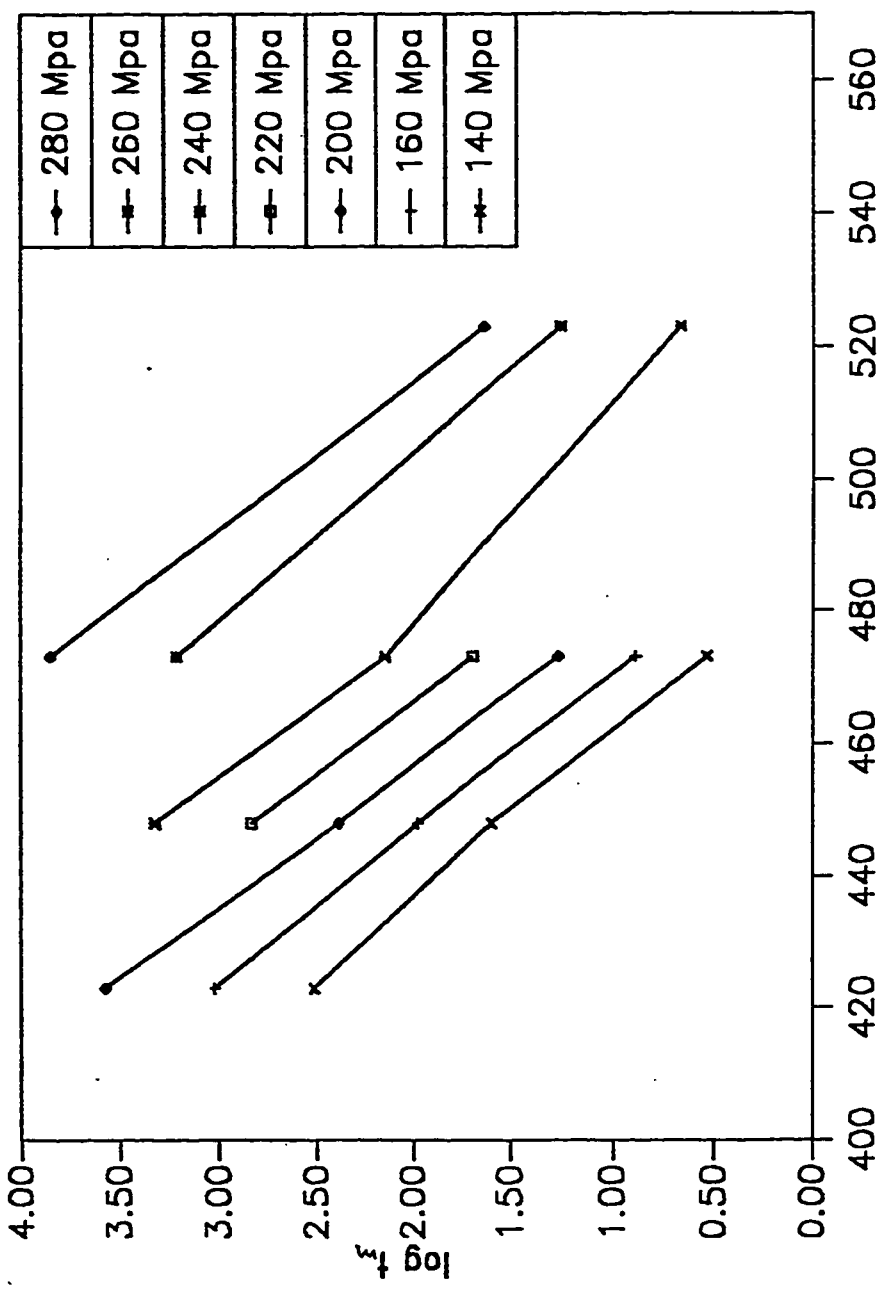

Fig. 5.22 Variation of temperature with logarithmic time at different stress levels [76].

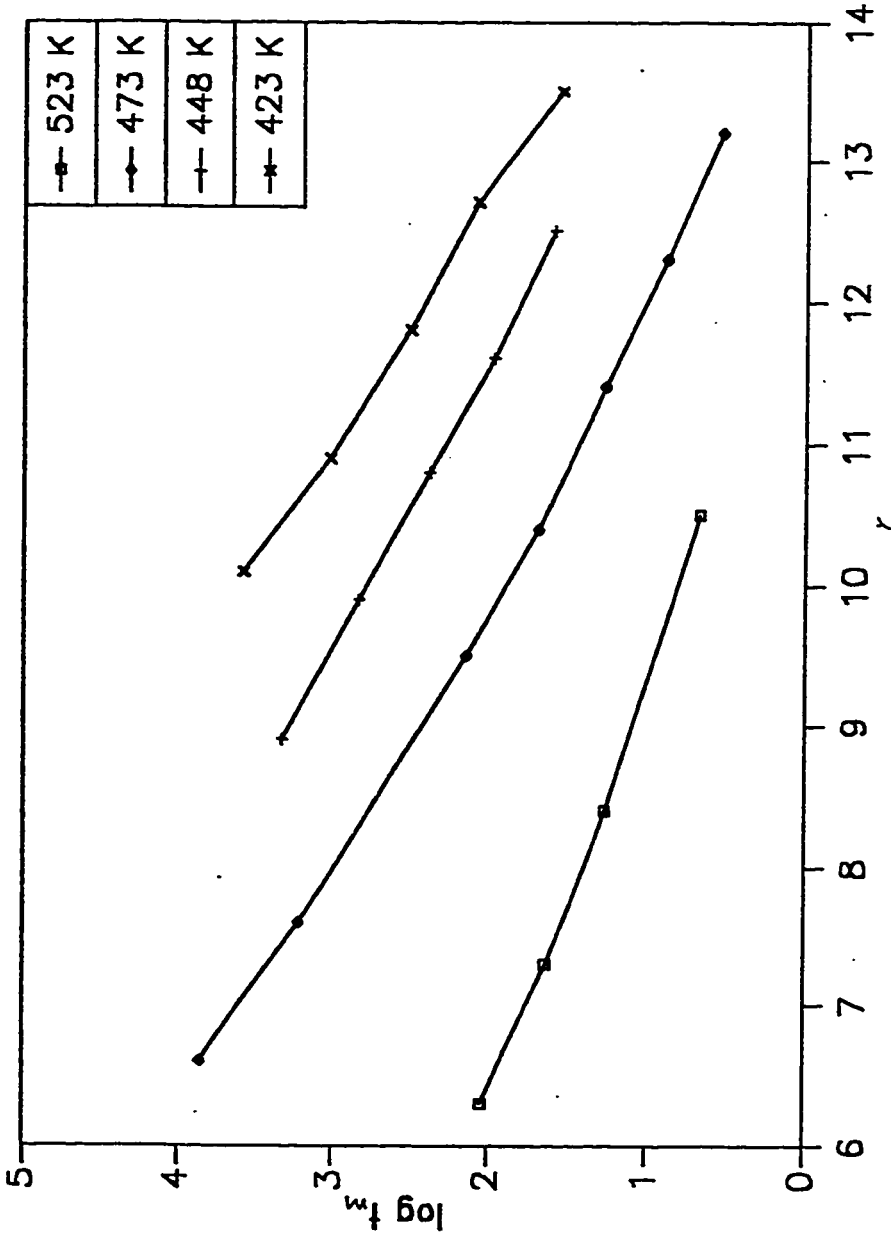

Fig. 5.23 Variation of product of stress and temperature with logarithmic time at different temperatures [76].

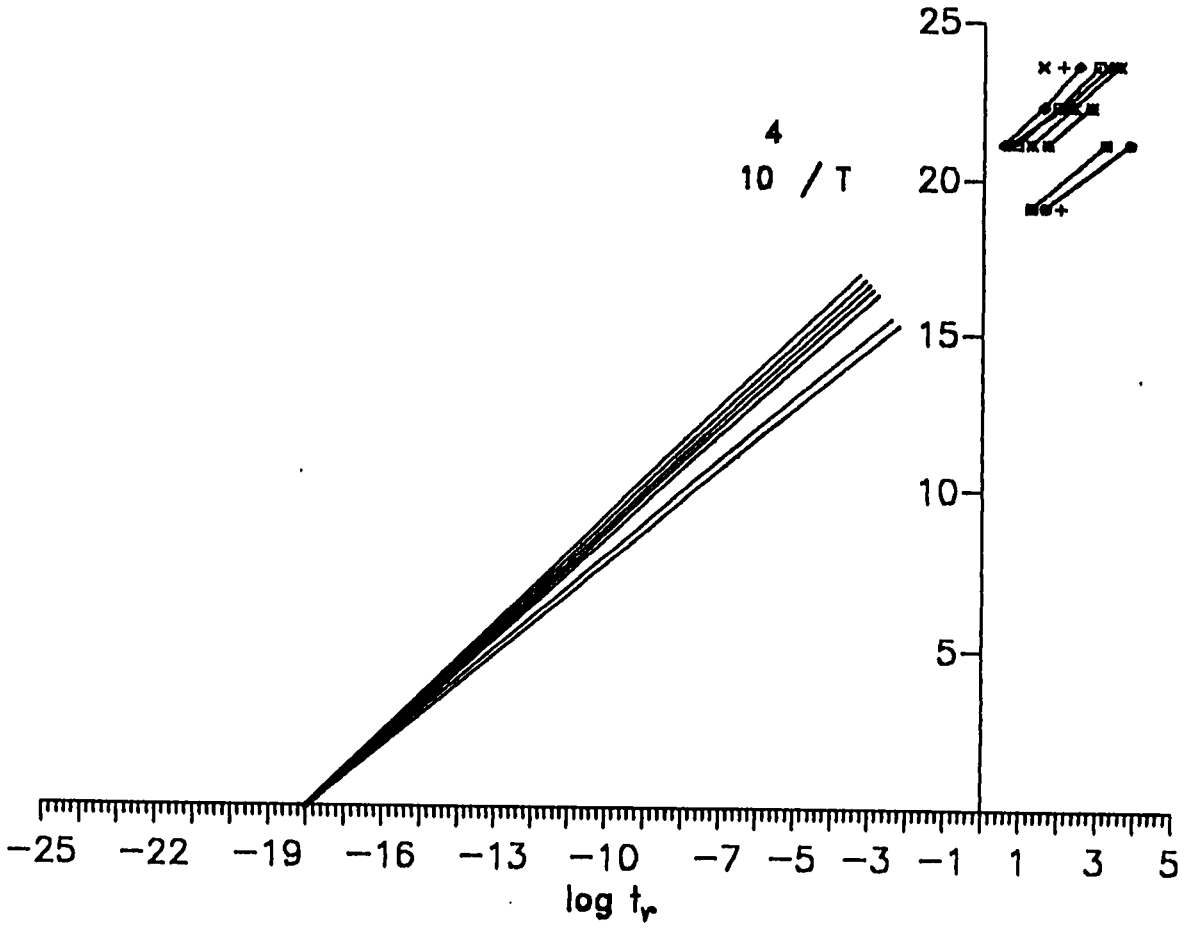

Fig. 5.24 Larson-Miller method for correlating creep data for Ak4-1. Data from Ref [76].

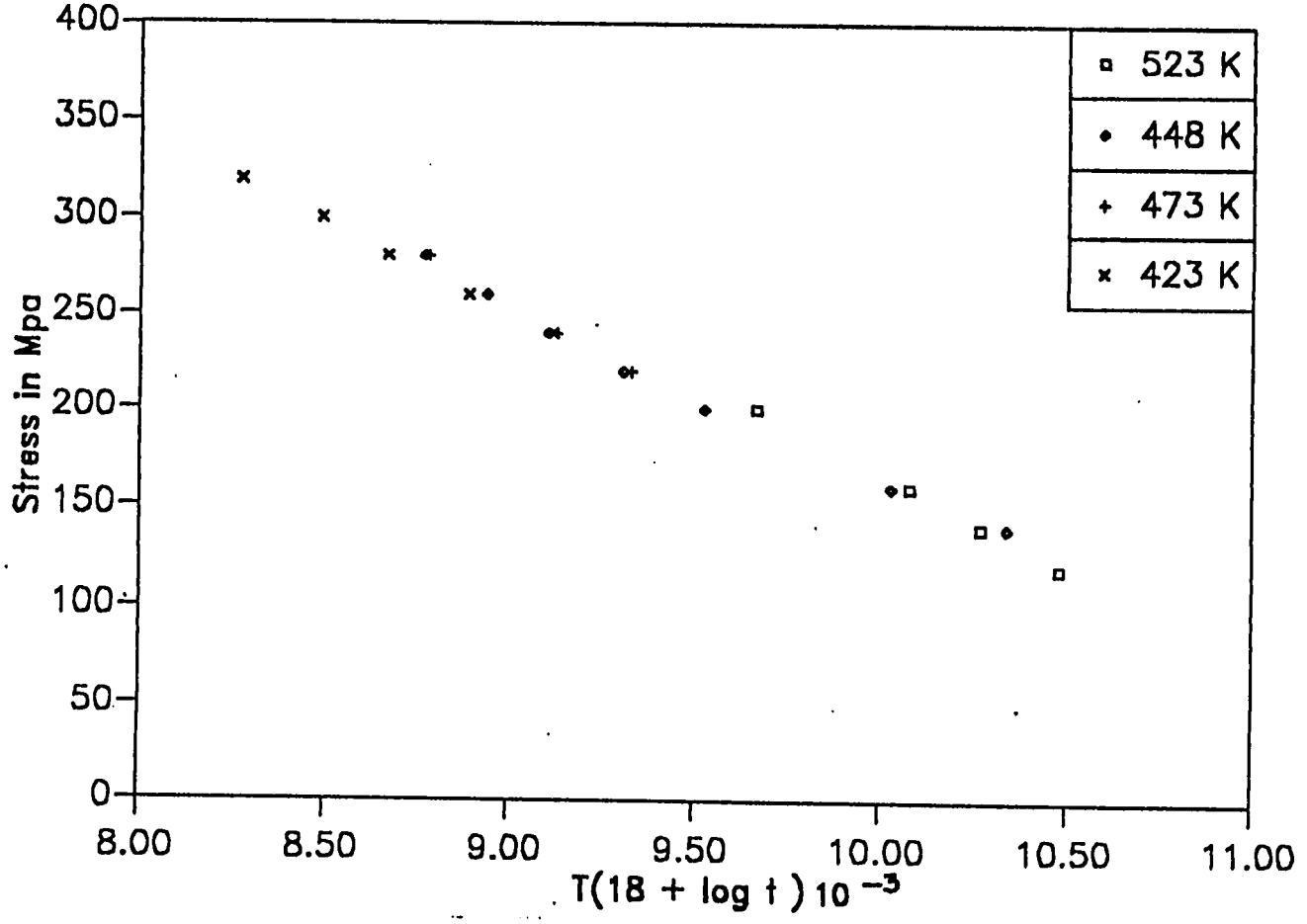

Fig. 5.25 Correlation curve for creep rupture using Larson-Miller correlation parameter at different temperatures for creep data for Ak4-1. Data from Ref [76].

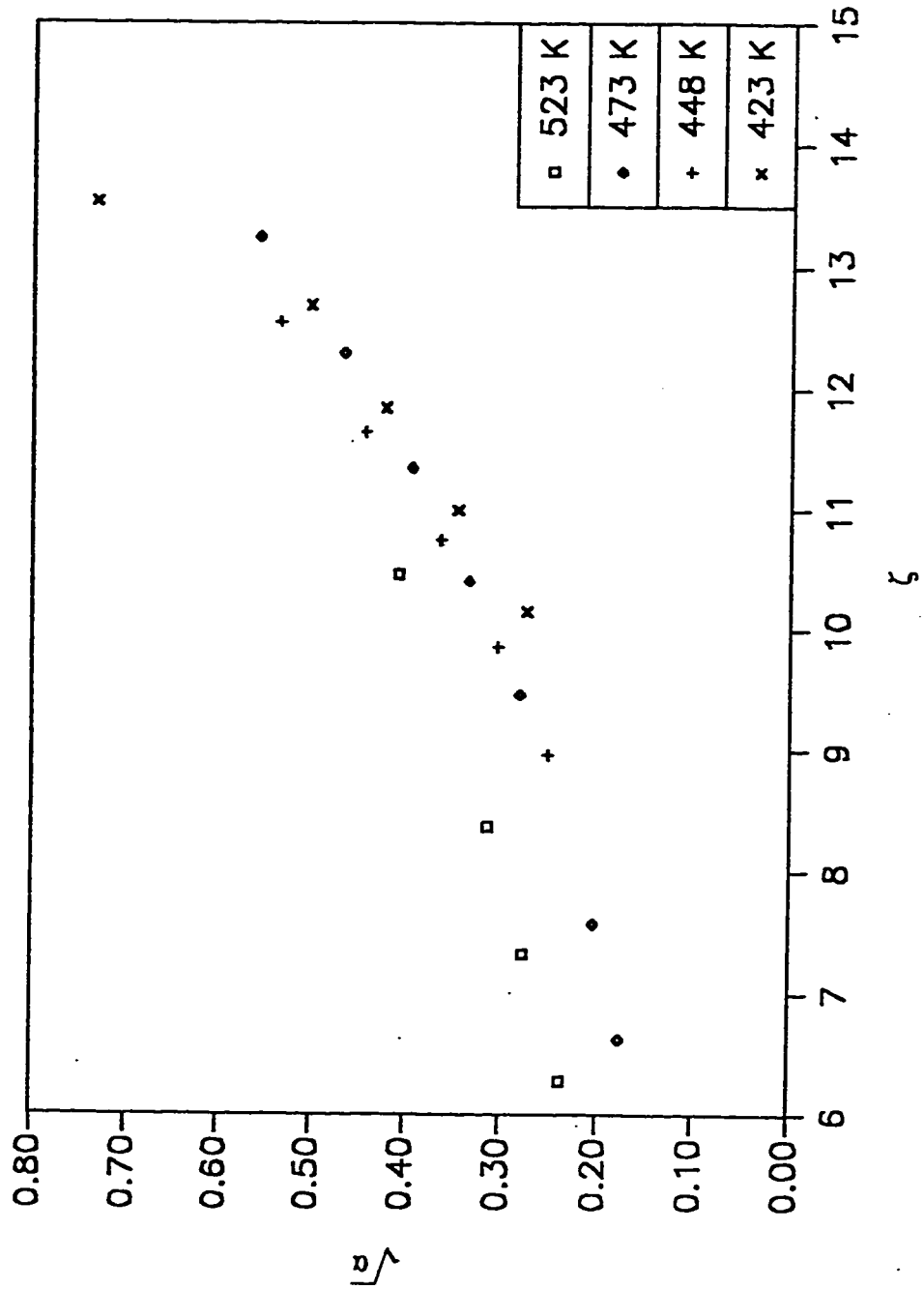

Fig. 5.26 Variation of product of stress and temperature with scatter parameter $\sqrt{\alpha}$.

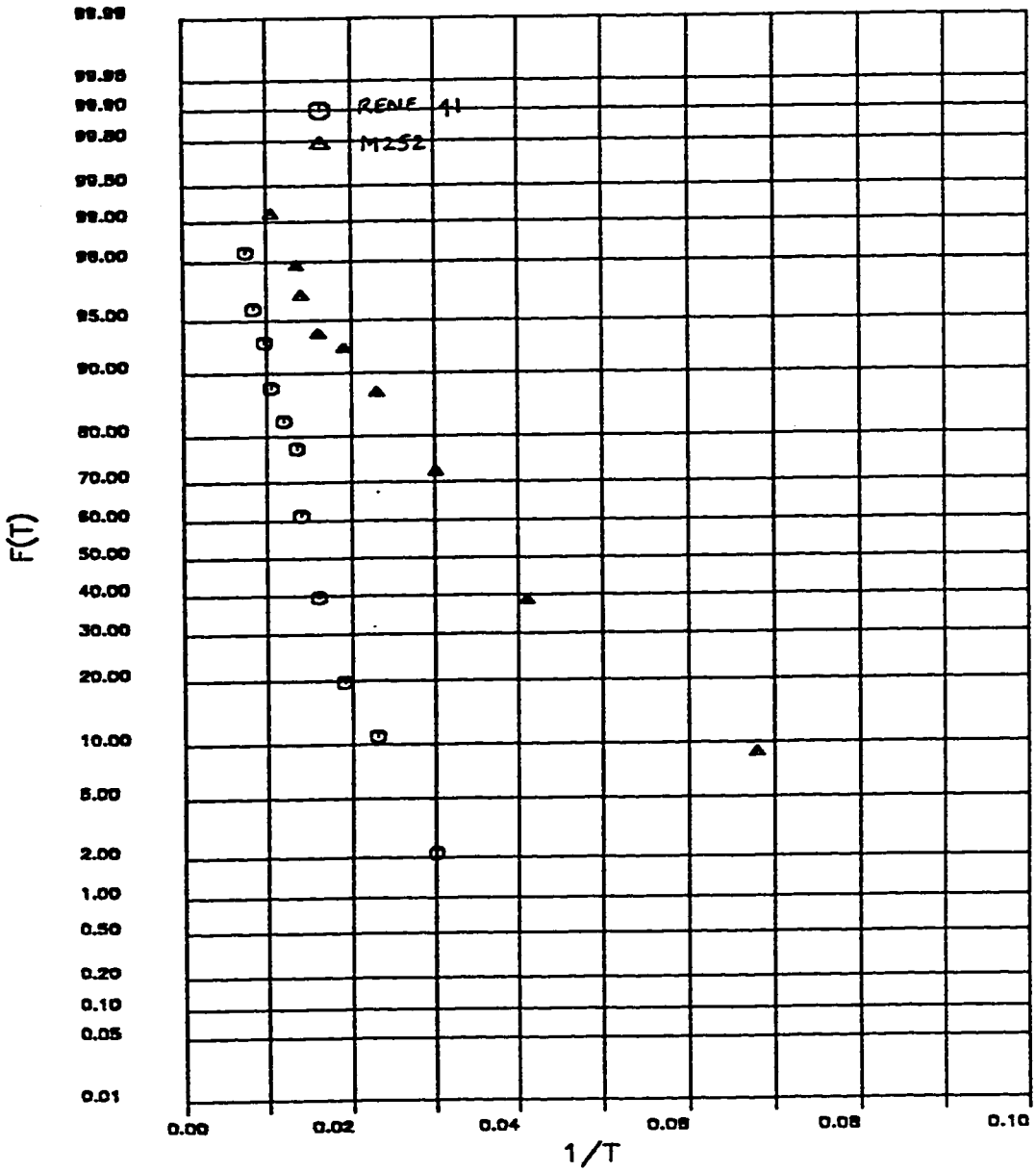

Fig. 5.27 Inverted normal distribution of time to rupture data for different materials [78].

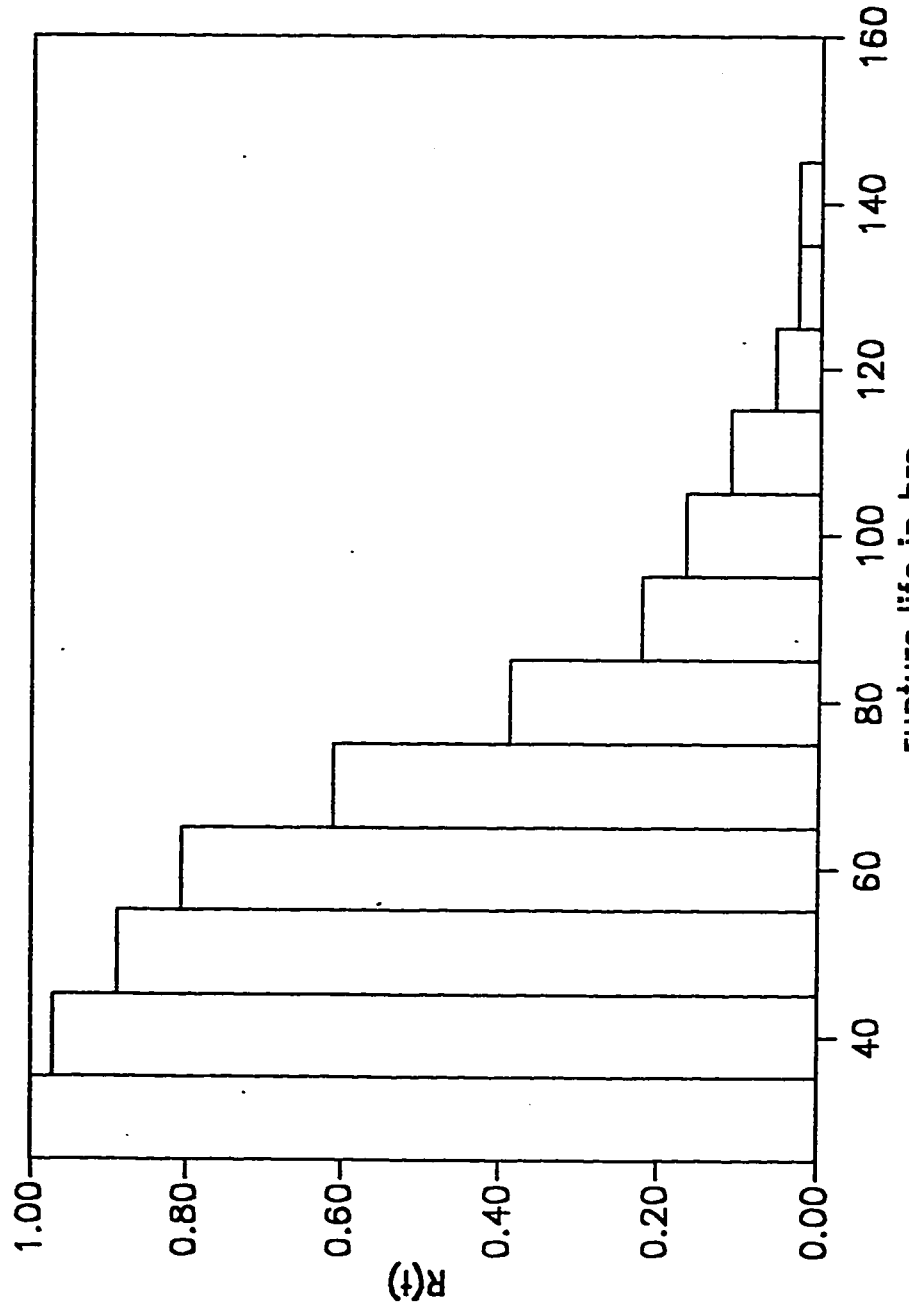

Fig. 5.28 Reliability function for inverted normal distribution for Renc 41 [78].

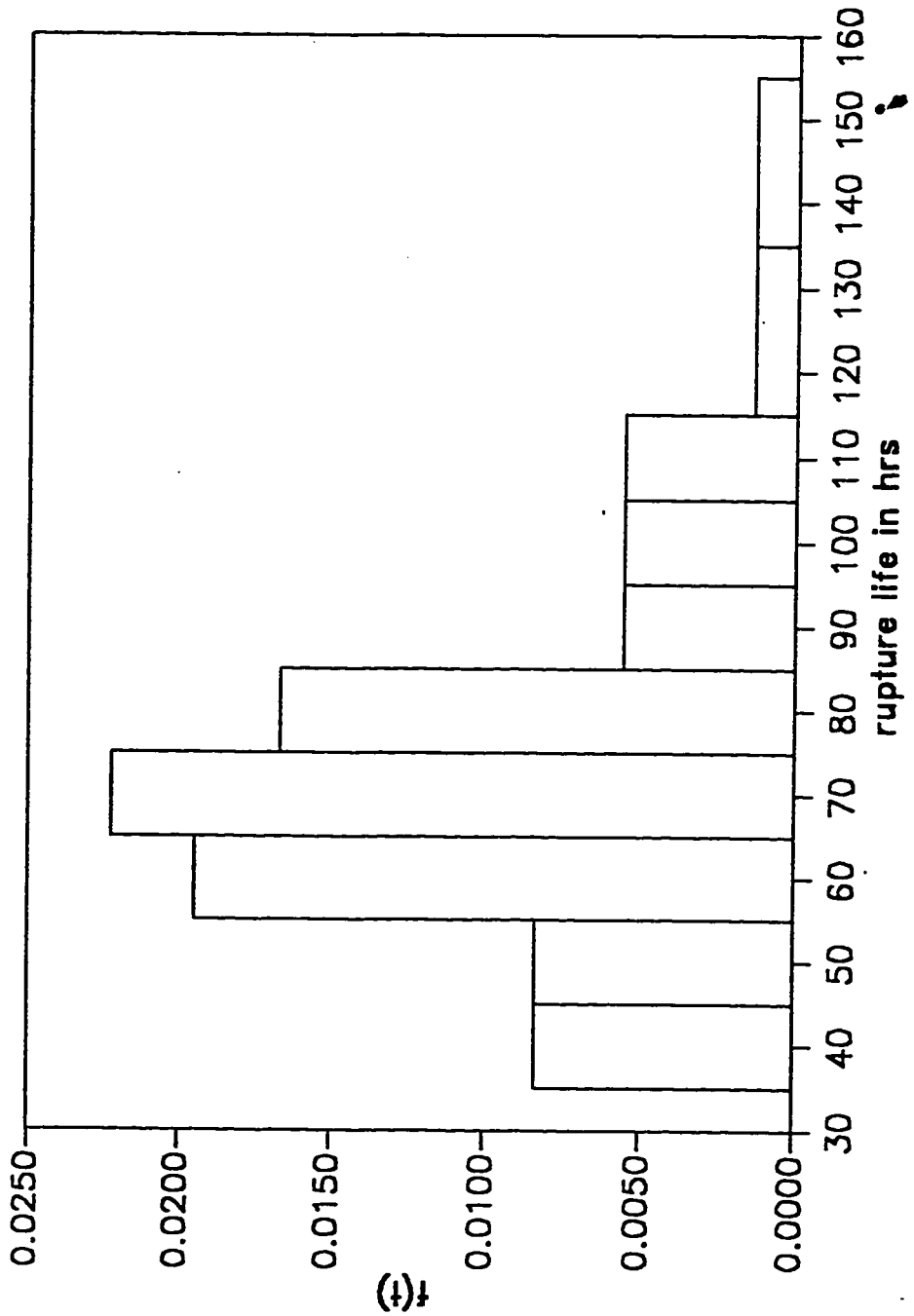

Fig. 5.29 Probability density function for inverted normal distribution for Rene 41 [78].

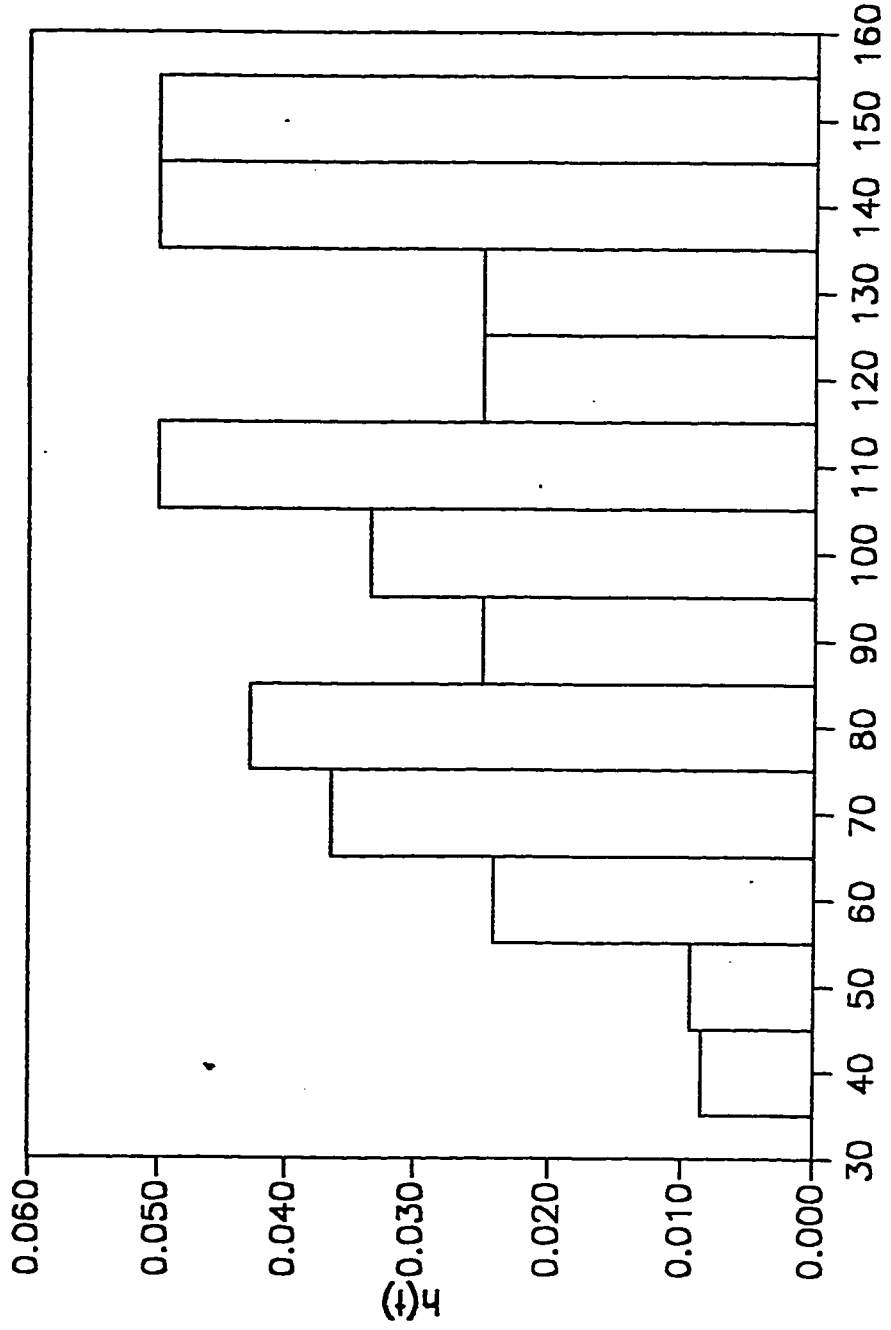

Fig. 5.30 Hazard function for inverted normal distribution for Rene 41 [78].

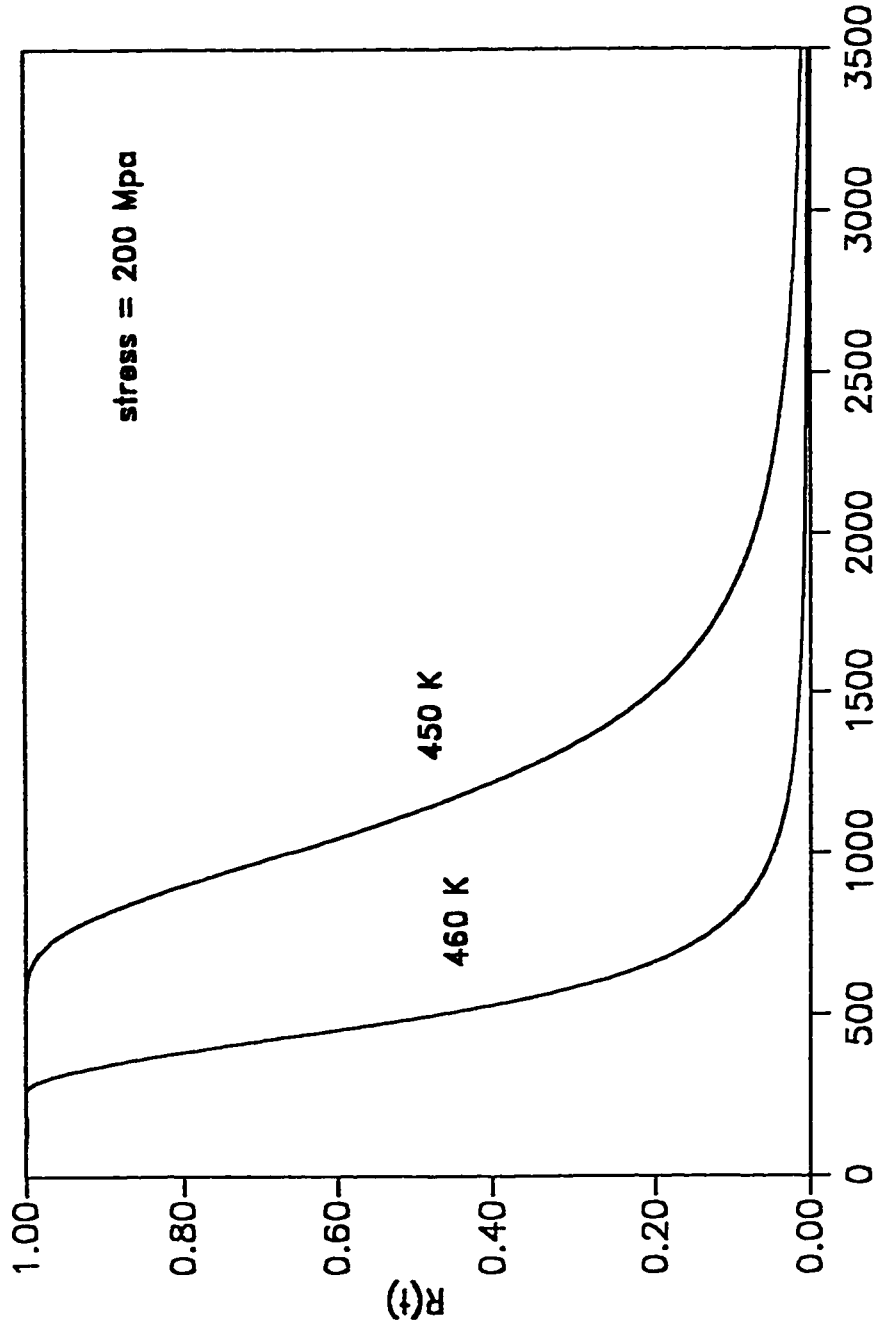

Fig. 5.31 Reliability function for inverted normal distribution at fixed stress for different temperatures.

Table 5.1 Parameters of the distribution for creep at stress 8.6414 N/mm² [70]

Fig.	Symbol	Basis	Distribution	Distribution parameters			
5.8	———	Damage function	Bernstein model	D_1	c	α	β
				0.06 0.07 0.08	5.331 11.701 18.070	0.0322 0.0322 0.0322	12.698 12.698 12.698
	—·—·—	Time to failure	Inverted normal	D_1	$\hat{c}$		$\hat{\alpha}$
				0.06 0.07 0.08	16.77 10.05 5.10		0.117 0.154 0.186

Table 5.2 Parameters of the distribution for creep at stress 9.5055 N/mm² [70]

Fig.	Symbol	Basis	Distribution	Distribution paramcters			
5.9	———	Damage function	Bernstein model	D_1	c	α	β
				0.06 0.07 0.08	1.003 3.662 6.322	0.1952 0.1952 0.1952	3.250 3.250 3.250
	—·—·—·—	Time to failure	Inverted normal	D_1	$\hat{c}$		$\hat{\alpha}$
				0.06 0.07 0.08	1.603 2.561 5.350		0.264 0.358 0.327

Table 5.3 Parameters of the distribution for creep at stress 10.3697 N/mm² [70]

Fig.	Symbol	Basis	Distribution	Distribution parameters			
5.10	———	Damage function	Bernstein model	D_1	c	α	β
				0.08	1.878	0.1381	0.699
				0.09	3.100	0.1381	0.699
				0.10	4.323	0.1381	0.699
	—·—·—·—	Time to failure	Inverted normal	D_1	$\hat{c}$		$\hat{\alpha}$
				0.08	1.935		0.129
				0.09	2.797		0.260
				0.10	4.243		0.236

Table 5.4 Parameters of the distribution for creep at stress 11.2338 N/mm^2 [70]

Fig.	Symbol	Basis	Distribution	Distribution parameters			
5.11	———	Damage function	Bernstein model	D_l	c	α	β
				0.09 0.10	1.045 1.495	0.5956 0.5956	0.189 0.189
	—·—·—·—	Time to failure	Inverted normal	D_l	$\hat{c}$		$\hat{\alpha}$
				0.09 0.10	1.26 1.91		0.217 0.061

CHAPTER 6

CONCLUSIONS

1. Various material damage processes are normally treated as deterministic functions of time in literature, where as in real life their behavior is stochastic with their average and dispersion characteristics and associated distributions at various time locations.

2. Conventional approach to develop reliability is to analyse time to failure data and select the most appropriate model to fit it. However if time to failure data is not directly available then the damage process which lead to the failure can be used to develop these reliability models. In this manner starting from the physics of the damage process and its average and dispersion characteristics the reliability models are developed.

3. Utilizing the similarity in the mathematical representation of various types of material damage, a generalized systems approach in modelling these damage processes and their corresponding time to failure distributions are developed. This systems approach also establish link between the parameters of the damage process and time to failure distribution parameters.

4. Using this systems approach, the reliability models were developed from appropriate damage functions and these distributions were compared with empirical distribution obtained directly from time to failure data analysis. Reliability models were developed and compared for a variety of material damage processes such as wear, corrosion and creep, and systems damage process such as fouling.

5. It was observed that in general the following reliability models are valid for specific type of damage process :

Process	Time dependence	Best model
1. Wear	Linear	Inverted normal
2. Corrosion		
(a) Pitting	Logarithmic	Weibull
	Power law	Inverted lognormal
(b) SCC	Logarithmic	Inverted normal and log Bernstein
(c) Oxidation	Linear	Inverted normal
	Logarithmic	Inverted lognormal
3. Fouling	Linear	Inverted normal
	Logarithmic	Inverted lognormal
	Asymptotic	Weibull
4. Creep	Linear	Inverted normal

6. Reliability models developed based on damage function analysis and time to

failure analysis are identical in those cases where initial damage and its scatter is accurately determined. Whenever the initial damage and its scatter is estimated by extrapolated values of regression lines, it always introduced distortion in the estimated parameter, which resulted in a poor fit to the data. In such cases if the initial scatter is ignored the fit of the resulting two parameter model was improved.

7. These proposed reliability models can be utilized in various applications such as maintenance and replacement strategies, economic forecasts, spare parts predictions and for improving the performance of the existing design as well as in field comparison of the performance of similar products supplied by different manufacturers.

NOMENCLATURE

A	:	area
A'	:	material constant
C	:	constant
D_i	:	initial level of damage at $t=0$
D_l	:	critical damage level
D_{max}	:	asymptotic value of damage
$D(t)$	:	represents a certain manifestation of damage at time t
$\tilde{D}$	:	parameter of extreme value type I model (mode)
E	:	mean life
F_n	:	applied normal force
H	:	hardness
K	:	wear coefficient
K	:	coefficient of variation
P	:	critical plastic displacement
P_{LM}	:	Larson-Miller parameter
Q	:	activation energy
Q_p	:	constant for given material
R	:	universal gas constant
R_f	:	fouling resistance

R_1	:	radius of curvature of asperity
R^*	:	asymptotic value of fouling resistance
T	:	absolute temperature
T_a	:	material constant
T_m	:	median life
$\bar{T}$	:	mean life
V	:	volume of wear
V(T)	:	variance
W	:	wear rate
W_o	:	oxidation rate
a	:	constant
b	:	constant
c	:	median life
f	:	fraction of oxide which is oxygen
h	:	thickness of layer
l	:	sliding distance
m	:	mass of the particle
n	:	fixed quantity
q	:	probability = 1 - p
r	:	rate of damage
r_1	:	random number
r_2	:	random number

t	:	time
t_a	:	material constant
t_m	:	median time to failure
t_o	:	induction time
t_r	:	rupture time
t'	:	fatigue curve exponent power
v	:	velocity
x	:	depth of penetration

Greek Symbols

α	:	scatter parameter
α'	:	ratio of nominal area to frictional area of contact
α_1	:	constant
α_2	:	constant
α_3	:	constant
α_4	:	constant
β	:	shape parameter
β_1	:	material constant
ε_{el}	:	effective strain
ε_e	:	external factors
ε_i	:	internal factors
ε_o	:	initial quality factors

ε_{pl}	:	plastic strain
$\dot{\varepsilon}_s$	:	secondary creep rate
η	:	scale parameter of the weibull model
η_o	:	critical oxide thickness
γ	:	shape parameter of weibull model
λ	:	constant
μ	:	mean
ρ	:	constant
ρ_o	:	average density of the oxide
σ	:	stress
$\sigma(T)$	:	standard deviation
θ_o	:	constant
θ'_o	:	constant
ζ	:	product of stress and temperature

REFERENCES

[1] Sheikh, A.K., and Ahmad, M., 'A Reliability Model for a Non-Linear Damage Process', Reliability Engineering, Vol 18, pp. 73-99, 1987.

[2] Sheikh, A.K., Hussain, S.J., Ahmad, M.,'Cutting Tool Reliability and Machining Economics when Tool Wear follows a linear nonstationary random wear process', Proceedings of the 8th International Conference on Production Research, University of Stuttgart, Stuttgart, West Germany, [Ed. H.J. Bullinger and H.J. Warwacke], Springer - Verlag, .pp 163-178, August, 1985.

[3] Finley, M.J., 'An Extreme Value Statistical Analysis of Maximum Pit Depths and Time to First Perforation', Corrosion, Vol. 23, No. 4, pp. 83-87, 1967.

[4] Crews, D.L., 'Interpretation of Pitting Corrosion Data from Statistical Prediction Interval Calculations', ASTM STP576, ASTM Philadelphia, Pennsylvania, pp. 217-230, 1976.

[5] Sheikh, A.K., 'Generalized Non-Linear Damage Process and reliability models', Unpublished Work.

[6] Kern, D.Q., and Seaton, R.E., 'A Theoretical Analysis of Thermal Surface Fouling', British Chemical Engineering, Vol. 4, No. 5, pp. 258-262, 1959.

[7] Gertsbakh, I.B., and Kordonsky, Kh.B., 'Models of Failure', Springer -

Verlag, Inc., New York, 1969.

[8] Ahmad, M., and Sheikh, A.K., 'Bernstein Reliability Model: Derivation and Estimation of Parameters', Reliability Engineering, Vol 8, No. 6, pp. 131-148, 1984.

[9] Sheikh, A.K., Boah, J., and Younus, M., 'Reliability aspects of Corrosion', paper submitted for publication.

[10] Holm, R., 'Electrical contacts', Almquist and Wiksells, Stockholm, Section 40, 1946.

[11] Archard J.F., 'Contact and rubbing of flat surfaces', Journal of Applied Physics, 24, 24, 1953.

[12] Rabinowicz, E., 'The least wear' 100, pp. 533-541, 1984.

[13] Archard J.F., Wear, Proceedings of symposium on interdisciplinary approach to Friction and Wear, NASA SR181, ed. Ku, P.M., San Antorio, Texas, pp. 267-333, 1967.

[14] Suh N.P., 'An overview of the delamination theory of wear', Wear, 44, 1, pp. 1-16, 1977.

[15] Quinn, T.F.J., Sullivan, J.I., and Rowson, D.M., 'New developments in the oxidational theory of mild wear of metals', Proc. Int. Conference on wear of materials, ASME, Dearborn, Mich., pp. 1-11, 1979.

[16] Kragelsekii, I.V., and Marchenko, E.A., 'Wear of machine components', Trans. ASME, Lubrication Technology, 104, 1, pp. 1-7, 1982.

[17] Rabinowicz, E., 'Wear coefficients - metals', Wear control Handbook, ASME, pp. 475-506, 1980.

[18] Rabinowicz, E., 'The Wear coefficients - magnitude, scatter, uses', Trans. of ASME, Journal of lubrication Technology, Vol 103, pp. 188-194, 1981.

[19] Wallbridge, N.C., and Dowson, D., 'Distribution of wear rate data and a statistical approach to sliding wear theory' Wear, 119, pp. 295-312, 1987.

[20] Shahab, F.Q., 'A quantitative analysis of adhesive wear processes in metals', M.S. Thesis, King Fahd Univ. of Petroleum and Minerals, 1984.

[21] Kragelsky, I.V., and Alisin, V.V, Friction and wear lubrication, Vol 1., Tribology Handbook, Mir Publishers, Moscow, pp. 152, 1981.

[22] Metals Handbook Vol 1., American society for metals, pp. 687, 1977.

[23] Kececioglu, D., and Koharcheck, A., 'Wear reliability of Aircraft splines', Proceeding of Annual reliability and maintainability Symposium, pp. 155-163, 1977.

[24] Chow, E., 'Analysis of surface coatings using Bernstein distribution', M.S. Research Project, M.E. department, Washington State University, 1983.

[25] Raymond, G.B., 'Wear testing', Meatals Handbook Vol 7.

[26] Fontana, M.G., 'Corrosion Engineering', McGraw Hill Book Company, 1986.

[27] Staehle, R.W., 'Predictions and Experimental Verification of the Slip Dissolution Model for Stress Corrosion Cracking of Low Strength Alloys', NACE-5, NACE, pp. 180-208, 1973.

[28] Evans, V.R., 'The Corrosion and Oxidation of Metals' Edward Arnold, pp. 911, 1960.

[29] Booth, F.F., and Tucker, G.E.G, 'Statistical Distribution of Endurance in Electrochemical Stress Corrosion Tests', Corrosion, 21, 173, 1975.

[30] Cochran, R.W., and Stachle, R.W., 'Effects of Surface Preparation of Stress Corrosion Backing of Type 310 Stainless Stell in Building 42%, Magnesium Chloride', Corrosion, pp. 24, 367, 1968.

[31] Pelensky, M.A., and Gallaccio, A., 'Stress Corrosion Susceptibility of Aluminum Cartridge Cases', Corrosion, pp. 32, 312, 1976.

[32] Harshberger, J.H., Lemppiren, A.I., and Strum, B.W., Handbook on Corrosion testing and Evaluation', ed. W.H., Aitor, John Wiley and Sons, pp. 87, 1970.

[33] Locks, M.O., Corrosion, 27, .pp 386, 1971.

[34] Clarke, W.L., and Gordon, G.M., Corrosion, 29, 1, 1973.

[35] Strecker, E., Ryder, D.A., Davies, T.J., Journal of Iron and Steel Inst., 207, pp. 1639, 1969.

[36] Kaneko, R.S., and Simenz, R.F., 'Corrosion thresholds for interference fit fasteners and cold worked holes', Stress Corrosion New Approaches, ASTM STP 610, ASTM, pp. 252-266, 1976.

[37] Hines, J.G., and Jones, E.R.W., 'Some effects of alloy composition on the stress corrosion behavior of austenitic Cr-Ni steels', Corrosion Science, Vol 1, pp. 88-107, 1961.

[38] Evans, V.R., Mears, R.B., Quenea P.E., Engineering, Vol 136, pp. 689, 1933.

[39] Aziz, P.M. and Goclard, H.D., 'Industrial Engineering Chemistry', Vol. 44, pp. 1791, 1952.

[40] Summerson T.J., Pryor, M.J., Keir, D.S., Hogan R.J., Metals, ASTM, STP 196, ASTM, Philadelphia, Pennsylvannia, pp. 157, 1957.

[41] Rosenfeld, I.L., Industrial Metallurgia, 1970.

[42] Flaks, V.YA., Protection of Metals, Vol 9, No. 4, pp. 407-409, 1973.

[43] Aziz, P.M., 'Application of Statistical theory of extreme values to the analysis of maximum pit depth data for aluminium', Corrosion, Vol 12, pp. 495t-506t, 1956.

[44] Eldredge, G.G. 'Analysis of Corrosion Pitting by Extreme Value Statistics and its Application to oilwell tubing caliper survey', Corrosion, Vol 13, pp. 511t-601t, 1957.

[45] Ishikawa, Y., Ozaki, T., Hosaka, N., and Nishida, O., 'Prediction of localized Corrosion damage of some Machine Aspects by Means of Extreme Value Statistical Analysis', Transactions ISIJ, Vol 22, pp. 997-983, 1982.

[46] Korkosh, S.V., and Yondinshkin, K.N., 'Determination of the reliability of piping elements made from MNZh 5 -1 alloy,

Translation from Russian, Zashichita Metallov, Vol 6, No. 3, pp. 297-301, 1970.

[47] Leidheiser, H., 'The corrosion of Copper, Tin and their alloys', John Wiley & sons, 1971.

[48] Drazic, D.M., and Vascic, V., 'The Correlation between accelerated laboratory corrosion tests on Steels', Corrosion Science, Vol. 29, No. 10, pp. 1197-1204, 1989.

[49] Legault, R.A., and Pearson, V.P., 'The kinetics of the atmospheric corrosion of aluminized steel', Corrosion, Vol 34, No. 10, 1978.

[50] Dunn, J.S., Proceedings of Royal Society, [A], 111, 203, 1926.

[51] Vernon, W.H.J., Akeroyd, E., and Stroud, E.G., Journal of Institution of Metals, 65, pp. 301, 1939.

[52] Taborek, J., Aoki, T., Ritter, R.B., Palen, J.W., and Knudsen, J.G., 'Fouling: The major unresolved problem in Heat transfer', Chemical Engineering Progress, Vol. 68, No. 2, pp. 59-67, 1972.

[53] Taborek, J., Aoki, T., Ritter, R.B., Palen, J.W., and Knudsen, J.G., 'Predictive Methods for Fouling Behavior', Chemical Engineering Progress, Vol. 68, No. 7, pp. 69-78, 1972.

[54] Suitor, J.W., Marner, W.J., and Ritter, R.B., 'The History and Status of Research in Fouling of Exchangers in Cooling Water Service', The Canadian Journal of Chemical Engineering, Vol 55, pp. 374-380, 1976.

[55] Gudmundsson, J.S., 'Particulate Fouling', Fouling of Heat Transfer

Equipment, eds. E.F.C. Sommerscales and J.G. Knudsen, pp. 645-652, Hemisphere, Washington, D.C., 1981.

[56] Morse, R.W., and Knudsen, J.W., 'Effect of Alkalinity on the Scaling of Simulated Colling Tower Water', Chemical Engineering Progress, Vol. 55, No. 6, pp. 272-278, 1977.

[57] Story, M., and Knudsen, J.G., 'The Effect of Heat Transfer Surface Temperature on the Scaling Behavior of Simulated Colling Tower Water', Heat Transfer : Research and Application, ed. J.C. Chen, AIChE Symposium Series, Vol 74, No. 124, pp. 25-30, 1978. 25-xx.

[58] Lee, S.H., and Knudsen, J.G., 'Scaling Characteristics of Colling Tower Water', ASHRAE Transaction, Vol.85, Part 1, pp. 281-302, 1979.

[59] Watkinson, A.P., and Epstein, N., Chemical Engineering Progress Symposium Series, 65, No. 92, pp. 84-90, 1976.

[60] Sommerscales, E.F.C., 1981, 'Corrosion Fouling', Fouling in Heat Exchange Equipment, eds. J.M.Chenoweth and M. Impagliazzo, ASME HTD, Vol 17, pp. 17-27, 1981.

[61] Lister, D.H., 'Corrosion Products in Power Generating Systems', Fouling of Heat Transfer Equipment, eds. E.F.C. Sommerscales and J.G. Knudsen, Hemisphere, Washington, D.C., pp. 135-200, 1981.

[62] Characklis, W.G., 'Microbial Fouling: A Process Analysis', Fouling of Heat Transfer Equipment, eds. E.F.C. Sommerscales and J.G. Knudsen, Hemisphere, Washington, D.C., pp. 251-291, 1981.

[63] Siegel, R., and Savino, J.M., 'An Analysis of the Transient Solidification of a Flowing Warm Liquid on a Convectively Cooled Wall', Proceedings of the 3rd International Heat Transfer Conference, Vol. 4, pp. 141-151, 1966.

[64] Bott, T.R., 'Fouling due to Liquid Solidification', Fouling Heat Transfer Equipment, eds. E.F.C. Sommerscales and J.G. Knudsen, Hemisphere, Washington, D.C., pp. 201-226, 1981.

[65] Bell, K.J., and Mueller, A.C., 'Wolverine Heat Transfer Data Book II', A publication of Wolverine Division of UOP Inc., pp.36-37, 1984.

[66] McCabe, W.L., and Robinson, C.S., 'Evaporator scale formation', Industrial Engineering chemistry, Vol 16, pp. 478-479, 1924.

[67] Dunqi, Xu., and Knudsen, J.G., 'Functional correlation of surface temperature and flow velocity on fouling of cooling tower water', Heat transfer engineering, Vol 7, Nos. 1-2, pp. 63-70, 1986.

[68] Robinson, S.L., and Sherby, O.D., 'Mechanical behavior of Polycrystaline tungsten at elevated temperature', Acta. Metallurgica., Vol 17, pp. 109, 1969.

[69] Larson, F.R., and Miller, J., 'A time temperature relationship for rupture and creep stress' Transaction ASME, Vol 74, pp. 765, 1952.

[70] Sheikh, A.K., 'An investigation of creep tests variability using lead as a model' Unpublished research work, 1988.

[71] Hahn, G.J., 'The Role of Statistics', Chapter 4 of Development of a Standard Methodology for the Correlation and Extrapolation of

Elevated Temperature.

[72] Hahn, G.J., 'The Role of Statistical Methods in the Analysis of Creep and Rupture Data', General Electric Co. Report 78CRD237, 1978.

[73] Manson. S.S., and Ensign, A., 'Achievements in the last quarter century in the development of methods of correlation and extrapolation of results of long time strength tests', Teor. Osn. Inzh. Rachetov, Sev, D, 101, No. 4, pp. 9-18, 1979.

[74] Samrin, Yu.P., 'Application of stochastic equations in the theory of creep of materials', Izv. Aked. Nank SSSR, Mekh. Tvevd. Tela, No. 1, pp. 83-95, 1974.

[75] Peralta Duran, A., and Wirsching P.H., 'Creep rupture reliability analysis' Journal of Vibration, Acoustics, Stress and Reliability in Design, Vol 107, pp. 339-345, 1985.

[76] Stephov, M.N., Inozemtseva, I.A., and Maklakov, V.G., 'Regularities in the Change in scatter characteristics for the stress-rupture strength of high temperature alloys', Translated from Problemy Prochnosh, No. 8, pp. 59-64, 1988.

[77] Goldhoff, P.M., 'Towards the standardization of time temperature parameter usage in elevated temperature data analysis', Journal of Testing and Evaluation, Vol 2, No. 5, pp. 387-424, 1972.

[78] Metals Handbook Vol 1., American society for metals, 1977.